eISSN 2508-2612

KJIR
Korean Journal of Interventional Radiology

Vol. 31 No. 2 September 2026

https://kjironline.org

Korean Society of Interventional Radiology

KJIR
Korean Journal of
Interventional Radiology

eISSN 2508-2612
https://kjironline.org

Vol. 31 No. 2 September 2026

Aims and Scope

Korean Journal of Interventional Radiology, the official English-language journal of the *Korean Society of Interventional Radiology (KSIR)*, is an international peer-reviewed academic journal dedicated to interventional radiology. *KJIR* will publish cutting-edge and impactful scientific research articles in the field of interventional radiology.

KJIR will feature peer-reviewed original articles, authoritative reviews, systematic reviews and meta-analysis, case reports, and expert opinion on novel techniques and technologies.

Open Access

This is an Open Access article distributed under the terms of the Creative Commons Attribution Non-Commercial License (http://creativecommons.org/licenses/by-nc/4.0) which permits unrestricted non-commercial use, distribution, and reproduction in any medium, provided the original work is properly cited.

Publisher Korean Society of Interventional Radiology
Editor-in-Chief Jin Wook Chung, MD

Editorial Office
Korean Society of Interventional Radiology
Room 1401, 42, Seocho-daero 78-gil, Seocho-gu, Seoul 06626, Republic of Korea
Tel: +82-2-465-9070, Fax: +82-2-465-9072, E-mail: editor@kjironline.org

Publishing Office
M2PI
#805, 26 Sangwon 1-gil, Seongdong-gu, Seoul 04779, Korea
Tel: +82-2-6966-4930, Fax: +82-2-6966-4945, E-mail: support@m2-pi.com

Published on September 30, 2026

© 2026 Korean Society of Interventional Radiology

Editorial Board

Editor-in-Chief

Jin Wook Chung, MD	Department of Radiology, Seongnam Citizens Medical Center, Korea

Deputy Editor

Dong Jae Shim, MD, PhD	Department of Radiology, Incheon St. Mary's Hospital, College of Medicine, The Catholic University of Korea, Korea

Editorial Board

Youngjong Cho, MD, PhD	Department of Radiology, Gangneung Asan Hospital, University of Ulsan College of Medicine, Korea
Chang-ho Jeon, MD, PhD	Department of Radiology, Eunpyeong St. Mary's Hospital, College of Medicine, The Catholic University of Korea, Korea
Hyoung Nam Lee, MD., PhD	Aorta· Peripheral Vascular Clinic, Department of Radiology, Soonchunhyang University College of Medicine, Korea
Gun Ha Kim, MD	Asan Medical Center, University of Ulsan College of Medicine, Korea
Kun Yung Kim, MD, PhD	Department of Radiology, Seoul National University College of Medicine, Division of Intervention, Department of Radiology, Seoul National University Bundang Hospital, Korea
Jae Hwan Lee, MD, PhD	Department of Radiology, Seoul National University College of Medicine, Division of Intervention, Department of Radiology, Seoul National University Bundang Hospital, Korea
Sung-Joon Park, MD	Korea University Ansan Hospital, Korea
Suyoung Park, MD, PhD	Department of Radiology, Gil Medical Center, Gachon University College of Medicine, Korea
Chang Hoon Oh, MD	Department of Radiology, Samsung Medical Center, Sungkyunkwan University School of Medicine, Korea

KJIR
Korean Journal of
Interventional Radiology

eISSN 2508-2612
https://kjironline.org

Contents

Vol. 31 No. 2 September 2026

Editorial

47 Ethanol-Based Embolization for Renal Angiomyolipoma: Is the Embolic Agent the Answer, or the Strategy?
Ho Jong Chun

Case Reports

50 Transjugular Biliary Stenting: Case Report and Literature Review
Soumil Singhal, Heera Ram, Anubhav Khandelwal, Sanjay Saran Baijal

56 Plug-Assisted Thrombectomy for Extensive SVC Thrombosis: A Case Report
Tae Wook Baek, Ji Hoon Kim, Dong Il Gwon, Ji Hoon Shin, Jin Hyoung Kim

62 Sheath-Assisted Percutaneous Forceps Biopsy of the Cyst Wall under Ultrasound Guidance for the Histological Diagnosis of Complex Hepatic Cystic Lesions
Soumil Singhal, Vinamrita Patni, Sudhir Yadav, Anubhav Khandelwal, Sanjay Saran Baijal

69 A Side-Hole Catheter Technique for Overcoming Hostile Vascular Anatomy during Chemoembolization: A Case Report
Min Gwan Kim, Hyo-Cheol Kim

74 Recurrent Caudate Lobe HCC Supplied by a Variant Right Inferior Adrenal Artery: A Case Report
Donghyun Kim, Hyo-Cheol Kim

79 Transarterial Radioembolization via Right Internal Thoracic Artery in a Patient with HCC: A Case Report
Hyo-Cheol Kim

85 Comprehensive Interventional Management of Postoperative Duodenal Perforation: A Case Report
Jae Hwan Lee, Kun Yung Kim, Chang Jin Yoon

Review Articles

92 Drug-Coated Balloon Angioplasty for Dysfunctional Hemodialysis Access: An Update
Kichang Han

103 Endovascular Treatment of Below-the-Knee Arterial Disease in Chronic Limb-Threatening Ischemia
Tae Won Choi, Je Hwan Won, Jinoo Kim

113 Endovascular Management of Type 2 Endoleak after Endovascular Aneurysm Repair: An Interventional Radiologist's Perspective
Joon Ho Kwon

© 2026 Korean Society of Interventional Radiology

KJIR
Korean Journal of
Interventional Radiology

eISSN 2508-2612
https://kjironline.org

Vol. 31 No. 2 September 2026

Original Articles

125 Impact of Tumor Location on Radiofrequency Ablation Outcomes as First-Line Therapy for Hepatocellular Carcinoma
Gwang Hyeon Choi, Chang Jin Yoon, Chong-ho Lee, Kun Yung Kim, Eun Sun Jang, Jin-Wook Kim, Seung Jae Lee, Sook-Hyang Jeong, Minuk Kim, Jae Hwan Lee

136 Two-Session Catheter-Directed Ethanol Sclerotherapy for Symptomatic Peritoneal Inclusion Cysts: A Preliminary Case Series
Byung Soo Im, Ji-Hoon Kim, Gun Ha Kim, Shakir Ali H. Aljerdah, Ji Hoon Shin

145 Securement of Central Venous Catheters: Suture Fixation vs. Stabilization Devices in a Multicenter Retrospective Study
Jung Ui Hong, Yohan Kwon, Dong Jae Shim, Jae Hwan Lee

156 Clinical Efficacy and Patency of Stents for Malignant Iliocaval Venous Occlusion
Wonseon Shin, Gyoung Min Kim, Kichang Han, Man Deuk Kim, Joon Ho Kwon, Jong Yun Won, Juil Park

Letter-to-Editor

164 Risk-Adapted Central Venous Catheter Securement: Which Strategy, for Which Catheter, in Which Patient?
Jeong Ho Kim

How I Do It

167 Single-Incision Technique for Placement of Totally Implantable Venous Access Port via the Axillary Vein
Woo Jin Yang, Myung Gyu Song, Tae-Seok Seo

© 2026 Korean Society of Interventional Radiology

Editorial

eISSN 2508-2612
https://doi.org/10.64961/kjir.2026.00094
Korean J Interv Radiol 2026;31(2):47-49

KJIR
Korean Journal of
Interventional Radiology

Ethanol-Based Embolization for Renal Angiomyolipoma: Is the Embolic Agent the Answer, or the Strategy?

Ho Jong Chun*

Department of Radiology, College of Medicine, The Catholic University of Korea, Seoul, Republic of Korea

Transcatheter arterial embolization (TAE) is widely accepted as a nephron-sparing, minimally invasive treatment for renal angiomyolipoma (AML), particularly in symptomatic patients and those with large lesions or high-risk vascular features such as intratumoral aneurysms. As embolization devices and microcatheter techniques have advanced, TAE has become an increasingly preferred alternative to surgery in selected cases. Nevertheless, a critical question persists: which embolic material or procedural approach best achieves durable tumor control while maintaining an acceptable safety profile?

This lack of consensus is unsurprising. AML is a heterogeneous entity with variable proportions of adipose tissue, smooth muscle, and abnormal vasculature, and embolization practice varies considerably across institutions with respect to material selection, endpoint definition, and adjunctive techniques. Comparative studies are further constrained by small sample sizes, single-center designs, and inconsistent outcome metrics. Against this backdrop, the dual-center retrospective cohort study by Kim et al. [1] offers timely and valuable evidence, comparing ethanol-based embolization with polyvinyl alcohol (PVA) particle embolization and evaluating the incremental effect of microcoil use within ethanol-based therapy.

The investigators analyzed 119 adult patients with single renal AML treated between 2005 and 2023. To address baseline imbalance, they applied inverse probability treatment weighting using age, sex, and baseline tumor volume, followed by linear mixed-effects modeling for longitudinal volume change. Tumor response was assessed volumetrically using an ellipsoid formula derived from three orthogonal diameters on CT or MRI. The authors report that ethanol-based embolization achieved higher response rates (≥50% volume reduction) than PVA (92.1% vs. 78.4%), and that ethanol combined with microcoils demonstrated superior response and lower recurrence compared with ethanol alone. These findings suggest that ethanol-based approaches, particularly when reinforced with proximal occlusion, may offer meaningful advantages in AML embolization.

Agent Comparison Is Inseparable from Procedural Strategy

A central challenge in interpreting comparative embolization studies is procedural heterogeneity. In this study, ethanol-based embolization encompassed both ethanol-only and ethanol-plus-microcoil cases, whereas the PVA cohort consisted exclusively of PVA without coil use. This design preserves internal clarity within the PVA group but creates an important interpretive limitation: the comparison effectively becomes "ethanol ± coil" versus "PVA without coil," rather than a fully strategy-matched analysis.

Received: April 17, 2026; **Revised:** April 22, 2026;
Accepted: April 22, 2026
***Corresponding email:** hojongchun@gmail.com

© 2026 Korean Society of Interventional Radiology

This is an Open Access article distributed under the terms of the Creative Commons Attribution Non-Commercial License (http://creativecommons.org/licenses/by-nc/4.0) which permits unrestricted non-commercial use, distribution, and reproduction in any medium, provided the original work is properly cited.

In routine practice, coils are frequently added after particulate embolization to reduce the risk of recanalization, especially in larger feeding arteries or lesions with aneurysmal components. Readers will naturally ask under what angiographic circumstances coils were added in the ethanol group. The authors note that coil use was left to operator discretion based on angiographic findings, and that PVA-plus-coil cases were excluded from the PVA group, a reasonable approach for maintaining group separation, but one that complicates interpretation, as "ethanol superiority" may in part reflect "strategy superiority". Future studies would benefit from explicitly reporting coil selection criteria, including feeder diameter thresholds, washout patterns, residual tumor staining after distal embolization, or aneurysm and shunt physiology, so that the combined approach can be reproduced in a standardized manner.

Is Ethanol Superiority Truly Material-Based, or Coil-Supported?

The most thought-provoking signal in this manuscript emerges from the subgroup analysis. The ethanol-only subgroup demonstrated a response rate of 73.8%, lower than that of the PVA group (78.4%), and a higher recurrence rate (30.2% vs. 14.8%). Although these values derive from separately weighted cohorts and no direct statistical comparison was performed, the numerical pattern is suggestive and reinforces the case for the coil-stratified reanalysis proposed below. These findings raise a plausible alternative explanation: the favorable outcomes attributed to ethanol-based embolization may be driven primarily by the ethanol-plus-microcoil subgroup rather than by ethanol itself.

This is not a semantic distinction. If the principal determinant of durability is coil-supported proximal stabilization, the practical conclusion shifts: rather than recommending ethanol as a preferred agent, the emphasis should fall on a procedural framework that integrates durable proximal control with distal devascularization. The authors argue that the benefit reflects synergy between ethanol and coils rather than coil use alone, citing improved response rates (91.3% vs. 73.8%) and markedly reduced recurrence (7.1% vs. 30.2%) in the ethanol-plus-microcoil group compared with ethanol only. This explanation is clinically plausible; however, because the PVA cohort excluded coil use by design, the independent contributions of coil support and embolic agent cannot be fully disentangled.

A potentially informative supplementary analysis, if feasible, would compare a "coil group" (ethanol-plus-coil) with a "non-coil group" (ethanol-only and PVA-only combined). Even if selection bias cannot be eliminated, such a comparison would shed additional light on whether the observed advantage is primarily material-driven or strategy-driven.

Mechanistic Plausibility: Why Ethanol May Benefit from Optimization

Another notable contribution of this study is its presentation of a mechanistic rationale for ethanol-based embolization. As a liquid embolic agent, ethanol penetrates distal microvasculature, induces endothelial destruction and tumor necrosis, and achieves permanent occlusion at the arteriolar and capillary levels. This theoretical advantage offers a coherent basis for improved response and durability compared with particulate agents, which may occlude more proximally or incompletely.

However, ethanol-only embolization may be vulnerable to rapid washout in high-flow vessels, increasing the risk of incomplete occlusion, recanalization, and recurrence. In this context, microcoil augmentation serves as a logical procedural reinforcement: ethanol provides distal endothelial injury, while coils stabilize proximal occlusion and reduce washout, thereby prolonging contact time and improving durability. This "distal ablation plus proximal stabilization" strategy aligns with established embolization principles and plausibly explains why the ethanol-plus-microcoil subgroup achieved the most favorable outcomes.

This strategy-focused interpretation is consistent with prior experience in AML embolization. In an earlier comparative study by Jin et al. [2], embolization with ethanol-lipiodol emulsion and PVA particles showed no significant difference in shrinkage rate, with both approaches demonstrating safety and efficacy. Notably, microcoils were used selectively to treat aneurysms or proximal feeding arteries larger than 2 mm after distal embolic occlusion, in order to prevent incomplete occlusion or recanalization. Taken together, these data suggest that durable outcomes depend less on identifying a universal-

ly superior agent and more on applying a tailored strategy that integrates both distal and proximal embolization components.

Toward Tailored Embolization Strategies and Clinically Meaningful Endpoints

Although volumetric response provides an objective endpoint, the ultimate measure of AML embolization success lies in clinically meaningful outcomes: prevention of hemorrhage, relief of symptoms, avoidance of retreatment, and preservation of renal function. Future investigations should incorporate standardized reporting of these endpoints alongside imaging response. Strategy-matched comparisons, such as PVA-plus-coil versus ethanol-plus-coil, would provide stronger evidence for true material superiority and help establish reproducible procedural algorithms.

In summary, the authors present valuable dual-center evidence suggesting that ethanol-based embolization, particularly the ethanol-plus-microcoil approach, may achieve high response rates and improved durability compared with PVA-only embolization. The broader implication is that AML embolization outcomes may be optimized when distal devascularization is paired with stable proximal control, especially in lesions with high-flow vascular physiology.

Clinical Implications

(1) Ethanol-based embolization may offer improved early response in renal AML, but outcomes should be interpreted within the context of procedural strategy, particularly the adjunctive use of microcoils. (2) When ethanol washout or high-flow feeding anatomy is anticipated, combining distal ethanol embolization with proximal coil stabilization may improve durability and reduce the risk of recurrence. (3) Future studies should incorporate AML composition and angiographic phenotype to guide individualized embolization strategies, moving beyond agent-only comparisons.

Conflict of interest

No potential conflict of interest relevant to this article was reported.

Funding

None.

Acknowledgments

None.

Author contributions

The author conducted all aspects of the study.

Data availability statement

Data sharing does not apply to this article as no datasets were generated or analyzed during the current study.

ORCID

Ho Jong Chun, https://orcid.org/0000-0003-4512-6152

References

1. Kim KY, Kim M, Yoon CJ, Lee CH, Yoon SH, Han YM, et al. Impact of embolic agents on outcomes of renal angiomyolipoma embolization: a dual-center retrospective cohort study. Korean J Interv Radiol. 2026;31:36-42. http://doi.org/10.64961/kjir.2025.00045
2. Jin L, Chun HJ, Oh JS, Choi BG, Lee HG, Kim IJ. Selective arterial embolization of renal angiomyolipoma: comparing ethanol-lipiodol emulsion and polyvinyl alcohol particles as embolic agents. Diagn Interv Radiol. 2023;29:170-174. http://doi.org/10.5152/dir.2022.21625

Case Report

eISSN 2508-2612
https://doi.org/10.64961/kjir.2026.00059
Korean J Interv Radiol 2026;31(2):50-55

KJIR
Korean Journal of
Interventional Radiology

Transjugular Biliary Stenting: Case Report and Literature Review

Soumil Singhal*, Heera Ram, Anubhav Khandelwal, Sanjay Saran Baijal

Department of Interventional Radiology, Medanta: The Medicity, Gurgaon, India

We report a 54-year-old woman with chronic pancreatitis, duodenal obstruction, massive ascites, and refractory thrombocytopenia who developed septic obstructive cholangitis after occlusion of a plastic common bile duct (CBD) stent. Endoscopic exchange failed and PTBD was prohibitively risky. Transjugular intrahepatic biliary stenting (TIBS) provides an alternative route that avoids transperitoneal hepatic capsule puncture. Via right internal jugular access, the right hepatic vein was catheterized, a posterior sectoral bile duct punctured, and a guidewire crossed the distal CBD stricture. A 12 × 80 mm self-expandable metallic stent was deployed and the transhepatic tract embolized with coils. The patient experienced rapid clinical and biochemical recovery (bilirubin, 13.3 to 1.37 mg/dL) over 9 days postprocedure without any hemorrhagic complications. TIBS is a decisive, life-saving alternative when standard routes are not possible.

Keywords: Intrahepatic bile ducts; Cholangitis; Obstructive jaundice; TIPSS; Stent

Introduction

Obstructive jaundice due to biliary stricture or blockage often requires urgent decompression to prevent cholangitis and liver failure. The standard approaches for biliary drainage are endoscopic retrograde stenting or PTBD. However, these conventional routes can be infeasible or high-risk in certain situations. Massive ascites and coagulopathy (severe thrombocytopenia or coagulopathy) are relative contraindications to percutaneous transhepatic biliary interventions due to the high risk of hemorrhage and bile leakage into the peritoneum [1]. In such high-risk cases—for example, when endoscopic access is blocked by duodenal obstruction or when coagulopathy cannot be corrected—an alternative route for biliary drainage is needed. A transjugular intrahepatic approach offers a viable alternative in these scenarios [1]. This technique involves accessing the biliary system through the internal jugular vein and hepatic veins, thereby avoiding puncture of the liver capsule from the peritoneal side. We present a case of successful transjugular intrahepatic biliary stenting (TIBS) in a patient with distal biliary obstruction, refractory coagulopathy, and ascites. A comprehensive review of the literature is also provided to contextualize this approach, its indications, technique, and outcomes.

Case Report

A 54-year-old woman presented with 15 days of progressive jaundice (yellowish discoloration of the eyes), intense pruritus, and upper abdominal pain. Her medical history was no-

Received: March 16, 2026; **Revised:** April 13, 2026;
Accepted: April 13, 2026
***Corresponding email:** drsoumilsinghal75@gmail.com

© 2026 Korean Society of Interventional Radiology

This is an Open Access article distributed under the terms of the Creative Commons Attribution Non-Commercial License (http://creativecommons.org/licenses/by-nc/4.0) which permits unrestricted non-commercial use, distribution, and reproduction in any medium, provided the original work is properly cited.

table for chronic calcific pancreatitis with pancreatic ductal calculi and a distal common bile duct (CBD) stricture seen on a prior magnetic resonance cholangiopancreatography. She had undergone endoscopic plastic biliary stenting for the CBD stricture a few weeks earlier and an attempted pancreatic duct stenting had been unsuccessful. On current admission, she was markedly icteric and had signs of cholestatic liver dysfunction. A multiphasic contrast-enhanced computed tomography scan showed changes of chronic pancreatitis with extensive intraductal pancreatic calcifications. There were fluid collections in the lesser sac and anterior to the left liver lobe, along with moderate ascites (Fig. 1). The previously placed biliary stent appeared to be occluded, with a significantly dilated biliary tree upstream. Notably, a small enhancing lesion in the head of the pancreas raised suspicion for pancreatic malignancy.

During the hospital course, the patient's condition deteriorated: she developed acute cholangitis with high fever and septic shock requiring intensive care unit admission and vasopressor support. An attempt at endoscopic biliary stent exchange was made, but it failed due to a tight duodenal stricture with deep ulceration in the duodenum that prevented endoscope passage to the papilla. With the endoscopic route not possible, percutaneous transhepatic access was considered next. However, the patient had profound thrombocytopenia (platelet count 7,000/mm^3, rising only to 12,000/mm^3, after two single-donor platelet transfusions) and evidence of consumptive coagulopathy (elevated immature platelet fraction ~30%, peripheral smear showing low platelets with megakaryocytes, consistent with low-grade disseminated intravascular coagulation). Her prothrombin time was mildly prolonged (international normalized ratio, 1.38). Given the uncorrectable coagulopathy and presence of ascites, standard PTBD was deemed exceedingly high-risk for uncontrollable bleeding. After multidisciplinary discussion, a transjugular intrahepatic route was selected for biliary decompression as a last resort.

The procedure was performed in the interventional radiology suite under fluoroscopic guidance. A 10-Fr access in the right internal jugular vein was taken and a 5-Fr Multipurpose catheter was advanced into the right hepatic vein (RHV). Over an Ultra-stiff Amplatz wire the TIPS cannula was advanced (Cook Medical, Bloomington, IN, USA). Using ultrasound guidance provided by a second operator, the Colapinto needle was advanced to puncture the right biliary radicle from the RHV. The puncture technique was similar to a portal vein puncture while performing a TIPS procedure. Indentation of the bile duct was confirmed on ultrasonography, following which the puncture was made (Video 1). Contrast was injected to confirm entry into the biliary tree with opacification of dilated intrahepatic ducts. A 0.035-inch Terumo guidewire along with a 4F Cobra (C1) glide-catheter (Terumo Corp., Tokyo, Japan) was used to negotiate through the obstructed bile duct. The stricture at the lower end of the CBD was successfully traversed, and the wire was advanced into the duodenum. The wire was exchanged for an Ultra-stiff Amplatz over which, a 12 × 80 mm self-expandable metallic stent (Luminexx, BD/BARD, Tempe, AZ, USA) was deployed across the distal CBD stricture, spanning from the proximal biliary tree into the duodenum. Free flow of contrast into the duodenum

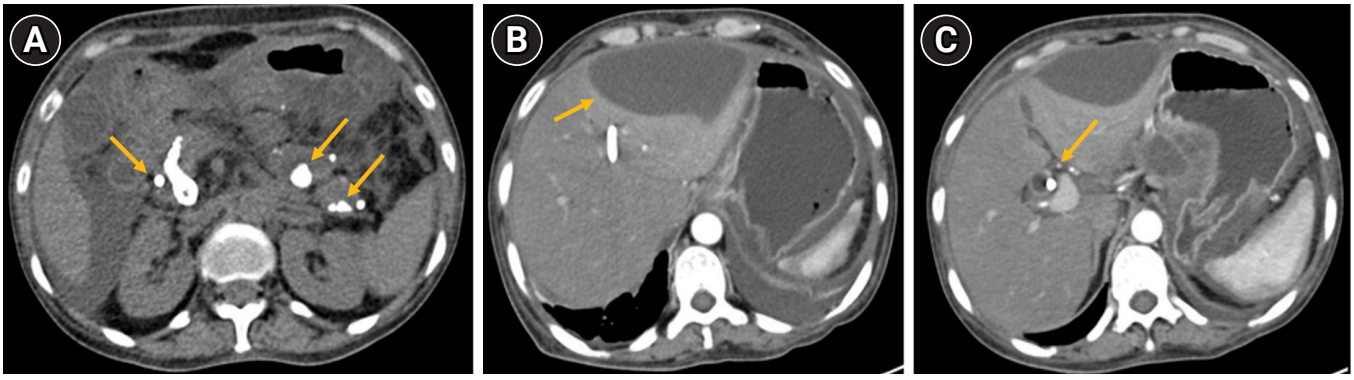


Fig. 1. Intraductal calculi (depicted by arrows) in the head, body, and tail region of pancreas (A), fluid collection (arrow) along the anterior aspect of the left lobe of the liver (B), and a common bile duct (CBD) stent (arrow) with dilated CBD and pseudocyst in the lesser sac and a fluid collection along the anterior aspect of the left lobe of liver (C).

confirmed adequate decompression of the biliary system. Finally, to prevent hemorrhage or bile leak along the needle tract, the transhepatic tract between the RHV and the biliary duct was embolized. Two pushable coils measuring 35-5-3 mm and 35-14-4 mm (Cook Medical) were placed in the tract to seal it. The internal jugular access was then removed and hemostasis achieved (Fig. 2).

Following the transjugular stent placement, the patient's condition improved markedly. Her jaundice and fever subsided over the next few days as cholangitis resolved. Liver function tests showed rapid improvement: total bilirubin decreased from 13.3 mg/dL pre-procedure to 1.37 mg/dL at discharge. She was monitored in the hospital for 9 days post-procedure, during which no procedure-related complications (such as bleeding or hemobilia) occurred. The patient was discharged in stable condition with instructions for outpatient follow-up. At a 1-month follow-up, she remained clinically improved with the biliary stent functioning and no recurrence of biliary obstruction symptoms.

This case was conducted in accordance with the Declaration of Helsinki. As a retrospective observational report involving anonymized clinical data, formal ethics committee approval was not required at our institution; however, institutional review board exemption was confirmed. Patient confidentiality has been maintained throughout. Written informed consent was obtained from the patient for the publication of this case and any accompanying images.

Discussion

This case highlights the role of TIBS as a salvage technique when conventional methods are contraindicated or have failed. The presence of severe coagulopathy and ascites in our patient made percutaneous transhepatic access extremely dangerous, as puncturing the liver capsule under these conditions carries a high risk of intraperitoneal hemorrhage and bile peritonitis [2]. Even with techniques like prior ascites drainage and tract embolization, PTBD in coagulopathic patients has a significantly elevated complication risk. The transjugular approach, first described in 1967 by Hanafee and Weiner [3] for cholangiography, avoids traversing the peritoneal cavity by accessing the biliary system via the hepatic veins. In essence, the needle puncture is entirely intrahepatic and any bleeding that occurs is more likely to be contained

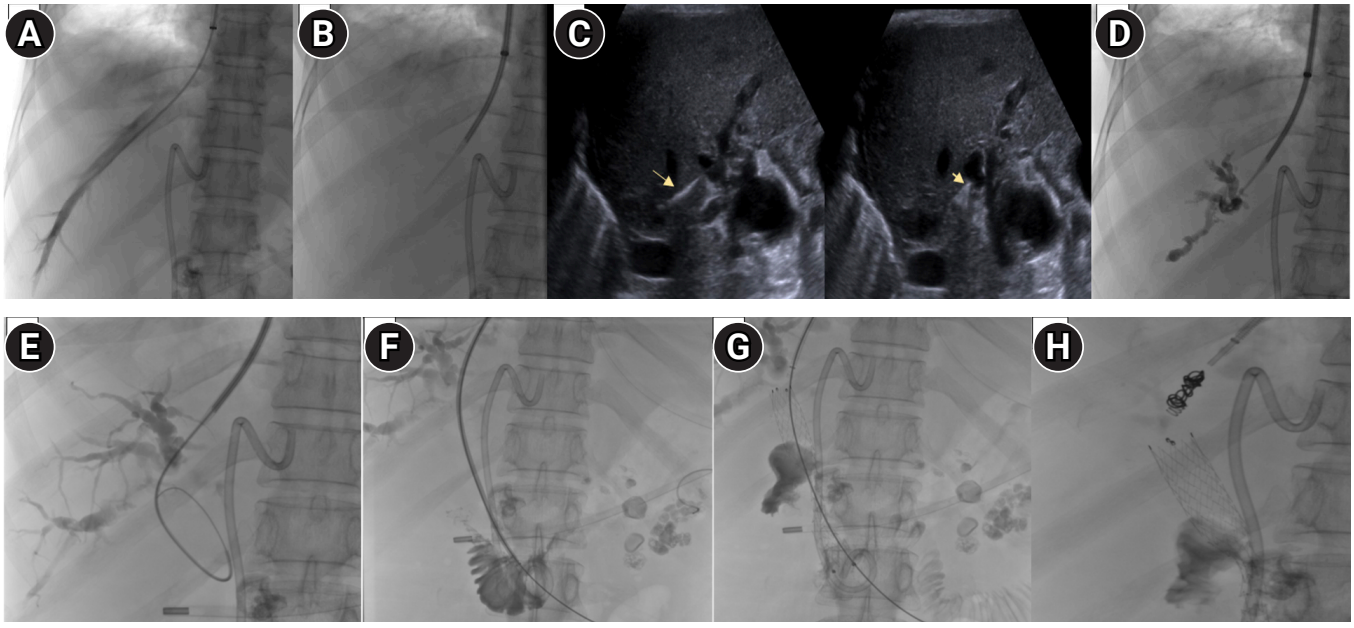


Fig. 2. (A) Right hepatic vein venography. (B) Transjugular liver biopsy (Cook Medical) set cannula through which a Rosch Uchida TIPS set (RUPS set, Cook Medical) catheter stylet combination advanced to puncture the right posterior sectoral duct (RPSD). (C) Ultrasonography guidance demonstrates sludge within dilated biliary ducts (arrowhead) and puncture of the RPSD (arrow). (D) Cholangiography. (E) A 0.035-inch angled glidewire (Terumo Corp.) negotiated into the common bile duct (CBD). (F) A 4-Fr catheter used to assist in negotiating the guidewire across the stricture into the duodenum. (G) Metallic stent deployed across the stricture. (H) The intrahepatic veno-biliary track embolized with pushable coils.

within the vascular system or tract, rather than filling the abdominal cavity. This approach was further developed in the 1990s, with early reports demonstrating transjugular insertion of biliary stents in patients with malignant obstructions complicated by ascites. Ring et al. reported the first use of an expandable metal stent via the transjugular route to palliate malignant biliary obstruction in a patient with refractory ascites [4]. Subsequent case reports, including the study by Amygdalos et al. in 1996 [1], reinforced that transjugular biliary catheterization is a valuable alternative when standard PTBD is contraindicated.

The TIBS requires advanced skill and careful technique. Under imaging guidance, a hepatic vein (usually RHV) is catheterized from the internal jugular route. A Colapinto or Rösch needle is used to puncture from the hepatic vein through a small portion of liver parenchyma into an intrahepatic bile duct [2]. Key technical steps include choosing a peripheral biliary branch to puncture (to minimize the tract size and bleeding risk) and using real-time ultrasound guidance to aid the needle puncture. Once access to a dilated bile duct is confirmed by cholangiography, a guidewire and catheter are advanced across the biliary obstruction. In our case and others, a hydrophilic guidewire can be maneuvered through a distal CBD stricture into the duodenum. If the guidewire successfully crosses the obstruction, the tract can be dilated to allow passage of catheters and eventually a stent. Self-expandable metal stents (uncovered or covered) of adequate length are then deployed across the stricture to re-establish biliary drainage into the gastrointestinal tract. A completion cholangiogram or radiograph is performed to ensure contrast flows freely past the stent into the duodenum or bowel, confirming patency. Finally, an important step—especially in coagulopathic patients—is embolization of the created tract. After stent placement, the needle tract through the liver is occluded using coils to prevent any bleeding leading to hemobilia. In the presented case, coils were used; some protocols use N-butyl cyanoacrylate (glue) mixed with lipiodol for tract sealing [5]. Tract embolization has been shown to reduce post-procedure hemorrhage and bile leak complications in both percutaneous and transvenous approaches.

Our patient's successful outcome aligns with the growing body of evidence supporting transjugular biliary interventions in high-risk patients. While no large randomized trials exist (owing to the relatively infrequent use of this technique), multiple small studies and case reports have documented its feasibility. A prospective study of 12 patients by Shim et al. (2019) [2] is one of the largest studies to date evaluating TIBS in malignant obstructions with massive ascites/coagulopathy. Technical success of 92% and clinical success of 73% was reported. The main complication noted in that study was hemobilia in two patients. Notably, all patients had advanced malignancy, and the median overall survival was only 19 days due to disease progression—emphasizing that TIBS in such contexts is often a palliative measure to improve quality of life in end-stage patients.

Another notable study by Tsauo et al. [5] reported on six patients with distal malignant biliary obstruction and uncorrectable coagulopathy who underwent transjugular bare-metal stent insertion. The authors concluded that when the risk of hemorrhage from percutaneous drainage is prohibitively high, TIBS is an effective alternative for palliation of obstructive jaundice. They reported an average survival of 4.5 months in their study, with 100% stent patency until death. This suggests that once the immediate hurdle of safely establishing drainage is overcome, TIBS can sustain biliary decompression adequately. Our case reinforces this conclusion, demonstrating that TIBS can be life-saving in the setting of disseminated intravascular coagulation and thrombocytopenia where PTBD is essentially impossible.

It is also valuable to compare the transjugular approach to the modified percutaneous strategies developed for patients with ascites. Seif et al. [6] described a "one-stage percutaneous triple procedure" for malignant biliary obstruction with marked ascites, which involves large-volume paracentesis (ascites drainage), immediate placement of a biliary metal stent, and then embolization of the tract with glue, all in one session. In a study of 25 patients treated with this method, technical success was 96% and major complications were avoided by prophylactically sealing the tract. While that approach is highly effective when ascites is the main issue, it still requires that coagulation parameters be reasonably controlled; bleeding can still occur if platelets or clotting factors are critically low. TIBS is technically demanding and not as widely practiced as standard PTBD or endoscopic stenting. The success of the procedure hinges on being able to target a suitable bile duct from the venous side. Failure can occur if

the bile ducts are small or not sufficiently dilated to be located, or if the stricture cannot be crossed with a guidewire.

Meticulous tract management is paramount during and after hepatic interventions: coil embolization under ultrasound guidance should be performed to prevent bile-venous communications. The rationale is hemodynamic—a higher pressure in the CBD (approximately 12–14 mmHg) relative to the hepatic vein (around 7 mmHg) can drive bile directly into the hepatic venous system. Clinically, this manifests as bilhemia, marked by a rapid rise in total and direct bilirubin without other evidence of hepatic dysfunction or biliary obstruction. It most often follows hepatic trauma but has also been observed after TIPS. This mechanism differs from portal venous–biliary fistulas, in which the higher-pressure portal circulation delivers blood into the biliary tree, resulting in hemobilia [7-9].

Our patient's recovery from multi-organ dysfunction after biliary decompression illustrates how critical timely drainage is, and TIBS provided a means to achieve it when no other safe option was available.

TIBS is an important alternative technique for biliary drainage in patients who have contraindications to the standard endoscopic or percutaneous approaches. In the presence of uncorrectable coagulopathy, severe thrombocytopenia, or massive ascites, the transjugular approach can be life-saving, allowing relief of biliary obstruction with a lower risk of catastrophic bleeding. The literature, though composed of case studies and reports, consistently demonstrates that TIBS is technically feasible and clinically effective in achieving jaundice relief in high-risk patients. The case presented here adds to this body of evidence, showing successful application of TIBS in a scenario of disseminated intravascular coagulation and duodenal obstruction. While TIBS requires specialized expertise and may not be available in all centers, it should be considered in the armamentarium for complex biliary obstruction cases. Transjugular route offers a robust solution to achieve biliary decompression and resolve obstructive cholangitis, ultimately improving patient outcomes in otherwise dire circumstances.

Conflict of interest

No potential conflict of interest relevant to this article was reported.

Funding

None.

Acknowledgments

None.

Author contributions

Conceptualization: SS, HR, AK, SSB. Writing – original draft: SS. Writing – review & editing: SS, SSB.

Data availability statement

Data sharing does not apply to this article as no datasets were generated or analyzed during the current study.

Supplementary material

The supplementary data are available with this article at https://doi.org/10.64961/kjir.2026.00059.

ORCID

Soumil Singhal, https://orcid.org/0000-0003-1688-3664
Heera Ram, https://orcid.org/0000-0001-6017-1643
Anubhav Khandelwal, https://orcid.org/0000-0003-2275-1457
Sanjay Saran Baijal, https://orcid.org/0000-0002-2797-4054

References

1. Amygdalos MA, Haskal ZJ, Cope C, Kadish SL, Long WB. Transjugular insertion of biliary stents (TIBS) in two patients with malignant obstruction, ascites, and coagulopathy. Cardiovasc Intervent Radiol. 1996;19:107-109. https://doi.org/10.1007/BF02563903
2. Shim DJ, Gwon DI, Ko GY, Yoon HK, Sung KB. Transjugular insertion of biliary stent in patients with malignant biliary obstruction complicated by ascites with/without coagulopathy: a prospective study of 12 patients. Diagn Interv Radiol. 2019;25:465-470. https://doi.org/10.5152/dir.2019.18470
3. Hanafee W, Weiner M. Transjugular percutaneous cholangiography. Radiology. 1967;88:35-39. https://doi.org/10.1148/88.1.35
4. Ring EJ, Gordon RL, LaBerge JM, Shapiro HA. Malignant biliary obstruction complicated by ascites: transjugular insertion of an expandable metallic endoprosthesis. Radiology. 1991;180:579-581. https://doi.org/10.1148/radiology.

180.2.2068334
5. Tsauo J, Li X, Li H, Wei B, Luo X, Zhang C, et al. Transjugular insertion of bare-metal biliary stent for the treatment of distal malignant obstructive jaundice complicated by coagulopathy. Cardiovasc Intervent Radiol. 2013;36:521-525. https://doi.org/10.1007/s00270-012-0453-6
6. Seif HM, Zidan M, Helmy A. One-stage percutaneous triple procedure for treatment of endoscopically unmanageable patients with malignant biliary obstruction and marked ascites. Arab J Gastroenterol. 2013;14:148-153. https://doi.org/10.1016/j.ajg.2013.10.004
7. Kruel CR, Guimaraes M, Chedid AD, Grezzana-Filho TM, Leipnitz I, de Araujo A, et al. Bilhemia following transjugular intrahepatic portosystemic shunt placement (TIPS): liver transplantation as a rescue procedure - case report. Arq Bras Cir Dig. 2013;26:238-240. https://doi.org/10.1590/s0102-67202013000300016
8. Blum U, Buitrago-Tellez C, el Seif M, Wimmer B. Posttraumatic bilhemia: conservative management by percutaneous drainage. Cardiovasc Intervent Radiol. 1993;16:55-57. https://doi.org/10.1007/BF02603040
9. Singal AK, Kathuria MK, Malhotra A, Goodgame RW, Soloway RD. Bilhemia after trans-jugular intra-hepatic porto-systemic shunt and its management with biliary decompression. World J Gastroenterol. 2009;15:3681-3683. https://doi.org/10.3748/wjg.15.3681

Case Report

eISSN 2508-2612
https://doi.org/10.64961/kjir.2026.00052
Korean J Interv Radiol 2026;31(2):56-61

KJIR
Korean Journal of
Interventional Radiology

Plug-Assisted Thrombectomy for Extensive SVC Thrombosis: A Case Report

Tae Wook Baek, Ji Hoon Kim*, Dong Il Gwon, Ji Hoon Shin, Jin Hyoung Kim

Department of Radiology and Research Institute of Radiology, Asan Medical Center, University of Ulsan College of Medicine, Seoul, Republic of Korea

Acute SVC syndrome caused by extensive thrombosis requires prompt endovascular intervention. We report a 48-year-old female with colon cancer presenting with massive chemoport-related thrombosis involving the SVC, right atrium (RA), and bilateral brachiocephalic veins. Due to the lack of an embolic protection filter landing zone, we performed a novel plug-assisted thrombectomy (PAT) technique. A 20-mm vascular plug was positioned at the SVC-RA junction as a temporary tethered filter without detachment. Following mechanical thrombectomy, plug retrieval, and adjunctive balloon dilatation, the patient recovered and was discharged on day 12. This case demonstrates the technical feasibility of PAT as a proof-of-concept approach for embolic protection in patients with extensive SVC thrombosis where conventional filter placement is anatomically precluded.

Keywords: Superior vena cava syndrome; Thrombosis; Thrombectomy; Case reports

Introduction

Upper-extremity deep vein thrombosis (UEDVT) accounts for approximately 10% of all deep vein thrombosis (DVT) cases, and its incidence has been steadily increasing—a trend closely associated with the growing use of indwelling central venous catheters [1,2]. Subsequent thrombosis of the innominate and subclavian veins may occur with severe SVC stenosis. Nowadays, most non-malignant SVC syndromes are attributed to indwelling central venous catheters or pacemaker leads [3]. The primary treatment for UEDVT is standard anticoagulation, aimed at alleviating symptoms, preventing thrombus progression, and reducing the risk of fatal pulmonary thromboembolism (PTE) [4]. However, despite the rising clinical burden of catheter-associated UEDVT, there is a lack of established consensus or specific guidelines regarding its optimal management, particularly concerning anticoagulation protocols and the indications for SVC filter placement. When acute UEDVT progresses to massive SVC thrombosis, it can cause severe hemodynamic instability, necessitating endovascular intervention. While catheter-directed thrombolysis [5,6] or mechanical thrombectomy (e.g., the FlowTriever system) [7] is increasingly utilized, supporting literature remains limited to case reports and small series. During aggressive mechanical thrombectomy for lower extremity DVT, an IVC filter is routinely and safely utilized to provide embolic protection [8]. While some studies have reported on the safety of placing filters in the SVC to protect against PTE in patients with UEDVT, its routine use remains controversial [9,10]. In contrast, using a conventional filter in the SVC for UEDVT presents significant anatomical challenges due to the lack of an adequate landing zone, and carries catastrophic complication risks, such as caval perforation and cardiac tamponade [11].

Received: March 1, 2026; **Revised:** April 20, 2026;
Accepted: April 21, 2026
***Corresponding email:** jihoonkim@amc.seoul.kr

© 2026 Korean Society of Interventional Radiology

This is an Open Access article distributed under the terms of the Creative Commons Attribution Non-Commercial License (http://creativecommons.org/licenses/by-nc/4.0) which permits unrestricted non-commercial use, distribution, and reproduction in any medium, provided the original work is properly cited.

Herein, we report a case of fatal hemodynamic compromise caused by extensive acute SVC thrombosis. To overcome the anatomical constraints and risks associated with conventional filters, we successfully performed mechanical thrombectomy using a vascular plug as an embolic protection device (plug-assisted thrombectomy, PAT).

Case Report

A 48-year-old woman with a history of laparoscopic anterior resection for sigmoid colon cancer 2 years earlier and subsequent adjuvant chemotherapy presented with syncope and abrupt, severe swelling of the face and bilateral arms. She had an indwelling chemoport actively used for palliative chemotherapy due to recently developed lymph node and peritoneal metastases. Upon arrival, the patient was hemodynamically unstable with an initially unmeasurable blood pressure, which marginally stabilized to 97/80 mmHg with compensatory tachycardia (124 bpm) and respiratory alkalosis (pH 7.460, $PaCO_2$ 13.5 mmHg, PaO_2 100.6 mmHg, and HCO_3 9.6 mmEq/L) on arterial blood gas analysis. Initial laboratory investigations revealed a significantly elevated D-dimer level, 30 μg/mL. Complete blood count showed anemia, with a hemoglobin of 8.8 g/dL and a hematocrit of 27.1%, while the platelet count was 141 × 10^3/μL. Coagulation studies indicated an INR of 1.62, with a corresponding prothrombin time of 18.5 seconds. Contrast-enhanced chest CT revealed extensive, diffuse thrombosis involving the bilateral subclavian, brachiocephalic veins, and the SVC, extending into the right atrium (RA) (Fig. 1A). Acute PTE was identified in right lower lobar and segmental pulmonary arteries (Fig. 1B). Given the massive thrombus burden, urgent endovascular thrombectomy was planned. At the time of intervention, the patient required dual vasopressor support with norepinephrine (0.24 μg/kg/min) and vasopressin (0.02 units/min), maintaining a blood pressure of 84/59 mmHg. To evaluate the risk of acute right ventricular (RV) volume overload following restoration of SVC flow, preprocedural echocardiography was performed and demonstrated no evidence of RV strain or dysfunction. Although extracorporeal membrane oxygenation was considered as a rescue strategy, it was deferred after multidisciplinary discussion given the patient's underlying malignancy and estimated prognosis of less than one year. Due to the severe risk of massive PTE during the procedure, prophylactic endotracheal intubation was performed under general anesthesia. When planning the procedure, our primary concern was how to effectively prevent thrombus migration into the RA during thrombectomy. We initially considered the use of an IVC filter-type device as a temporary barrier; however, given the absence of an appropriate landing zone within the SVC, this approach was not feasible. Instead, we considered a vascular plug, which offered both a sufficiently large diameter

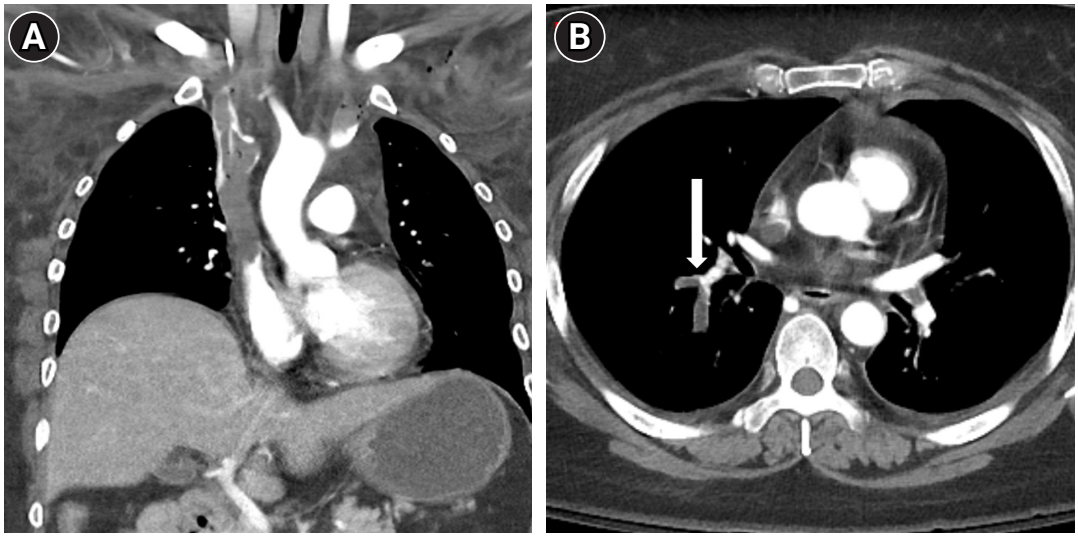


Fig. 1. A 48-year-old woman with a history of sigmoid colon cancer presented with syncope and abrupt, severe swelling of the face and bilateral arms. (A) CT image shows extensive, diffuse thrombosis involving the SVC. (B) Axial CT image at the level of the lower thorax reveals acute pulmonary thromboembolism in the right lower lobar segmental pulmonary arteries (arrow).

to be deployed within the SVC and the mechanical properties necessary to function as a temporary barrier against thrombus fragment migration during thrombectomy.

Right common femoral vein access was achieved under ultrasound guidance using a micropuncture set with a 21-gauge needle. A 7-Fr Shuttle Flexor guiding sheath (Cook Inc., Bloomington, IN, USA) was then placed, through which a 5-Fr C2 Cobra catheter (Boston Scientific, Cork, Ireland) was advanced. Venography through the 5-Fr angiographic catheter in the RA showed thrombotic occlusion and narrowing at the SVC-RA junction. Since the diameter of the SVC-RA junction was measured at 13 mm on venography, plug sizing was initially attempted with a 22-mm Amplatzer Vascular Plug II (Abbott Medical, Abbott Park, IL, USA); however, this plug failed to maintain stable positioning and was dislodged, likely due to excessive oversizing. A 20-mm plug was subsequently deployed, which provided adequate and stable anchoring throughout the procedure. To prevent potential migration, one lobe of the plug was intentionally positioned within the thrombotic segment, ensuring stable anchoring and complete occlusion at the junction. Crucially, instead of detachment, the plug was only deployed and maintained on the delivery cable throughout the procedure, serving as a temporary sieve and mechanical barrier against large emboli (Fig. 2A, 2B). A second access was established via the right internal jugular vein using ultrasound guidance and a micropuncture set. Ini-

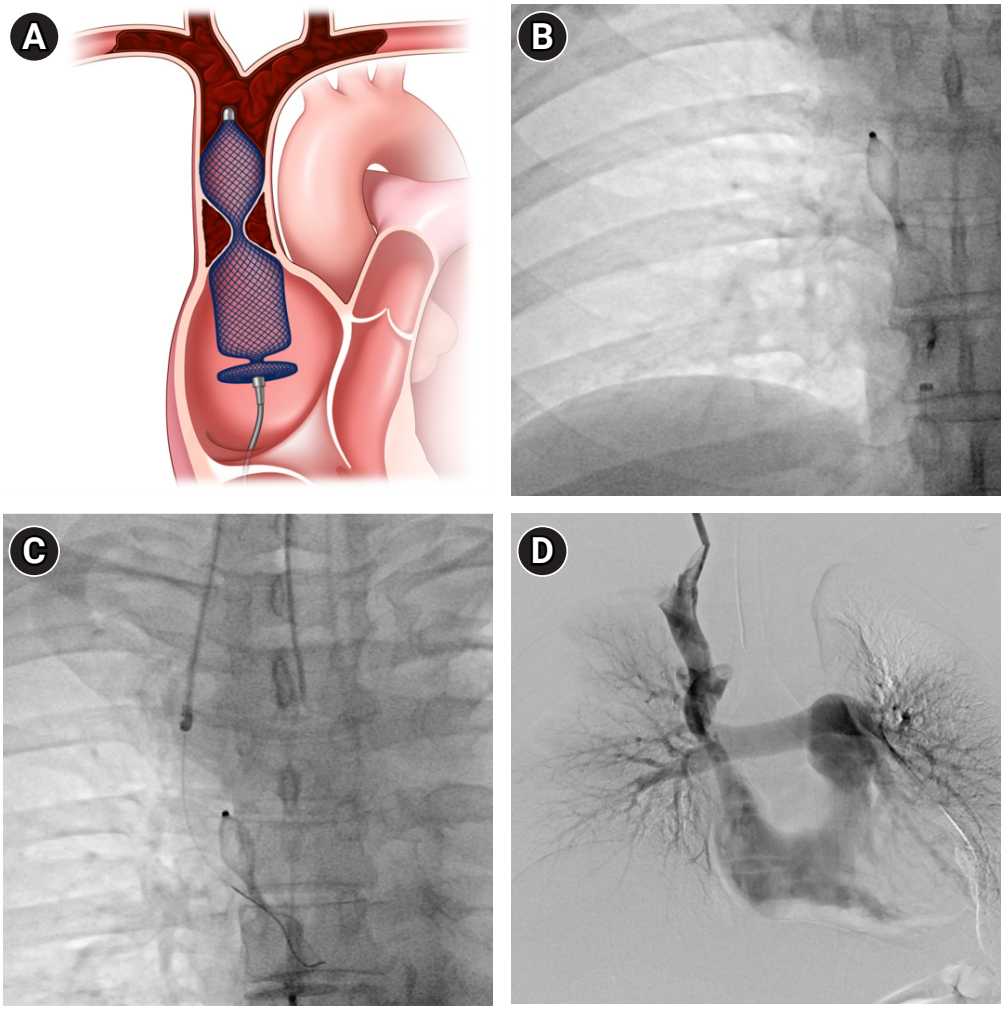


Fig. 2. Endovascular thrombectomy. (A) Illustration of a vascular plug deployed at the SVC–right atrium (RA) junction to prevent the migration of massive thrombus. (B) Vascular plug is deployed at the junction of SVC-RA, where the portion of vascular plug in the thrombosed SVC is partially opened. (C) Mechanical thrombectomy is performed via route of right internal jugular vein. (D) The deployed vascular plug was safely retrieved, with a small amount of residual thrombus remaining in the SVC.

tially, mechanical thrombectomy using an 8-Fr Aspirex device (Straub Medical AG, Wangs, Switzerland) was performed to reduce the overall thrombotic burden. During this process, the use of the Aspirex device was strictly avoided in the vicinity of the vascular plug to prevent potential device damage or entanglement (Fig. 2C). During plug retrieval, a critical technical consideration was the directionality of the capture maneuver. Rather than advancing the sheath toward the plug—which risks mechanically displacing the surrounding thrombus caudally into the RA—the 7-Fr Shuttle Flexor sheath was maintained in a stationary position while the plug was retracted cranially by pulling the delivery cable, drawing the plug back into the fixed sheath. This 'device-to-sheath' retrieval technique minimizes mechanical interaction with the peri-plug thrombus and reduces the risk of iatrogenic embolization during retrieval. Following the retrieval of the plug, residual thrombosis adjacent to the plug site was safely removed via manual aspiration using a 7-Fr Envoy guiding catheter (Codman Neurovascular, Raynham, MA, USA). Following the aspiration of the massive thrombus, a residual stenosis was identified in the SVC adjacent to the RA. Balloon angioplasty was performed using a 12 × 60-mm Mustang balloon (Boston Scientific, Marlborough, MA, USA). Final venography revealed that the main flow of the SVC was restored (Fig. 2D). Residual thrombus in the SVC and bilateral brachiocephalic veins was planned to be managed with anticoagulation. Following the procedure, anticoagulation was administered according to our institutional standard-dose heparinization protocol: an initial bolus of unfractionated heparin 3,000 IU was administered intravenously, followed by a continuous infusion of 20,000 IU in 500 mL normal saline at 20 mL/h (800 IU/h), targeting an activated partial thromboplastin time of 50–75 seconds.

The patient showed dramatic clinical improvement, with edema resolving over the next 10 days. A follow-up CT demonstrated near-complete resolution of the thrombosis (Fig. 3). She was successfully extubated and discharged 12 days after the initial presentation. At discharge, the patient was maintained on prophylactic-dose enoxaparin (40 mg once daily), as therapeutic-dose anticoagulation was de-escalated due to the development of hematuria during admission. Outpatient follow-up was scheduled with repeat laboratory evaluation including D-dimer.

Discussion

The management of extensive SVC thrombosis involving hemodynamic instability and a high thrombus burden extending into the RA remains clinically challenging. In the present case, the patient's clinical deterioration—characterized by syncope, hypotension, and severe respiratory alkalosis—necessitated immediate endovascular intervention.

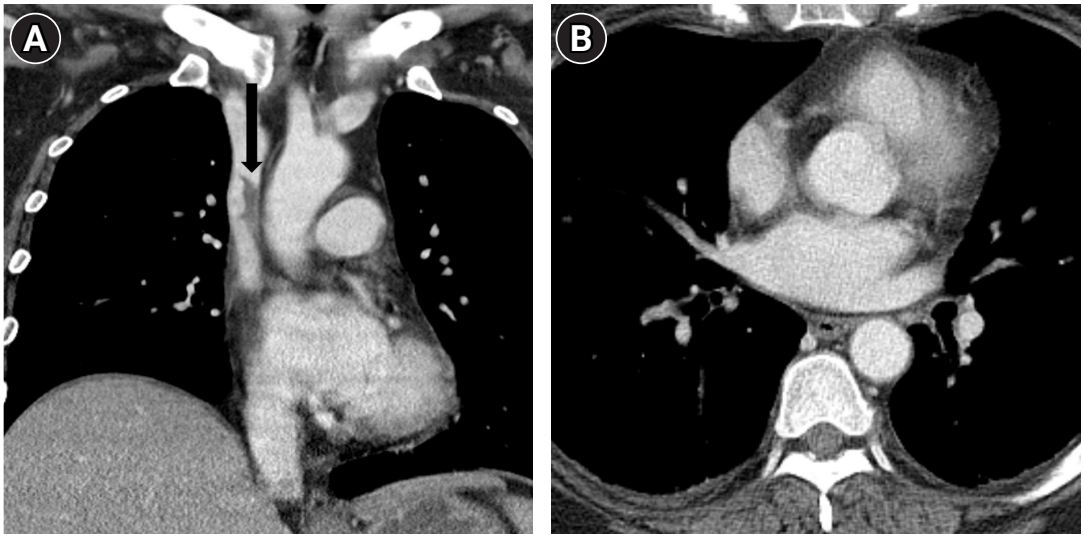


Fig. 3. Follow-up. (A) A 10-day follow-up CT scan shows near-complete resolution of the thrombus, with a small amount of residual thrombus remaining in the superior vena cava (arrow). (B) Axial CT image reveals complete resolution of the previous pulmonary thromboembolism (PTE), with no evidence of newly developed PTE.

However, the existing PTE and the massive thrombus burden at the SVC-RA junction presented a significant procedural dilemma: the high risk of treatment-induced fatal pulmonary embolism versus the lack of a safe landing zone for conventional embolic protection.

The anatomical constraints of the SVC often preclude the use of SVC filters, which are associated with risks of migration, caval perforation, and cardiac tamponade in this shorter and more mobile vessel segment [9,11]. Furthermore, since the thrombus in our patient had already extended adjacent to the RA, there was insufficient space for safe filter deployment. To overcome these challenges, we utilized a vascular plug as a temporary embolic protection device. We hypothesized that the fine nitinol mesh of the Amplatzer Vascular Plug II could similarly serve as a mechanical barrier against large, procedurally-dislodged thrombi.

The use of a vascular plug as a protection device in the SVC offers several distinct clinical advantages. First, when the plug is not detached from the delivery cable, it can be repositioned freely to accommodate real-time changes in thrombus morphology and can be easily retrieved into the sheath once the thrombectomy is completed [12]. Second, the availability of various sizes (2–22 mm) allows for precise fitting in large-caliber vessels like the SVC, ensuring a stable "sieve" effect. Third, the safety profile of these plugs is well-established across various clinical scenarios with minimal complications [13]. Although a delivery sheath of 7-Fr or larger is required, this is rarely a limiting factor in the context of large-bore SVC interventions. However, one important caveat is that plug stability may diminish as thrombectomy progresses. As the surrounding thrombus burden is reduced, the thrombus that initially contributes to plug anchoring is gradually eliminated, potentially rendering the plug susceptible to dislodgement. Continuous fluoroscopic monitoring of plug position throughout the procedure is therefore strongly advisable.

In this case, diffuse thrombosis in the SVC and right brachiocephalic vein was successfully resolved. The clinical improvement and the patient's discharge within 12 days underscore the feasibility of this technique. For patients with massive SVC thrombosis where the risk of procedural PTE is high and conventional filter placement is anatomically constrained, the use of a vascular plug as a temporary embolic protection device (PAT) may offer a feasible and versatile technical alternative.

Conflict of interest

No potential conflict of interest relevant to this article was reported.

Funding

None.

Acknowledgments

None.

Author contributions

Conceptualization: TWB, JHK (Ji Hoon Kim). Investigation: TWB, JHK (Ji Hoon Kim), DIG. Supervision: HS, JHK (Jin Hyoung Kim). Writing - original draft: TWB. Writing - review and editing and supervision: HS, JHK (Jin Hyoung Kim).

Data availability statement

Data sharing does not apply to this article as no datasets were generated or analyzed during the current study.

ORCID

Tae Wook Baek, https://orcid.org/0000-0001-8743-022X
Ji Hoon Kim, https://orcid.org/0000-0002-9280-414X
Dong Il Gwon, https://orcid.org/0000-0002-3121-2853
Ji Hoon Shin, https://orcid.org/0000-0001-6598-9049
Jin Hyoung Kim, https://orcid.org/0000-0002-7300-6396

References

1. Munoz FJ, Mismetti P, Poggio R, Valle R, Barron M, Guil M, et al. Clinical outcome of patients with upper-extremity deep vein thrombosis: results from the RIETE Registry. Chest. 2008;133:143-148. https://doi.org/10.1378/chest.07-1432
2. Joffe HV, Kucher N, Tapson VF, Goldhaber SZ; Deep Vein Thrombosis (DVT) FREE Steering Committee. Upper-extremity deep vein thrombosis: a prospective registry of 592 patients. Circulation. 2004;110:1605-1611. https://doi.org/10.1161/01.CIR.0000142289.94369.D7
3. Rice TW, Rodriguez RM, Light RW. The superior vena cava syndrome: clinical characteristics and evolving etiology. Medicine (Baltimore). 2006;85:37-42. https://doi.org/10.1097/01.md.0000198474.99876.f0

4. Engelberger RP, Kucher N. Management of deep vein thrombosis of the upper extremity. Circulation. 2012;126:768-773. https://doi.org/10.1161/CIRCULATIONAHA.111.051276
5. Cui J, Kawai T, Irani Z. Catheter-directed thrombolysis in acute superior vena cava syndrome caused by central venous catheters. Semin Dial. 2015;28:548-551. https://doi.org/10.1111/sdi.12362
6. Carroll H, Dineen F, Ryan P, Crowley M, Power S, O'Reilly S. Catheter-directed thrombolysis for acute SVC obstruction in a patient with metastatic breast cancer: catheter-directed thrombolysis for SVC obstruction. Arch Breast Cancer. 2022;9:407-410. https://doi.org/10.32768/abc.202293407-410
7. Sousou JM, Sherard DM, Edwards JR, Negron-Rubio E. Successful removal of a thrombus in the setting of SVC syndrome using the INARI FlowTriever device. Radiol Case Rep. 2022;17:744-747. https://doi.org/10.1016/j.radcr.2021.12.032
8. Lee SH, Kim HK, Hwang JK, Kim SD, Park SC, Kim JI, et al. Efficacy of retrievable inferior vena cava filter placement in the prevention of pulmonary embolism during catheter-directed thrombectomy for proximal lower-extremity deep vein thrombosis. Ann Vasc Surg. 2016;33:181-186. https://doi.org/10.1016/j.avsg.2015.10.034
9. Usoh F, Hingorani A, Ascher E, Shiferson A, Tran V, Marks N, et al. Long-term follow-up for superior vena cava filter placement. Ann Vasc Surg. 2009;23:350-354. https://doi.org/10.1016/j.avsg.2008.08.012
10. Yim NY, Chang NK, Lim JH, Kim JK. Retrograde Tempofilter II placement within the superior vena cava in a patient with acute upper extremity deep venous thrombosis: the filter stands on its head. Korean J Radiol. 2011;12:140-143. https://doi.org/10.3348/kjr.2011.12.1.140
11. Hussain SM, McLafferty RB, Schmittling ZC, Zakaria AM, Ramsey DE, Larson JL, et al. Superior vena cava perforation and cardiac tamponade after filter placement in the superior vena cava: a case report. Vasc Endovascular Surg. 2005;39:367-370. https://doi.org/10.1177/153857440503900412
12. Vaidya S, Tozer KR, Chen J. An overview of embolic agents. Semin Intervent Radiol. 2008;25:204-215. https://doi.org/10.1055/s-0028-1085930
13. Lopera JE. The Amplatzer vascular plug: review of evolution and current applications. Semin Intervent Radiol. 2015;32:356-369. https://doi.org/10.1055/s-0035-1564810

Case Report

eISSN 2508-2612
https://doi.org/10.64961/kjir.2026.00115
Korean J Interv Radiol 2026;31(2):62-68

KJIR
Korean Journal of
Interventional Radiology

Sheath-Assisted Percutaneous Forceps Biopsy of the Cyst Wall under Ultrasound Guidance for the Histological Diagnosis of Complex Hepatic Cystic Lesions

Soumil Singhal*, Vinamrita Patni, Sudhir Yadav, Anubhav Khandelwal, Sanjay Saran Baijal

Department of Interventional Radiology, Medanta: The Medicity, Gurugram, India

Complex hepatic cystic lesions with inconclusive imaging pose a recurring diagnostic problem: cyst-fluid cytology and conventional core-needle biopsy seldom capture the epithelial lining needed for a histological diagnosis, and current guidelines advise against simple cyst aspiration. We describe a sheath-assisted percutaneous forceps biopsy technique for direct cyst-wall sampling under ultrasound guidance, illustrated in two male patients (76 and 48 years). After Seldinger placement of an 8-Fr sheath into the cyst, rat-tooth forceps obtained direct biopsies of the wall epithelium, and the tract was embolized with Gelfoam. Technical success was achieved in both cases; histology showed columnar biliary epithelium consistent with mucinous cystic neoplasm, whereas fluid cytology was non-diagnostic. No complications occurred. This technique offers a feasible means of obtaining a histological diagnosis in complex hepatic cystic lesions when conventional methods are inconclusive.

Keywords: Mucinous cystic neoplasm; Percutaneous biopsy; Hepatic cystic lesion; Rat-tooth forceps; Ultrasound guidance; Cyst wall sampling

Introduction

Mucinous cystic neoplasm of the liver (MCN), historically termed biliary cystadenoma (BCA), is a rare cyst-forming epithelial tumor accounting for fewer than 5% of hepatic cystic lesions [1-3]. Under the current World Health Organization classification, the entity is defined by subepithelial ovarian-like stroma and distinguished from intraductal papillary neoplasm of the bile duct by the absence of biliary communication; lesions are graded from low-grade dysplasia to associated invasive carcinoma [3]. Although MCN occurs predominantly in women, well-documented occurrence in men is recognized [3]. The lesions are slow-growing, follow a stepwise tumorigenic progression, and carry a risk of malignant transformation, so complete surgical excision is the accepted standard and a tissue diagnosis materially influences management [2,4].

Preoperative distinction of MCN from simple, complicated, hydatid, and other cystic lesions is unreliable, as cross-sectional imaging features overlap substantially [3,5]. This uncertainty carries a clinical cost in both directions: a meaningful proportion of patients undergo major hepatectomy on presumptive grounds, while a cautious radiological differential of

Received: June 7, 2026; **Revised:** July 7, 2026; **Accepted:** July 7, 2026
***Corresponding email:** drsoumilsinghal75@gmail.com

© 2026 Korean Society of Interventional Radiology

This is an Open Access article distributed under the terms of the Creative Commons Attribution Non-Commercial License (http://creativecommons.org/licenses/by-nc/4.0) which permits unrestricted non-commercial use, distribution, and reproduction in any medium, provided the original work is properly cited.

"rule out biliary cystadenoma" for what is in fact a simple cyst drives unnecessary surgery. In one tertiary series, 19 of 20 lesions resected for presumed BCA proved to be simple cysts [6]. Tissue diagnosis would resolve this, yet conventional approaches fail: cyst-fluid cytology is limited by low cellularity and patchy epithelial desquamation, standard trucut biopsy is designed to core solid tissue, and contemporary multi-society guidance accordingly advises against cyto-aspiration or needle biopsy of complex cysts [2,7]. The diagnostic substrate—the columnar epithelial lining, and where present the ovarian-like stroma—is rarely captured by these methods.

Sampling tissue through an introducer sheath or working channel is a well-established principle, used routinely in endoscopy, cholangioscopy, and percutaneous transhepatic biliary procedures [8-11]. More recent endoscopic advances—such as endoscopic ultrasonography (EUS)–guided sampling of pancreatic cysts and cholangioscopy-guided forceps biopsy of biliary lesions—share the same underlying rationale: in cystic disease, the epithelial wall must be sampled directly to obtain a diagnosis [11,12]. Its application to percutaneous hepatic cyst-wall biopsy, however, has not been systematically described. We report a sheath-assisted percutaneous technique for direct cyst-wall sampling using rat-tooth forceps under ultrasound guidance, with technical and histopathological outcomes in two cases of complex hepatic cystic lesions confirmed as MCN in which conventional investigations were inconclusive. The contribution is not a new device but a reproducible adaptation of trans-sheath sampling to the percutaneous hepatic route, targeting the precise substrate that fluid cytology and core-needle biopsy miss.

Case Report

Case 1

A 76-year-old man presented with a six-month history of right upper quadrant pain, intermittent fever, and rigors. Examination revealed mild right hypochondrial tenderness. Investigations showed leukocytosis (14.47 × 10^3/μL), markedly elevated C-reactive protein (145.7 mg/L), and mildly raised gamma-glutamyl transferase (96 U/L); hydatid enzyme-linked immunosorbent assay serology was negative. Ultrasound demonstrated a multiloculated hypoechoic cyst (10 × 8 cm) in the right hepatic lobe with internal echogenic debris. Contrast-enhanced MRI confirmed a well-defined multiloculated cystic lesion (10.2 × 8.4 × 7.6 cm) involving segments VII, VIII, and IVa, with thin enhancing septations and a subcapsular component, and no solid component, diffusion restriction, or biliary communication (Fig. 1A–1D). The principal differentials were MCN, complicated simple cyst, and hydatid disease, the last considered unlikely given negative serology and

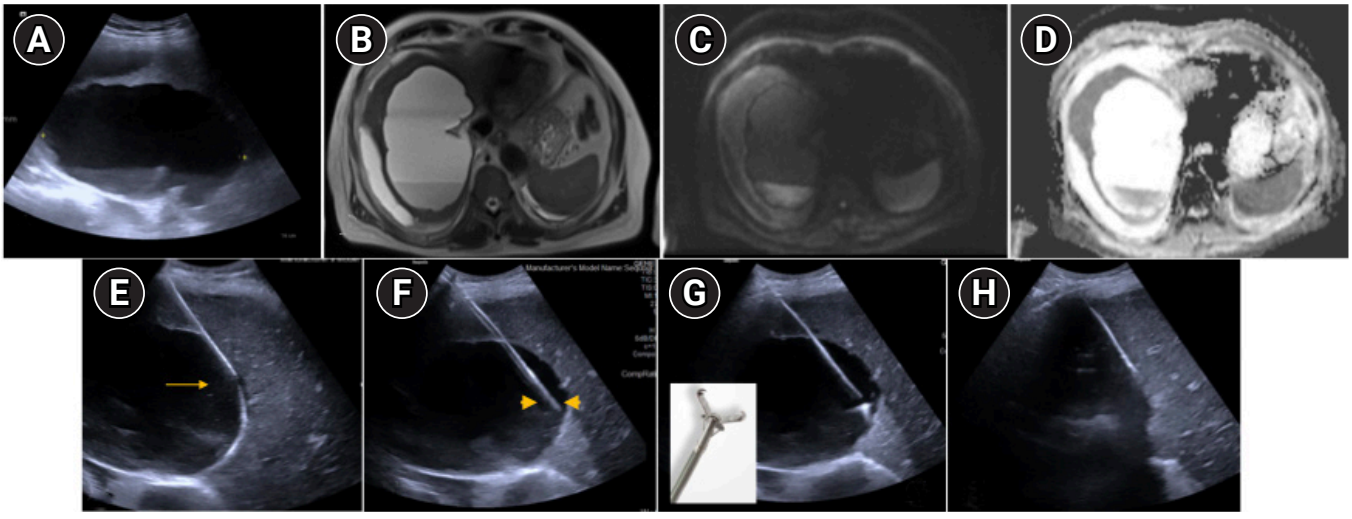


Fig. 1. Case 1 (76-year-old man). (A) Grayscale ultrasound: multiloculated hypoechoic cyst (10 × 8 cm) in the right hepatic lobe with internal echogenic debris. (B–D) Axial MRI (T2-weighted, diffusion-weighted, and apparent diffusion coefficient mapping): well-defined multiloculated cystic lesion (10.2 × 8.4 × 7.6 cm) in segments VII/VIII/IVa with subcapsular extension; diffusion restriction, no solid component or biliary communication. (E) Seldinger access: guidewire (arrow) within the cyst lumen prior to 8-Fr sheath insertion. (F) Rat-tooth forceps advanced through the sheath (arrowheads) and deployed against the cyst wall. (G) Ultrasonography: Forceps jaw opening against the wall and withdrawal with tissue sample. (H) Post-biopsy cyst-fluid aspiration and the tract was embolized with Gelfoam.

absent biliary communication. Following multidisciplinary team (MDT) review, percutaneous biopsy was agreed as the safest route to tissue diagnosis.

Case 2

A 48-year-old man presented with right upper quadrant pain and progressive abdominal fullness. Investigations showed borderline IgG anti-Echinococcus antibody (12.83 IU/mL), mildly raised total bilirubin (2.2 mg/dL), and normal serum CA 19-9 (31.8 U/mL). Ultrasound showed a large multiloculated hypoechoic lesion in segment IVa with heterogeneous contents and dependent debris. MRI demonstrated a T2-hyperintense multiloculated cystic lesion (6.3 × 7.9 × 6.6 cm) in segments VIII/IVa with a T2-hypointense rim, delayed peripheral enhancement, and partial T1 hyperintensity indicating proteinaceous contents, without solid component, diffusion restriction, or biliary communication (Fig. 2A–2C). Given the borderline serology, an initial diagnosis of hydatid disease was made and oral albendazole (400 mg twice daily) commenced; after 12 weeks without clinical or radiological response, MDT review recommended percutaneous biopsy before surgical planning.

Technique

Both procedures were performed under local anesthesia with pre-procedural intravenous antibiotic prophylaxis, using continuous real-time ultrasound guidance and full aseptic precautions; local anesthetic was infiltrated to the level of the hepatic capsule. An access route traversing a cuff of intervening hepatic parenchyma was selected in both patients. An 18-gauge needle was used to puncture the anterior cyst wall under direct visualization; a 0.035-inch guidewire was advanced into the cavity and the tract serially dilated to accept an 8-Fr introducer sheath positioned with its tip just within the lumen (Figs. 1E, 2). Rat-tooth biopsy forceps (Olympus FB-230U, Olympus Medical Systems, Tokyo, Japan) were advanced through the sheath and deployed against the inner wall under real-time ultrasound guidance (Fig. 1F), obtaining multiple full-thickness punch biopsies of the epithelial lining (Figs. 1G, 2E)—three samples in case 1 and four in case 2. Cyst fluid was then aspirated for cytology (Figs. 1H, 2F), and the access tract was embolized with Gelfoam slurry to mitigate hemorrhage.

Procedural and Pathological Outcomes

Technical success was achieved in both cases. Histopathology of the forceps specimens showed the cyst wall lined by a single layer of tall columnar biliary epithelium in both patients (Fig. 3). In contrast, cyst-fluid cytology demonstrated only inflammatory cells with no diagnostic epithelial ele-

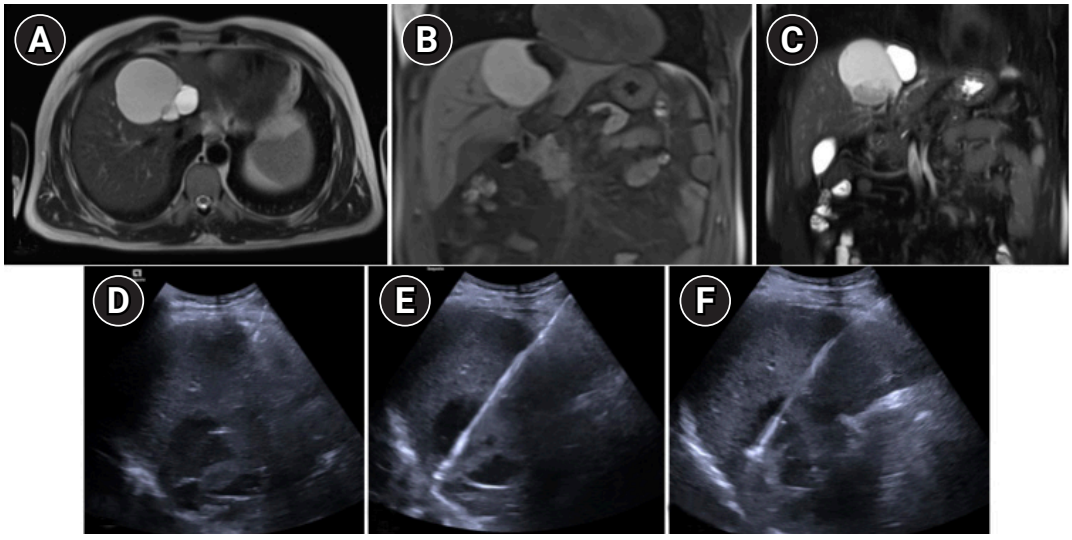


Fig. 2. Case 2 (48-year-old man). (A–C) Axial and coronal MRI: T2-hyperintense multiloculated cystic lesion (6.3 × 7.9 × 6.6 cm) in segments VIII/IVa with a T2-hypointense rim, delayed peripheral enhancement, and partial T1 hyperintensity consistent with proteinaceous contents; no solid component or biliary communication. (D) Grayscale ultrasound: multiloculated cyst with heterogeneous dependent debris. (E) Ultrasonography: Rat-tooth forceps deployed through the sheath for cyst-wall sampling. (F) Post-biopsy cyst-fluid aspiration (cytology: inflammatory cells only); the tract was embolized with Gelfoam.

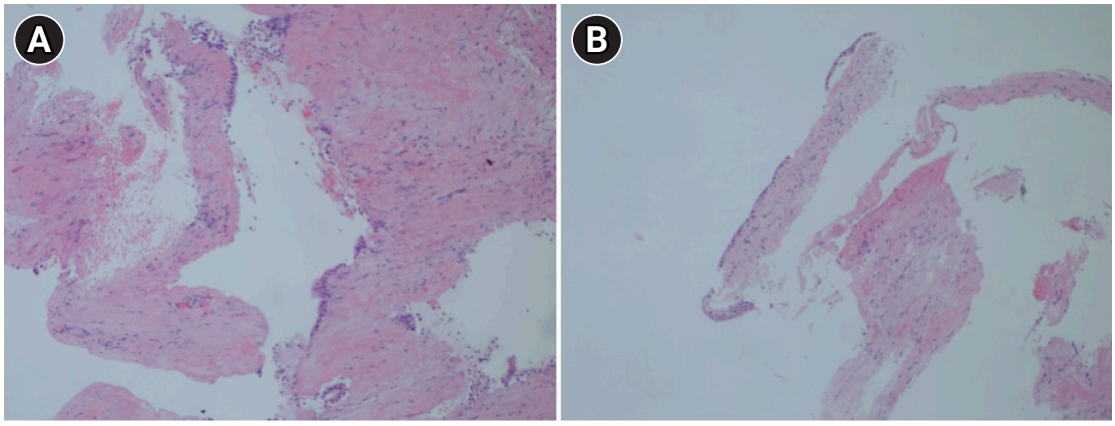


Fig. 3. Histopathology (H&E, ×100). Cyst-wall specimens from case 1 (A) and case 2 (B), each showing a single layer of tall columnar biliary epithelium lining the cyst wall, consistent with mucinous cystic neoplasm/biliary cystadenoma. Cyst-fluid cytology was non-diagnostic in both cases, confirming that direct wall sampling was essential for histological diagnosis.

ments. The diagnosis was subsequently confirmed on the resection specimens, which demonstrated ovarian-like stroma diagnostic of mucinous cystic neoplasm of the liver. Both patients were monitored until surgery and developed no persistent abdominal pain, clinically significant bleeding, bile leak, sepsis, or other procedure-related complication. Each underwent elective hepatic resection within one week, with no intraoperative evidence of tract-related sequelae.

Ethics Statement

This report was conducted in accordance with the Declaration of Helsinki. The Institutional Review Board granted a waiver of formal approval for this retrospective report of two de-identified cases. Written informed consent for the procedure and for publication of clinical details and accompanying images was obtained from both patients.

Discussion

The histological diagnosis of MCN is a recognized challenge. On imaging, it presents as a multiloculated cystic lesion with enhancing septations, features shared by hydatid cysts, complicated, hemorrhagic simple cysts, cystic metastases, and hepatic abscess, so confident imaging-based diagnosis is unreliable [3,5]. Cyst-fluid cytology yields a diagnosis only when intact columnar epithelium is sampled—uncommon, given desquamation and patchy neoplastic distribution and serum and intracystic tumor markers lack specificity [2,7]. The described technique addresses this gap directly: whereas tru-cut biopsy traverses a cystic wall tangentially or exits into fluid, rat-tooth forceps advanced through an indwelling coaxial sheath can be deployed under real-time ultrasound control against the inner wall and withdrawn with a full-thickness epithelial bite, capturing the diagnostic epithelial lining—mechanistically analogous to forceps biopsy through a bronchoscope or cholangioscope working channel, transposed to a percutaneous hepatic route. In both cases, direct wall sampling yielded diagnostic columnar epithelium whereas cyst-fluid cytology showed only inflammatory cells, illustrating the potential diagnostic advantage of sampling the epithelial lining directly; this observation, based on two cases, requires confirmation in larger series.

Trans-sheath forceps biopsy is itself established in several clinical settings—and recent endoscopic experience with EUS through-the-needle microforceps for pancreatic cysts and cholangioscopy-guided forceps biopsy underscores the shared move toward direct epithelial sampling in cystic disease [11,12]. The novel element here is the percutaneous hepatic adaptation: Seldinger sheath placement into the cyst, intraluminal forceps deployment using ultrasound guidance for full-thickness epithelial bites, and Gelfoam tract embolization.

Regarding the site of sampling, no high-level evidence directly compares biopsy of the free surface of the cyst with a wall buttressed by parenchyma. By analogy with percutaneous liver-mass biopsy, a trajectory through a cuff of intervening normal parenchyma is conventionally preferred, the parenchyma providing a tamponade effect and limiting

intraperitoneal leakage of cyst contents—of particular relevance to a potentially neoplastic mucinous lesion, in which peritoneal spillage is undesirable [13]. Since cystic lesions have a thin wall, diagnostic yield would be higher when the sample is acquired from the free wall than from an area surrounded by liver parenchyma. In both cases, the route was planned through intervening parenchyma where feasible, with Gelfoam tract embolization, an established hemostatic adjunct [14,15]. A sheathed working channel may also reduce seeding relative to repeated needle passes, although this risk cannot be eliminated completely for a potentially malignant cystic neoplasm.

Nomenclature warrants comment. Current World Health Organization terminology designates this entity a mucinous cystic neoplasm, defined by ovarian-like stroma, reserving intraductal papillary neoplasm of the bile duct for lesions with biliary communication; the older term biliary cystadenoma persists in clinical and surgical usage, and the two are frequently used interchangeably [1-3]. Definitive subclassification rests on the resection specimen, as ovarian-like stroma and focal dysplasia may not be represented in a wall biopsy. Both patients here were male—an uncommon but documented presentation [3]—underscoring that, where ovarian-like stroma is not demonstrated, classification as MCN should be made with caution and the differential of intraductal papillary neoplasm considered.

Complete surgical excision remains the cornerstone of management for mucinous cystic neoplasm, serving both as definitive treatment and as the only reliable means of excluding associated invasive carcinoma, since a non-targeted percutaneous biopsy may not sample the most atypical focus [3]. Non-resective approaches such as aspiration, sclerotherapy, and fenestration carry high recurrence and are inappropriate for a neoplastic lesion [3].

Establishing the necessity of tissue confirmation is central to the rationale for this technique. Because MCN cannot be reliably distinguished from simple, complicated, hydatid, or other cystic lesions on imaging, and because its malignant potential mandates resection whereas benign mimics do not, a preoperative histological diagnosis directly determines the management pathway. Confirmation of MCN averts two opposing errors: unnecessary major hepatectomy for a lesion that proves to be a simple cyst—reported in up to 19 of 20 resections for presumed BCA [6]—and inappropriate non-resective treatment (aspiration or sclerotherapy) of a neoplastic lesion, which risks recurrence and peritoneal dissemination of mucinous contents. It also redirects management away from unnecessary medical therapy, as in case 2, where 12 weeks of empirical albendazole for presumed hydatid disease preceded a tissue-proven diagnosis of MCN. Accordingly, this technique is not a first-line investigation for all hepatic cysts but should be reserved—by MDT consensus involving interventional radiology, hepatobiliary surgery, and hepatology—for lesions that remain indeterminate after full imaging and cytological workup, where non-operative management has failed, or where histology will alter the management pathway.

This report is limited to two cases, insufficient to establish safety, efficacy, or generalizability, and includes no formal comparison with alternative techniques. The approach adds modest procedural complexity relative to simple aspiration. Larger prospective or multicenter series are needed to define diagnostic yield, the number of passes required for adequacy, complication and tract-seeding rates at follow-up, and the technique's place relative to EUS-guided wall biopsy within the diagnostic algorithm.

Sheath-assisted percutaneous forceps biopsy of the cyst wall under ultrasound guidance is a technically feasible means of obtaining a histological diagnosis in complex hepatic cystic lesions when imaging and cytology are inconclusive. In two cases of MCN, direct epithelial sampling yielded diagnostic epithelium where fluid cytology did not, contributing to a histological diagnosis that informed surgical management. Prospective evaluation in larger cohorts is warranted to define its safety profile, optimal procedural parameters, and role within the diagnostic algorithm for complex hepatic cystic lesions.

Conflict of interest

No potential conflict of interest relevant to this article was reported.

Funding

None.

Acknowledgments

None.

Author contributions

Conceptualization: SSB. Data curation: VP. Formal analysis: VP, SY. Methodology: VP, SY, SSB. Writing - original draft: SS. Writing - review & editing: SS, AK, SSB.

Data availability statement

Data sharing does not apply to this article as no datasets were generated or analyzed during the current study.

ORCID

Soumil Singhal, https://orcid.org/0000-0003-1688-3664
Vinamrita Patni, https://orcid.org/0009-0008-0259-0047
Sudhir Yadav, https://orcid.org/0009-0004-1605-6794
Anubhav Khandelwal, https://orcid.org/0000-0003-2275-1457
Sanjay Saran Baijal, https://orcid.org/0000-0002-2797-4054

References

1. Hutchens JA, Lopez KJ, Ceppa EP. Mucinous cystic neoplasms of the liver: epidemiology, diagnosis, and management. Hepat Med. 2023;15:33-41. https://doi.org/10.2147/HMER.S284842
2. Soares KC, Arnaoutakis DJ, Kamel I, Anders R, Adams RB, Bauer TW, et al. Cystic neoplasms of the liver: biliary cystadenoma and cystadenocarcinoma. J Am Coll Surg. 2014;218:119-128. https://doi.org/10.1016/j.jamcollsurg.2013.08.014
3. Lee MH, Katabathina VS, Lubner MG, Shah HU, Prasad SR, Matkowskyj KA, et al. Mucin-producing cystic hepatobiliary neoplasms: updated nomenclature and clinical, pathologic, and imaging features. Radiographics. 2021;41:1592-1610. https://doi.org/10.1148/rg.2021210011
4. Aziz H, Hamad A, Afyouni S, Kamel IR, Pawlik TM. Management of mucinous cystic neoplasms of the liver. J Gastrointest Surg. 2023;27:1963-1970. https://doi.org/10.1007/s11605-023-05709-6
5. Kim JY, Kim SH, Eun HW, Lee MW, Lee JY, Han JK, et al. Differentiation between biliary cystic neoplasms and simple cysts of the liver: accuracy of CT. AJR Am J Roentgenol. 2010;195:1142-1148. https://doi.org/10.2214/AJR.09.4026
6. Kumar A, Zendel A, Batres M, Gerber DA, Desai CS. Radiologic reporting of simple hepatic cyst versus biliary cystadenoma may lead to unnecessary surgery. Am Surg. 2023;89:1392-1395. https://doi.org/10.1177/00031348211054077
7. Pompili M, Ardito F, Brunetti E, Cabibbo G, Calliada F, Cillo U, et al. Benign liver lesions 2022: guideline for clinical practice of Associazione Italiana Studio del Fegato (AISF), Societa Italiana di Radiologia Medica e Interventistica (SIRM), Societa Italiana di Chirurgia (SIC), Societa Italiana di Ultrasonologia in Medicina e Biologia (SIUMB), Associazione Italiana di Chirurgia Epatobilio-Pancreatica (AICEP), Societa Italiana Trapianti d'Organo (SITO), Societa Italiana di Anatomia Patologica e Citologia Diagnostica (SIAPEC-IAP) - Part I - Cystic lesions. Dig Liver Dis. 2022;54:1469-1478. https://doi.org/10.1016/j.dld.2022.08.030
8. Liu Y, Zhou X, Kong L, Han X, Jiao D. Percutaneous transhepatic intraluminal forceps biopsy for patients with biliary stricture after endoscopic retrograde approach failure: a retrospective study. Quant Imaging Med Surg. 2023;13:2605-2619. https://doi.org/10.21037/qims-22-915
9. Pawlak KM, Juzwiak J, Brzosko M, Piatkowski J, Jackowski M, Jagielski M. Fluoroscopy-guided, sheath-assisted biopsy for indeterminate intraductal biliary masses. Endoscopy. 2026;58:E156-E157. https://doi.org/10.1055/a-2777-6802
10. Sakamoto H, Ishiwatari H, Yamamura M, Doi T, Sato J, Kakuda Y, et al. Utility of a novel sheath designed for mapping biopsy for preoperative malignant hilar biliary obstruction. Endosc Int Open. 2026;14:a27871325. https://doi.org/10.1055/a-2787-1325
11. Perez-Cuadrado-Robles E, Phillpotts S, Bronswijk M, Conrad CC, Binda C, Monino L, et al. PERcutaneous transhepatic CHOLangioscopy using a new single-operator short cholangioscope (PERCHOL): European feasibility study. Dig Endosc. 2024;36:719-725. https://doi.org/10.1111/den.14697
12. Guilabert L, Nikolic S, de-Madaria E, Vanella G, Capurso G, Tacelli M, et al. Endoscopic ultrasound for pancreatic cystic lesions: a narrative review. BMJ Open Gastroenterol. 2025;12:e001893. https://doi.org/10.1136/bmjgast-2025-001893
13. Thanos L, Zormpala A, Papaioannou G, Malagari K, Brountzos E, Kelekis D. Safety and efficacy of percutaneous CT-guided liver biopsy using an 18-gauge automated needle. Eur J Intern Med. 2005;16:571-574. https://doi.org/10.1016/j.ejim.2005.06.010
14. Singhal S, M DP, Inuganti S, Botcha S, Deepashree DT,

Uthappa MC. Percutaneous ultrasound-guided plugged liver biopsy: a single-centre experience. Pol J Radiol. 2021;86:e239-e245. https://doi.org/10.5114/pjr.2021.105852

15. Nota T, Kageyama K, Yamamoto A, Jogo A, Sohgawa E, Yonezawa H, et al. Feasibility of gel-like radiopaque embolic material using gelatin sponge and contrast agent for tract embolization after percutaneous treatment. PLoS One. 2023;18:e0281384. https://doi.org/10.1371/journal.pone.0281384

Case Report

eISSN 2508-2612
https://doi.org/10.64961/kjir.2026.00150
Korean J Interv Radiol 2026;31(2):69-73

KJIR
Korean Journal of
Interventional Radiology

A Side-Hole Catheter Technique for Overcoming Hostile Vascular Anatomy during Chemoembolization: A Case Report

Min Gwan Kim[1], **Hyo-Cheol Kim**[1,2,3,*]

[1]Department of Radiology, Seoul National University Hospital, Seoul, Republic of Korea
[2]Department of Radiology, Seoul National University College of Medicine, Seoul, Republic of Korea
[3]Institute of Radiation Medicine, Seoul National University Medical Research Center, Seoul National University Hospital, Seoul, Republic of Korea

In a 58-year-old man with HCC undergoing TACE, a segment III tumor was supplied by an accessory left hepatic artery arising from the left gastric artery (LGA). The dominant technical challenge shifted from acute angulation at the LGA origin to inadequate back support in distal branches. To overcome repeated dislodgement, the catheter was exchanged for a 5-Fr catheter with a hand-cut side hole, positioned at the LGA orifice while the tip was anchored in the celiac trunk. This technique allowed a microcatheter to traverse in a single well-supported pass, enabling successful superselective TACE without immediate complications. This case emphasizes the importance of distinguishing ostial angulation from back-support failure and highlights the utility of proximal side-hole anchoring in complex multivessel selection.

Keywords: Chemoembolization, therapeutic; Carcinoma, hepatocellular; Hepatic artery; Anatomic variation; Catheterization

Introduction

Knowledge of variant hepatic arterial anatomy is essential for safe and effective TACE of HCC. An accessory or replaced left hepatic artery (LHA) arising from the left gastric artery (LGA) is among the most common hepatic arterial variants, reported in up to 16% of patients undergoing hepatic angiography [1].

Selective catheterization of acutely angulated branches remains a technical challenge during TACE. When the primary obstacle is the acute takeoff angle itself, a shepherd's hook-shaped microguidewire is often effective for engaging the ostium by allowing rotation and withdrawal maneuvers [2,3]. In contrast, when the main limitation is inadequate back support—particularly in small-caliber or tortuous distal vessels—the microcatheter-guidewire system tends to dislodge repeatedly despite successful initial engagement. In such situations, a catheter with a surgically created side hole can provide stable support by anchoring the main catheter shaft in a proximal, larger-caliber vessel while permitting the microcatheter to exit laterally through the side hole toward the target branch [4-7].

We report a case in which both problems occurred sequentially during a single TACE procedure: acute angulation at the LGA origin and subsequent back-support failure in the accessory LHA and its tumor feeder.

Received: June 24, 2026; **Revised:** July 19, 2026; **Accepted:** July 19, 2026
***Corresponding email:** radioembolization@snu.ac.kr

© 2026 Korean Society of Interventional Radiology

This is an Open Access article distributed under the terms of the Creative Commons Attribution Non-Commercial License (http://creativecommons.org/licenses/by-nc/4.0) which permits unrestricted non-commercial use, distribution, and reproduction in any medium, provided the original work is properly cited.

Case Report

Institutional Review Board approval was waived for this case report in accordance with the policy of Seoul National University Hospital. A 58-year-old man with hepatitis B virus–related liver cirrhosis on entecavir and HCC (Child-Pugh class A5) presented for further locoregional treatment. He had previously undergone transarterial radioembolization, radiation therapy to segment II, and four prior sessions of conventional TACE. Contrast-enhanced CT demonstrated a hypervascular nodule in segment III, and three-dimensional CT angiography suggested an accessory LHA from the mid-portion of LGA (Fig. 1).

Celiac arteriography was performed with a 5-Fr Rösch hepatic (RH) catheter (Grafia, Sungjin-Hitech, Suwon, Korea), which showed the LGA arising from the celiac trunk at an acute angle. A shepherd's hook technique using a microcatheter (Progreat Lambda, 1.7-Fr, Terumo, Tokyo, Japan) and microguidewire (Transend, Boston Scientific, Marlborough, MA, USA) was used to select the LGA successfully. An accessory LHA arose from an intermediate portion of the LGA's course; selecting this vessel caused the microcatheter-guidewire system to dislodge from the ostium on two occasions before successful selection of the accessory LHA was achieved on a third attempt (Video 1).

From the accessory LHA, a segment III tumor-feeding branch arose, as confirmed by cone-beam CT obtained via the catheter positioned in the accessory LHA (Fig. 1D). While advancing toward this feeder, the catheter could not provide adequate back support, and the microcatheter system repeatedly dislodged before reaching the feeder (Video 1). The catheter was therefore exchanged for a 5-Fr Simmons type 1 catheter (J.S Angio Catheter, Simmons 1, A&A M.D., Seongnam, Korea), and a side hole approximately 3 mm in length was

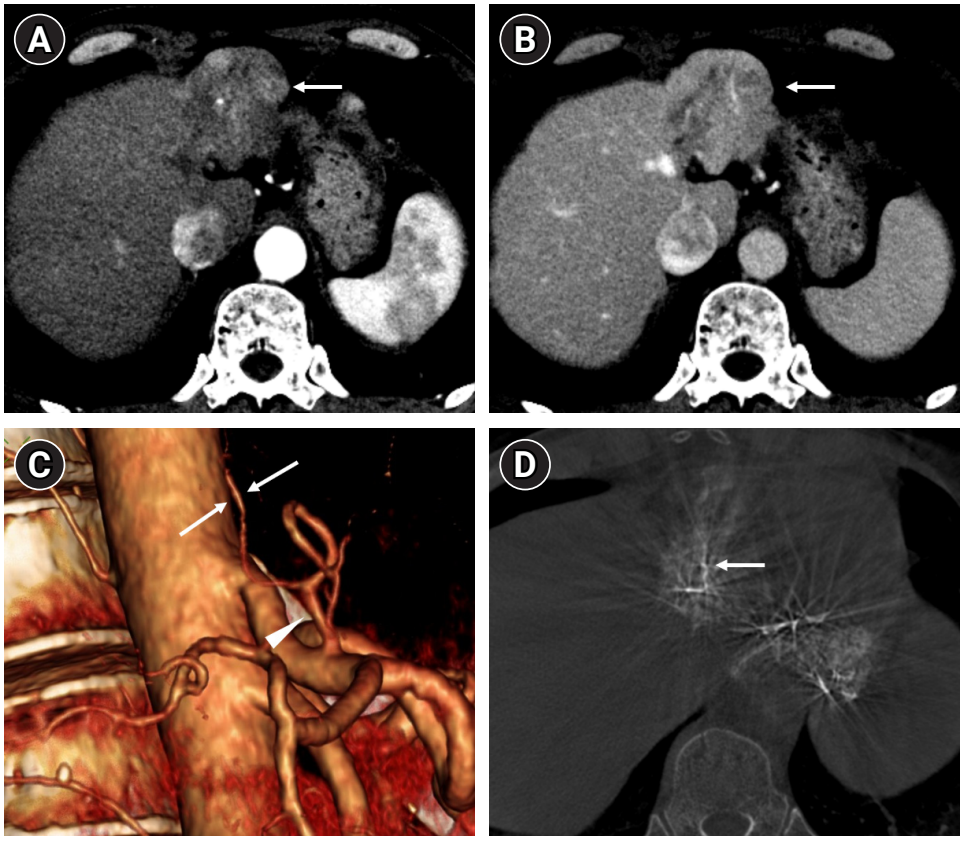


Fig. 1. A 58-year-old man was referred for TACE of HCC in liver segment III. Preprocedural contrast-enhanced CT shows a typical HCC (arrow) with early arterial enhancement (A) and washout on the portal venous phase (B). (C) Volume-rendered CT angiography shows the left gastric artery (LGA) (arrowhead) arising from the celiac trunk at an acute angle, with the accessory left hepatic artery (LHA) (arrows) originating from the mid-portion of the LGA. (D) Cone-beam CT obtained via the catheter positioned in the accessory LHA after shepherd's hook selection shows the feeding vessel (arrow) of the segment III tumor, corresponding to the lipiodol deposition in the same tumor shown in Fig. 3.

carefully and gradually incised into the catheter wall using a No. 11 scalpel blade (Fig. 2A). In this case, the side hole was created approximately 7 mm proximal to the catheter tip; the exact location relative to the tip was individualized according to the distance and angular relationship between the celiac trunk and the LGA origin. After creation, the catheter was flushed once with heparinized saline to confirm patency. The microcatheter was subsequently advanced through the side hole to verify that the opening was adequately sized for smooth passage. No sharp edges were produced at the cut margin. The Simmons catheter was seated at the proximal portion of the celiac trunk, and the side hole was aligned with the orifice of the LGA (Fig. 2B). The microcatheter was then advanced through the side hole over a 0.016-inch microguidewire (ASAHI Meister, Asahi Intecc, Seto, Japan). No resistance or shearing was encountered during microcatheter manipulation, and the system traversed the LGA and accessory LHA in a single, well-supported pass, achieving successful superselective catheterization of the segment III feeder (Video 2). Angiography via the microcatheter confirmed a tumor blush corresponding to the segment III nodule.

TACE was performed by infusing an emulsion of 5 mL of iodized oil (Lipiodol Ultra-Fluid, Guerbet, Paris, France) and 5 mg of idarubicin (Zavedos, Pfizer, New York, NY, USA) into the segment III feeder, followed by embolization with gelatin sponge particles (100–150 μm [PrimeGel, PLmicromed, Yansan, Korea] and 350–560 μm [EGgel, Engain, Hwaseong, Korea]) until flow stasis was achieved. The procedure was completed without complications. Follow-up CT demonstrated compact, dense lipiodol uptake confined to the treated tumor, consistent with a favorable treatment response (Fig. 3).

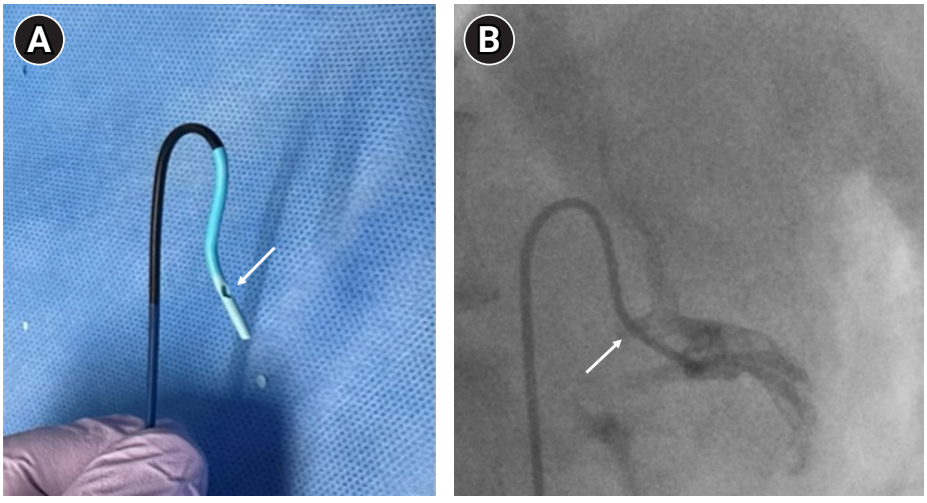


Fig. 2. (A) A side hole (arrow) was created near the tip portion of a 5-Fr Simmons catheter using a No. 11 scalpel blade. (B) The side hole was aligned precisely with the orifice (arrow) of the left gastric artery.

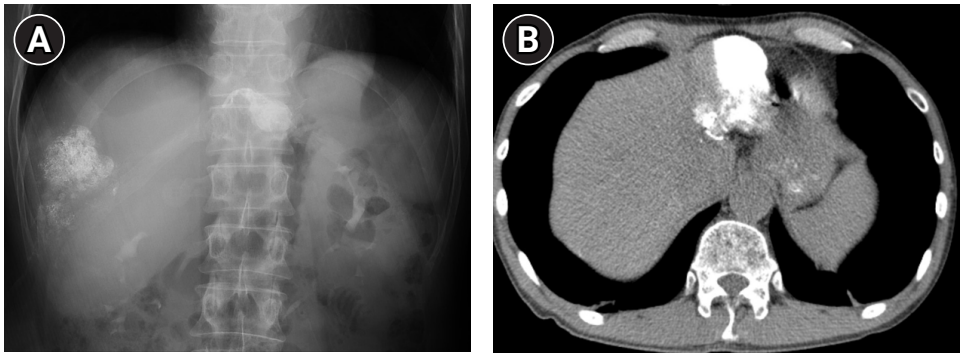


Fig. 3. (A) Spot fluoroscopic image obtained at the end of the procedure shows dense, compact lipiodol uptake confined to the segment III tumor. (B) Follow-up CT shows compact, dense lipiodol deposition confined to the treated tumor, consistent with a favorable treatment response.

Discussion

This case illustrates that the dominant technical challenge during selective catheterization can shift within a single TACE procedure, necessitating real-time recognition and adaptation of strategies. Initially, the acute angulation of the LGA origin from the celiac trunk was effectively overcome using the shepherd's hook microguidewire technique [2,3]. However, once the accessory LHA was engaged, repeated dislodgement occurred during advancement toward the segment III feeder despite no sharp angulation at that level. This pattern clearly indicates inadequate back support rather than ostial angulation as the limiting factor. Such failure typically reflects an inability of the catheter shaft to transmit forward pushing force to the microcatheter: rather than advancing distally, the shaft buckles or loops within the larger, more compliant vessel just proximal to the target ostium. Differentiating these two mechanisms is clinically important because the optimal solution differs: shepherd's hook reshaping primarily addresses engagement failure, whereas back-support failure requires enhanced stability during distal advancement [4-7].

The side-hole catheter technique was first introduced by Miyayama et al. [4] for selective catheterization of the inferior phrenic artery and has since been applied to various difficult branches, including the internal mammary artery [5], anomalous bronchial and subclavian arteries [6], and hepatic arterial variants [7-9]. In most reported cases, the side hole was created near the catheter tip and positioned directly at or immediately adjacent to the target vessel ostium, with the catheter tip acting as a distal anchor [4,5,8-10]. In the present case, we applied a proximally anchored configuration, in which the side hole was aligned with the LGA orifice while the main catheter tip remained stable in the large-caliber celiac trunk. This allowed the microcatheter to traverse the LGA, accessory LHA, and segment III feeder in one continuous, well-supported pass without repeated re-engagement of the parent vessels. A Simmons type 1 catheter was chosen for the side-hole technique because its reformed, reverse-curve tip forms a self-retaining, hook-shaped anchor once seated in the celiac trunk, providing reliable back support for the side-hole maneuver by bracing the catheter shaft at this fixed distal anchor point. A similar proximal anchoring approach was described by Meng et al. [7] using transradial access for a replaced LHA. Our case further demonstrates the utility of this proximal configuration in complex multivessel selection during conventional transfemoral TACE, especially when cumulative loss of back support develops across multiple distal branches.

The success of this technique also relies on precise orientation of the side hole toward the target ostium under fluoroscopic guidance. Creation of a side hole using a scalpel blade is technically simple and requires no specialized equipment [9,10]. Nevertheless, operators should be cautious of potential drawbacks, including weakening of the catheter shaft, risk of microcatheter or guidewire shearing at the sharp edges, and possible interaction with embolic materials. In this case, the microcatheter advanced smoothly without any resistance or shearing, and no procedure-related complications occurred.

In conclusion, systematic evaluation of the failure pattern after each catheterization step—whether the system fails to engage the ostium or dislodges during advancement—can guide timely selection between shepherd's hook and side-hole techniques. When cumulative loss of back support across multiple distal branches is the main issue, a proximally anchored side-hole catheter offers a practical solution. This adaptive approach may improve procedural efficiency and safety in patients with challenging hepatic arterial anatomy during TACE.

Conflict of interest

No potential conflict of interest relevant to this article was reported.

Funding

None.

Acknowledgments

None.

Author contributions

Conceptualization: HCK. Data curation: MGK. Project administration: HCK. Resources: HCK. Supervision: HCK. Visualization: MGK, HCK. Writing - original draft: MGK. Writing - review & editing: HCK.

Data availability statement

The datasets generated or analyzed during the study are

available from the corresponding author on reasonable request.

Supplementary material

The supplement data are available with this article at https://doi.org/10.64961/kjir.2026.00150.

ORCID

Min Gwan Kim, https://orcid.org/0000-0002-9947-2125
Hyo-Cheol Kim, https://orcid.org/0000-0002-6016-247X

References

1. Choi TW, Chung JW, Kim HC, Lee M, Choi JW, Jae HJ, et al. Anatomic variations of the hepatic artery in 5625 patients. Radiol Cardiothorac Imaging. 2021;3:e210007. https://doi.org/10.1148/ryct.2021210007
2. Baek JH, Chung JW, Jae HJ, Lee W, Park JH. A new technique for superselective catheterization of arteries: preshaping of a micro-guide wire into a shepherd's hook form. Korean J Radiol. 2007;8:225-230. https://doi.org/10.3348/kjr.2007.8.3.225
3. Kim HC, Chung JW. Shepherd's hook technique for superselective catheterization of hepatic arteries. J Vasc Interv Radiol. 2014;25:1993-1996. https://doi.org/10.1016/j.jvir.2014.07.029
4. Miyayama S, Matsui O, Akakura Y, Yamamoto T, Fujinaga Y, Koda W, et al. Use of a catheter with a large side hole for selective catheterization of the inferior phrenic artery. J Vasc Interv Radiol. 2001;12:497-499. https://doi.org/10.1016/s1051-0443(07)61890-9
5. Oh JS, Choi BG, Chun HJ, Lee HG. A side-hole catheter for catheterization of a difficult internal mammary artery. Acta Radiol. 2017;58:307-310. https://doi.org/10.1177/0284185116642633
6. Won JH, Park SI, Park KJ, Oh YJ, Hwang SC. Microcatheter placement through a side hole created in a 5-F catheter into proximal subclavian arterial branches causing hemoptysis. J Vasc Interv Radiol. 2004;15:881-884. https://doi.org/10.1097/01.RVI.0000136996.50373.E4
7. Meng XX, Liao HQ, Liu HC, Jiang HL, Gu YF, Li X, et al. Application of side-hole catheter technique for transradial arterial chemoembolization in patients with hepatocellular carcinoma. Abdom Radiol (NY). 2019;44:3195-3199. https://doi.org/10.1007/s00261-019-02072-6
8. Kim HC, Miyayama S, Choi JW, Kim GM, Chung JW. Hepatocellular carcinoma supplied by the inferior phrenic artery or cystic artery: anatomic and technical considerations. Radiographics. 2023;43:e220076. https://doi.org/10.1148/rg.220076
9. Miyayama S, Yamashiro M, Nagai K, Yokka A. Use of a catheter with a large side hole or cleft in selective catheterization of small branch arteries. Interv Radiol (Higashimatsuyama). 2016;1:67-74. https://doi.org/10.22575/interventionalradiology.1.2_67
10. Miyayama S, Yamashiro M, Okuda M, Aburano H, Shigenari N, Morinaga K, et al. Creation of a cleft in an angiography catheter to facilitate catheterization of branches of the aorta arising at an acute angle. J Vasc Interv Radiol. 2008;19:1769-1771. https://doi.org/10.1016/j.jvir.2008.08.024

Case Report

eISSN 2508-2612
https://doi.org/10.64961/kjir.2026.00143
Korean J Interv Radiol 2026;31(2):74-78

KJIR
Korean Journal of
Interventional Radiology

Recurrent Caudate Lobe HCC Supplied by a Variant Right Inferior Adrenal Artery: A Case Report

Donghyun Kim, Hyo-Cheol Kim*

Department of Radiology, Seoul National University Hospital, Seoul National University College of Medicine, Seoul, Republic of Korea

Variant right inferior adrenal arterial supply to caudate lobe HCC is rare and may be overlooked. We report a 53-year-old man with recurrent caudate lobe HCC after 12 TACE sessions. During the 13th TACE, cone-beam CT of the common hepatic artery did not reveal tumor vascularity. At the 14th TACE, performed 3 days later, the right inferior phrenic artery, the most common extrahepatic collateral feeder to caudate lobe HCC, showed no tumor supply. Angiography and cone-beam CT from a small aortic common trunk giving rise to a variant right inferior adrenal artery and the right renal capsular artery revealed predominant supply from the variant right inferior adrenal artery. Embolization through these branches achieved compact iodized oil uptake without immediate complications.

Keywords: Carcinoma, hepatocellular; Chemoembolization, therapeutic; Angiography; Collateral circulation

Introduction

HCC in the caudate lobe is technically challenging to treat because of its deep location and variable arterial anatomy, which can limit surgical or percutaneous approaches and make intra-arterial therapy an important treatment option [1]. Caudate arterial branches are usually small, may be multiple, and often communicate with one another; therefore, the tumor-feeding artery can differ according to the subsegmental location of the caudate tumor [2]. Recurrent caudate lobe HCC, particularly after repeated TACE, may also recruit extrahepatic collateral arteries [2,3]. The right inferior phrenic artery (RIPA) is the most frequent extrahepatic collateral artery supplying caudate lobe HCC [3]. In contrast, inferior adrenal arterial supply to caudate lobe HCC has only rarely been described [3,4]. We report a case of recurrent caudate lobe HCC after multiple prior TACE sessions in which the dominant tumor feeder was an adrenal branch interpreted as a variant right inferior adrenal artery.

Case Report

Institutional Review Board approval was waived for this case report in accordance with the policy of Seoul National University Hospital. A 53-year-old man with HCC was referred for treatment of recurrent HCCs, including a recurrent caudate lobe lesion and a separate recurrent lesion in segment IV. He had hepatitis B virus-related liver cirrhosis. Between December 2016 and September 2025, he had undergone 12 sessions of TACE for multifocal recurrent HCC, as well as radiofrequency ablation and stereotactic ablative radiotherapy. The prior TACE sessions included chemoembolization via several segmental hepatic arteries and the RIPA.

The caudate lobe HCC relevant to this report was first treated in November 2024. At that time, the tumor was located in

Received: June 22, 2026; **Revised:** July 16, 2026; **Accepted:** July 19, 2026
***Corresponding email:** radioembolization@snu.ac.kr

© 2026 Korean Society of Interventional Radiology

This is an Open Access article distributed under the terms of the Creative Commons Attribution Non-Commercial License (http://creativecommons.org/licenses/by-nc/4.0) which permits unrestricted non-commercial use, distribution, and reproduction in any medium, provided the original work is properly cited.

the inferior portion of the Spiegel lobe. Angiography demonstrated tumor supply from a caudate artery, and selective TACE resulted in dense accumulation of iodized oil. In September 2025, marginal recurrence developed in the adjacent caudate process. This recurrence was again supplied by a caudate artery and was treated with selective TACE, resulting in dense accumulation of iodized oil.

In April 2026, follow-up liver MRI demonstrated a 1-cm nodule in segment IV and a 3.6-cm recurrent lesion involving both the Spiegel lobe and caudate process. Both lesions represented recurrence within a previously TACE-treated site. Because the prior stereotactic ablative radiotherapy had been directed to a separate segment IV lesion and the caudate lesion itself had not been treated with radiation, the caudate lesion was assessed using the Liver Imaging Reporting and Data System (LI-RADS) CT/MRI Nonradiation Treatment Response Algorithm v2024. Mass-like arterial phase hyperenhancement within the treated caudate lesion (Fig. 1) met the criteria for the LI-RADS Treatment Response Viable. The lesion also showed washout on delayed-phase imaging, hypointensity on hepatobiliary-phase imaging, and high signal intensity on diffusion-weighted imaging. Before the planned TACE, the patient had preserved liver function, with Child-Pugh class A5 and an Eastern Cooperative Oncology Group performance status of 0. Preprocedural laboratory tests showed total bilirubin, 0.7 mg/dL; albumin, 4.0 g/dL; prothrombin time/INR, 0.89; platelet count, $240 \times 10^3/\mu L$; serum creatinine, 1.01 mg/dL; AFP, 2805.69 ng/mL; and PIVKA, 1026 mAU/mL.

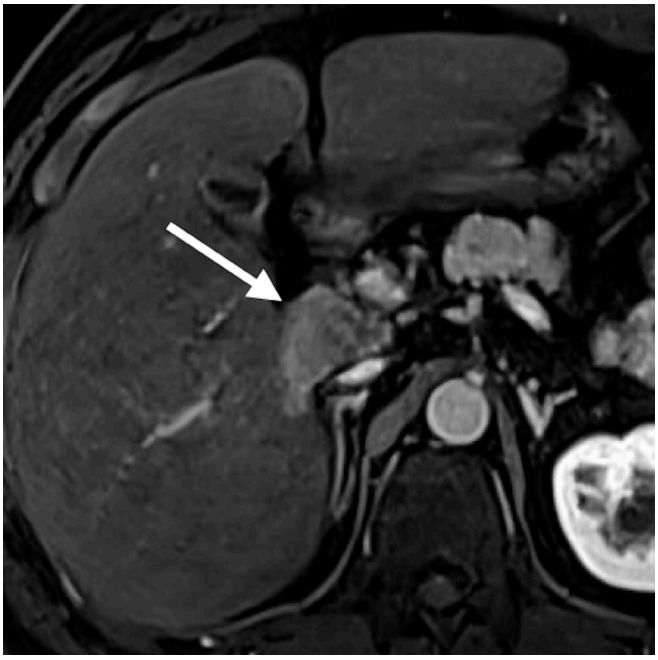


Fig. 1. Preprocedural liver MRI of hepatic arterial phase shows the recurrent tumor involving the Spiegel lobe and caudate process (arrow).

The 13th TACE session was performed in June 2026. Through right common femoral arterial access, cone-beam CT of the common hepatic artery showed a small enhancing tumor in segment IV, but no enhancement of the recurrent caudate lobe tumor. Because the operator thought that the caudate lobe tumor had no tumor vascularity, he performed chemoembolization through the segment IV hepatic artery and recommended external beam radiation therapy for the caudate lobe tumor. He did not interrogate the RIPA.

Immediate postembolization unenhanced CT scan after the 13th TACE demonstrated iodized oil uptake in the segment IV lesion, indicating a technically satisfactory immediate embolization result for the segment IV nodule. At the multidisciplinary team meeting 2 days after the 13th TACE, further treatment for the caudate HCC was discussed. Occult extrahepatic collateral supply to the caudate lobe tumor was suspected based on the discordance between the preprocedural MRI findings and the angiographic findings during the 13th TACE session. The definite arterial phase hyperenhancement on preprocedural MRI indicated arterial vascularity that was not demonstrated on common hepatic arteriography or cone-beam CT. The history of repeated caudate-directed TACE and prior RIPA chemoembolization further supported the possibility of occult extrahepatic collateral supply. The 14th TACE session was performed 3 days later to evaluate and treat the caudate lobe tumor. The RIPA was first selectively catheterized; however, angiography and cone-beam CT showed no tumor staining. Selective angiography of the left inferior phrenic artery and right middle adrenal artery also showed no tumor supply. Careful catheter exploration along the abdominal aorta was then performed using a 5-Fr RH catheter (GRAFIA, Sungjin-Hitech Co., Ltd., Suwon, Korea) to identify small periaortic branches (Video 1). This revealed a separate, more caudal aortic common trunk giving rise to an adrenal branch and the right renal capsular artery. The adrenal branch was interpreted as a variant right inferior adrenal artery based on its caudal origin, common trunk with the right renal capsular artery, and course toward the inferior aspect of

the right adrenal gland. Selective angiography from this common trunk demonstrated intense tumor staining (Fig. 2A), and cone-beam CT confirmed enhancement corresponding to the target recurrent caudate lobe HCC (Fig. 2B).

A hypertrophied tumor-feeding branch from the variant right inferior adrenal artery was then superselectively catheterized with a 1.7-Fr Progreat Lambda microcatheter (Terumo, Tokyo, Japan) over a 0.016-inch ASAHI Meister 16 guidewire (Asahi Intecc, Seto, Japan). TACE was performed using a mixture of 5 mL of iodized oil and 5 mg of idarubicin, followed by smaller calibrated gelatin particles (Prime-Gel, 100–150 μm, PL Micromed Co., Ltd., Yangsan, Korea) for distal embolization. Because residual arterial flow persisted, larger particles (EGgel 350–560 μm, ENGAIN Co., Ltd., Hwaseong, Korea) were subsequently administered to provide additional, relatively proximal flow reduction until angiographic stasis was achieved. Most of the tumor showed dense accumulation of iodized oil, with a small residual unstained portion (Fig. 2C). The residual portion was supplied by fine branches from the right renal capsular artery. These branches were subsequently superselectively embolized using the same sequence of the iodized oil–idarubicin mixture, smaller calibrated gelatin particles, and larger particles until angiographic stasis was achieved, resulting in iodized oil uptake in the residual tumor portion (Fig. 2D).

Postprocedural noncontrast CT demonstrated compact iodized oil uptake within the target recurrent caudate lobe HCC (Fig. 3). Focal iodized oil deposition was also noted in the right adrenal gland and was interpreted as non-target adrenal parenchymal embolization through the variant right inferior adrenal arterial route. Direct adrenal involvement was considered unlikely because preprocedural MRI showed no adrenal mass, no definite continuity between the caudate lobe tumor and the right adrenal gland, and no imaging findings

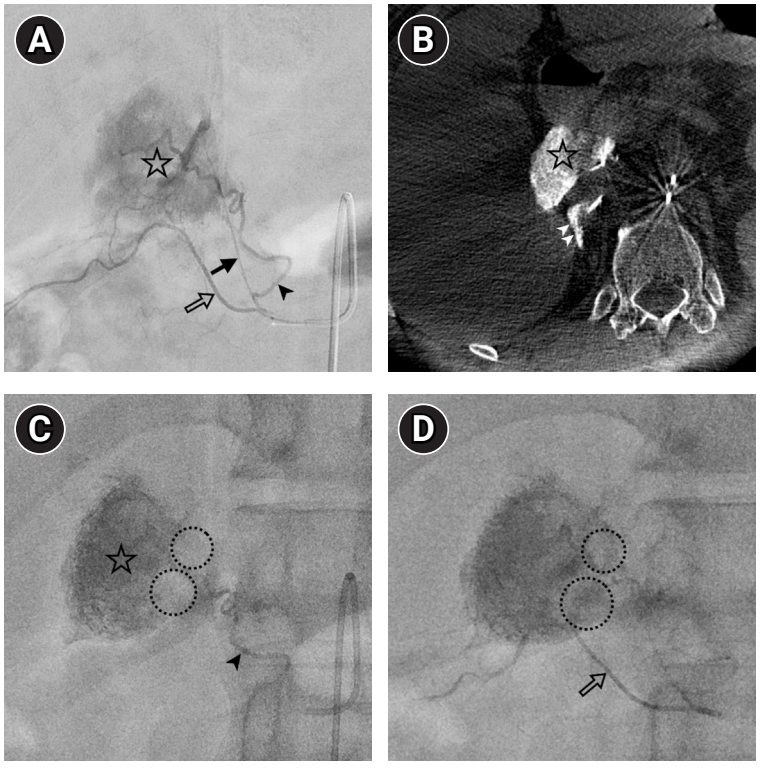


Fig. 2. Angiographic and cone-beam CT findings during the 14th TACE session. (A) Selective angiography from a small common trunk arising from the abdominal aorta demonstrates a variant right inferior adrenal artery (arrow), a hypertrophied tumor-feeding branch arising near its origin (arrowhead), and the right renal capsular artery (open arrow). Intense tumor staining corresponding to the recurrent caudate lobe HCC is also identified (asterisk). (B) Cone-beam CT from the same common trunk confirms enhancement of the bulk of the target caudate lobe tumor (asterisk). Concomitant enhancement of the right adrenal gland is also noted (double arrowhead). (C) After superselective catheterization of a hypertrophied tumor-feeding branch from the variant right inferior adrenal artery (arrowhead), TACE shows dense iodized oil accumulation in most of the tumor (asterisk), with a small residual unstained portion (dashed circles). (D) Subsequent superselective embolization through fine branches from the right renal capsular artery (open arrow) results in iodized oil accumulation within the residual tumor portion (dashed circles).



Fig. 3. Postprocedural noncontrast CT after the 14th TACE session. Noncontrast CT demonstrates compact iodized oil uptake throughout the target recurrent caudate lobe HCC (asterisk), indicating technically successful superselective TACE. Concomitant focal iodized oil deposition is also noted in the right adrenal gland (double arrowhead).

suggestive of adrenal parenchymal tumor involvement. Nevertheless, microscopic adrenal involvement could not be definitively excluded in the absence of histologic confirmation. Throughout and immediately after the procedure, the patient's vital signs remained stable, and no immediate adrenal-related or other procedure-related complication was observed. The patient was discharged on postprocedural day 1. CT scan 1 month after 14th TACE showed no viable tumor, and longer-term imaging follow-up to formally assess the treatment response of both the caudate lobe and segment IV lesions was scheduled.

Discussion

This case illustrates a rare extrahepatic collateral pathway to recurrent caudate lobe HCC. The caudate lobe has variable arterial supply, and caudate arteries can arise from both right and left hepatic arterial systems. These arteries are frequently small and interconnected, and the dominant feeder can differ according to the subsegmental location of the tumor [2]. Therefore, careful evaluation of caudate arterial supply is essential during TACE.

The RIPA is the most common extrahepatic collateral artery supplying caudate lobe HCC. Woo et al. [3] reported that 31 of 35 caudate lobe HCCs treated through extrahepatic collateral arteries were supplied by the RIPA, whereas non-RIPA collaterals were uncommon and included the gastroduodenal, dorsal pancreatic, right gastric, and left gastric arteries. Our case differed from this usual pattern. During the 13th TACE session, the operator did not suspect extrahepatic collateral supply to the caudate lobe HCC, and regarded it as a hypovascular tumor that was not a good candidate for TACE, and recommended external beam radiation therapy. At the 14th TACE session, the RIPA did not supply the tumor. Instead, the tumor was supplied by a small common trunk arising from the abdominal aorta, which gave rise to a variant right inferior adrenal artery and right renal capsular artery. This variant right inferior adrenal artery served as the dominant tumor feeder, with fine ancillary supply from the right renal capsular branch.

Several factors may have contributed to this unusual collateral pathway. Repeated caudate-directed TACE may have attenuated the usual intrahepatic caudate arterial supply, a mechanism that has been suggested to promote extrahepatic collateralization, particularly through the RIPA, in caudate lobe HCC [3]. In our patient, however, the potential RIPA route may have been limited by previous RIPA chemoembolization, which has been associated with a higher incidence of non-RIPA extrahepatic collateral supply [3]. Although prior stereotactic ablative radiotherapy had been directed to a separate segment IV lesion rather than the caudate lesion, a possible contribution of regional radiation-related vascular injury could not be entirely excluded. However, its role in the development of this collateral pathway remains uncertain [5]. In addition, the recurrent tumor involved the lower Spiegel lobe and caudate process, placing it close to the retroperitoneal space, right adrenal gland, and right kidney. This location may have favored recruitment of the variant right inferior adrenal and renal capsular arteries, consistent with adjacent-organ collateralization and known communications among the inferior phrenic, adrenal, and retroperitoneal arterial networks [6,7].

Non-target embolization of the adrenal gland is a potential concern when the adrenal artery is used as a collateral route. A small preliminary series of transarterial embolization/TACE performed through adrenal arteries for HCC reported no embolization-related complications [8]; however, the available evidence remains limited. Therefore, careful superselective catheterization is important to minimize non-target adrenal

embolization. In this case, focal iodized oil deposition was noted in the right adrenal gland, but no immediate adrenal-related or other procedure-related complication was observed. This case underscores the importance of superselective catheterization and careful monitoring when performing TACE through an adrenal arterial feeder.

This case provides a practical angiographic lesson. In recurrent caudate lobe HCC after repeated TACE, extrahepatic collateral supply should be kept in mind when cone-beam CT of the hepatic artery fails to demonstrate tumor blush. For tumors involving the lower Spiegel lobe or caudate process, especially in patients with prior caudate-directed and RIPA chemoembolization, small periaortic adrenal–renal capsular collateral pathways, including variant adrenal arterial branches, should be considered after exclusion of the usual caudate arterial and RIPA routes. Recognition of this rare pathway may help identify occult tumor supply and enable complete tumor embolization with superselective TACE.

Conflict of interest

No potential conflict of interest relevant to this article was reported.

Funding

None.

Acknowledgments

None.

Author contributions

Conceptualization: DK, HCK. Data curation: DK. Formal analysis: DK, HCK. Investigation: DK, HCK. Methodology: DK, HCK. Project administration: HCK. Resources: HCK. Supervision: HCK. Validation: HCK. Visualization: DK. Writing - original draft: DK. Writing - review & editing: DK, HCK.

Data availability statement

The datasets generated or analyzed during the study are not publicly available due to patient privacy but are available from the corresponding author on reasonable request.

Supplementary material

The supplement data are available with this article at https://doi.org/10.64961/kjir.2026.00143.

ORCID

Donghyun Kim, https://orcid.org/0000-0002-9353-775X
Hyo-Cheol Kim, https://orcid.org/0000-0002-6016-247X

References

1. Kim HC, Chung JW, Jae HJ, Yoon JH, Lee JH, Kim YJ, et al. Caudate lobe hepatocellular carcinoma treated with selective chemoembolization. Radiology. 2010;257:278-287. https://doi.org/10.1148/radiol.10100105
2. Kim HC, Miyayama S, Chung JW. Selective chemoembolization of caudate lobe hepatocellular carcinoma: anatomy and procedural techniques. Radiographics. 2019;39:289-302. https://doi.org/10.1148/rg.2019180110
3. Woo S, Kim HC, Chung JW, Jung HS, Hur S, Lee M, et al. Chemoembolization of extrahepatic collateral arteries for treatment of hepatocellular carcinoma in the caudate lobe of the liver. Cardiovasc Intervent Radiol. 2015;38:389-396. https://doi.org/10.1007/s00270-014-0929-7
4. Rash C, Lee E, Klinsky S, Angel W. Case study of inferior adrenal artery as an extrahepatic collateral arterial supply to hepatocellular carcinoma. Radiol Case Rep. 2025;20:129-132. https://doi.org/10.1016/j.radcr.2024.10.026
5. Park HJ, Griffin RJ, Hui S, Levitt SH, Song CW. Radiation-induced vascular damage in tumors: implications of vascular damage in ablative hypofractionated radiotherapy (SBRT and SRS). Radiat Res. 2012;177:311-327. https://doi.org/10.1667/rr2773.1
6. Kim HC, Chung JW, Lee W, Jae HJ, Park JH. Recognizing extrahepatic collateral vessels that supply hepatocellular carcinoma to avoid complications of transcatheter arterial chemoembolization. Radiographics. 2005;25 Suppl 1:S25-S39. https://doi.org/10.1148/rg.25si055508
7. Kim HC, Miyayama S, Choi JW, Kim GM, Chung JW. Hepatocellular carcinoma supplied by the inferior phrenic artery or cystic artery: anatomic and technical considerations. Radiographics. 2023;43:e220076. https://doi.org/10.1148/rg.220076
8. Hu S, Tu J, Jia Z, Huang Y, Jiang G. Transarterial embolization/chemoembolization therapy for hepatocellular carcinoma fed by adrenal artery: preliminary results. Medicine (Baltimore). 2016;95:e5762. https://doi.org/10.1097/MD.0000000000005762

Case Report

eISSN 2508-2612
https://doi.org/10.64961/kjir.2026.00157
Korean J Interv Radiol 2026;31(2):79-84

KJIR
Korean Journal of
Interventional Radiology

Transarterial Radioembolization via Right Internal Thoracic Artery in a Patient with HCC: A Case Report

Hyo-Cheol Kim*

Department of Radiology, Seoul National University Hospital, Seoul National University College of Medicine, Seoul, Republic of Korea

Extrahepatic collateral supply from the Sappey superior artery of the right internal thoracic artery (RITA) is an uncommon but important source of perfusion to HCC located in segment IV. Preprocedural CT demonstrated a large segment IV HCC supplied by the Sappey superior artery. Initial transfemoral angiography confirmed tumor vascularization but failed to achieve superselective catheterization because of marked tortuosity of the aortic arch. The procedure was converted to a right transradial approach, which provided stable access to the RITA and enabled successful superselection of the Sappey superior artery. Y-90 radioembolization via the Sappey superior artery and hepatic artery was completed without complications.

Keywords: Carcinoma, hepatocellular; Radioembolization, therapeutic; Mammary arteries; Radial artery; Yttrium radioisotopes

Introduction

Extrahepatic collateral arterial supply is frequently encountered in HCC, particularly in large or subcapsular tumors [1]. Among these collateral pathways, the inferior phrenic artery is the most common source [1]; however, the internal thoracic artery and its branches, including the Sappey superior artery, may also contribute to tumor perfusion, especially for lesions located in segment IV or abutting the anterior hepatic surface [2,3]. Recognition of these vessels is essential because incomplete treatment of collateral supply may compromise the efficacy of locoregional therapy.

Yttrium-90 (Y-90) transarterial radioembolization has increasingly been performed through parasitized extrahepatic arteries when superselective catheterization can be safely achieved. Recent reports have demonstrated the feasibility of radioembolization via the inferior phrenic artery, internal thoracic artery, and adrenal artery [4-9].

We report a case of successful Y-90 radioembolization performed through the Sappey superior artery originating from the right internal thoracic artery (RITA). Because severe tortuosity of the aortic arch prevented superselective catheterization from a transfemoral approach, conversion to a right transradial approach enabled stable catheterization and successful treatment.

Case Report

Institutional Review Board approval was waived for this case report in accordance with the policy of Seoul National University Hospital. An 86-year-old man presented with an 8.5-cm-sized single nodular HCC located in hepatic segment IV (Fig. 1). He had preserved liver function with Child-Pugh class A5. Preprocedural laboratory tests showed total bilirubin, 0.8 mg/dL; albumin, 4.6 g/dL; prothrombin time/INR,

Received: July 2, 2026; **Revised:** July 22, 2026; **Accepted:** July 22, 2026
***Corresponding email:** radioembolization@snu.ac.kr

© 2026 Korean Society of Interventional Radiology

This is an Open Access article distributed under the terms of the Creative Commons Attribution Non-Commercial License (http://creativecommons.org/licenses/by-nc/4.0) which permits unrestricted non-commercial use, distribution, and reproduction in any medium, provided the original work is properly cited.

1.03; platelet count, 244 × 10^3/μL; serum creatinine, 0.7 mg/dL; serum α-fetoprotein, 5.6 ng/mL; and protein induced by vitamin K antagonist-II, 305 mAU/mL. Contrast-enhanced CT demonstrated a parasitized extrahepatic arterial supply arising from the Sappey superior artery, which originated from the RITA and coursed through the falciform ligament to supply the tumor (Video 1). Because of the absence of dysmorphic intratumoral vessel, same-day radioembolization with resin microspheres (SIR-Spheres, SIRTEX, Woburn, MA, USA) was planned.

The procedure was initially performed via a right common femoral artery approach with a 5-Fr catheter (RH, Cook, Bloomington, IN, USA). Celiac angiography and cone-beam CT obtained at the proper hepatic artery revealed a hypervascular tumor in segment IV (Fig. 2A), but focal unenhancement of the anterior portion of the tumor was noted on cone-beam CT (Fig. 2B), which suggested the presence of extrahepatic collateral blood supply. Selective angiography and cone-beam CT of the RITA demonstrated that the anterior portion of the tumor was supplied by the Sappey superior artery of the RITA (Fig. 3). ^{99m}Tc-macroaggregated albumin (MAA) was injected via the left hepatic artery, but not via the RITA. The patient was transferred to the department of nuclear medicine to obtain SPECT/CT, resulting in a lung shunt fraction of 3.17% and a tumor-to-normal ratio of 3.5. The total liver volume was 1,041 mL, of which 419 mL was planned for treatment. The total tumor volume was 181 mL, with 168 mL supplied by the segment IV artery and 13 mL by the RITA, as determined by cone-beam CT.

The virtual tumor absorbed dose (vTAD) was calculated under the assumption that all radioactive microspheres were deposited within the tumor. Based on the tumor volume of 13 mL supplied by the RITA, an activity of 0.19 GBq was required to achieve the target vTAD of 700 Gy. Therefore, the prescribed activity for the RITA was set at 0.2 GBq. For treatment via the segment IV artery, partition dosimetry was used. Given a treated liver volume of 406 mL, a treated tumor volume of 168 mL, and a tumor-to-normal ratio of 3.5, an activity of 2.45 GBq was required to achieve the target tumor absorbed dose (TAD) of 500 Gy. Accordingly, the prescribed activity for the segment IV artery was set at 2.5 GBq.

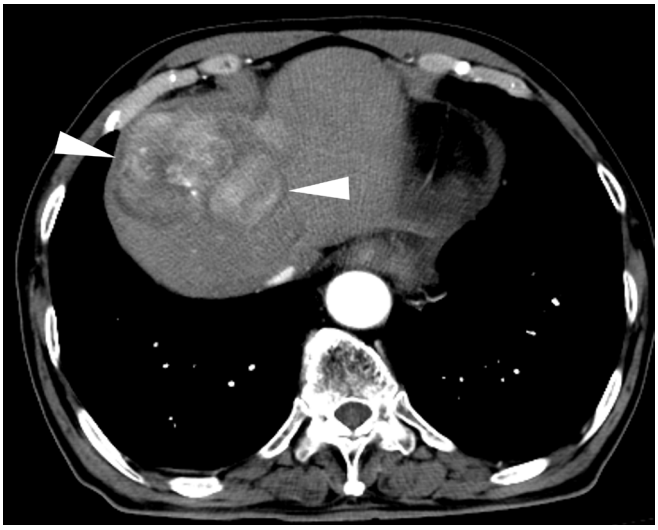


Fig. 1. CT scan shows a large enhancing tumor (arrowheads) in liver segment IV.



Fig. 2. (A) Celiac angiogram shows large tumor blush (arrowheads) supplied by the segment IV artery. (B) Axial image of cone-beam CT obtained at the proper hepatic artery shows tumor blush (arrowheads) in the liver dome. The anterior part (arrow) of the tumor was not enhanced.

The patient was sent back to the angiography suite, and then the treatment procedure was initiated 30 minutes after SPECT/CT. Treatment via the Sappey superior artery was first attempted. However, because of marked elongation and tortuosity of the aortic arch, advancement of the microcatheter into the Sappey superior artery was technically unsuccessful. To overcome this limitation, vascular access via the right radial artery was added using a 5-Fr sheath (Prelude, Merit Medical, South Jordan, UT, USA). Through the transradial route, the RITA was readily catheterized with a 5-Fr Omni catheter (A&A, Seoul, Korea), which improved coaxial support and allowed advancement of a 1.7-Fr microcatheter (Progreat Lambda, Terumo, Tokyo, Japan) into the Sappey superior artery (Fig. 4). Resin microspheres (SIR-Spheres, SIRTEX) of 0.2 GBq were delivered via the Sappey superior artery. Through the femoral approach, the segment IV artery was treated with resin microspheres of 2.5 GBq. Residual activity was measured after the procedure, and the actual delivered radiation activity was 0.18 GBq and 2.46 GBq via the Sappey superior artery and segment IV artery, respectively. Post-treatment PET/CT imaging was obtained the next morning, which demonstrated hot radiation activity within the entire tumor and no significant extrahepatic uptake, and mean TAD was calculated as 586 Gy.

The patient tolerated the procedure well without access-site complications or clinically significant adverse events. Follow-up CT scan 6 months after radioembolization demonstrated partial response with minimal residual tumor by modified Response Evaluation Criteria in Solid Tumors (Fig. 5). CT scan 8 months after radioembolization demonstrated a slight increase in the residual viable tumor, and a second radioembolization was performed. During the second procedure, selective angiography and cone-beam CT showed that the residual viable tumor was supplied exclusively by the segment IV artery, with no tumor supplied by the RITA. A total activity of 1.1 GBq was administered through the segment IV artery. Post-treatment PET/CT demonstrated a TAD of 578 Gy. Until the last follow-up, no complications occurred.



Fig. 4. Selective angiogram of the Sappey superior artery shows tumor blush (arrowhead). Note a microcatheter tip (arrow) in the Sappey superior artery and a 5-Fr catheter (open arrow) inserted via the right radial artery.

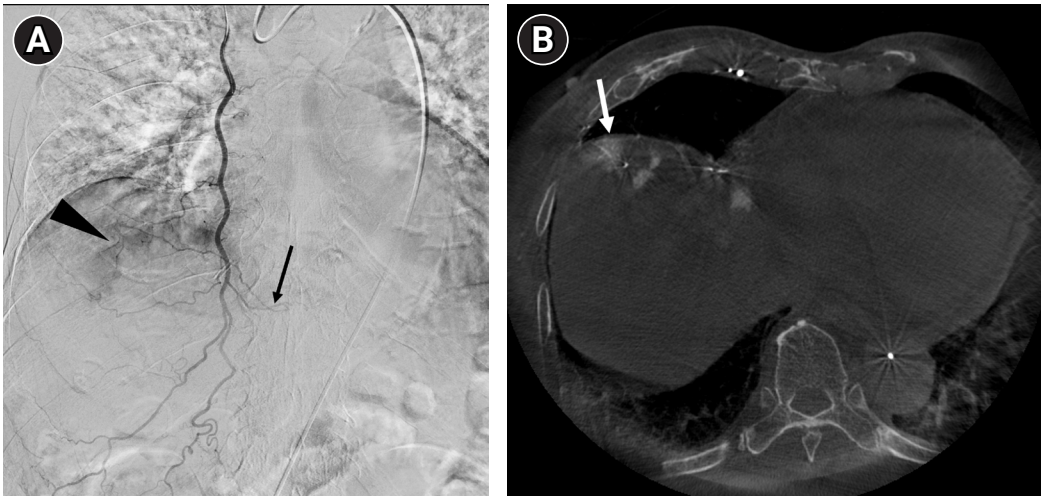


Fig. 3. (A) Right internal thoracic angiogram shows tumor blush (arrowhead) supplied by Sappey superior artery (arrow) from the right internal thoracic artery. (B) Axial image of cone-beam CT obtained at the right internal thoracic artery shows tumor blush (arrow) in the anterior part of the tumor.

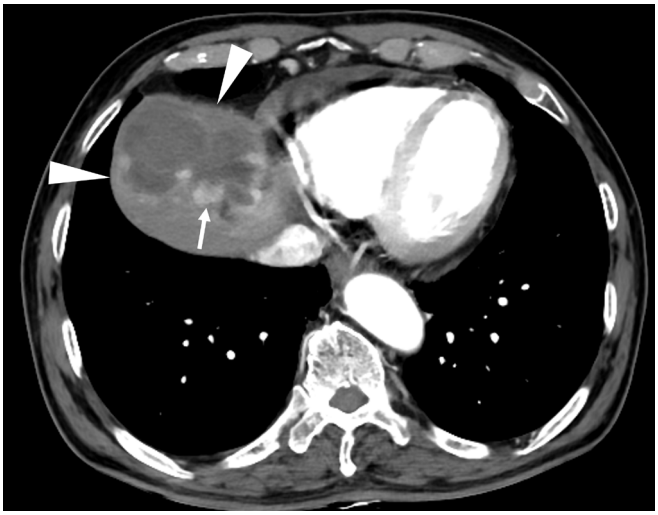


Fig. 5. CT scan 6 months after radioembolization shows small residual enhancing foci (arrow) within the treated tumor (arrowheads).

Discussion

The Sappey superior artery is an important but underrecognized collateral pathway supplying HCCs located in the anterior superior liver, particularly segment IV lesions adjacent to the falciform ligament [2]. Previous anatomic studies have shown that this vessel may arise from the internal thoracic artery and communicate with the inferior phrenic circulation through the diaphragm [2]. Consequently, careful review of preprocedural cross-sectional imaging and angiography is required to identify this collateral source [10].

Although several reports have described transarterial chemoembolization or radioembolization through parasitized internal thoracic or extrahepatic arteries, experience with Y-90 delivery through the Sappey superior artery remains extremely limited [8]. Complete treatment of all arterial supplies is particularly important for radioembolization when curative or ablative intent is pursued, because omission of a collateral feeder may leave viable tumor tissue untreated.

The RITA gives rise to the anterior intercostal arteries and the superior epigastric artery, which supply the anterior chest/abdominal wall and overlying skin. Consequently, non-selective radioembolization through the RITA carries a substantial risk of radiation dermatitis. In contrast, the Sappey superior artery supplies the tumor and the diaphragm without providing arterial supply to the skin. Therefore, superselective radioembolization through the Sappey superior artery is unlikely to result in radiation dermatitis. Because resin microspheres have a relatively high particle load, microsphere reflux may occur during administration. If reflux occurs into the non-target branches of the RITA, radiation dermatitis may develop. To minimize this risk, the author continuously infused a 1:1 mixture of contrast medium and 5% dextrose through the injection line at a very slow rate, allowing real-time monitoring of antegrade flow and immediate detection of any reflux. This technique facilitated maintenance of antegrade flow throughout the procedure and helped prevent microsphere reflux into non-target vessels.

This case also highlights an important technical consideration regarding vascular access. Transfemoral catheterization of the RITA may be difficult in elderly patients with severe elongation and tortuosity of the aortic arch. In contrast, a right transradial approach provides a shorter and more favorable trajectory to the RITA, improving catheter stability and facilitating distal microcatheter advancement. In this patient, conversion from femoral to radial access transformed an unsuccessful procedure into successful superselective catheterization and definitive treatment.

The present case supports two practical messages. First, the Sappey superior artery should be actively sought in patients with segment IV HCC demonstrating incomplete hepatic arterial perfusion. Second, when transfemoral access fails because of unfavorable aortic anatomy, a transradial approach should be considered as an effective alternative for selective catheterization of the RITA and its distal branches.

Appropriate patient selection is essential for safe implementation of same-day radioembolization. Based on previous studies and our prospective ISTAR-01 protocol [11,12], imaging findings suggestive of elevated lung shunting include hepatic vein invasion, early hepatic vein enhancement on arterial-phase CT or MRI, the presence of transjugular intrahepatic portosystemic shunt, and dysmorphic intratumoral vessels measuring ≥3 mm. Marked portal vein enhancement on arterial-phase CT or MRI indicates a massive arterioportal shunt, which is generally considered a contraindication to radioembolization because of the risk of unintended whole-liver irradiation. Therefore, the ideal candidates for same-day radioembolization are patients without any imaging features suggestive of high lung shunting and without evidence of a massive arterioportal shunt on preprocedural imaging. Even

in patients without these imaging findings, same-day treatment should proceed only after MAA-based dosimetry confirms that an adequate TAD can be delivered while maintaining the estimated lung dose within accepted safety limits.

In conclusion, Y-90 radioembolization through the Sappey superior artery arising from the RITA is feasible and can be safely performed when meticulous superselective catheterization is achieved. In patients with severe aortic arch tortuosity, the right transradial approach may provide superior catheter stability compared with the transfemoral approach and facilitate successful treatment of HCC supplied by this uncommon extrahepatic collateral artery.

Conflict of interest

No potential conflict of interest relevant to this article was reported.

Funding

None.

Acknowledgments

None.

Author contributions

The author conducted all aspects of the study.

Data availability statement

The datasets generated or analyzed during the study are available from the corresponding author on reasonable request.

Supplementary material

The supplementary data are available with this article at https://doi.org/10.64961/kjir.2026.00157.

ORCID

Hyo-Cheol Kim, https://orcid.org/0000-0002-6016-247X

References

1. Kim HC, Chung JW, Lee W, Jae HJ, Park JH. Recognizing extrahepatic collateral vessels that supply hepatocellular carcinoma to avoid complications of transcatheter arterial chemoembolization. Radiographics. 2005;25 Suppl 1:S25-S39. https://doi.org/10.1148/rg.25si055508
2. Kim HC, Miyayama S, Choi JW, Kim GM, Chung JW. Hepatocellular carcinoma supplied by the inferior phrenic artery or cystic artery: anatomic and technical considerations. Radiographics. 2023;43:e220076. https://doi.org/10.1148/rg.220076
3. Kim HC, Chung JW, Choi SH, Jae HJ, Lee W, Park JH. Internal mammary arteries supplying hepatocellular carcinoma: vascular anatomy at digital subtraction angiography in 97 patients. Radiology. 2007;242:925-932. https://doi.org/10.1148/radiol.2423060220
4. Kim HC, Kim YJ, Paeng JC, Chung JW. Yttrium-90 radioembolization of the right inferior phrenic artery in 20 patients with hepatocellular carcinoma. J Vasc Interv Radiol. 2018;29:556-563. https://doi.org/10.1016/j.jvir.2017.10.010
5. Kim HC, Kim DH, Suh M, Paeng JC, Choi JW. High-dose radioembolization limited by lung shunt for hepatocellular carcinoma supplied by the inferior phrenic artery. J Vasc Interv Radiol. 2025;36:1427-1435. https://doi.org/10.1016/j.jvir.2025.05.027
6. Vidal LL, Frey GT, Ritchie C, Lewis A, Paz-Fumagalli R, McKinney M, et al. Ablative transarterial radioembolization of a parasitized adrenal artery for the treatment of hepatocellular carcinoma. J Vasc Interv Radiol. 2019;30:473-476. https://doi.org/10.1016/j.jvir.2018.10.022
7. Arotzarena G, Toskich BB, Lewis AR, Paz-Fumagalli R. Ablative radioembolization of hepatocellular carcinoma with total arterial supply originating from the superior adrenal artery achieved complete pathologic necrosis. Radiol Case Rep. 2023;18:196-199. https://doi.org/10.1016/j.radcr.2022.10.025
8. Alhussaini A, Qazi SA, AlZahrani YA. Successful transcatheter arterial radioembolization of hepatocellular carcinoma via left internal mammary artery: a case report. Cureus. 2022;14:e22954. https://doi.org/10.7759/cureus.22954
9. Okinedo I, Frageau J, Krishnarao A, Figueira T, Resnick N, Li NP. Yttrium-90 transarterial radioembolization of a hepatocellular carcinoma via parasitized adrenal and renal capsular arteries. J Vasc Interv Radiol. 2026;37:108739. https://doi.org/10.1016/j.jvir.2026.108739
10. Kim HC, Chung JW, Jae HJ, Jeon UB, Son KR, Park JH. Hepatocellular carcinoma: prediction of blood supply from an

internal mammary artery with multi-detector row CT. J Vasc Interv Radiol. 2008;19:1419-1425. https://doi.org/10.1016/j.jvir.2008.06.015

11. Kim HC, Suh M, Paeng JC, Choi JW. Same-day versus multiday planning/treatment radioembolization with yttrium-90 resin microspheres in patients with liver cancer ≥5 cm. J Vasc Interv Radiol. 2025;36:2010-2020. https://doi.org/10.1016/j.jvir.2025.08.028
12. Kim HC, Lee IJ, Hyun DH, Kim GM. Same-day radioembolization for large hepatocellular carcinoma (≥5 cm) using yttrium-90 resin microspheres: protocol for a multicenter prospective registry study (ISTAR-01). Cardiovasc Intervent Radiol. (in press).

Case Report

eISSN 2508-2612
https://doi.org/10.64961/kjir.2026.00178
Korean J Interv Radiol 2026;31(2):85-91

KJIR
Korean Journal of
Interventional Radiology

Comprehensive Interventional Management of Postoperative Duodenal Perforation: A Case Report

Jae Hwan Lee[1,2,3,*], **Kun Yung Kim**[1], **Chang Jin Yoon**[1,2,3]

[1]Department of Radiology, Seoul National University Bundang Hospital, Seongnam, Republic of Korea
[2]Department of Radiology, Seoul National University College of Medicine, Seoul, Republic of Korea
[3]Institute of Radiation Medicine, Seoul National University Hospital, Seoul, Republic of Korea

Duodenal perforation is an uncommon but potentially fatal complication of pancreatic surgery. We report a 73-year-old man who presented with hematochezia after laparoscopic distal pancreatectomy with splenectomy for pancreatic body cancer, complicated by a postoperative pancreatic fistula that led to gastroduodenal artery bleeding treated with a stent-graft. Contrast-enhanced CT showed active duodenal bleeding with a surrounding hematoma. The bleeding duodenal branch was embolized, and the hematoma was drained percutaneously; a fistulous communication between the periduodenal collection and the duodenal lumen was subsequently demonstrated. Through the drainage tract, an 8-Fr Foley catheter was advanced into the duodenal lumen and its balloon inflated to secure a controlled fistula, while a percutaneous gastrojejunostomy provided distal enteral feeding. The catheter was maintained for approximately 2 months, and the tract was embolized at the time of removal to minimize residual leakage. The patient recovered fully. This case demonstrates the feasibility of staged interventional management for postoperative duodenal perforation when reoperation is not feasible.

Keywords: Intestinal perforation; Postoperative complications; Drainage; Case reports

Introduction

Duodenal perforation is a full-thickness disruption of the duodenal wall that constitutes a life-threatening emergency associated with substantial morbidity and mortality. It arises from diverse etiologies, including peptic ulcer disease, iatrogenic injury during ERCP or endoscopic ultrasound, blunt or penetrating trauma, malignancy, and abdominal surgery. Iatrogenic perforation is uncommon; post-ERCP perforation occurs in fewer than 1% of procedures but carries a reported mortality of 4.2%–37% depending on perforation type, timing of diagnosis, and management strategy [1]. The predominantly retroperitoneal location of the duodenum and its proximity to the pancreas and biliary tree contribute to atypical presentation, delayed diagnosis, and persistent leakage, which together account for the disproportionate morbidity relative to perforations elsewhere in the gastrointestinal tract.

Classical management has centered on open surgical repair—primary closure with an omental patch, peritoneal lavage, and drainage. Although effective for source control, open repair imposes considerable physiological stress, particularly in elderly patients, those with multiple comorbidities, or those presenting late, and reported complication rates reach 42%–58% with hospital stays of 5–15 days [2,3]. In the postoperative setting, reoperation is further constrained by

Received: July 22, 2026; **Revised:** August 10, 2026;
Accepted: August 18, 2026
***Corresponding email:** lzhwanmd@gmail.com

© 2026 Korean Society of Interventional Radiology

This is an Open Access article distributed under the terms of the Creative Commons Attribution Non-Commercial License (http://creativecommons.org/licenses/by-nc/4.0) which permits unrestricted non-commercial use, distribution, and reproduction in any medium, provided the original work is properly cited.

adhesions, tissue friability, and inflammation within a recently manipulated surgical field, and revision surgery has been required in up to 67% of retroperitoneal duodenal perforations managed surgically [4]. These limitations underscore the need for less invasive alternatives in selected patients.

Advances in interventional radiology and endoscopy have established minimally invasive techniques as viable alternatives or adjuncts to surgery. Image-guided percutaneous drainage achieves source control with reported success of 77%–88% [5,6], covered self-expandable metal stents attain technical success approaching 100% and clinical healing of 87%–93% [7,8], and endoscopic vacuum therapy has reported 100% technical and 80% clinical closure [9]. A randomized trial of combined endoscopic and radiologic management versus surgery for perforated peptic ulcer showed shorter hospital stay (1 vs. 7 days) and lower complication rates (24% vs. 58%) in the interventional arm [3], while a meta-analysis of post-ERCP perforations found no significant difference in mortality between non-operative and surgical management [10]. Beyond reduced physiological insult, these techniques permit staged, patient-tailored management—stabilizing the patient first and combining drainage with defect sealing according to perforation size, location, and degree of contamination—thereby enabling an individualized rather than uniformly operative strategy.

Duodenal perforation following pancreatic surgery represents a particularly challenging scenario, as early reoperation within a fresh operative field carries high risk and is often technically difficult or infeasible. Herein, we report a case of postoperative duodenal perforation managed by percutaneous drainage followed by catheter-based tract sealing, illustrating the feasibility of a staged, minimally invasive approach when reoperation is not a favorable option.

Case Report

A 73-year-old man presented with hematochezia 5 weeks after laparoscopic distal pancreatectomy with splenectomy for pancreatic body cancer. His postoperative course had been complicated by a postoperative pancreatic fistula (POPF). Three weeks after surgery, enzymatic erosion associated with the POPF resulted in bleeding from the gastroduodenal artery (GDA), which was treated by stent-graft placement. On arrival, he was hemodynamically unstable, with a blood pressure of 99/46 mmHg and a heart rate of 105 beats/min. Initial laboratory studies showed a hemoglobin level of 9.5 g/dL, a hematocrit of 30.6%, and a platelet count of 369 × 10^3/μL; coagulation studies were within normal limits. Contrast-enhanced multiphasic abdominal CT demonstrated active bleeding from the duodenum with a surrounding hematoma (Fig. 1).

Emergency transarterial embolization of the bleeding duodenal branch was performed with a Concerto detachable coil (Medtronic, Minneapolis, MN, USA) and a 1:1 mixture of N-butyl cyanoacrylate (Histoacryl, B. Braun, Melsungen, Germany) and ethiodized oil (Lipiodol, Guerbet, Villepinte, France). Percutaneous catheter drainage (PCD) of the hematoma was then undertaken under combined ultrasonographic and cone-beam CT guidance. Because the left hepatic lobe and the gastric antrum lay anterior to the collection, a transhepatic route was selected, and cone-beam CT was used to plan and confirm a trajectory that traversed the left hepatic lobe while avoiding the stomach. The aspirated fluid was dark brown, bile-tinged, and purulent on gross inspection. Fluid amylase and lipase levels were 112 U/L and 1,007 U/L, re-



Fig. 1. A 73-year-old man presented with hematochezia 5 weeks after laparoscopic distal pancreatectomy with splenectomy for pancreatic body cancer. Contrast-enhanced CT shows active contrast extravasation from a duodenal branch, with an adjacent perilesional hematoma.

spectively, and culture grew *Klebsiella pneumoniae*. Fluid bilirubin was not measured, so a biliary contribution could not be quantified biochemically; however, the bile-tinged appearance was consistent with an infected collection receiving enteric content, in the setting of the previously documented POPF. The biochemical findings alone could not establish direct communication with the pancreatic fistula. Daily drainage was approximately 300 mL/day immediately after PCD placement and persisted at this level over the subsequent 5 days (Fig. 2).

Three days later, a tubogram through the PCD demonstrated a fistulous communication between the drainage cavity and the duodenum, with injected contrast passing into the duodenal lumen (Fig. 3). Because the enteric output persisted despite adequate drainage, a catheter-directed approach to occlude the fistula was undertaken on day 5 after PCD placement. The fistula was cannulated through the PCD tract using a 5-Fr Kumpe catheter (Cook Medical, Bloomington, IN, USA) and a 0.035-inch guidewire. After access into the duodenal lu-

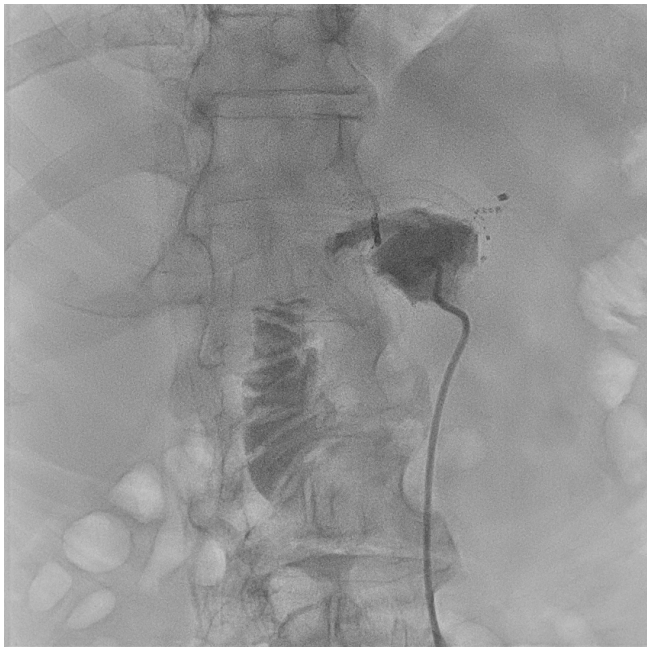


Fig. 3. Tubogram obtained 3 days after drainage. Contrast injected through the percutaneous drainage catheter opacifies the cavity and passes into the duodenal lumen through a fistulous communication, confirming a duodenal fistula.

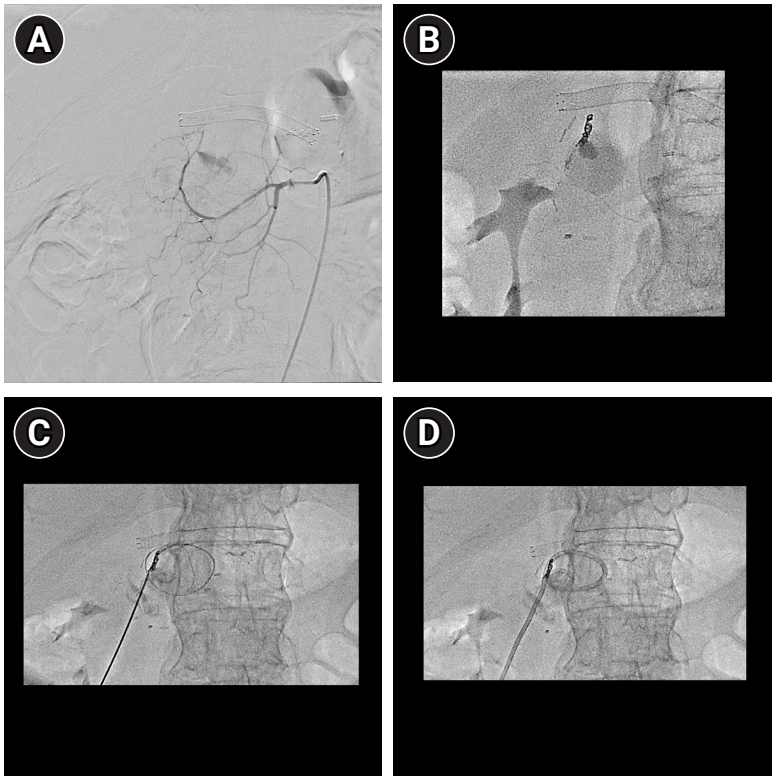


Fig. 2. Emergency transarterial embolization and percutaneous drainage. (A) Selective angiography demonstrates active bleeding from the duodenal branch. (B) Post-embolization spot image after microcoil placement and injection of a 1:1 glue-lipiodol mixture shows cessation of bleeding. (C) The hematoma is punctured under combined ultrasonographic and cone-beam CT guidance via a transhepatic route, avoiding the gastric antrum, and (D) a percutaneous drainage catheter is placed.

men was achieved, an 8-Fr silicone-coated latex Foley balloon catheter (SEWOON Medical, Cheonan, Korea) was positioned in exchange for the existing drainage catheter, the balloon was inflated within the lumen, and slight tension was applied to secure the tube. Output thereafter declined to approximately 20 mL/day and remained minimal until removal. Because a separate drainage catheter was not maintained, the catheter and the residual cavity were monitored by tubography every 2 days for the first week and weekly thereafter; no re-accumulation was observed. A percutaneous gastrojejunostomy was subsequently created to enable enteral feeding beyond the duodenal fistula (Fig. 4).

The catheter was maintained for approximately 2 months, during which the patient received enteral feeding through the gastrojejunostomy and underwent rehabilitation therapy. The patient recovered, and the gastrojejunostomy was removed once oral feeding was tolerated. At the time of catheter removal, tubography confirmed a mature fistulous tract without extraluminal leakage. To minimize residual leakage along the tract after catheter withdrawal, the tract was embolized with a 1:1 mixture of N-butyl cyanoacrylate and ethiodized oil. After balloon deflation, the catheter was withdrawn until its tip lay immediately outside the duodenal wall, and approximately 1 mL of the mixture was injected while the catheter was gradually withdrawn, so that embolization was confined to the extraluminal tract outside the fistula and no glue was delivered into the duodenal lumen. Dextrose flushing was not used (Fig. 5). After the absence of leakage or abdominal pain was confirmed, the patient was discharged the following day. No procedure-related adverse events occurred during the course of

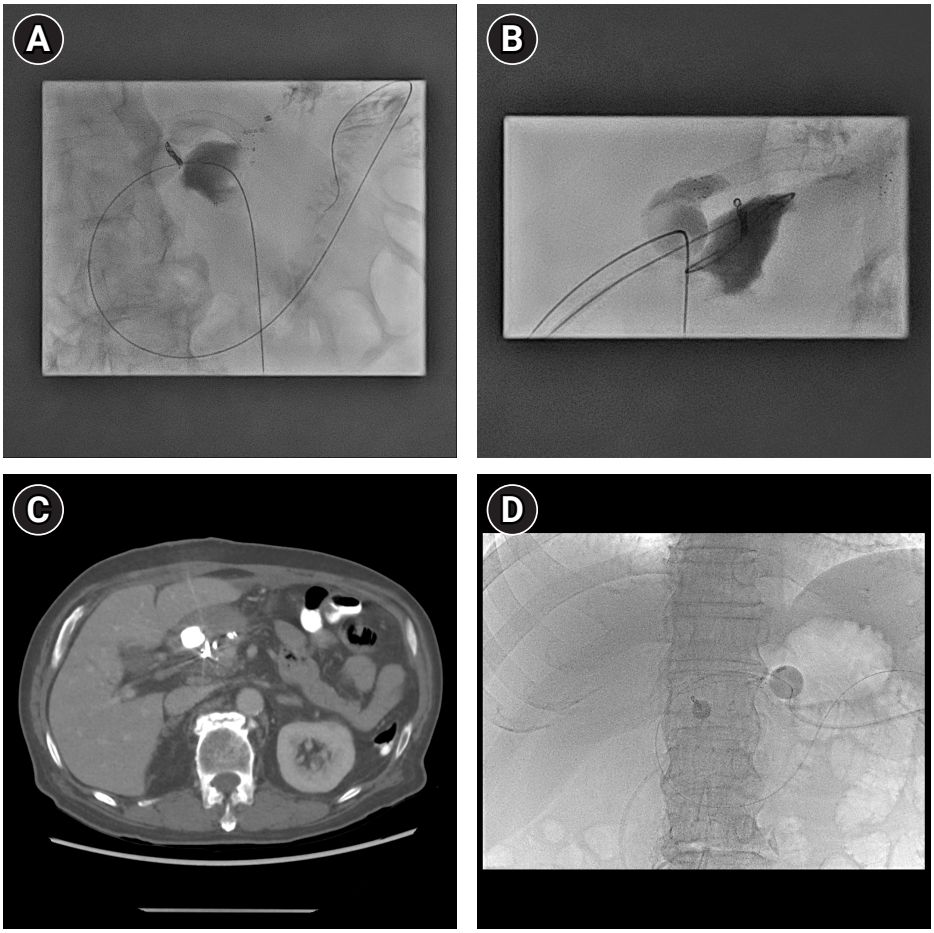


Fig. 4. Catheter-directed controlled fistula formation. (A) Through the drainage tract, the fistula was cannulated with a 5-Fr Kumpe catheter and a 0.035-inch guidewire, and access into the duodenal lumen was achieved. (B) An 8-Fr silicone-coated latex Foley balloon catheter (SEWOON Medical, Cheonan, Korea) was positioned across the fistula and its balloon inflated within the duodenal lumen to secure the tract. (C) Axial CT after the procedure demonstrates the balloon within the duodenal lumen. (D) A percutaneous gastrojejunostomy was created to deliver enteral nutrition distal to the fistula.

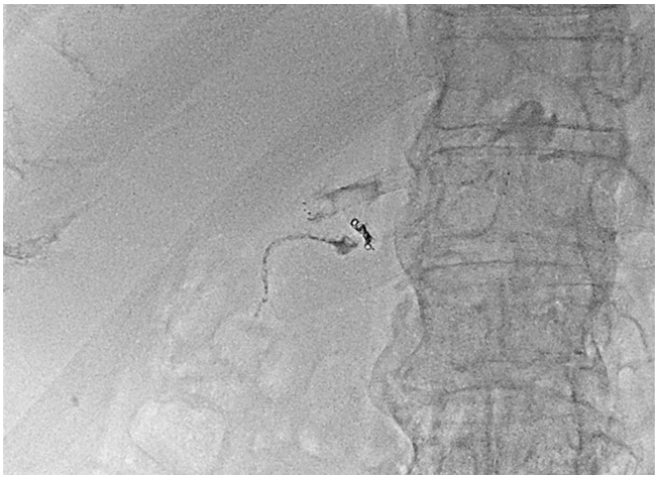


Fig. 5. Removal of the Foley catheter and embolization of the percutaneous tract. Tubography demonstrated a mature fistulous tract without extraluminal leakage. The tract was then embolized with a 1:1 mixture of N-butyl cyanoacrylate and ethiodized oil while the catheter was gradually withdrawn, to minimize residual leakage.

interventional management. At the outpatient visit 2 weeks after discharge, the patient was asymptomatic and tolerated oral intake, with no clinical evidence of recurrent leakage; follow-up was clinical, and no follow-up imaging was obtained.

The requirement for institutional review board review was waived by the Institutional Review Board of Seoul National University Bundang Hospital because of the retrospective nature of this case report (IRB No. B-2608-1065-102). Written informed consent for publication of this case and the accompanying images was obtained from the patient.

Discussion

Duodenal fistula arising after pancreatic and periduodenal surgery is an uncommon but potentially lethal complication, and its management in the postoperative setting is particularly problematic. Early reoperation within a recently operated field is technically demanding because of altered anatomy, dense adhesions, and tissue friability, and primary repair or omental patch closure frequently fails under these conditions. Reported complication rates after surgical management of duodenal perforation range from 42% to 58% [2,3], and revision surgery has been required in up to 67% of retroperitoneal duodenal perforations managed operatively [4]. A meta-analysis of post-ERCP perforations found no mortality advantage for initial surgery over non-operative management [10], supporting consideration of less invasive alternatives in appropriately selected patients.

Advances in endoscopy and interventional radiology have expanded the non-operative options for duodenal perforation. Covered self-expandable metal stents can seal iatrogenic defects with high technical and clinical success [7,8], and endoscopic vacuum therapy has yielded promising closure rates in early series [9]. These endoscopic approaches, however, depend on adequate luminal access, may require repeated endoscopic sessions for device exchange or removal, and are supported mainly by small, heterogeneous reports. In the postoperative abdomen with distorted anatomy, repeated transluminal intervention may be impractical, increasing the appeal of a purely percutaneous, image-guided strategy.

The mechanism of the duodenal fistula in this case appears multifactorial. The patient had an established POPF, and enzyme-rich pancreatic fluid is itself capable of eroding adjacent vascular and enteric structures; indeed, the GDA bleeding 3 weeks after surgery is attributable to this process. Superimposed on this, the duodenal wall had been subjected to sequential loss of arterial inflow—first stent-graft exclusion of the GDA and, approximately 2 weeks later, embolization of a duodenal branch with a liquid agent that penetrates to the distal arteriolar level. Although the pancreaticoduodenal arcades usually provide robust collateral supply, cumulative devascularization within a field already compromised by enzymatic inflammation and hematoma may reduce mural perfusion beyond the compensatory capacity of the arcade. The fistula was demonstrated only three days after embolization, a sequence compatible with post-embolization mural ischemia in addition to enzymatic and operative injury. The relative contributions of these mechanisms cannot be established from a single case; nevertheless, the sequence is clinically instructive, since embolization of duodenal branches in a patient whose proximal inflow has already been excluded may warrant anticipatory surveillance for mural injury, for which percutaneous techniques such as those described here offer a means of management without reoperation.

The core principle of interventional management is to eliminate the fluid collection and convert an uncontrolled leak into a controlled, externally drained fistula using image-guided PCD [5,6,11]. Percutaneous Foley catheter placement has been reported as a safe and effective means of achieving this

conversion in postoperative duodenal stump leakage, with successful luminal placement and no procedure-related complications in a consecutive series [12]. The duodenum, however, is a high-pressure, high-motility segment continuously exposed to bile and pancreatic secretions, so drainage alone may be insufficient to divert luminal content and allow the tract to close. In the present case, a Foley catheter was advanced across the fistula and its balloon inflated within the duodenal lumen, reducing free efflux of enteric content into the tract. The objective effect of this maneuver was reflected in the drainage output, which fell from approximately 300 mL/day, sustained over the preceding 5 days despite adequate drainage, to approximately 20 mL/day after balloon occlusion. We additionally considered whether the tissue reactivity of latex-based catheters, relative to all-silicone drains, might favor fibrous tract maturation, an inference extrapolated from urological biocompatibility data in which latex catheters provoke greater inflammatory reaction and tissue trauma than silicone [13,14]. This rationale remains speculative. It has not been validated for enteric fistula tracts; the catheter used here was silicone-coated latex, so the tissue-contacting surface was not bare latex; and in a single case the contribution of catheter material cannot be separated from those of prolonged indwelling and mechanical balloon occlusion. We therefore regard balloon occlusion as the principal mechanism and any material-related effect as unproven and hypothesis-generating. A conceptually similar catheter-based approach has been reported for post-ERCP duodenal perforation [1].

To further support healing, a percutaneous gastrojejunostomy was placed so that enteral nutrition could be delivered distal to the fistula, maintaining nutritional status while minimizing passage of ingested content across the defect—a consideration of particular relevance for proximal, higher-output fistulas [11]. Tract embolization at the time of catheter removal was performed to minimize residual leakage along the mature tract rather than as salvage for failed tract formation, and we regard it as an integral final step of the technique. Under this combined strategy the patient recovered and was discharged approximately 2 months after the initial drainage. This report describes a single case and should be regarded as proof of concept; the technique requires validation in larger series, and criteria for patient selection and for conversion to surgery when interventional management fails remain to be defined. Nonetheless, the case illustrates that a staged, entirely percutaneous strategy—collection drainage, balloon-assisted controlled fistula formation, distal enteral feeding, and tract embolization at catheter removal—can be a feasible option for complex postoperative duodenal fistula or perforation, including cases in which ischemic injury after sequential arterial interventions may have contributed, when reoperation is difficult or infeasible.

Conflict of interest

No potential conflict of interest relevant to this article was reported.

Funding

None.

Acknowledgments

None.

Author contributions

Conceptualization: JHL, CJY. Investigation: JHL, KYK. Supervision: CJY. Writing - original draft: JHL. Writing - review & and editing: JHL, KYK, CJY.

Data availability statement

Data sharing does not apply to this article as no datasets were generated or analyzed during the current study.

ORCID

Jae Hwan Lee, https://orcid.org/0000-0001-6513-3224
Kun Yung Kim, https://orcid.org/0000-0002-2018-8130
Chang Jin Yoon, https://orcid.org/0000-0002-7660-0489

References

1. Ma Y, Bi Y, Wei C, Ding X, Zhou G, Yin M, et al. Interventional three-tube method for the management of duodenal perforation after endoscopic retrograde cholangiopancreatography for choledocholithiasis: a case series. Quant Imaging Med Surg. 2025;15:7563-7571. https://doi.org/10.21037/qims-2024-2650
2. Arroyo Vazquez JA, Khodakaram K, Bergstrom M, Park PO.

Stent treatment or surgical closure for perforated duodenal ulcers: a prospective randomized study. Surg Endosc. 2021;35:7183-7190. https://doi.org/10.1007/s00464-020-08158-3

3. Negm S, Mohamed H, Shafiq A, AbdelKader T, Ismail A, Yassin M, et al. Combined endoscopic and radiologic intervention for management of acute perforated peptic ulcer: a randomized controlled trial. World J Emerg Surg. 2022;17:24. https://doi.org/10.1186/s13017-022-00429-9
4. Yurttas C, Thiel C, Wichmann D, Horvath P, Strohaker J, Bongers MN, et al. Retrospective analysis of different therapeutic approaches for retroperitoneal duodenal perforations. Sci Rep. 2022;12:10243. https://doi.org/10.1038/s41598-022-14278-8
5. McCarthy CJ, Butros SR, Dawson SL, Arellano RS. Image-guided percutaneous management of duodenal perforation following endoscopic retrograde cholangiopancreatography (ERCP): assessment of efficacy and safety. Clin Radiol. 2018;73:319.e9-319.e15. https://doi.org/10.1016/j.crad.2017.09.014
6. Rahman MM, Al Mamun A, Hossain MD, Das MK. Peptic ulcer perforation: management of high-risk cases by percutaneous abdominal drainage. Trop Doct. 2005;35:30-31. https://doi.org/10.1258/0049475053001822
7. Sbrozzi-Vanni A, Galloro G, Piciucchi M, Castellani D, Germani U, Dell'Amico I, et al. Over-the-scope technique for partially covered self-expandable metal stent placement to treat duodenal perforation during EUS. J Gastrointestin Liver Dis. 2023;32:65-69. https://doi.org/10.15403/jgld-4625
8. Bergstrom M, Arroyo Vazquez JA, Park PO. Self-expandable metal stents as a new treatment option for perforated duodenal ulcer. Endoscopy. 2013;45:222-225. https://doi.org/10.1055/s-0032-1325885
9. Chevallay M, Lorenz F, Bichard P, Frossard JL, Schmidt T, Goeser T, et al. Outcome of endoscopic vacuum therapy for duodenal perforation. Surg Endosc. 2023;37:1846-1853. https://doi.org/10.1007/s00464-022-09686-w
10. Samara A, Diamantis A, Perivoliotis K, Mavrovounis G, Simeonidis D, Baloyiannis I, et al. Initial management of duodenal perforations after ERCP: a systematic review and meta-analysis. HPB (Oxford). 2022;24(Suppl 1):S541. https://doi.org/10.1016/j.hpb.2022.05.1172
11. Ghimire P. Management of enterocutaneous fistula: a review. JNMA J Nepal Med Assoc. 2022;60:93-100. https://doi.org/10.31729/jnma.5780
12. Oh JS, Lee HG, Chun HJ, Choi BG, Lee SH, Hahn ST, et al. Percutaneous management of postoperative duodenal stump leakage with Foley catheter. Cardiovasc Intervent Radiol. 2013;36:1344-1349. https://doi.org/10.1007/s00270-012-0518-6
13. Liedberg H. Catheter induced urethral inflammatory reaction and urinary tract infection: an experimental and clinical study. Scand J Urol Nephrol Suppl. 1989;124:1-43.
14. Nickel JC, Olson ME, Costerton JW. In vivo coefficient of kinetic friction: study of urinary catheter biocompatibility. Urology. 1987;29:501-503. https://doi.org/10.1016/0090-4295(87)90037-9

Review Article

eISSN 2508-2612
https://doi.org/10.64961/kjir.2026.00045
Korean J Interv Radiol 2026;31(2):92-102

KJIR

Drug-Coated Balloon Angioplasty for Dysfunctional Hemodialysis Access: An Update

Kichang Han*

Department of Radiology, University of California Los Angeles (UCLA) Medical Center, Los Angeles, CA, USA

Hemodialysis vascular access dysfunction remains a major cause of morbidity and repeated interventions. Stenosis related to neointimal hyperplasia and altered hemodynamics leads to access flow limitation and thrombosis, particularly in AVFs. While percutaneous transluminal angioplasty is the standard first-line treatment, durability is often limited, resulting in frequent reinterventions. Drug-coated balloons, most commonly paclitaxel-based, have been introduced to inhibit restenosis and have demonstrated improved target lesion patency compared with conventional balloon angioplasty in several randomized trials, though outcomes vary by lesion location and study design. This narrative review summarizes the current evidence for drug-coated balloon angioplasty in dysfunctional arteriovenous access, discusses key trial endpoints, reviews safety and practical considerations, and highlights ongoing controversies and future directions.

Keywords: Angioplasty; Arteriovenous fistula; Hemodialysis

Introduction

Maintaining long-term patency of hemodialysis vascular access remains a persistent challenge in patients with end-stage renal disease. AVFs, although preferred for durability and lower infection risk, frequently develop stenosis that compromises access flow and necessitates repeated interventions. Percutaneous transluminal angioplasty (PTA) has long been the cornerstone of treatment and provides excellent immediate technical success [1,2]. However, contemporary outcomes after plain balloon angioplasty remain suboptimal: post-PTA primary patency at 1 year is typically only 40% to 65% for AVFs and 20 to 50% for AVGs [3-6]. Consequently, restenosis is common, and many patients require multiple repeat procedures to maintain access function.

Over the past decade, drug-coated balloon (DCB) angioplasty has emerged as a strategy to improve the durability of endovascular treatment by combining mechanical dilation with local delivery of antiproliferative therapy. Overall, available evidence suggests that DCBs tend to provide favorable outcomes compared with plain balloon angioplasty in dysfunctional arteriovenous (AV) access; however, several randomized controlled trials (RCTs) and registry studies have also reported no statistically significant benefit in certain settings [7-9]. These mixed findings likely reflect differences in lesion location, access type, device characteristics, and procedural technique.

In this review, we first outline the pathophysiology of AV access stenosis from an interventional radiology perspective, then summarize the scientific rationale and clinical evidence

Received: February 27, 2026; **Revised:** April 21, 2026;
Accepted: April 21, 2026
***Corresponding email:** kichang.rad@gmail.com

© 2026 Korean Society of Interventional Radiology

This is an Open Access article distributed under the terms of the Creative Commons Attribution Non-Commercial License (http://creativecommons.org/licenses/by-nc/4.0) which permits unrestricted non-commercial use, distribution, and reproduction in any medium, provided the original work is properly cited.

for DCB angioplasty, discuss key technical and safety considerations, and highlight current knowledge gaps and future directions in the management of failed AVFs.

An AV Access Stenosis: An Interventional Radiology Perspective on Pathophysiology

From an interventional radiology perspective, AV access stenosis can be understood as a cycle of repeated vascular injury followed by an exaggerated healing response. The initiating or upstream events include surgical manipulation during fistula creation, exposure of the vein to high-pressure arterial flow and abnormal shear stress, uremia-related endothelial dysfunction, and repeated needle cannulation during dialysis. These injuries activate endothelial inflammation and thrombotic signaling, which lead to the downstream biologic response including migration and proliferation of vascular smooth muscle cells and fibroblasts, extracellular matrix deposition, and progressive intimal thickening known as neointimal hyperplasia (NIH) [10-12]. As the lumen narrows, disturbed flow further amplifies endothelial injury, creating a self-perpetuating cycle of stenosis. Importantly for interventionalists, balloon angioplasty relieves the obstruction mechanically but also causes additional barotrauma, which represents another upstream injury that can trigger the same downstream proliferative cascade and explains the high rate of restenosis [13-15]. Thus, AV access stenosis is not purely a mechanical problem but a biologic response to repeated injury, providing the rationale for antiproliferative strategies such as DCBs to interrupt this upstream–downstream cycle and potentially improve long-term patency.

Biological Rationale and Device Characteristics of DCBs

Recurrent stenosis in dysfunctional AV access is driven by NIH resulting from repeated vascular injury, as described above. DCBs were developed to interrupt this proliferative cascade at the time of angioplasty [16]. Unlike plain balloon angioplasty, which mechanically fractures the lesion but leaves the biological response unchecked, DCBs deliver an antiproliferative drug directly to the vessel wall during balloon inflation. Paclitaxel, the most widely used agent, stabilizes microtubules and arrests smooth muscle cell division, suppressing neointimal growth while allowing endothelial recovery [17,18]. Because of its lipophilicity, brief balloon contact can achieve sustained tissue retention and prolonged biologic effect [19].

The concept of local antiproliferative drug delivery has been validated in other vascular territories. DCBs were first widely adopted in femoropopliteal peripheral artery disease, where randomized trials showed improved patency compared with plain balloon angioplasty in selected lesions, and they later became an established treatment for coronary instent restenosis and small-vessel coronary disease [20,21]. Experience has also extended to venous stenoses, including AV access stenoses and central venous lesions, although outcomes have been more variable due to differences in vessel biology and hemodynamics [22]. These cross-territory experiences support the biologic rationale for DCB use while highlighting that AVFs represent a unique environment characterized by extreme flow, repetitive puncture injury, and complex upstream–downstream dynamics that may modify treatment response.

Commercial DCB platforms differ in several design features that may influence clinical performance (Table 1). Each device combines a balloon catheter, an antiproliferative drug, and an excipient that facilitates drug transfer. Balloon compliance and surface properties affect vessel wall contact, while drug dose density, coating stability, and excipient chemistry determine how much drug is retained during delivery and transferred into the vessel wall [23]. In practice, these differ-

Table 1. Drug-coated balloon used in hemodialysis access trials

Brand name (manufacturer)	Paclitaxel dose (μg/mm^2)	Excipient material	Balloon diameter (mm)
In.Pact (Medtronic)	3.5	Urea	4–12
Lutonix (Becton Dickison)	2.0	Polysorbate and sorbitol	4–12
APERTO (Cardionovum)	3.0	Ammonium salt	5–10
Passeo-18 Lux (Biotronik)	3.0	Hydrophobic butyryl-tri-hexyl citrate	2–7
AcoArt Orchid (Acotec)	3.3	Magnesium stearate	4–12

ences contribute to variable patency outcomes among devices, particularly in lesions with elastic recoil, calcification, or inadequate predilation [24-27]. Accordingly, careful lesion preparation, appropriate balloon sizing, sufficient inflation time, and avoidance of geographic miss remain essential to maximize drug delivery and clinical benefit.

Evolution of Randomized Evidence for DCB Angioplasty in Dialysis Access

To date, most RCTs evaluating DCB angioplasty in dialysis access have focused predominantly on AVFs rather than grafts. Since the initial clinical reports in 2012, multiple RCTs have examined whether DCB angioplasty improves patency compared with plain balloon angioplasty [28,29]. Overall, a substantial portion of the literature suggests meaningful benefit, but results remain heterogeneous across trials.

Evidence in Native AV Fistula

The most influential evidence comes from the IN.PACT AV Access, a multicenter RCT enrolling 330 patients with dysfunctional native AVFs [24]. The target lesion primary patency (TLPP) was significantly higher with DCB than conventional balloon (CB) (82.2% vs. 59.5% at 6 months, $p < 0.001$). The advantage persisted at 12 months (63.8% vs. 43.6%, $p < 0.001$) with a 35.4% reduction in reinterventions required to maintain TLPP (total 93 vs. 144) [30]. Extended follow-up through 36 months further supported durability: event-free TLPP remained higher (43.1% vs. 28.6%, $p < 0.001$), and access-circuit primary patency was improved (33.2% vs. 21.1%, $p < 0.001$) in the DCB group [31].

By contrast, the Lutonix AV trial showed a smaller and time-dependent signal. At the prespecified primary analysis, TLPP at 6 months was 71% (DCB) vs. 63% (CB) ($p = 0.06$), narrowly missing statistical significance. An analysis allowing a 30-day window (9 months) showed TLPP 64% vs. 53% ($p = 0.02$). In the 2-year follow-up, TLPP differences were modest and time-dependent (12 months: 44% vs. 36%, $p = 0.04$; 24 months: 27% vs. 24%, $p = 0.09$), with no mortality difference through 2 years [25,32]. Importantly, even recent RCTs continue to report opposing signals, underscoring persistent controversy. In a contemporary RCT by Zhao et al. [33], 12-month TLPP remained significantly higher with DCB than CB (66.1% [74/112] vs. 46.4% [52/112], $p = 0.0037$), with higher freedom from reintervention at 12 months (67.5% vs. 48.6%, $p = 0.0006$) and fewer reinterventions to maintain target lesion patency (48 vs. 94 total; mean, 0.4 vs 0.8 per patient; $p = 0.001$) [33]. In contrast, the multicenter APERTO trial did not demonstrate a significant improvement in its primary clinical outcome at 1 year: functional hemodialysis access without reintervention at 12 months was achieved in 19.6% (10/51) of DCB group versus 9.6% (5/52) in the CB group ($p = 0.612$), and the authors concluded that longer adequate circuit function with DCB could not be shown [34].

Within the native AV access circuit, lesion location appears to influence treatment response. In particular, cephalic arch stenosis is a lesion in which restenosis after CB angioplasty is frequent, largely because elastic recoil, marked vessel angulation with turbulent hemodynamics, and potential extrinsic compression often limit durable luminal gain. In this setting, a systematic review and meta-analysis focused on cephalic arch stenosis found no significant difference between DCB and CB angioplasty in primary patency at 6 and 12 months, suggesting that biologic inhibition of NIH alone may not fully overcome the predominant mechanical failure mechanisms [35]. For central venous stenosis, clinical evidence specifically evaluating DCB angioplasty remains sparse. By analogy to cephalic arch stenosis, central venous lesions are frequently driven by elastic recoil, extrinsic compression, and long-segment fibrotic remodeling, mechanisms that can limit durable luminal gain after angioplasty. Therefore, it is plausible that the clinical effect of DCB angioplasty may likewise be attenuated in central venous stenosis.

Key aspects of trial design and major outcomes are presented in Tables 2 and 3 [24-28,31-34,36-47]. As shown in these tables, there is substantial heterogeneity across studies with respect to the DCB platform, procedural technique, and the definitions of clinical and patency endpoints. In particular, differences between TLPP and access-circuit primary patency (ACPP) may contribute to variability in reported outcomes, as improvements in lesion-level patency do not necessarily translate into overall access durability. Taken together, the randomized evidence base in native AVFs more often suggests improved patency with DCB angioplasty; however, recent trials continue to report both positive and neutral findings. This pattern supports the concept that the clinical benefit of DCBs

Table 2. Design characteristics and procedural techniques in randomized trials

Study	Publication year	No. of patients	Access type (AVF or AVG)	Lesion type (de novo or recurrent)	Vessel preparation	DCB type	Inflation time (s)
Katsanos et al. [28]	2012	40	Both	NR	No	In.Pact	>60
Kitrou et al. [36]	2015	40	AVF	Both	No	In.Pact	90
Irani et al. [37]	2018	119	Both	Both	Yes	In.Pact	60
Trerotola et al. [25,32]	2018	285	AVF	Both	Yes	Lutonix	>30
Maleux et al. [38]	2018	64	AVF	Both	Yes	In.Pact	NA
Bjorkman et al. [39]	2019	36	AVF	Both	Yes	In.Pact	90
Kim et al. [26]	2020	39	AVF	Both	Yes	In.Pact	120
Karmota [40]	2020	60	AVF	NR	Yes	Lutonix	180
Liao et al. [41]	2020	44	AVG	Recurrent	No	In.Pact	60
Lookstein et al. [24]	2020	330	AVF	Both	Yes	In.Pact	>180
Moreno-Sanchez et al. [42]	2020	148	Both	Both	Yes	Passeo-Lux	45
Pang et al. [43]	2021	40	Both	Both	Yes	In.Pact	180
Karunanithy et al. [27]	2021	212	AVF	Both	Yes	Lutonix	>60
Yin et al. [44]	2021	161	AVF	Both	Yes	APERTO	120–180
Therasse et al. [45]	2021	120	Both	Both	Yes	Passeo-Lux	60
Goo et al. [46]	2024	190	AVG	Both	Yes	In.Pact	180
Zhao et al. [33]	2024	244	AVF	Both	Yes	AcoArt	120
Maleux et al. [34]	2025	103	Both	Both	No	APERTO	60–120

DCB, drug-coated balloon; NR, not reported; NA, not available.

is context-dependent and underscores the need for additional standardized, lesion-specific randomized trials.

Evidence in AVGs

Evidence supporting DCB angioplasty in AVGs has historically been limited, as most randomized trials enrolled predominantly AVF patients and included only small numbers of graft lesions. One early single-center randomized trial by Liao et al. [41] evaluated 44 dysfunctional AVGs with venous anastomotic stenosis and reported significantly higher 6-month TLPP in the DCB group compared with CB angioplasty (41% vs. 9%, p = 0.001), as well as higher 6-month ACPP (36% vs. 9%, p = 0.002) [42]. However, this benefit was not sustained at 1 year, with 1-year ACPP of 14% vs. 9% (p = 0.273), suggesting that short-term improvement may not translate into durable long-term outcomes in AVGs.

More recently, a prospective multicenter RCT by Goo et al. [46] specifically enrolled patients with dysfunctional AVGs caused by venous anastomotic stenosis and randomized 94 patients to DCB and 92 to CB angioplasty after successful lesion preparation. DCB angioplasty demonstrated significantly higher TLPP at 3 months (91.1% vs. 74.4%, p < 0.001) and 6 months (64.6% vs. 43.2%, p = 0.002), as well as improved ACPP at 6 months (63.4% vs. 42.0%, p = 0.002) and 12 months (29.1% vs. 14.6%, p = 0.022). Mortality at 12 months was similar between groups, although early thrombotic events within 3 months were more frequent in the DCB arm. This finding suggests a potential trade-off between short-term patency benefit and early thrombotic risk. Clinically, close early surveillance may help mitigate its impact, and further studies are needed to clarify the role of peri-procedural management in influencing these events.

Together, these studies suggest that DCB angioplasty may improve short- to mid-term patency in AVG stenosis but the evidence base remains smaller than that for AVFs, and long-term durability and lesion-specific benefit require further investigation.

Technical Considerations for DCB Angioplasty

Vessel Preparation

DCBs should be viewed primarily as drug delivery platforms rather than definitive angioplasty tools. Therefore, outcomes often depend on how well the lesion is prepared before DCB use. In AV access, DCBs are compliant or semi-compliant and are not designed for high-pressure dilation. Their nominal inflation pressures are typically around 5 to 8 atmo-

Table 3. Clinical outcomes of randomized trials comparing DCB and CB angioplasty

Study	Publication year	Primary endpoint	Outcomes	Significant effect	Significant AE difference
Katsanos et al. [28]	2012	TLPP at 6 mo	70% (DCB) vs. 25% (CB), $p < 0.001$	Yes	No
Kitrou et al. [36]	2015	TLPP at 12 mo	35% (DCB) vs. 5% (CB), $p < 0.001$	Yes	No
Irani et al. [37]	2018	TLPP at 6 mo	81% (DCB) vs. 61% (CB), $p = 0.03$	Yes	No
Trerotola et al. [25,32]	2018	TLPP at 6, 9, 12, 24 mo	71% (DCB) vs. 63% (CB) at 6 mo, $p = 0.06$ 58% (DCB) vs. 46% (CB) at 9 mo, $p = 0.02$ 44% (DCB) vs. 36% (CB) at 12 mo, $p = 0.04$ 27% (DCB) vs. 24% (CB) at 24 mo, $p = 0.09$	No[a]	No
Maleux et al. [38]	2018	ACPP at 6, 12 mo	68% (DCB) vs. 65% (CB) at 6 mo, $p = 0.8$ 42% (DCB) vs. 39% (CB) at 12 mo, $p = 0.95$	No	No
Bjorkman et al. [39]	2019	TLR at 12 mo	89% (DCB) vs. 22% (CB), $p = 0.001$	No	No
Kim et al. [26]	2020	TLPP at 12 mo	65% (DCB) vs. 58% (CB) at 12 mo, $p = 0.9$	No	No
Karmota [40]	2020	TLPP at 6, 12 mo	97% (DCB) vs. 90% (CB) at 6 mo, $p = 0.3$ 90% (DCB) vs. 67% (CB) at 12 mo, $p = 0.03$	No[a]	No
Liao et al. [41]	2020	TLPP at 6 mo	41% (DCB) vs. 9% (CB), $p = 0.006$	Yes	No
Lookstein et al. [24,31,47]	2020	TLPP at 6, 12, 24, 36 mo	82% (DCB) vs. 60% (CB) at 6 mo, $p < 0.001$ 63.8% (DCB) vs. 43.6% (CB) at 12 mo, $p < 0.001$ 52.1% (DCB) vs. 36.7% (CB) at 24 mo, $p < 0.001$ 43.1% (DCB) vs. 28.6% (CB) at 36 mo, $p < 0.001$	Yes	No
Moreno-Sanchez et al. [42]	2020	TLPP at 6 and 12 mo	153 days (DCB) vs. 142 days (CB) at 6 mo, $p = 0.07$ 266 days (DCB) vs. 238 days (CB) at 12 mo, $p = 0.37$	No	No
Pang et al. [43]	2021	TLPP at 12 mo	65% (DCB) vs. 30% (CB), $p = 0.007$	Yes	No
Karunanithy et al. [27]	2021	Time to lose TLPP at 6 mo	159 days (DCB) vs. 215 days (CB), $p = 0.44$	No	No
Yin et al. [44]	2021	TLR-free survival at 6 mo	86% (DCB) vs. 78% (CB), $p = 0.3$	No	No
Therasse et al. [45]	2021	LLL at 6 mo	0.64 mm (DCB) vs. 1.13 mm (CB), $p = 0.08$	No	No
Goo et al. [46]	2024	TLPP at 3, 6 mo	91.1% (DCB) vs. 64.6% (CB) at 3 mo, $p = 0.001$ 74.4% (DCB) vs. 43.2% (CB) at 6 mo, $p = 0.001$	Yes	Yes (thrombosis)
Zhao et al. [33]	2024	TLPP at 6 mo	91% (DCB) vs. 67% (CB), $p < 0.001$	Yes	No
Maleux et al. [34]	2025	TLPP at 12 mo	19.6% (DCB) vs. 9.6% (CB), $p = 0.612$	No	No

DCB, drug-coated balloon; CB, conventional balloon; AE, adverse event; TLPP, target lesion primary patency; ACPP, access-circuit primary patency; TLR, target lesion revascularization; LLL, late lumen loss.
[a]No, partially met.

spheres, with burst pressures around 12 to 14 atmospheres for commonly used platforms [23,48]. As a result, resistant venous stenoses that require higher pressures to fully eliminate balloon waist may not respond well to a DCB alone. For this reason, operators should first perform predilation with a high-pressure plain balloon to achieve an acceptable mechanical result. Trials commonly define this as 30% or less residual stenosis and no flow-limiting dissection [24,25]. Adequate predilation is also a simple angiographic test of whether the lesion is treatable with a DCB. For long or tandem lesions, careful measurement and segment-by-segment preparation help ensure full coverage and reduce the risk of geographic miss.

Balloon Handling and Transit Time

Because part of the drug coating can be lost before balloon inflation, keeping balloon transit time short is an important step. Drug loss may occur during device preparation, advancement through the sheath, or navigation across tight or tortuous segments [49,50]. To reduce avoidable coating loss, it is practical to complete all preparatory steps before opening the DCB package and to prepare the DCB only when the operator is ready for immediate deployment. Once introduced, the DCB should be advanced efficiently to the target lesion to minimize transit time, avoiding repeated push and pull maneuvers, unnecessary repositioning, or prolonged dwell time within the sheath [51]. When feasible, selecting an access route that shortens the distance to the lesion and using an adequately sized sheath to reduce friction may further help pre-

serve the coating during delivery. These workflow details are rarely captured in clinical trial endpoints, but they can influence the effective drug dose delivered in real-world practice.

Inflation Time

Because DCB angioplasty is intended to achieve local pharmacologic effect, inflation time should be selected to ensure sustained and uniform balloon-wall contact that supports drug deposition and tissue uptake. In contemporary AV access practice, inflation durations commonly fall within 60- to 180-second range per treated segment, with some protocols favoring longer inflations when balloon position is stable and the patient can tolerate prolonged occlusion [52].

Notably, real-world registry data have suggested a time-dependent signal. In the prospective registry, 6-month TLPP was higher with longer inflation, with TLPP increasing across longer inflation time (68% for 50–120 seconds vs. 80% for 120–180 seconds; p = 0.007), implying that longer contact may improve clinical durability [53]. Similar themes have been raised in meta-analyses, although it remains difficult to isolate the independent contribution of inflation time from other tightly linked determinants of success, such as lesion preparation quality, balloon sizing, device platform, and avoidance of geographic miss [22].

Accordingly, when satisfactory vessel preparation has already been achieved and the balloon can be maintained in a stable position, a minimum DCB inflation time of ≥3 minutes (≥180 seconds) seems to be reasonable to maximize the likelihood of effective drug transfer, while acknowledging that the optimal duration is not definitively established and should be refined by future protocolized studies.

Safety Profile of DCBs in Dialysis Access Interventions

The safety of DCB angioplasty in AV access has been evaluated with attention to systemic paclitaxel exposure, downstream embolization, and long-term outcomes. Although DCBs are designed for local drug delivery, a small amount of drug may be lost during device handling, transit, or inflation, resulting in only limited systemic exposure. The total paclitaxel dose used in AV access procedures is far lower than that used in systemic cancer therapy, and current clinical trials in dialysis access have not shown a consistent increase in morbidity and mortality [54].

Concerns about possible late mortality from paclitaxel-coated devices were first raised in peripheral arterial disease studies [55]. However, this signal has not been clearly reproduced in AV access trials, and subsequent individual patient data analyses in femoropopliteal peripheral arterial disease have also not demonstrated a significant increase in mortality associated with paclitaxel-coated devices [56,57]. These findings are generally reassuring; however, they should be interpreted with caution in the dialysis population. Patients with hemodialysis access frequently undergo repeated endovascular interventions, which may result in higher cumulative paclitaxel exposure over time compared with patients treated for peripheral arterial disease. In addition, their distinct comorbidity profile and competing risks may modify both short- and long-term outcomes, underscoring the need for continued surveillance and long-term safety evaluation in this population.

Additional procedural safety considerations include non-target particulate embolization from balloon coatings, especially with excessive device handling or prolonged transit time, and the possibility of vessel injury if DCBs are used without adequate lesion preparation [49,50]. Overall, available evidence suggests that DCB angioplasty has an acceptable safety profile in AV access interventions [9,58,59]. Nevertheless, careful patient selection, standardized technique, and long-term follow-up remain essential to fully define its risk-benefit balance.

Korean Reimbursement Landscape and Real-World Practice Considerations

In Korea, reimbursement for DCB angioplasty in hemodialysis access was introduced in May 2025, but its application remains restricted to narrowly defined clinical scenarios. Under the current national insurance criteria, DCB use is reimbursed for stenotic lesions in native AVFs or AVG when recurrent stenosis is documented within 3 months after prior plain balloon angioplasty at the same lesion. Accordingly, primary DCB use without evidence of early restenosis after conventional angioplasty is not reimbursed, which has an important impact on real-world case selection and treatment strategy. From a prac-

tice standpoint, these criteria concentrate DCB use in patients with biologically aggressive restenosis or early failure after PTA, thereby enriching Korean DCB-treated cohorts for higher-risk lesions compared with many Western settings where DCB use may be more readily implemented in routine practice. This reimbursement-driven selection effect should be considered when interpreting domestic outcomes, comparing Korean real-world data with international studies, and designing future studies, as observed effectiveness may be attenuated or appear more variable when the treated population is skewed toward early recurrent stenosis. As Korean experience expands under the current reimbursement system, prospective registries and lesion-specific studies that explicitly account for these policy constraints will be valuable to define the most cost-effective and clinically impactful indications for DCB use in dialysis access maintenance.

Knowledge Gaps and Future Directions

DCBs show promise for maintaining AV access, but evidence remains heterogeneous. A major gap is that outcomes are highly lesion- and technique-dependent; differences in lesion preparation, balloon sizing, inflation strategy, and technical endpoints likely contribute to inconsistent RCT results. Accordingly, future multicenter trials should standardize procedural protocols and stratify by lesion location and access characteristics to clarify where DCBs provide the most benefit.

Another key gap is the unique biology and hemodynamics of AV access such as high flow, repeated cannulation injury, and complex upstream–downstream stresses, which may alter drug transfer and durability compared with arterial applications. Mechanistic studies linking hemodynamics, tissue drug retention, and imaging/pathology are needed. Finally, device variability lacks robust head-to-head data and comparative effectiveness and safety studies including repeated exposure in patients needing frequent reinterventions remain priorities. Overall, progress will depend on combining better lesion selection with standardized technique and evaluating emerging platforms such as sirolimus-based coatings or combination strategies with lesion preparation devices.

Conclusion

DCB angioplasty offers a biologically targeted adjunct to conventional angioplasty for dysfunctional AV access by suppressing the NIH that drives recurrent stenosis. While randomized trials suggest improved patency in selected settings, results remain heterogeneous and appear dependent on lesion characteristics, device design, and procedural technique. Overall, DCBs have an acceptable safety profile and may provide meaningful benefit when used after high-quality vessel preparation with careful attention to delivery factors. Future studies should standardize technique and refine lesion-specific selection to better define where DCBs add the greatest value in AV access maintenance.

Conflict of interest

No potential conflict of interest relevant to this article was reported.

Funding

None.

Acknowledgments

None.

Author contributions

The author conducted all aspects of the study.

Data availability statement

The datasets generated or analyzed during the study are available from the corresponding author on reasonable request.

ORCID

Kichang Han, https://orcid.org/0000-0002-9701-9757

References

1. Lok CE, Moist L. KDOQI 2019 Vascular access guidelines: what is new? Adv Chronic Kidney Dis. 2020;27:171-176. https://doi.org/10.1053/j.ackd.2020.02.003
2. Beathard GA. Percutaneous transvenous angioplasty in the treatment of vascular access stenosis. Kidney Int. 1992;42:

1390-1397. https://doi.org/10.1038/ki.1992.431
3. Lawson JH, Niklason LE, Roy-Chaudhury P. Challenges and novel therapies for vascular access in haemodialysis. Nat Rev Nephrol. 2020;16:586-602. https://doi.org/10.1038/s41581-020-0333-2
4. Rajan DK, Bunston S, Misra S, Pinto R, Lok CE. Dysfunctional autogenous hemodialysis fistulas: outcomes after angioplasty: are there clinical predictors of patency? Radiology. 2004;232:508-515. https://doi.org/10.1148/radiol.2322030714
5. Heye S, Maleux G, Vaninbroukx J, Claes K, Kuypers D, Oyen R. Factors influencing technical success and outcome of percutaneous balloon angioplasty in de novo native hemodialysis arteriovenous fistulas. Eur J Radiol. 2012;81:2298-2303. https://doi.org/10.1016/j.ejrad.2011.09.004
6. Yan Wee IJ, Yap HY, Hsien Ts'ung LT, Lee Qingwei S, Tan CS, Tang TY, et al. A systematic review and meta-analysis of drug-coated balloon versus conventional balloon angioplasty for dialysis access stenosis. J Vasc Surg. 2019;70:970-979. https://doi.org/10.1016/j.jvs.2019.01.082
7. Xu ZW, Li HB, Yang XS, Qin HS, Hao QZ. Comparison of drug-coated balloon versus plain balloon angioplasty for the treatment of arteriovenous fistula stenosis: a systematic review and meta-analysis of randomized controlled trials. Cardiovasc Intervent Radiol. 2026;49:17-31. https://doi.org/10.1007/s00270-025-04279-1
8. Elahi A, Qamar M, Khan FM, Babar R, Zahid MJ, Ahmad MO, et al. Efficacy of drug-coated balloon versus uncoated balloon for dysfunctional dialysis access: a systematic review and meta-analysis. Clin Exp Nephrol. 2025;29:974-986. https://doi.org/10.1007/s10157-025-02642-7
9. Lee H, Choi H, Han E, Kim YJ. Comparison of clinical effectiveness and safety of drug-coated balloons versus percutaneous transluminal angioplasty in arteriovenous fistulae: a review of systematic reviews and updated meta-analysis. J Vasc Interv Radiol. 2024;35:949-962. https://doi.org/10.1016/j.jvir.2024.03.027
10. Lee T, Ul Haq N. New developments in our understanding of neointimal hyperplasia. Adv Chronic Kidney Dis. 2015;22:431-437. https://doi.org/10.1053/j.ackd.2015.06.010
11. Remuzzi A, Ene-Iordache B. Novel paradigms for dialysis vascular access: upstream hemodynamics and vascular remodeling in dialysis access stenosis. Clin J Am Soc Nephrol. 2013;8:2186-2193. https://doi.org/10.2215/CJN.03450413
12. Roy-Chaudhury P, Sukhatme VP, Cheung AK. Hemodialysis vascular access dysfunction: a cellular and molecular viewpoint. J Am Soc Nephrol. 2006;17:1112-1127. https://doi.org/10.1681/ASN.2005050615
13. Portugaller RH, Kalmar PI, Deutschmann H. The eternal tale of dialysis access vessels and restenosis: are drug-eluting balloons the solution? J Vasc Access. 2014;15:439-447. https://doi.org/10.5301/jva.5000271
14. Davidson CJ, Newman GE, Sheikh KH, Kisslo K, Stack RS, Schwab SJ. Mechanisms of angioplasty in hemodialysis fistula stenoses evaluated by intravascular ultrasound. Kidney Int. 1991;40:91-95. https://doi.org/10.1038/ki.1991.185
15. Lee T. Novel paradigms for dialysis vascular access: downstream vascular biology: is there a final common pathway? Clin J Am Soc Nephrol. 2013;8:2194-2201. https://doi.org/10.2215/CJN.03490413
16. Gray WA, Granada JF. Drug-coated balloons for the prevention of vascular restenosis. Circulation. 2010;121:2672-2680. https://doi.org/10.1161/CIRCULATIONAHA.110.936922
17. Weaver BA. How taxol/paclitaxel kills cancer cells. Mol Biol Cell. 2014;25:2677-2681. https://doi.org/10.1091/mbc.E14-04-0916
18. Scheller B, Speck U, Abramjuk C, Bernhardt U, Bohm M, Nickenig G. Paclitaxel balloon coating, a novel method for prevention and therapy of restenosis. Circulation. 2004;110:810-814. https://doi.org/10.1161/01.CIR.0000138929.71660.E0
19. Granada JF, Stenoien M, Buszman PP, Tellez A, Langanki D, Kaluza GL, et al. Mechanisms of tissue uptake and retention of paclitaxel-coated balloons: impact on neointimal proliferation and healing. Open Heart. 2014;1:e000117. https://doi.org/10.1136/openhrt-2014-000117
20. Rosenfield K, Jaff MR, White CJ, Rocha-Singh K, Mena-Hurtado C, Metzger DC, et al. Trial of a paclitaxel-coated balloon for femoropopliteal artery disease. N Engl J Med. 2015;373:145-153. https://doi.org/10.1056/NEJMoa1406235
21. Unverdorben M, Vallbracht C, Cremers B, Heuer H, Hengstenberg C, Maikowski C, et al. Paclitaxel-coated balloon catheter versus paclitaxel-coated stent for the treatment of coronary in-stent restenosis. Circulation. 2009;119:2986-2994. https://doi.org/10.1161/CIRCULATIONAHA.108.

839282
22. Kitrou PM, Katsanos K, Spyridonidis I, Theofanis M, Papachristou E, Papadoulas S, et al. Use of drug-coated balloons in dysfunctional arteriovenous dialysis access treatment: the effect of consecutive treatments on lesion patency. J Vasc Interv Radiol. 2019;30:212-216. https://doi.org/10.1016/j.jvir.2018.11.013
23. Shazly T, Torres WM, Secemsky EA, Chitalia VC, Jaffer FA, Kolachalama VB. Understudied factors in drug-coated balloon design and evaluation: a biophysical perspective. Bioeng Transl Med. 2023;8:e10370. https://doi.org/10.1002/btm2.10370
24. Lookstein RA, Haruguchi H, Ouriel K, Weinberg I, Lei L, Cihlar S, et al. Drug-coated balloons for dysfunctional dialysis arteriovenous fistulas. N Engl J Med. 2020;383:733-742. https://doi.org/10.1056/NEJMoa1914617
25. Trerotola SO, Lawson J, Roy-Chaudhury P, Saad TF; Lutonix AV Clinical Trial Investigators. Drug coated balloon angioplasty in failing AV fistulas: a randomized controlled trial. Clin J Am Soc Nephrol. 2018;13:1215-1224. https://doi.org/10.2215/CJN.14231217
26. Kim JW, Kim JH, Byun SS, Kang JM, Shin JH. Paclitaxel-coated balloon versus plain balloon angioplasty for dysfunctional autogenous radiocephalic arteriovenous fistulas: a prospective randomized controlled trial. Korean J Radiol. 2020;21:1239-1247. https://doi.org/10.3348/kjr.2020.0067
27. Karunanithy N, Robinson EJ, Ahmad F, Burton JO, Calder F, Coles S, et al. A multicenter randomized controlled trial indicates that paclitaxel-coated balloons provide no benefit for arteriovenous fistulas. Kidney Int. 2021;100:447-456. https://doi.org/10.1016/j.kint.2021.02.040
28. Katsanos K, Karnabatidis D, Kitrou P, Spiliopoulos S, Christeas N, Siablis D. Paclitaxel-coated balloon angioplasty vs. plain balloon dilation for the treatment of failing dialysis access: 6-month interim results from a prospective randomized controlled trial. J Endovasc Ther. 2012;19:263-272. https://doi.org/10.1583/11-3690.1
29. Manaki V, Bontinis V, Giannopoulos A, Kontes I, Rafailidis V, Ktenidis K. Drug-eluting stents for the treatment of arteriovenous access stenosis: a systematic review and individual patient data (IPD) meta-analysis. Ann Vasc Surg. 2026;123:514-523. https://doi.org/10.1016/j.avsg.2025.10.028
30. Holden A, Haruguchi H, Suemitsu K, Isogai N, Ross J, Hull J, et al. IN.PACT AV access randomized trial: 12-month clinical results demonstrating the sustained treatment effect of drug-coated balloons. J Vasc Interv Radiol. 2022;33:884-894. https://doi.org/10.1016/j.jvir.2022.03.606
31. Lookstein R, Haruguchi H, Suemitsu K, Isogai N, Gallo V, Madassery S, et al. IN.PACT AV access randomized trial of drug-coated balloons for dysfunctional arteriovenous fistulae: clinical outcomes through 36 months. J Vasc Interv Radiol. 2023;34:2093-2102. https://doi.org/10.1016/j.jvir.2023.07.007
32. Trerotola SO, Saad TF, Roy-Chaudhury P; Lutonix AV Clinical Trial Investigators. The lutonix AV randomized trial of paclitaxel-coated balloons in arteriovenous fistula stenosis: 2-year results and subgroup analysis. J Vasc Interv Radiol. 2020;31:1-14. https://doi.org/10.1016/j.jvir.2019.08.035
33. Zhao Y, Wang P, Wang Y, Zhang L, Zhao Y, Li H, et al. Drug-coated balloon angioplasty for dysfunctional arteriovenous hemodialysis fistulae: a randomized controlled trial. Clin J Am Soc Nephrol. 2024;19:336-344. https://doi.org/10.2215/CJN.0000000000000359
34. Maleux G, van der Linden E, Heijboer RJJ, Serafino GP, Wust AFJ, Dol JA, et al. Multicenter randomized controlled trial of APERTO-paclitaxel drug-eluting balloon angioplasty versus standard percutaneous transluminal angioplasty in dysfunctional hemodialysis grafts and native fistulae. J Endovasc Ther. 2025;32:1580-1588. https://doi.org/10.1177/15266028231215212
35. Kim H, Kim YS, Labropoulos N. Management of cephalic arch stenosis in hemodialysis access: updated systematic review and meta-analysis. J Vasc Access. 2025;26:1229-1240. https://doi.org/10.1177/11297298241264583
36. Kitrou PM, Katsanos K, Spiliopoulos S, Karnabatidis D, Siablis D. Drug-eluting versus plain balloon angioplasty for the treatment of failing dialysis access: final results and cost-effectiveness analysis from a prospective randomized controlled trial (NCT01174472). Eur J Radiol. 2015;84:418-423. https://doi.org/10.1016/j.ejrad.2014.11.037
37. Irani FG, Teo TK, Tay KH, Yin WH, Win HH, Gogna A, et al. Hemodialysis arteriovenous fistula and graft stenoses: randomized trial comparing drug-eluting balloon angioplasty with conventional angioplasty. Radiology. 2018;289:238-

247. https://doi.org/10.1148/radiol.2018170806
38. Maleux G, Vander Mijnsbrugge W, Henroteaux D, Laenen A, Cornelissen S, Claes K, et al. Multicenter, randomized trial of conventional balloon angioplasty versus paclitaxel-coated balloon angioplasty for the treatment of dysfunctioning autologous dialysis fistulae. J Vasc Interv Radiol. 2018;29:470-475. https://doi.org/10.1016/j.jvir.2017.10.023
39. Bjorkman P, Weselius EM, Kokkonen T, Rauta V, Alback A, Venermo M. Drug-coated versus plain balloon angioplasty in arteriovenous fistulas: a randomized, controlled study with 1-year follow-up (the Drecorest Ii-Study). Scand J Surg. 2019;108:61-66. https://doi.org/10.1177/1457496918798206
40. Karmota AG. Paclitaxel coated-balloon (PCB) versus standard plain old balloon (POB) fistuloplasty for failing dialysis access. Ann R Coll Surg Engl. 2020;102:601-605. https://doi.org/10.1308/rcsann.2020.0121
41. Liao MT, Lee CP, Lin TT, Jong CB, Chen TY, Lin L, et al. A randomized controlled trial of drug-coated balloon angioplasty in venous anastomotic stenosis of dialysis arteriovenous grafts. J Vasc Surg. 2020;71:1994-2003. https://doi.org/10.1016/j.jvs.2019.07.090
42. Moreno-Sanchez T, Moreno-Ramirez M, Machancoses FH, Pardo-Moreno P, Navarro-Vergara PF, Garcia-Revillo J. Efficacy of paclitaxel balloon for hemodialysis stenosis fistulae after one year compared to high-pressure balloons: a controlled, multicenter, randomized trial. Cardiovasc Intervent Radiol. 2020;43:382-390. https://doi.org/10.1007/s00270-019-02372-w
43. Pang SY, Au-Yeung KC, Liu GY, Tse RO, Lai D, Leung WK, et al. Randomized controlled trial for paclitaxel-coated balloon versus plain balloon angioplasty in dysfunctional hemodialysis vascular access: 12-month outcome from a non-sponsored trial. Ann Vasc Surg. 2021;72:299-306. https://doi.org/10.1016/j.avsg.2020.10.005
44. Yin Y, Shi Y, Cui T, Li H, Chen J, Zhang L, et al. Efficacy and safety of paclitaxel-coated balloon angioplasty for dysfunctional arteriovenous fistulas: a multicenter randomized controlled trial. Am J Kidney Dis. 2021;78:19-27. https://doi.org/10.1053/j.ajkd.2020.11.022
45. Therasse E, Caty V, Gilbert P, Giroux MF, Perreault P, Bouchard L, et al. Safety and efficacy of paclitaxel-eluting balloon angioplasty for dysfunctional hemodialysis access: a randomized trial comparing with angioplasty alone. J Vasc Interv Radiol. 2021;32:350-359. https://doi.org/10.1016/j.jvir.2020.10.030
46. Goo DE, Kim YJ, Park SW, Cheon HJ, Won YD, Yang SB. A prospective multicenter randomized controlled trial for comparing drug-coated and conventional balloon angioplasty in venous anastomotic stenosis of hemodialysis arteriovenous grafts. Cardiovasc Intervent Radiol. 2024;47:36-44. https://doi.org/10.1007/s00270-023-03536-5
47. Pietzsch JB, Geisler BP, Manda B, Misra S, Lyden SP, Pflederer TA, et al. IN.PACT AV access trial: economic evaluation of drug-coated balloon treatment for dysfunctional arteriovenous fistulae based on 12-month clinical outcomes. J Vasc Interv Radiol. 2022;33:895-902. https://doi.org/10.1016/j.jvir.2022.04.014
48. Boitet A, Massy ZA, Goeau-Brissonniere O, Javerliat I, Coggia M, Coscas R. Drug-coated balloon angioplasty for dialysis access fistula stenosis. Semin Vasc Surg. 2016;29:178-185. https://doi.org/10.1053/j.semvascsurg.2016.08.002
49. Faenger B, Heinrich A, Hilger I, Teichgraber U. Drug loss from paclitaxel-coated balloons during preparation, insertion and inflation for angioplasty: a laboratory investigation. Cardiovasc Intervent Radiol. 2022;45:1186-1197. https://doi.org/10.1007/s00270-022-03164-5
50. Heinrich A, Engler MS, Guttler FV, Matthaus C, Popp J, Teichgraber UK. Systematic evaluation of particle loss during handling in the percutaneous transluminal angioplasty for eight different drug-coated balloons. Sci Rep. 2020;10:17220. https://doi.org/10.1038/s41598-020-74227-1
51. Villar-Matamoros E, Stokes L, Lloret A, Todd M, Tillman BW, Yazdani SK. Understanding the mechanism of drug transfer and retention of drug-coated balloons. J Cardiovasc Pharmacol Ther. 2022;27:10742484221119559. https://doi.org/10.1177/10742484221119559
52. DePietro DM, Trerotola SO. Choosing the right treatment for the right lesion, Part II: a narrative review of drug-coated balloon angioplasty and its evolving role in dialysis access maintenance. Cardiovasc Diagn Ther. 2023;13:233-259. https://doi.org/10.21037/cdt-22-497
53. Karnabatidis D, Kitrou PM, Ponce P, Chong TT, Pietura R, Pegis JD, et al. A multicenter global registry of paclitaxel drug-coated balloon in dysfunctional arteriovenous fistulae and grafts: 6-month results. J Vasc Interv Radiol. 2021;32:360-368. https://doi.org/10.1016/j.jvir.2020.11.018

54. Dinh K, Limmer AM, Paravastu SCV, Thomas SD, Bennett MH, Holden A, et al. Mortality after paclitaxel-coated device use in dialysis access: a systematic review and meta-analysis. J Endovasc Ther. 2019;26:600-612. https://doi.org/10.1177/1526602819872154
55. Katsanos K, Spiliopoulos S, Kitrou P, Krokidis M, Karnabatidis D. Risk of death following application of paclitaxel-coated balloons and stents in the femoropopliteal artery of the leg: a systematic review and meta-analysis of randomized controlled trials. J Am Heart Assoc. 2018;7:e011245. https://doi.org/10.1161/JAHA.118.011245
56. Rocha-Singh KJ, Duval S, Jaff MR, Schneider PA, Ansel GM, Lyden SP, et al. Mortality and paclitaxel-coated devices: an individual patient data meta-analysis. Circulation. 2020;141:1859-1869. https://doi.org/10.1161/CIRCULATIONAHA.119.044697
57. Parikh SA, Schneider PA, Mullin CM, Rogers T, Gray WA. Mortality in randomised controlled trials using paclitaxel-coated devices for femoropopliteal interventional procedures: an updated patient-level meta-analysis. Lancet. 2023;402:1848-1856. https://doi.org/10.1016/S0140-6736(23)02189-X
58. Yang Q, Xia C. Angioplasty for dysfunctional arteriovenous fistulas: A meta-analysis of recent randomized controlled trials compared paclitaxel-coated balloon versus conventional balloon angioplasty. J Vasc Access. 2025;26:81-88. https://doi.org/10.1177/11297298231213724
59. Zhang Y, Yuan FL, Hu XY, Wang QB, Zou ZW, Li ZG. Comparison of drug-coated balloon angioplasty versus common balloon angioplasty for arteriovenous fistula stenosis: a systematic review and meta-analysis. Clin Cardiol. 2023;46:877-885. https://doi.org/10.1002/clc.24078

Review Article

eISSN 2508-2612
https://doi.org/10.64961/kjir.2026.00087
Korean J Interv Radiol 2026;31(2):103-112

KJIR
Korean Journal of
Interventional Radiology

Endovascular Treatment of Below-the-Knee Arterial Disease in Chronic Limb-Threatening Ischemia

Tae Won Choi*, Je Hwan Won, Jinoo Kim

Department of Radiology, Ajou University Hospital, Ajou University School of Medicine, Suwon, Republic of Korea

Chronic limb-threatening ischemia represents the most severe form of peripheral artery disease and is associated with high risks of limb loss and mortality. It is closely associated with below-the-knee arterial disease, with substantial overlap between the two conditions, particularly in patients with diabetes. Endovascular treatment plays a central role in restoring distal tibial and pedal perfusion, which is critical for wound healing and limb salvage. However, it remains technically challenging due to small vessel size, diffuse disease, and heavy calcification, which limit luminal expansion and predispose to recoil, dissection, and restenosis. Procedural success requires a structured approach integrating access strategy, guidewire crossing, and subsequent treatment. Crossing strategies, including subintimal tracking, retrograde tibio-pedal access, and bidirectional techniques such as controlled antegrade and retrograde tracking, are often required in complex lesions. Plain balloon angioplasty remains the most broadly applicable treatment, whereas drug-coated balloons show inconsistent benefit. Drug-eluting stents provide favorable outcomes in selected short focal lesions, whereas other technologies have more limited evidence. Overall, treatment should be individualized based on lesion characteristics and clinical context.

Keywords: Peripheral artery disease; Chronic limb-threatening ischemia; Below-the-knee; Endovascular treatment

Introduction

Below-the-knee (BTK) arterial disease should be understood within the broader epidemiologic context of peripheral artery disease (PAD). PAD affects approximately 12% to 14% of the general population, increases markedly with age, and has grown substantially worldwide, from 164 million people in 2000 to 202 million in 2010 [1,2]. This expanding and aging PAD population represents a major driver of the increasing global burden of advanced limb ischemia.

Chronic limb-threatening ischemia (CLTI) represents the most severe clinical subset of PAD. The 2024 American College of Cardiology/American Heart Association guidelines for lower-extremity PAD identify CLTI as one of the major clinical presentations of PAD and frame it as a limb-threatening condition requiring timely evaluation and treatment [3]. Epidemiologically, CLTI represents a substantial disease burden, with an estimated prevalence of approximately 6.5 million individuals across the United States, Europe, and Japan, and is associated with a 1-year mortality of about 20%–25% and a 5-year all-cause mortality exceeding 50% [4-6]. Clinically, CLTI presents with rest pain, non-healing wound, or gangrene, and reflects not only arterial obstruction itself but also the combined burden of impaired perfusion, tissue loss, infection risk, and systemic frailty.

Received: March 31, 2026; **Revised:** June 3, 2026; **Accepted:** June 3, 2026
***Corresponding email:** dllimit@naver.com

© 2026 Korean Society of Interventional Radiology

This is an Open Access article distributed under the terms of the Creative Commons Attribution Non-Commercial License (http://creativecommons.org/licenses/by-nc/4.0) which permits unrestricted non-commercial use, distribution, and reproduction in any medium, provided the original work is properly cited.

Importantly, CLTI and BTK disease overlap to a very large extent. BTK disease has been reported in more than 70% of patients with CLTI, particularly among patients with diabetes [6]. In addition, approximately one-third of patients with critical limb ischemia present with isolated BTK lesions, which have been associated with a higher incidence of limb loss than multilevel disease [7]. Accordingly, restoration of distal tibial and pedal perfusion is a critical determinant of wound healing and limb salvage in patients with CLTI. Treatment of more proximal disease alone is insufficient when distal runoff remains severely compromised [6,8].

This close relationship between CLTI and BTK disease explains why endovascular revascularization has a central role in contemporary management. The therapeutic goal is not simply angiographic patency, but restoration of perfusion sufficient to relieve ischemic pain, promote wound healing, and prevent major amputation [8]. Current guidelines consistently position revascularization as a key treatment component in CLTI management [3,9]. The 2024 European Society of Cardiology (ESC) Guidelines for the management of peripheral arterial and aortic diseases recommend revascularization as soon as possible in CLTI and state that endovascular revascularization is the treatment of choice for short BTK lesions [9].

Pathophysiology

BTK PAD differs from more proximal lower-extremity disease not only in lesion distribution but also in arterial structure and biomechanics. Compared with femoropopliteal arteries, BTK arteries are smaller, thinner, more frequently calcified, and mechanically stiffer in the longitudinal direction, with distinct structural composition including lower elastin, collagen, and glycosaminoglycan content [10].

The distribution and morphology of calcification also differ along the lower-extremity arterial tree. As the arterial tree progresses distally toward the tibial vessels, calcified plaques increase while fibrofatty plaques decrease, reflecting a progressive shift in plaque composition [6]. In BTK arteries, calcification is not only more prevalent but also a key determinant of vessel behavior, as it directly affects arterial compliance and response to endovascular treatment.

In particular, calcification in BTK arteries may involve both the intimal and medial layers, which have distinct biological and mechanical implications [11,12]. Intimal calcification is typically associated with atherosclerotic plaque and contributes directly to luminal narrowing, whereas medial calcification is more closely linked to systemic metabolic disease, particularly diabetes mellitus and chronic kidney disease, and results primarily in circumferential stiffening and loss of arterial compliance [12,13]. In a histopathologic study of lower-extremity arteries, hemodialysis was identified as an important factor associated with severe medial calcification in BTK lesions, whereas diabetes was not independently associated with severe medial calcification after multivariable adjustment [12].

These structural and pathologic differences have direct procedural implications. Compared with femoropopliteal arteries, BTK intervention is more vulnerable to limited luminal gain, elastic recoil, dissection, and restenosis [10,14]. In heavily calcified BTK arteries, particularly when circumferential calcification predominates, balloon angioplasty may produce limited luminal expansion despite successful wire crossing because the artery behaves as a rigid, poorly compliant tube rather than a readily expandable stenotic plaque. This often results in substantial residual stenosis or elastic recoil. In contrast, more focal or eccentric calcification may predispose the vessel to flow-limiting dissection during balloon expansion [11,13]. Accordingly, the morphologic pattern of calcification, rather than its mere presence, directly influences endovascular strategy. This provides a mechanistic basis for the growing use of lesion-modifying techniques such as specialty balloons, atherectomy, or intravascular lithotripsy when conventional angioplasty alone is unlikely to achieve adequate expansion, although their clinical benefit remains uncertain [11,13,15].

Technical Considerations in BTK Intervention

Target Vessel Selection

In CLTI with tissue loss, target vessel selection should first aim to establish in-line flow to the foot through at least one patent tibial artery [3,9]. Beyond this general principle, the angiosome concept may guide selection of the wound-related artery [3,8,9]. Direct revascularization of the artery supplying the wound territory is generally preferred when technically feasible, whereas indirect revascularization through collateral

networks may be acceptable when direct targeting is not feasible [3,8]. Lesion anatomy, vessel quality, collateral networks, pedal arch integrity, and technical feasibility should also be considered when selecting the target vessel.

Access Strategy

In BTK intervention, antegrade femoral access is generally preferred when there is no significant disease in the common femoral artery or at the ostium of the superficial femoral artery. As lesions become longer, more calcified, and more distal, wire control and torque transmission become increasingly important. Antegrade access shortens the working distance and improves support, pushability, and particularly torquability of the guidewire and devices during tibial and pedal interventions. Consistent with this concept, advancement of the sheath as distally as feasible, often to the popliteal segment, has been recommended to further improve device support and control during BTK procedures [16].

Wire Crossing Strategy

Crossing strategy in BTK chronic total occlusion (CTO) is largely lesion dependent. The Japanese BTK CTO score is useful because it translates angiographic morphology into practical crossing difficulty and predicts the likelihood of successful antegrade guidewire passage. In the original derivation cohort, five adverse angiographic variables predicted unsuccessful crossing: blunt proximal stump, calcification at the proximal entry, reference vessel diameter <2.0 mm, CTO length ≥ 200 mm, and absence of distal outflow in the target vessel. Successful guidewire crossing decreased from 97.3% in grade A to 76.8% in grade B, 19.3% in grade C, and 0% in grade D lesions [17]. Prospective validation confirmed similar directional performance, with successful antegrade crossing rates of 97.5%, 89.1%, 62.5%, and 27.3% across grades A through D, respectively [18]. Although the score is not universally adopted in routine practice, it highlights a fundamental concept: complex BTK CTO morphology is a major predictor of failure of simple antegrade intraluminal navigation. In such situations, subintimal tracking, retrograde tibio-pedal access, or bidirectional approaches frequently become necessary components of the procedural strategy [6,15,16,19].

Retrograde tibial or pedal access is primarily used as a bail-out strategy in complex BTK CTO intervention when antegrade crossing is unsuccessful [15]. One theoretical advantage is that the distal cap of the occlusion is often softer and more penetrable than the proximal cap, which may facilitate guidewire entry from below [6].

In addition, retrograde access is essential for conversion to a bidirectional strategy, such as controlled antegrade and retrograde subintimal tracking (CART) or reverse CART (Fig. 1) [6]. This technique is typically used when both antegrade and retrograde guidewire attempts fail to achieve true lumen re-entry, and the wires remain within separate subintimal spaces. A balloon is introduced from one direction to enlarge the subintimal space and create communication between the two channels. After balloon deflation, a guidewire in the opposite direction is advanced to enter the same subintimal plane and establish continuity between the antegrade and retrograde tracks. This bidirectional approach can substantially increase the likelihood of successful wire crossing when a single-directional wiring attempt fails.

Pedal Arch and Pedal-Plantar Loop Intervention

Anatomically, the pedal–plantar loop is formed by the dorsalis pedis artery, deep perforating artery, lateral plantar artery, and posterior tibial artery, providing potential collateral continuity between the anterior and posterior tibial circulations in the majority of individuals (Fig. 2) [16].

Pedal arch intervention should not be performed routinely and should be reserved for selected cases because of the relatively high risk of complications and restenosis [6]. It becomes most relevant in wound-oriented revascularization when restoration of forefoot perfusion is required, particularly in patients with tissue loss involving the distal foot or multiple angiosomes [6,16]. Observational studies suggest that pedal arch patency is associated with improved wound healing, limb salvage, and survival in CLTI populations, particularly among patients with diabetes [20,21]. In addition, in selected cases, restoration of pedal arch continuity may improve distal runoff and thereby support the durability of BTK interventions, as inadequate distal outflow can promote thrombosis and restenosis in the treated segment.

The pedal arch may also serve as a conduit for trans-arch recanalization [15]. A guidewire can be advanced across the pedal–plantar loop from the anterior tibial–dorsalis pedis system into the plantar and posterior tibial circulation, or in the oppo-

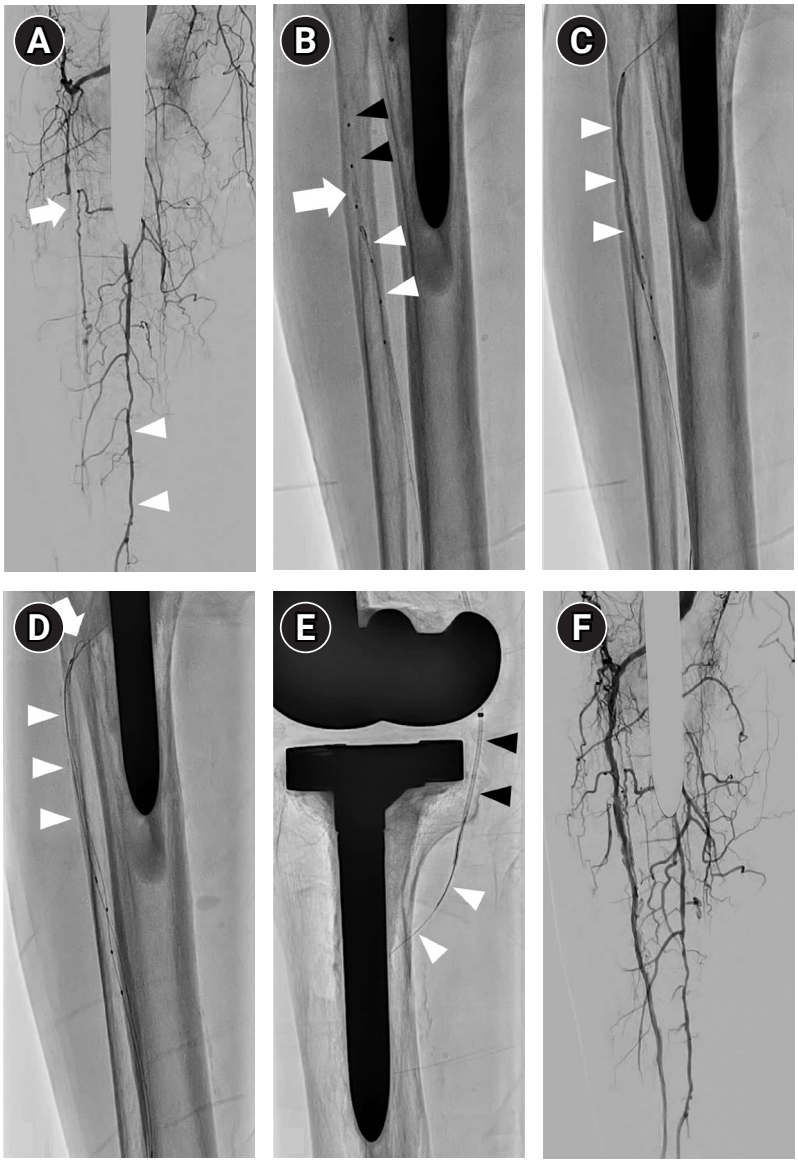


Fig. 1. Reverse controlled antegrade and retrograde tracking technique for guidewire crossing. (A) Pre-procedural angiography demonstrates chronic total occlusion of the anterior tibial artery (arrow) and posterior tibial artery, with foot perfusion maintained only through collateral flow from the peroneal artery (arrowheads). (B) To cross a severely calcified chronic total occlusion of the anterior tibial artery (white arrow), antegrade (black arrowheads) and retrograde tracking via pedal puncture (white arrowheads) were attempted but ended in different subintimal spaces. (C) A balloon catheter was introduced over the antegrade wire and inflated in the subintimal space to create a channel between the two different subintimal spaces (arrowheads). (D) After deflation of the balloon catheter (arrowheads), the retrograde guidewire successfully passed through the common channel (arrow). (E) The retrograde guidewire (white arrowheads) entered the true lumen and was captured in the popliteal artery using a 4-Fr catheter (black arrowheads) to establish a through-and-through rail. (F) Post-procedural angiography following balloon angioplasty demonstrates successful revascularization of the anterior tibial artery.

site direction, thereby enabling retrograde crossing of tibial occlusions when direct retrograde pedal puncture is difficult.

Technical execution requires particular caution because pedal arch vessels are small in caliber and frequently tortuous [6]. Navigation is typically performed using soft 0.014-inch guidewires together with low-profile microcatheters or balloons to minimize the risk of dissection injury. If pedal arch angioplasty is required, conservative balloon sizing is generally preferred in order to reduce the risk of rupture or flow-limiting dissection. Manipulation within the plantar circulation should also be minimized because excessive instrumentation can injure fragile distal vessels.

https://doi.org/10.64961/kjir.2026.00087

Balloon-Uncrossable Lesions

Failure of balloon passage after successful guidewire crossing is a common technical challenge in BTK intervention and is usually related to severe calcification, vessel tortuosity, or insufficient device support. In such situations, predilation with a low-profile single-marker balloon in the 1.2–1.5 mm range should be the first step [22].

If balloon crossing remains unsuccessful, wire externalization using additional retrograde pedal access and creation of a through-and-through tensioned rail should be considered early. This configuration can substantially improve pushability and facilitate device delivery across resistant segments [23,24].

When these strategies fail, advanced plaque-modifying techniques may be considered as bailout options. Percutaneous direct needle puncture of calcified plaque (PIERCE) and its variants, including inner PIERCE, involve direct puncture of heavily calcified plaque using a needle to disrupt the calcification and facilitate subsequent device advancement [25,26]. Although these techniques can enable balloon delivery in otherwise uncrossable lesions, they carry risks such as perforation, dissection, or loss of collateral channels [22]. Therefore, these advanced plaque-modifying techniques should be regarded as expert-level bailout maneuvers rather than routine procedural steps and should be reserved for patients with advanced diseases. The overall procedural workflow for BTK intervention is summarized in Fig. 3.

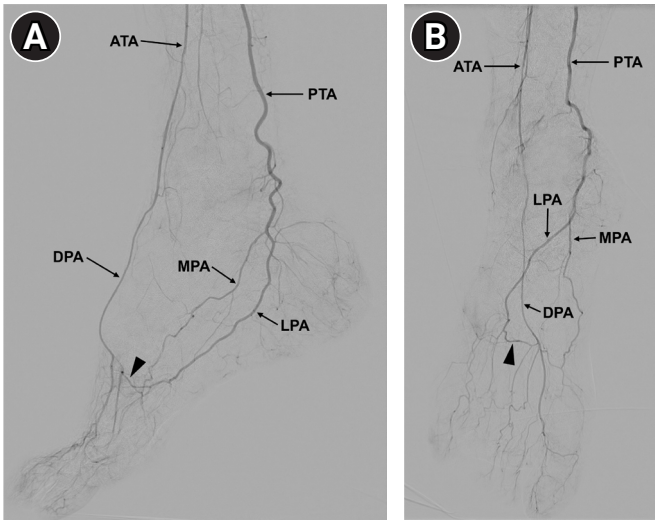


Fig. 2. Pedal arch anatomy. The deep plantar arch (arrowhead) is demonstrated on lateral (A) and anteroposterior (B) pedal angiography. ATA, anterior tibial artery; PTA, posterior tibial artery; DPA, dorsalis pedis artery; LPA, lateral plantar artery; MPA, medial plantar artery.

Endovascular Treatment Strategies in BTK Disease

Plain Balloons vs. Drug-Coated Balloons

Percutaneous transluminal angioplasty (PTA), referring to plain balloon angioplasty without drug coating, remains the most commonly used treatment and continues to serve as a practical first-line approach in many settings, and the evidence comparing drug-coated balloons (DCB) with PTA in BTK disease remains inconsistent and does not demonstrate a clear clinical advantage. Positive signals have been reported

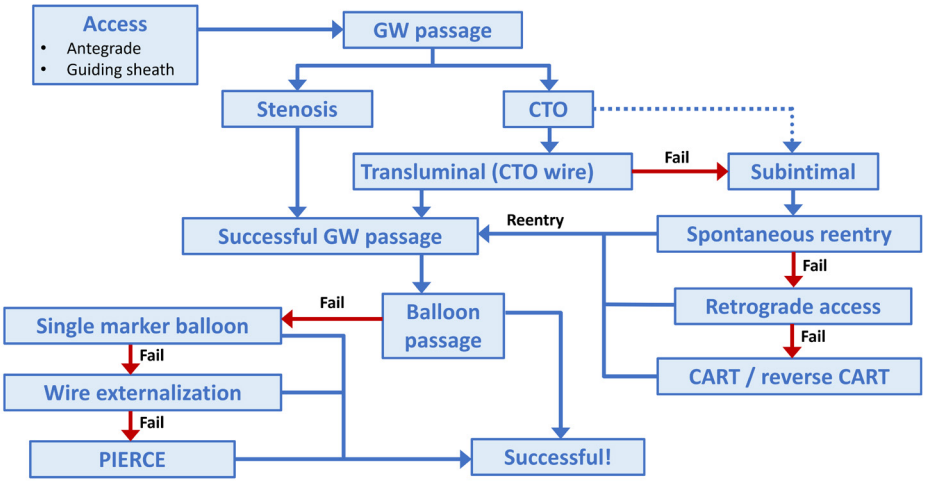


Fig. 3. Procedural workflow for below-the-knee intervention. GW, guidewire; CTO, chronic total occlusion; CART, controlled antegrade and retrograde tracking; PIERCE, percutaneous direct needle puncture of calcified plaque.

in some single-center randomized trials. In the DEBATE-BTK trial, freedom from clinically driven target lesion revascularization (CD-TLR) at 1 year was 82% with DCB versus 63% with PTA (p = 0.002). However, by 5 years, differences in CD-TLR, major amputation, and all-cause mortality were no longer statistically significant [27]. These findings are broadly consistent with those of a recent meta-analysis comparing DCB with PTA in CLTI patients, which found that DCB reduced CD-TLR at 12 months (OR, 0.39; 95% CI, 0.04 to 0.73). However, no significant differences were observed in major amputation, all-cause mortality, 6-month primary patency, or late lumen loss [28]. These findings indicate that DCB may reduce early repeat revascularization but do not provide a sustained benefit in major clinical outcomes. In addition, the benefit of DCB in reducing early repeat revascularization has not been consistently demonstrated across the broader literature, including another meta-analysis or randomized trials [15,29-33], and therefore does not support routine use of DCB in BTK artery disease.

Guideline recommendations reflect this uncertainty. The ESC guidelines state that drug-eluting balloons have not demonstrated superiority over PTA in BTK disease [9]. In CLTI requiring BTK artery revascularization, contemporary guidelines emphasize timely revascularization and limb-salvage goals rather than prioritizing a specific device platform [3,9].

Drug-Eluting Stents

Unlike bare-metal stents (BMS), which demonstrate limited long-term patency in BTK arteries, drug-eluting stents (DES) provide both mechanical scaffolding and local delivery of antiproliferative agents, and represent one of the most studied implant-based therapies for BTK lesions. However, most of the available evidence is derived from studies involving selected patients with relatively short focal lesions [34]. In the DESTINY trial, everolimus-eluting stents were compared with BMS in BTK lesions with a mean lesion length of 15.9 ± 10.2 mm [35]. DES demonstrated significantly higher primary patency and lower target lesion revascularization (TLR) at 12 months. Similarly, the ACHILLES trial showed superiority of sirolimus-eluting stents over PTA in BTK lesions with a mean lesion length of 27 ± 21 mm [36]. The DESTINY2 study assessed DES in slightly longer BTK lesions (mean lesion length, 47.4 ± 25 mm) and showed 12-month outcomes of 75.4% primary patency, 94.4% limb salvage, and 84.9% freedom from TLR [37]. In addition, Giaquinta et al. [38] reported outcomes of everolimus-eluting stents in BTK lesions with an average lesion length of 52.7 mm. Primary patency, limb salvage, and freedom from TLR were 88.9%, 93%, and 91.5% at 1 year, and 80.1%, 89.3%, and 85.1% at 3 years, respectively.

Taken together, the available evidence supports the use of DES primarily for selected short, focal BTK lesions. However, these results should be extrapolated with caution to the long, diffuse, and heavily calcified lesions commonly encountered in CLTI, as occlusion of the stented segment may complicate subsequent reintervention.

Bioresorbable Scaffolds

Bioresorbable scaffolds were developed to provide temporary mechanical support and drug delivery without leaving a permanent metallic implant in the tibial artery. The early experience was encouraging. In a pooled individual-patient analysis of 161 lesions in 121 patients treated with everolimus-eluting bioresorbable vascular scaffolds, freedom from restenosis was 91.7% at 12 months and 86.6% at 24 months, freedom from CD-TLR was 97.2% and 96.6%, and major amputation rate was 1.6% [39]. The strongest randomized evidence now comes from the LIFE-BTK trial [40]. In that multicenter trial, 261 CLTI patients were randomized 2:1 to a drug-eluting resorbable scaffold or PTA, and the mean lesion length was 44.1 ± 30.9 mm. At 2 years, the primary efficacy endpoint was achieved in 68.8% of the scaffold group compared with 45.4% in the PTA group (p < 0.001). Binary restenosis and CD-TLR were also significantly lower in the scaffold group, while the primary safety endpoint was similar between groups [41]. Overall, although bioresorbable scaffolds have shown promising early outcomes and theoretical advantages over permanent metallic stents, the current evidence remains limited, and further studies are required to clarify their long-term efficacy and safety.

Atherectomy and Plaque-Modifying Devices

Atherectomy has an intuitively attractive role in BTK intervention because tibial lesions are frequently long, diffusely diseased, and heavily calcified, and conventional balloon angioplasty in this setting is often limited by inadequate luminal expansion, recoil, and dissection [13]. In theory, plaque

Table 1. Summary of endovascular treatment modalities in BTK disease

Modality	Mechanism	Key evidence summary	Clinical considerations
PTA	Mechanical dilation with a plain balloon	Remains the reference standard in BTK disease	Limited by recoil, dissection, and restenosis
DCB	Mechanical dilation + drug delivery	Mixed results, without consistent improvement in major clinical outcomes	Role remains uncertain in BTK disease
DES	Mechanical support + drug delivery	Improved patency and reduced TLR in short focal lesions	Evidence limited in long, diffuse lesions
Bioresorbable scaffolds	Temporary mechanical support + drug delivery	Promising early results, but overall evidence remains limited	Further evidence is required
Atherectomy	Plaque debulking or modification	No consistent benefit over PTA in current studies	Risk of distal embolization; selective use may be considered

PTA, percutaneous transluminal angioplasty; DCB, drug-coated balloon; BTK, below-the-knee; DES, drug-eluting stent; TLR, target lesion revascularization.

debulking or calcium modification before adjunctive balloon angioplasty could improve vessel compliance and reduce severe balloon-related vessel injury. However, despite this mechanistic appeal, the clinical evidence supporting atherectomy in BTK disease remains limited and inconsistent. Most available data are derived from small prospective series or retrospective observational studies, with only very limited randomized evidence and substantial heterogeneity in lesion characteristics across studies [42,43]. Importantly, the overall literature does not show a reproducible clinical advantage of atherectomy over balloon angioplasty alone in terms of procedural success, limb salvage, or freedom from TLR [42]. In contrast, safety considerations can particularly be relevant because distal embolization from atherectomy in small-caliber tibial vessels with limited distal runoff may lead to significant harm in patients with CLTI, while distal embolic protection is not well established [15,44].

Taken together, the current evidence does not support the routine use of atherectomy for BTK disease. Atherectomy may be considered selectively in heavily calcified tibial lesions in which balloon expansion is expected to be inadequate, but its use should remain individualized, lesion-specific, and cautious. The treatment options for BTK intervention are summarized in Table 1.

Conclusion

BTK intervention is a central component in the management of CLTI, but outcomes are constrained by the intrinsic characteristics of tibial arteries, including small vessel size, diffuse disease, and heavy calcification.

No single device strategy has demonstrated consistent superiority across the full spectrum of BTK disease. Balloon angioplasty remains the most broadly applicable approach, while DES show benefit in selected short focal lesions; other technologies, including bioresorbable scaffolds and plaque-modifying devices, have more limited and context-dependent evidence.

Ultimately, the key challenge is not simply achieving procedural success, but improving the durability of revascularization to sustain wound healing and limb preservation in a disease setting characterized by diffuse pathology and frequent restenosis.

Conflict of interest

No potential conflict of interest relevant to this article was reported.

Funding

None.

Acknowledgments

The authors used ChatGPT for language editing. The authors take full responsibility for the content.

Author contributions

Conceptualization: TWC. Investigation: TWC, JHW, JK. Supervision: JHW, JK. Writing - original draft: TWC. Writing - review & and editing: TWC, JHW, JK.

Data availability statement

No new data were generated or analyzed in this study. Data

sharing is not applicable to this article.

ORCID

Tae Won Choi, https://orcid.org/0000-0002-0396-728X
Je Hwan Won, https://orcid.org/0000-0002-5901-295X
Jinoo Kim, https://orcid.org/0000-0001-7238-2528

References

1. Toledo Barros MG, Fonseca AV, Amorim JE, Vasconcelos V. Retrograde distal access versus femoral access for below the knee angioplasty. Cochrane Database Syst Rev. 2024;1:CD013637. https://doi.org/10.1002/14651858.CD013637.pub2
2. Fowkes FG, Rudan D, Rudan I, Aboyans V, Denenberg JO, McDermott MM, et al. Comparison of global estimates of prevalence and risk factors for peripheral artery disease in 2000 and 2010: a systematic review and analysis. Lancet. 2013;382:1329-1340. https://doi.org/10.1016/S0140-6736(13)61249-0
3. Gornik HL, Aronow HD, Goodney PP, Arya S, Brewster LP, Byrd L, et al. 2024 ACC/AHA/AACVPR/APMA/ABC/SCAI/SVM/SVN/SVS/SIR/VESS guideline for the management of lower extremity peripheral artery disease: a report of the American College of Cardiology/American Heart Association joint committee on clinical practice guidelines. Circulation. 2024;149:e1313-e1410. https://doi.org/10.1161/CIR.0000000000001251
4. Fereydooni A, Gorecka J, Dardik A. Using the epidemiology of critical limb ischemia to estimate the number of patients amenable to endovascular therapy. Vasc Med. 2020;25:78-87. https://doi.org/10.1177/1358863X19878271
5. Armstrong DG, Swerdlow MA, Armstrong AA, Conte MS, Padula WV, Bus SA. Five year mortality and direct costs of care for people with diabetic foot complications are comparable to cancer. J Foot Ankle Res. 2020;13:16. https://doi.org/10.1186/s13047-020-00383-2
6. Li J, Varcoe R, Manzi M, Kum S, Iida O, Schmidt A, et al. Below-the-knee endovascular revascularization: a position statement. JACC Cardiovasc Interv. 2024;17:589-607. https://doi.org/10.1016/j.jcin.2023.11.040
7. Fernandez N, McEnaney R, Marone LK, Rhee RY, Leers S, Makaroun M, et al. Multilevel versus isolated endovascular tibial interventions for critical limb ischemia. J Vasc Surg. 2011;54:722-729. https://doi.org/10.1016/j.jvs.2011.03.232
8. Fitridge R, Chuter V, Mills J, Hinchliffe R, Azuma N, Behrendt CA, et al. Editor's choice - The Intersocietal IWGDF, ESVS, SVS guidelines on peripheral artery disease in people with diabetes mellitus and a foot ulcer. Eur J Vasc Endovasc Surg. 2023;66:454-483. https://doi.org/10.1016/j.ejvs.2023.07.020
9. Mazzolai L, Teixido-Tura G, Lanzi S, Boc V, Bossone E, Brodmann M, et al. 2024 ESC guidelines for the management of peripheral arterial and aortic diseases. Eur Heart J. 2024;45:3538-3700. https://doi.org/10.1093/eurheartj/ehae179
10. Struczewska P, Razian SA, Townsend K, Jadidi M, Shahbad R, Zamani E, et al. Mechanical, structural, and physiologic differences between above and below-knee human arteries. Acta Biomater. 2024;177:278-299. https://doi.org/10.1016/j.actbio.2024.01.040
11. Akers NM, Dugas TR. Peripheral artery disease and local drug delivery: a review of disease pathology and drug delivery systems for therapy below the knee. Exp Biol Med (Maywood). 2025;250:10754. https://doi.org/10.3389/ebm.2025.10754
12. Kato T, Torii S, Nakamura N, Aihara K, Terabe Y, Iida O, et al. Pathological analysis of medial and intimal calcification in lower extremity artery disease: impact of hemodialysis. JACC Adv. 2023;2:100656. https://doi.org/10.1016/j.jacadv.2023.100656
13. Lichtenberg M, Patrone L, Rammos C, Stavroulakis K, Bailey C, Herbert J, et al. Recoil, dissection, and restenosis in Below-The-Knee (BTK) arteries following standard balloon angioplasty. Vasa. 2026;55:259-268. https://doi.org/10.1024/0301-1526/a001254
14. Tirziu D, Saleh A, Huang H, Akhlaghi N, Breen TJ, Parikh SA, et al. Safety and efficacy of endovascular treatment modalities for below-the-knee arterial disease: a systematic review and network meta-analysis. J Endovasc Ther. 2026;33:2139-2155. https://doi.org/10.1177/15266028251344809
15. Spiliopoulos S, Del Giudice C, Manzi M, Reppas L, Rodt T, Uberoi R. CIRSE standards of practice on below-the-knee revascularisation. Cardiovasc Intervent Radiol. 2021;44:1309-1322. https://doi.org/10.1007/s00270-021-02891-5
16. Tummala S, Briley K. Advanced limb salvage: pedal artery

interventions. Semin Vasc Surg. 2022;35:200-209. https://doi.org/10.1053/j.semvascsurg.2022.04.007
17. Tan M, Ueshima D, Urasawa K, Hayakawa N, Dannoura Y, Itoh T, et al. Prediction of successful guidewire crossing of below-the-knee chronic total occlusions using a Japanese scoring system. J Vasc Surg. 2021;74:506-513. https://doi.org/10.1016/j.jvs.2021.01.059
18. Tan M, Ueshima D, Iida O, Soga Y, Tobita K, Hayakawa N, et al. Clinical validity of the Japanese below-the-knee chronic total occlusion scoring system for the prediction of successful guidewire crossing. J Vasc Surg. 2024;80:1786-1795. https://doi.org/10.1016/j.jvs.2024.07.025
19. Ysa A, Lobato M, Patrone L, Arruabarrena A, Monasterio A, Metcalfe M, et al. Tips and tricks for simple and complex below-the-ankle punctures. J Endovasc Ther. 2025;32:1846-1856. https://doi.org/10.1177/15266028241234506
20. Troisi N, Turini F, Chisci E, Ercolini L, Frosini P, Lombardi R, et al. Impact of pedal arch patency on tissue loss and time to healing in diabetic patients with foot wounds undergoing infrainguinal endovascular revascularization. Korean J Radiol. 2018;19:47-53. https://doi.org/10.3348/kjr.2018.19.1.47
21. Jung HW, Ko YG, Hong SJ, Ahn CM, Kim JS, Kim BK, et al. Editor's choice: impact of endovascular pedal artery revascularisation on wound healing in patients with critical limb ischaemia. Eur J Vasc Endovasc Surg. 2019;58:854-863. https://doi.org/10.1016/j.ejvs.2019.07.034
22. Lobato M, Ysa A, Villani F, Chisci E, Michelagnoli S, Patrone L. The guidewire crosses but nothing else does: a pictorial review. Vasa. 2026;55:40-48. https://doi.org/10.1024/0301-1526/a001251
23. Delgadillo D, Liang T, Hegazi M, Sharma N, Kabutey NK. In the loop: endovascular pedal arch revascularization. Ann Vasc Surg. 2024;107:84-92. https://doi.org/10.1016/j.avsg.2023.12.099
24. McGuirl D, Giles KA. Retrograde tibio-pedal access for endovascular interventions for treating peripheral arterial disease. Ann Vasc Surg. 2024;107:136-139. https://doi.org/10.1016/j.avsg.2023.12.105
25. Ichihashi S, Sato T, Iwakoshi S, Itoh H, Kichikawa K. Technique of percutaneous direct needle puncture of calcified plaque in the superficial femoral artery or tibial artery to facilitate balloon catheter passage and balloon dilation of calcified lesions. J Vasc Interv Radiol. 2014;25:784-788. https://doi.org/10.1016/j.jvir.2014.01.016
26. Takei T, Miyamoto A, Takagi T, Yamauchi Y. A novel technique of percutaneous intraluminal cracking using a puncture needle for severe calcified lesions of below-the-knee and below-the-ankle arteries. Diagn Interv Radiol. 2021;27:413-417. https://doi.org/10.5152/dir.2021.20675
27. Liistro F, Reccia MR, Angioli P, Ducci K, Ventoruzzo G, Falsini G, et al. Drug-eluting balloon for below the knee angioplasty: five-year outcome of the DEBATE-BTK randomized clinical trial. Cardiovasc Intervent Radiol. 2022;45:761-769. https://doi.org/10.1007/s00270-022-03104-3
28. Modi K, Joseph T, Shah R, Ranga R, Markel L. Drug-coated balloon angioplasty versus percutaneous transluminal angioplasty for below-the-knee interventions in chronic limb-threatening ischemia patients: systematic review and meta-analysis. Ann Vasc Surg. 2026;123:104-118. https://doi.org/10.1016/j.avsg.2025.09.022
29. Cai H, Dong J, Ye Y, Song Q, Lu S. Safety and efficacy of drug-coated balloon in the treatment of below-the-knee artery: a meta-analysis. J Surg Res. 2022;278:303-316. https://doi.org/10.1016/j.jss.2022.04.055
30. Fransson T, Mohammed Y, Gottsater A, Resch T. Prospective randomized clinical trial comparing paclitaxel-coated balloon versus conventional balloon angioplasty in treating below the knee arterial lesions in chronic limb threatening ischemia: the CRURAL DEB study. J Endovasc Ther. 2025 Nov 20 [Epub]. https://doi.org/10.1177/15266028251388746
31. Zeller T, Baumgartner I, Scheinert D, Brodmann M, Bosiers M, Micari A, et al. Drug-eluting balloon versus standard balloon angioplasty for infrapopliteal arterial revascularization in critical limb ischemia: 12-month results from the IN.PACT DEEP randomized trial. J Am Coll Cardiol. 2014;64:1568-1576. https://doi.org/10.1016/j.jacc.2014.06.1198
32. Zeller T, Beschorner U, Pilger E, Bosiers M, Deloose K, Peeters P, et al. Paclitaxel-coated balloon in infrapopliteal arteries: 12-month results from the BIOLUX P-II randomized trial (BIOTRONIK'S-First in Man study of the Passeo-18 LUX drug releasing PTA balloon catheter vs. the uncoated Passeo-18 PTA balloon catheter in subjects requiring revascularization of infrapopliteal arteries). JACC Cardiovasc Interv. 2015;8:1614-1622. https://doi.org/10.1016/j.jcin.2015.07.011

33. Patel A, Irani FG, Pua U, Tay KH, Chong TT, Leong S, et al. Randomized controlled trial comparing drug-coated balloon angioplasty versus conventional balloon angioplasty for treating below-the-knee arteries in critical limb ischemia: the SINGA-PACLI trial. Radiology. 2021;300:715-724. https://doi.org/10.1148/radiol.2021204294
34. Dadrass F, Raja SC, Lookstein R. Below-the-knee stents and scaffolds: a comprehensive review. Semin Intervent Radiol. 2023;40:167-171. https://doi.org/10.1055/s-0043-57263
35. Bosiers M, Scheinert D, Peeters P, Torsello G, Zeller T, Deloose K, et al. Randomized comparison of everolimus-eluting versus bare-metal stents in patients with critical limb ischemia and infrapopliteal arterial occlusive disease. J Vasc Surg. 2012;55:390-398. https://doi.org/10.1016/j.jvs.2011.07.099
36. Scheinert D, Katsanos K, Zeller T, Koppensteiner R, Commeau P, Bosiers M, et al. A prospective randomized multicenter comparison of balloon angioplasty and infrapopliteal stenting with the sirolimus-eluting stent in patients with ischemic peripheral arterial disease: 1-year results from the ACHILLES trial. J Am Coll Cardiol. 2012;60:2290-2295. https://doi.org/10.1016/j.jacc.2012.08.989
37. Bosiers MJ, Deloose K, Peeters P, Torsello G, Zeller T, Scheinert D, et al. Outcome of a drug-eluting stent in longer below-the-knee lesions in patients with critical limb ischemia. J Cardiovasc Surg (Torino). 2017;58:49-54. https://doi.org/10.23736/S0021-9509.16.09546-X
38. Giaquinta A, Vincenzo A, De Marco E, Veroux M, Veroux P. Everolimus-eluting stent for patients with critical limb ischemia and infrapopliteal arterial occlusive disease. Vasc Endovascular Surg. 2017;51:60-66. https://doi.org/10.1177/1538574416689429
39. Huizing E, Kum S, Ipema J, Varcoe RL, Shah AP, de Vries JP, et al. Mid-term outcomes of an everolimus-eluting bioresorbable vascular scaffold in patients with below-the-knee arterial disease: a pooled analysis of individual patient data. Vasc Med. 2021;26:195-199. https://doi.org/10.1177/1358863X20977907
40. Varcoe RL, DeRubertis BG, Kolluri R, Krishnan P, Metzger DC, Bonaca MP, et al. Drug-eluting resorbable scaffold versus angioplasty for infrapopliteal artery disease. N Engl J Med. 2024;390:9-19. https://doi.org/10.1056/NEJMoa2305637
41. DeRubertis BG, Varcoe RL, Krishnan P, Bonaca MP, O'Connor DJ, Pin R, et al. Drug-eluting resorbable scaffold versus balloon angioplasty for below-the-knee peripheral artery disease: 2-year results from the LIFE-BTK trial. Circulation. 2025;152:1076-1086. https://doi.org/10.1161/CIRCULATIONAHA.125.075080
42. Benfor B, Sinha K, Lumsden AB, Roy TL. Scoping review of atherectomy and intravascular lithotripsy with or without balloon angioplasty in below-the-knee lesions. J Vasc Surg Cases Innov Tech. 2023;9:101185. https://doi.org/10.1016/j.jvscit.2023.101185
43. Zilinyi RS, Alsaloum M, Snyder DJ, Raja A, Mintz AJ, Sethi SS, et al. Surgical and endovascular therapies for below-the-knee peripheral arterial disease: a contemporary review. J Soc Cardiovasc Angiogr Interv. 2024;3:101268. https://doi.org/10.1016/j.jscai.2023.101268
44. Feldman ZM, Mohapatra A. Endovascular management of complex tibial lesions. Semin Vasc Surg. 2022;35:190-199. https://doi.org/10.1053/j.semvascsurg.2022.04.008

Review Article

eISSN 2508-2612
https://doi.org/10.64961/kjir.2026.00122
Korean J Interv Radiol 2026;31(2):113-124

KJIR
Korean Journal of
Interventional Radiology

Endovascular Management of Type 2 Endoleak after Endovascular Aneurysm Repair: An Interventional Radiologist's Perspective

Joon Ho Kwon*

Department of Radiology and Research Institute of Radiological Science, Yonsei University College of Medicine, Seoul, Korea

Type 2 endoleak (T2EL) is the most common complication after endovascular aneurysm repair (EVAR), occurring in 10%–25% of patients. Although many T2ELs follow a benign course, persistent T2EL is associated with sac expansion, secondary endoleaks, rupture, and aneurysm-related mortality. Endovascular treatment is indicated in cases of progressive sac growth and is broadly divided into the transarterial approach and the direct sac puncture approach—the latter encompassing transabdominal, translumbar, and transcaval routes. Each approach has distinct technical advantages and limitations, and selection should be tailored to the source vessel of the endoleak, sac location, surrounding anatomy, and patient-related factors. Coils, N-butyl cyanoacrylate, and ethylene vinyl alcohol copolymer (Onyx) constitute the principal embolic agents, with liquid embolics showing improved durability over coils alone in recent comparative studies. Prophylactic embolization of the inferior mesenteric artery, lumbar arteries, or the aneurysm sac during EVAR has recently emerged as a promising preventive strategy. This review summarizes the current approaches, embolic materials, prophylactic strategies, and clinical outcomes of T2EL management from the perspective of the interventional radiologist.

Keywords: Aortic aneurysm, abdominal; Endoleak; Endovascular aneurysm repair; Embolization, therapeutic

Introduction

Type 2 endoleak (T2EL) is the most common complication after endovascular aneurysm repair (EVAR) for abdominal aortic aneurysm (AAA), occurring in approximately 10%–25% of patients [1,2]. T2EL results from retrograde flow into the aneurysm sac via patent aortic side branches, most commonly the inferior mesenteric artery (IMA) and lumbar arteries (LAs), and less frequently from accessory renal, median sacral, vasa vasorum, or intercostal arteries [2,3]. It typically behaves as a hemodynamic system with inflow and outflow vessels, analogous to an arteriovenous malformation nidus, which has important implications for treatment strategy [4].

Although many T2ELs follow a benign course and resolve spontaneously, persistent T2EL may lead to sac expansion, secondary type I or III endoleaks, sac rupture, and the need for reintervention or open conversion [5]. Recent evidence has challenged the long-held notion that T2EL is uniformly benign. Large-scale registries and systematic reviews have shown that persistent T2EL—particularly when it persists beyond 1 year—is significantly associated with sac enlargement, reintervention, rupture, and AAA-related mortality after EVAR, and that active management is warranted in patients with progressive sac growth [6-8].

Current treatment guidelines have been updated to reflect

Received: June 10, 2026; **Revised:** June 26, 2026;
Accepted: June 27, 2026
***Corresponding email:** golilla82@yuhs.ac

© 2026 Korean Society of Interventional Radiology

This is an Open Access article distributed under the terms of the Creative Commons Attribution Non-Commercial License (http://creativecommons.org/licenses/by-nc/4.0) which permits unrestricted non-commercial use, distribution, and reproduction in any medium, provided the original work is properly cited.

this evolving evidence. The Society for Vascular Surgery recommends intervention when aneurysm sac expansion is ≥5 mm, whereas the updated European Society for Vascular Surgery (ESVS) guidelines use a sac growth threshold of >10 mm and provide revised recommendations on the diagnostic step-up and management of endoleaks, including a strengthened role for active management in high-risk patients with persistent T2EL [9,10].

This review provides a comprehensive update on the endovascular management of T2EL from the interventional radiologist's perspective, focusing on (1) approach techniques, (2) embolic materials, (3) prophylactic embolization, and (4) clinical outcomes.

Approach Techniques

Endovascular access routes for T2EL embolization are broadly divided into the transarterial approach (TAA) and the direct sac puncture approach. Alternative and emerging techniques are presented at the end of this section. A comparative summary is provided in Table 1.

Transarterial Approach

The TAA is one of the most commonly used techniques for T2EL embolization. Access is typically obtained from a femoral or brachial route, and catheterization of the endoleak is performed via collateral pathways depending on the source vessel. For IMA-driven endoleaks, the most common route is via the SMA through the marginal artery of Drummond or the arc of Riolan into the IMA, and subsequently into the endoleak nidus (Fig. 1). For LA-driven endoleaks, the internal iliac artery and its iliolumbar collateral branches serve as the principal access route (Fig. 2).

To minimize the risk of recurrence, both the feeding vessel and the endoleak nidus should be embolized. Embolization of the feeder alone is associated with high recurrence rates due to recruitment of additional collateral vessels [4,11]. Recent advances such as triaxial microcatheter systems and small-caliber microcatheters have improved the technical feasibility of navigating long and tortuous collateral pathways [12].

Advantages of TAA include supine patient positioning, familiarity to the interventional radiologist, the minimally invasive nature of the procedure, and the ability to address multiple feeding vessels in a single session. However, this approach carries important technical limitations. In particular, LA-driven endoleaks require navigation through the iliolumbar collateral pathway from the internal iliac artery, which is frequently tortuous, narrow-caliber, and prone to spasm. As a result, super-selective access to the endoleak nidus through this circuitous route is technically demanding and often unsuccessful. Even when the feeding vessel is reached, definitive nidus embolization may be limited by the inability to advance the microcatheter sufficiently into the sac. These anatomic and technical considerations make TAA particularly suitable for IMA-dominant endoleaks with a favorable SMA-IMA collateral, whereas alternative direct sac puncture approaches are frequently required for LA-dominant endoleaks.

Direct Sac Puncture Approach

Direct sac puncture approaches involve percutaneous access into the aneurysm sac, allowing direct catheterization

Table 1. Comparison of approach techniques for type 2 endoleak embolization

Approach	Advantages	Limitations
Transarterial	Familiar technique	Tortuous collateral pathway
	Supine position	Lower technical success in lumbar-driven endoleaks
	Minimally invasive	
Transabdominal	Direct sac access	Risk of bowel/visceral injury
	Supine position	Requires safe anterior window
	Ultrasound guided procedure	
	Useful when sac is anteriorly located	
Translumbar	Direct sac access	Prone position
	Lower risk of bowel injury	Risk of retroperitoneal hematoma
		Limited by kidney interposition
Transcaval	Supine position	Risk of endograft injury
	Concurrent arterial access	Aneurysm sac must abut to IVC

https://doi.org/10.64961/kjir.2026.00122

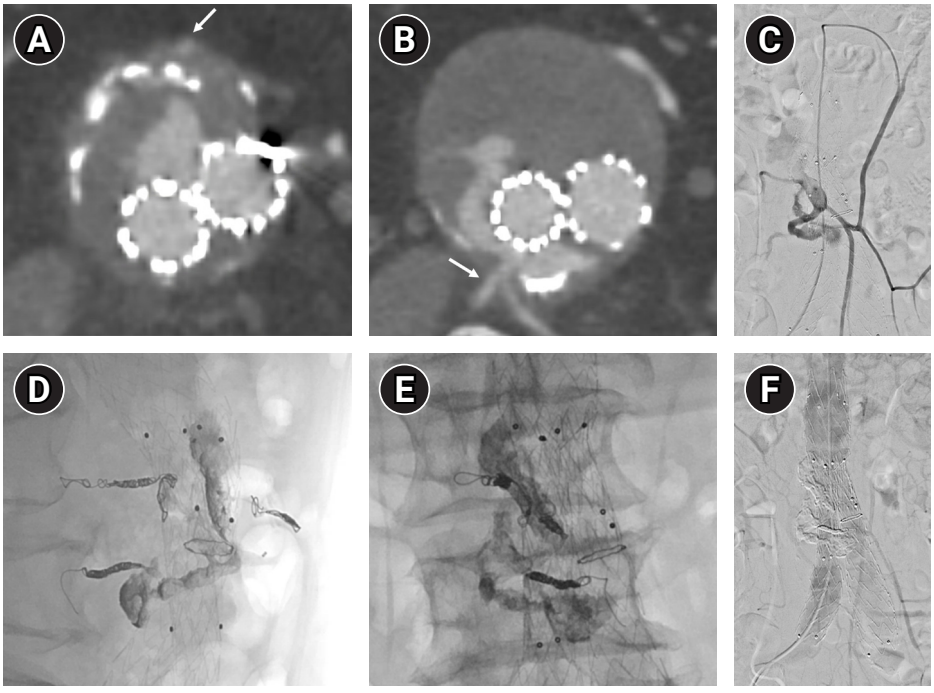


Fig. 1. Transarterial embolization of a type 2 endoleak via the SMA–arc of Riolan–inferior mesenteric artery (IMA) pathway in a 76-year-old man. (A) Axial CT image showing a type 2 endoleak fed by the inferior mesenteric artery (arrow). (B) Axial CT image at a more inferior level demonstrating additional feeding from bilateral lumbar arteries (arrow) connecting to the same endoleak nidus. (C) Selective superior mesenteric arteriography showing opacification of the IMA, endoleak nidus, and feeding lumbar arteries via the arc of Riolan. (D, E) Lateral (D) and anteroposterior (E) fluoroscopic images obtained after embolization of the IMA and lumbar arteries with coils and of the residual endoleak nidus with Onyx. (F) Post-embolization aortography demonstrating complete resolution of the type 2 endoleak.

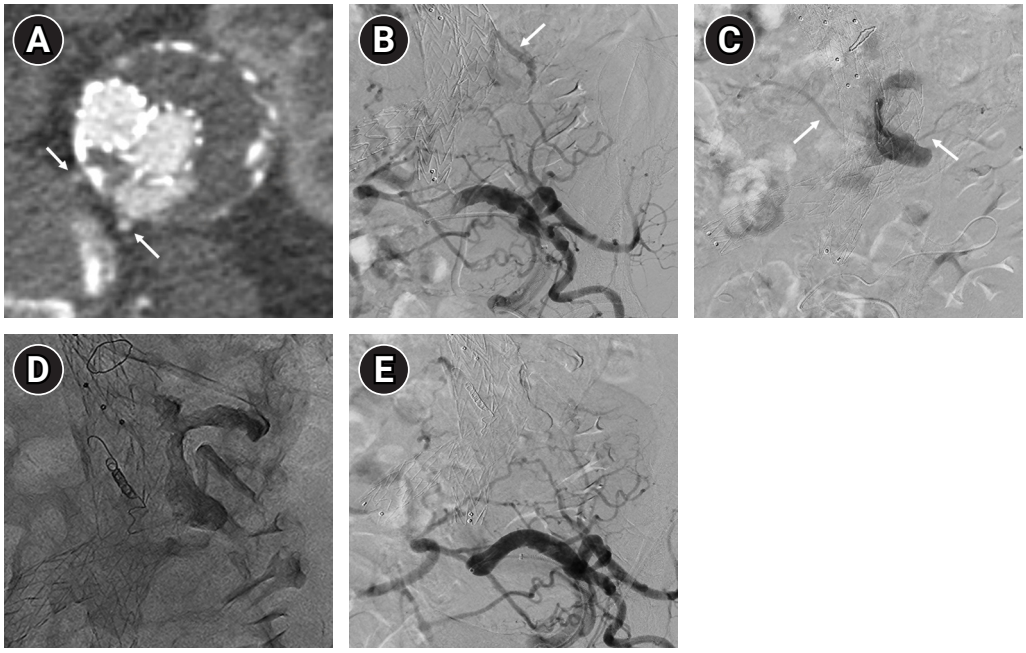


Fig. 2. Transarterial embolization of a type 2 endoleak via the internal iliac artery–iliolumbar collateral pathway in an 84-year-old woman. (A) Axial CT image showing a type 2 endoleak fed by bilateral lumbar arteries (arrows). (B) Left internal iliac arteriography demonstrating opacification of the endoleak nidus (arrow) through an iliolumbar collateral. (C) Angiography obtained after advancing a microcatheter through the iliolumbar collateral into the endoleak nidus, showing opacification of bilateral lumbar arteries (arrows). (D) Post-embolization image showing coil embolization of the right lumbar artery and Onyx embolization of the endoleak nidus and the left lumbar artery. (E) Final angiography demonstrating complete resolution of the type 2 endoleak.

and embolization of the endoleak nidus and outflow vessels. These techniques are generally associated with higher technical success rates than the TAA, particularly for complex or multi-source endoleaks [13]. Three principal routes have been described—transabdominal, translumbar, and transcaval—each chosen based on sac location, surrounding anatomy, and patient positioning constraints.

The technical workflow for both transabdominal and translumbar approaches follows a common sequence. Under CT, fluoroscopy, or ultrasound guidance, the endoleak nidus is punctured with a 21-gauge Chiba needle, and intrasac position is confirmed by free backflow of arterial blood. Selective angiography is then performed to delineate the endoleak nidus, feeding artery, and outflow vessels. A 0.018-inch guidewire is then introduced, and a 4-Fr coaxial introducer sheath is placed. A Y-connector is attached to the sheath to permit coaxial introduction of a microcatheter (Fig. 3). In selected cases with low-flow dynamics and simple sac anatomy—particularly endoleaks supplied by a small number (typically 1–2) of feeders arising from a single vertebral level—the liquid embolic agent may also be injected directly through the 21-gauge Chiba puncture needle without subsequent placement of a coaxial introducer sheath and microcatheter [14].

When the feeding artery can be selectively catheterized with the microcatheter, coil embolization is performed for feeder occlusion followed by a liquid embolic agent for nidus filling (Fig. 4). When selective feeder catheterization is not possible, a liquid embolic alone is used to obliterate both the nidus and the proximal portion of the feeding artery.

The direct transabdominal approach involves anterior percutaneous puncture of the aneurysm sac under CT or ultrasound guidance, typically with the patient in the supine position. This approach is most suitable when the aneurysm sac has an accessible anterior window, free of overlying bowel, kidney, or vascular structures. While the supine positioning is well tolerated, careful pre-procedural planning with cross-sectional imaging is essential to avoid injury to adjacent abdominal organs [15]. Disadvantages of the transabdominal approach include the risk of injury to overlying abdominal organs and limited applicability when no safe anterior puncture window is available.

The translumbar approach (TLA) is the most established direct sac puncture technique. With the patient in the prone position, percutaneous puncture is performed via a left posterolateral route under CT or cone-beam computed tomography guidance, and embolization is carried out under fluoros-

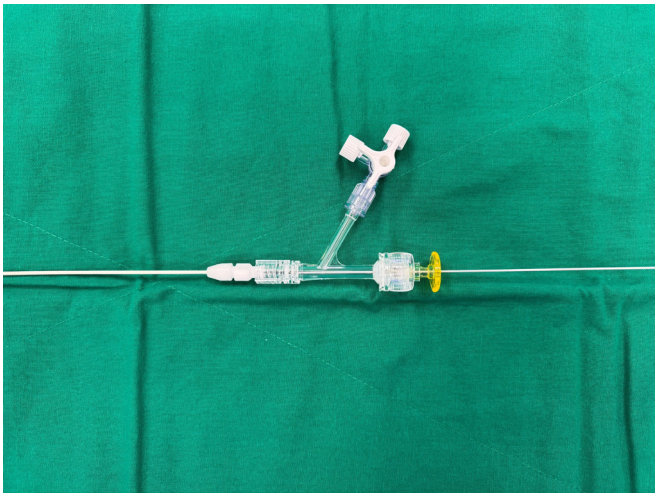


Fig. 3. Working assembly used for direct sac puncture embolization. A 4-Fr coaxial introducer sheath is connected to a Y-connector, allowing coaxial introduction of a microcatheter while maintaining hemostasis.

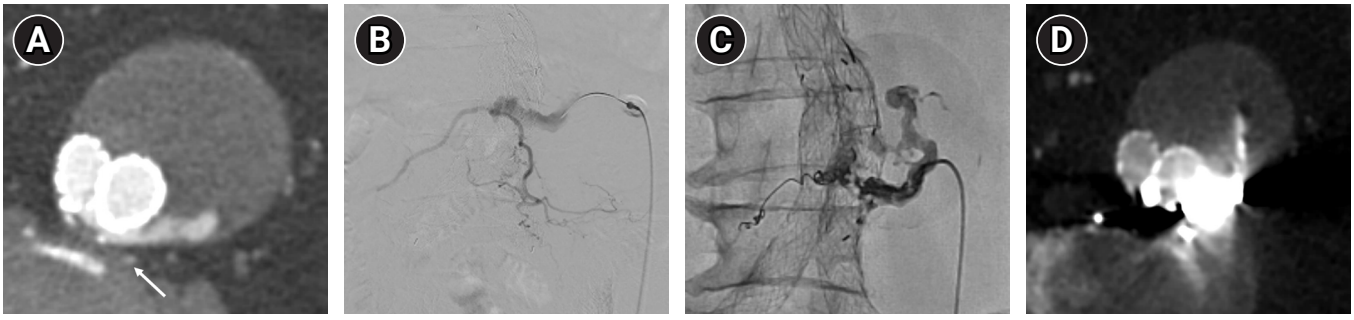


Fig. 4. Transabdominal direct sac puncture embolization of a type 2 endoleak in a 79-year-old woman. (A) Axial CT image showing a type 2 endoleak fed by a posteriorly arising lumbar artery (arrow) behind the aneurysm sac. (B) Selective angiography obtained after transabdominal direct sac puncture, demonstrating opacification of the endoleak nidus and bilateral lumbar arteries. (C) Post-embolization image showing coil embolization of the right lumbar artery and Onyx embolization of the residual endoleak nidus. (D) Follow-up CT image demonstrating complete resolution of the type 2 endoleak.

copy. TLA provides excellent direct access to the sac and is particularly useful for LA-driven endoleaks. Disadvantages include the requirement for prone positioning—which may be challenging in elderly or obese patients—the risk of retroperitoneal hematoma, and limited applicability when bowel, kidney, or graft components are interposed in the puncture trajectory [16-18].

Transcaval embolization (TCE) is performed via transfemoral or transjugular venous access, with direct puncture of the IVC into the aneurysm sac. The level of the endoleak nidus is identified on pre-procedural CT angiography. Under fluoroscopic and intravascular ultrasound guidance, the Colapinto needle or the Rösch-Uchida needle is advanced from the IVC into the aneurysm sac at the planned level. After confirmation of intrasac position by angiography, embolization is typically performed using a liquid embolic agent to fill the endoleak nidus and outflow vessels [19,20]. Ideal candidates have a sac abutting the IVC with minimal calcification at the puncture site. The transcaval approach is particularly valuable when the endoleak nidus is located in a region inaccessible to transabdominal or translumbar approaches (Fig. 5). Advantages of TCE include supine positioning, concurrent arterial access for completion angiography, and avoidance of risks associated with prone positioning, making it particularly valuable when transarterial and translumbar approaches have failed or are not feasible [20,21]. However, the main limitations are the risk of endograft injury and the technical complexity of caval-aortic crossing, although novel microwire-based caval traversal techniques have improved procedural safety [22].

Alternative and Emerging Approaches

Several alternative and emerging approaches have been described for selected cases or as salvage strategies when conventional techniques fail. The perigraft approach involves catheterization of the space between the stent graft and the native aortic wall, typically via a transfemoral arterial route, and is useful when the endoleak nidus communicates with the perigraft space [23]. The transgraft approach uses direct puncture through the stent graft into the aneurysm sac; although technically feasible, it carries a risk of creating a new type III endoleak and is therefore generally reserved for cases in which no other access is available [23]. In addition, a hybrid technique combining microsurgical–endovascular access via direct exposure and puncture of a lumbar segmental artery has been reported in a case not amenable to conventional endovascular access [24], and laparoscopic clipping of the IMA or LAs remains a surgical alternative reserved for refractory endoleaks after multiple failed endovascular attempts [25].

Embolic Materials

Selection of the embolic agent depends on the access route, the morphology of the endoleak, and operator experience.

Coils

Detachable and pushable microcoils remain the most widely used embolic agents, particularly for feeder vessel occlusion. They allow precise and controlled deployment but may be insufficient for nidus filling when used alone. Several stud-



Fig. 5. Transcaval embolization of a type 2 endoleak in a 64-year-old man, in whom both transabdominal and translumbar approaches were precluded because the endoleak nidus was located between the stent-graft and the vertebral body. (A) Axial CT image showing a type 2 endoleak fed by a posteriorly arising lumbar artery (arrow), with the nidus positioned between the stent-graft and the vertebral body. (B) Fluoroscopic image showing transcaval puncture of the endoleak nidus using a Rösch-Uchida needle introduced via the right internal jugular vein. (C) Angiography obtained after intrasac access demonstrating opacification of the endoleak nidus and the feeding lumbar artery. (D) Post-embolization image showing complete obliteration of the endoleak nidus using N-butyl cyanoacrylate glue mixed with ethiodized oil at a 1:4 ratio.

ies have shown higher reintervention rates with coil-only embolization compared with liquid embolic materials [11,26,27].

Liquid Embolic Materials

Liquid embolic agents have gained increasing prominence in T2EL embolization because of their ability to penetrate and fill the endoleak nidus and feeding vessels. The two most commonly used liquid agents are N-butyl cyanoacrylate (NBCA) and ethylene vinyl alcohol copolymer (Onyx).

NBCA (Histoacryl, B. Braun, Melsungen, Germany) is an adhesive liquid embolic that polymerizes rapidly upon contact with ionic environments, allowing rapid and durable sac occlusion at relatively low cost. The dilution ratio with ethiodized oil (Lipiodol, Guerbet, Villepinte, France) is typically tailored to the flow dynamics of the target endoleak and the number of feeding vessels. However, when multiple feeding vessels coexist within the endoleak nidus, the rapid polymerization of NBCA may result in early solidification of the embolic material before all feeders are occluded, leaving residual patent inflow channels that perpetuate the endoleak. Other major technical concerns include the risk of catheter retention and non-target embolization, both of which require careful technique and operator experience to mitigate [28].

Onyx (Medtronic, Minneapolis, MN, USA) is a non-adhesive liquid embolic agent dissolved in dimethyl sulfoxide that precipitates upon contact with blood. Its non-adhesive nature allows controlled, prolonged injection and excellent penetration of the endoleak nidus and outflow vessels [29]. However, the procedure is typically time-consuming, often requiring extended fluoroscopy time. In addition, because Onyx has a relatively high specific gravity and must be injected slowly ($\leq$0.2 mL/min) to allow gradual polymerization, retrograde filling of the inflow arteries against arterial pressure can be difficult, and the agent tends to layer dependently within the sac rather than refluxing into upstream feeders.

Combined Strategies

In clinical practice, a combination of coils for feeder vessel occlusion and a liquid embolic for nidus filling is often advocated, particularly with direct sac puncture techniques. This combined approach addresses both inflow and outflow components of the endoleak and may reduce recurrence [30].

Outcomes

A summary of representative outcome studies is provided in Table 2 [15,21,31-35].

Post-procedure Follow-up

Routine post-embolization follow-up imaging is typically performed with contrast-enhanced CT (CE-CT). According to current guidelines, surveillance imaging is recommended within 1–6 months of the procedure and annually thereafter, with modifications based on residual endoleak status, sac size changes, and renal function [10]. In patients with impaired renal function or contrast allergy in whom CE-CT is not feasible, non-contrast CT may be used to monitor changes in aneurysm sac diameter, or contrast-enhanced ultrasound (CE-US) with sulfur hexafluoride microbubbles (SonoVue, Bracco, Milan, Italy) may serve as a non-nephrotoxic alternative. CE-US offers several advantages, including the absence of nephrotoxicity (the microbubble contrast agent is eliminated via the lungs rather than the kidneys), the lack of ionizing radiation, and the ability to demonstrate real-time flow dynamics; pooled meta-analyses have reported sensitivities of approximately 91% for endoleak detection, comparable to CT angiography [36].

Table 2. Summary of representative outcome studies of type 2 endoleak embolization

Study	No. of patients	Approach	Embolic agent	Technical success	Clinical success
Zener et al. (2018) [15]	31	Transabdominal	Coils, NBCA, Onyx	100%	81%
Scallan et al. (2021) [31]	58	TAA/TLA	Onyx vs. coils	Not reported	Lower reintervention with Onyx
Hamidizadeh et al. (2021) [32]	129	TAA vs. TLA	NBCA, coils, Onyx	Higher with TLA	NBCA superior; access success a predictor
Nana et al. (2022, SR) [21]	117	Transcaval	Various	Pooled 96%	80% at 12 months
Vandenbulcke et al. (2023) [33]	60	TAA/TLA	Various	95%	Radiological 26.7%; sac stable in 48.3%
Nana et al. (2024) [34]	43	Transcaval	Coils, Onyx	97.7%	90% at 36 months
Chun et al. (2026) [35]	72	Mixed	Various	77%	82%/70%/59% at 12/24/60 months

NBCA, N-butyl cyanoacrylate; TAA, transarterial approach; TLA, translumbar approach; SR, systematic review.

Definitions of Success

Outcome reporting in T2EL embolization is heterogeneous, which complicates direct comparison across studies. The most commonly used endpoints are technical success defined as complete cessation of flow within the endoleak nidus and feeding vessels on completion angiography; radiological success defined as the absence of a visible endoleak on follow-up CE-CT; and clinical success defined as stabilization or shrinkage of the aneurysm sac on follow-up imaging, irrespective of residual endoleak.

Technical Success

Pooled technical success rates of T2EL embolization range from 84% to 100%, depending on the technique used [32]. Direct sac puncture approaches generally yield higher technical success than TAAs. Hamidizadeh et al. [32] reported a significantly higher technical success rate with TLA compared with TAA in a long-term study of 129 patients. For transabdominal direct sac puncture, Zener et al. [15] reported a 100% technical success rate in 31 patients, and for TLA, reported technical success rates range from 90% to 100% across published series [16-18]. Transcaval approaches in recent series have achieved technical success rates of 96%–98% [21,34].

Clinical Success and Long-term Outcomes

Clinical success rates vary widely (30%–90%), reflecting differences in definition, follow-up duration, embolic agent, and patient selection. Across direct sac puncture techniques, reported clinical success rates are approximately 81% for transabdominal embolization at 12 months [15], 70%–85% for translumbar embolization [16-18], and up to 90% at 36 months for TCE [34]. Long-term cohort data, however, have demonstrated a progressive decline in durability, with clinical success falling from approximately 82% at 12 months to 59% at 60 months [35]. Larger registry analyses, including data from the Vascular Quality Initiative and the Japanese Committee for Stentgraft Management registry, have similarly confirmed that persistent T2EL is associated with sac enlargement and increased reintervention rates [6,37]. Notably, although persistent sac expansion is associated with higher rates of reintervention and open conversion, it does not appear to be independently associated with worse overall survival [33,35].

Comparative Outcomes

Direct comparisons of access routes have shown that the early advantage of TLA over TAA in technical success [16] has narrowed in subsequent series using modified transarterial techniques, with comparable clinical success rates of 72%–78% reported between the two approaches [18,32]. With regard to embolic agents, Onyx has been associated with significantly lower reintervention rates than coils alone in long-term follow-up [31]. Among direct sac puncture techniques, TCE has produced particularly favorable outcomes, with a pooled clinical success of 80% at 12 months [21] and 90% at 36 months in a recent single-center series [34].

Factors Influencing Clinical Success

Several patient-, procedural-, and imaging-related factors have been identified as influencing clinical success after T2EL embolization. From a procedural standpoint, Hamidizadeh et al. [32] identified successful sac access during transarterial embolization and the use of NBCA glue as independent predictors of clinical success, with NBCA showing significantly higher success rates than other embolic agents ($p = 0.017$–0.037). Embolization of both the nidus and the feeding vessels—as opposed to feeder-only or nidus-only embolization—has also been associated with better long-term outcomes [4,11].

Imaging-based predictors are increasingly recognized. Pre-interventional CT findings such as unsharp or blurred T2EL delineation have been identified as predictors of persistent endoleak and continued sac expansion after embolization [33]. Earlier work has also shown that CT features of T2EL flow dynamics can predict subsequent sac enlargement [38]. These features include sharper delineation of the endoleak nidus on early arterial-phase CT angiography, persistent opacification across the venous and delayed phases, and a greater number and larger caliber of communicating branch vessels, all of which have been correlated with subsequent sac enlargement. Anatomic factors—a patent and large-caliber IMA, multiple patent LAs, and lower mural thrombus burden—are also associated with persistence and reduced response to embolization [39,40]. Such imaging- and anatomy-based predictors may help guide patient selection and inform decisions regarding alternative strategies, including open conversion in refractory cases.

Complications

Major complications are uncommon (<5%). Reported complications include non-target embolization (e.g., colonic ischemia, spinal cord injury), retroperitoneal hematoma, graft injury, infection, and—rarely—aneurysm rupture during or after the procedure [27,31].

Prophylactic Embolization

Given the limited durability of secondary embolization for established T2EL, prophylactic embolization of aortic side branches has emerged as a strategy to prevent T2EL after EVAR. Three main strategies have been described: selective IMA embolization-aneurysmal sac side branch (IMA-ASSB), in which a patent IMA is pre-emptively occluded with coils or a vascular plug before or during EVAR; non-selective aneurysmal sac side branch embolization (NS-ASSB), which combines IMA embolization with closure of patent LAs; and aneurysm sac coil embolization (ASCE), in which coils or a liquid embolic are placed directly within the aneurysm sac at the time of EVAR.

Rationale and Patient Selection

Anatomic predictors for T2EL include a patent IMA ≥3 mm in diameter, two or more patent LAs ≥2 mm in diameter, and an aortoiliac aneurysm configuration [39,40]. Patients with these features are considered high-risk for T2EL and may derive the greatest benefit from prophylactic embolization.

Evidence from Randomized Trials and Meta-Analyses

A landmark single-center randomized controlled trial evaluated pre-emptive IMA embolization in 106 high-risk patients with patent IMA and at least one additional anatomic risk factor (LAs ≥2 mm or aortoiliac configuration). At 5-year follow-up, the embolization group had significantly lower T2EL rates compared with controls (28.3% vs. 54.7%, p = 0.006), a higher freedom from sac enlargement, and a greater cumulative incidence of sac shrinkage [41]. The multicenter CLARIFY-IMA study protocol has been initiated to further confirm these findings on a broader scale [42].

Several recent systematic reviews and meta-analyses have consistently supported the efficacy of prophylactic side-branch embolization in reducing T2EL incidence, sac enlargement, and reintervention rates after EVAR compared with standard EVAR alone. These analyses, encompassing both retrospective cohort and updated randomized/registry data, have shown that all three strategies—IMA-ASSB, NS-ASSB, and ASCE—are superior to no embolization, with broadly comparable efficacy among them, although IMA-ASSB has shown a tendency toward better suppression of sac expansion and reintervention in network comparisons [43-47]. A summary of these key studies is provided in Table 3 [41,43-46].

Current Status and Considerations

Despite encouraging evidence, prophylactic embolization is not yet a standard of care. The ESVS 2024 guidelines acknowledge the accumulating data but note that broader implementation is not yet recommended without further high-quality evidence, including data on cost-effectiveness and the potential effect on rupture rates [10]. Practical considerations include added procedural time, contrast load, radiation exposure, and procedural cost. However, selective application in high-risk patients—defined by anatomic criteria—appears to provide the most favorable risk-benefit ratio.

Conclusion

Type 2 endoleak embolization remains a clinically chal-

Table 3. Summary of representative studies on prophylactic embolization to prevent T2EL

Author (Year)	Design	Strategy	T2EL rate (Emb vs. Ctrl)	Reintervention (Emb vs. Ctrl)
Yu et al. (2020) [43]	Meta-analysis	Side-branch embolization	18.5% vs. 38.6% (OR 0.34)	1.5% vs. 12.4% (OR 0.12)
Yu et al. (2023) [44]	Meta-analysis	Side-branch embolization	Reduced T2EL (OR 0.40)	Reduced
Takeuchi et al. (2024) [41]	Single-center RCT	IMA embolization	28.3% vs. 54.7% (p = 0.006)	Reduced
Niklas et al. (2022) [45]	Meta-analysis	IMA embolization	Reduced T2EL incidence	Reduced
Wu et al. (2022) [46]	Meta-analysis	IMA-ASSB vs. NS-ASSB vs. ASCE	All strategies superior to no embolization	IMA-ASSB tended to lower reintervention

T2EL, type 2 endoleak; Emb, embolization; Ctrl, control; RCT, randomized controlled trial; IMA, inferior mesenteric artery; IMA-ASSB, inferior mesenteric artery aortic side branch embolization; NS-ASSB, non-selective aortic side branch embolization; ASCE, aneurysm sac coil embolization.

lenging but evolving field within interventional radiology. No single approach can be regarded as universally first-line; rather, the optimal access route—whether transarterial, transabdominal, translumbar, or transcaval—should be tailored to each patient based on the source vessel of the endoleak, sac location and anatomy, surrounding structures, prior intervention history, and patient-related factors such as positional tolerance. For IMA-dominant endoleaks with favorable SMA-IMA collateral, transarterial embolization remains an effective option, while direct sac puncture approaches are often more effective for LA-dominant or multi-source endoleaks. The transcaval approach has emerged as a particularly valuable option for sacs abutting the IVC and for cases in which prone positioning is contraindicated.

Liquid embolic agents, particularly Onyx and NBCA, have shown improved durability over coils alone, although optimal material selection remains individualized and dependent on the access route and endoleak morphology. Prophylactic embolization in carefully selected high-risk patients—supported by a recent randomized trial and multiple meta-analyses—appears to reduce T2EL incidence, sac enlargement, and reintervention rates. Nevertheless, its routine use is not yet endorsed by current guidelines.

In conclusion, we have summarized the current evidence on endovascular management of T2EL after EVAR. Multidisciplinary collaboration, careful patient selection, and tailored technique selection remain the cornerstones of successful management. Further prospective randomized trials with longer follow-up are needed to standardize practice and define the optimal role of each technique and embolic material.

Conflict of interest

No potential conflict of interest relevant to this article was reported.

Funding

None.

Acknowledgments

None.

Author contributions

The author conducted all aspects of the study.

Data availability statement

The datasets generated or analyzed during the study are available from the corresponding author on reasonable request.

ORCID

Joon Ho Kwon, https://orcid.org/0000-0002-6178-7252

References

1. White GH, Yu W, May J, Chaufour X, Stephen MS. Endoleak as a complication of endoluminal grafting of abdominal aortic aneurysms: classification, incidence, diagnosis, and management. J Endovasc Surg. 1997;4:152-168. https://doi.org/10.1177/152660289700400207
2. Baum RA, Stavropoulos SW, Fairman RM, Carpenter JP. Endoleaks after endovascular repair of abdominal aortic aneurysms. J Vasc Interv Radiol. 2003;14:1111-1117. https://doi.org/10.1097/01.rvi.0000085773.71254.86
3. Rhee SJ, Ohki T, Veith FJ, Kurvers H. Current status of management of type II endoleaks after endovascular repair of abdominal aortic aneurysms. Ann Vasc Surg. 2003;17:335-344. https://doi.org/10.1007/s10016-003-0002-5
4. Chuter TA, Faruqi RM, Sawhney R, Reilly LM, Kerlan RB, Canto CJ, et al. Endoleak after endovascular repair of abdominal aortic aneurysm. J Vasc Surg. 2001;34:98-105. https://doi.org/10.1067/mva.2001.111487
5. Pineda DM, Calligaro KD, Tyagi S, Troutman DA, Dougherty MJ. Late type II endoleaks after endovascular aneurysm repair require intervention more frequently than early type II endoleaks. J Vasc Surg. 2018;67:449-452. https://doi.org/10.1016/j.jvs.2017.05.124
6. Seike Y, Matsuda H, Shimizu H, Ishimaru S, Hoshina K, Michihata N, et al. Nationwide analysis of persistent type II endoleak and late outcomes of endovascular abdominal aortic aneurysm repair in Japan: a propensity-matched analysis. Circulation. 2022;145:1056-1066. https://doi.org/10.1161/CIRCULATIONAHA.121.056581
7. Iwakoshi S, Ogawa Y, Dake MD, Ono Y, Higashihara H, Ikoma A, et al. Outcomes of embolization procedures for type II endoleaks following endovascular abdominal aortic repair. J Vasc Surg. 2023;77:114-121. https://doi.org/10.1016/j.jvs.2022.07.168

8. Ultee KH, Buttner S, Huurman R, Bastos Goncalves F, Hoeks SE, Bramer WM, et al. Editor's choice: systematic review and meta-analysis of the outcome of treatment for type II endoleak following endovascular aneurysm repair. Eur J Vasc Endovasc Surg. 2018;56:794-807. https://doi.org/10.1016/j.ejvs.2018.06.009
9. Chaikof EL, Dalman RL, Eskandari MK, Jackson BM, Lee WA, Mansour MA, et al. The Society for Vascular Surgery practice guidelines on the care of patients with an abdominal aortic aneurysm. J Vasc Surg. 2018;67:2-77. https://doi.org/10.1016/j.jvs.2017.10.044
10. Wanhainen A, Van Herzeele I, Bastos Goncalves F, Bellmunt Montoya S, Berard X, Boyle JR, et al. Editor's choice: European Society for Vascular Surgery (ESVS) 2024 clinical practice guidelines on the management of abdominal aorto-iliac artery aneurysms. Eur J Vasc Endovasc Surg. 2024;67:192-331. https://doi.org/10.1016/j.ejvs.2023.11.002
11. Sarac TP, Gibbons C, Vargas L, Liu J, Srivastava S, Bena J, et al. Long-term follow-up of type II endoleak embolization reveals the need for close surveillance. J Vasc Surg. 2012;55:33-40. https://doi.org/10.1016/j.jvs.2011.07.092
12. Onishi Y, Shimizu H, Kawatou M, Minatoya K, Nakamoto Y. Transarterial embolization of type 2 endoleak post thoracic endovascular aortic repair (TEVAR) using a triaxial system with a 1.3-F microcatheter: a case report. Cureus. 2024;16:e51694. https://doi.org/10.7759/cureus.51694
13. Yang RY, Tan KT, Beecroft JR, Rajan DK, Jaskolka JD. Direct sac puncture versus transarterial embolization of type II endoleaks: an evaluation and comparison of outcomes. Vascular. 2017;25:227-233. https://doi.org/10.1177/1708538116663992
14. Burke CT, Yu H. How I do it: computed tomography-guided modified translumbar embolization of type 2 endoleak. Semin Intervent Radiol. 2021;38:576-580. https://doi.org/10.1055/s-0041-1736656
15. Zener R, Oreopoulos G, Beecroft R, Rajan DK, Jaskolka J, Tan KT. Transabdominal direct sac puncture embolization of type II endoleaks after endovascular abdominal aortic aneurysm repair. J Vasc Interv Radiol. 2018;29:1167-1173. https://doi.org/10.1016/j.jvir.2018.04.002
16. Baum RA, Carpenter JP, Golden MA, Velazquez OC, Clark TW, Stavropoulos SW, et al. Treatment of type 2 endoleaks after endovascular repair of abdominal aortic aneurysms: comparison of transarterial and translumbar techniques. J Vasc Surg. 2002;35:23-29. https://doi.org/10.1067/mva.2002.121068
17. Stavropoulos SW, Carpenter JP, Fairman RM, Golden MA, Baum RA. Inferior vena cava traversal for translumbar endoleak embolization after endovascular abdominal aortic aneurysm repair. J Vasc Interv Radiol. 2003;14:1191-1194. https://doi.org/10.1097/01.rvi.0000085771.71254.14
18. Stavropoulos SW, Park J, Fairman R, Carpenter J. Type 2 endoleak embolization comparison: translumbar embolization versus modified transarterial embolization. J Vasc Interv Radiol. 2009;20:1299-1302. https://doi.org/10.1016/j.jvir.2009.07.003
19. Mansueto G, Cenzi D, Scuro A, Gottin L, Griso A, Gumbs AA, et al. Treatment of type II endoleak with a transcatheter transcaval approach: results at 1-year follow-up. J Vasc Surg. 2007;45:1120-1127. https://doi.org/10.1016/j.jvs.2007.01.063
20. Giles KA, Fillinger MF, De Martino RR, Hoel AW, Powell RJ, Walsh DB. Results of transcaval embolization for sac expansion from type II endoleaks after endovascular aneurysm repair. J Vasc Surg. 2015;61:1129-1136. https://doi.org/10.1016/j.jvs.2014.12.002
21. Nana P, Spanos K, Heidemann F, Panuccio G, Kouvelos G, Rohlffs F, et al. Systematic review on transcaval embolization for type II endoleak after endovascular aortic aneurysm repair. J Vasc Surg. 2022;76:282-291. https://doi.org/10.1016/j.jvs.2022.02.032
22. Van Sickler AP, Smith AH, Ellis RC, Steenberge SP, Quatromoni JG, Rowse JW, et al. A novel technique and outcomes for transcaval endoleak embolization. Ann Vasc Surg. 2023;93:300-307. https://doi.org/10.1016/j.avsg.2023.01.013
23. Chen JX, Stavropoulos SW. Type 2 endoleak management. Semin Intervent Radiol. 2020;37:365-370. https://doi.org/10.1055/s-0040-1715873
24. Nguyen VN, Rennert RC, Sternbach S, Cavaleri J, Abedi A, Atai NA, et al. A novel combined microsurgical and endovascular approach for type II endoleak embolization through direct puncture of a lumbar segmental artery: a technical case instruction. Neurosurg Pract. 2024;5:e00115. https://doi.org/10.1227/neuprac.0000000000000115
25. Spanos K, Tsilimparis N, Larena-Avellaneda A, Giannoukas AD, Debus SE, Kolbel T. Systematic review of laparoscopic ligation of inferior mesenteric artery for the treatment of

type II endoleak after endovascular aortic aneurysm repair. J Vasc Surg. 2017;66:1878-1884. https://doi.org/10.1016/j.jvs.2017.07.066

26. Stavropoulos SW, Kim H, Clark TW, Fairman RM, Velazquez O, Carpenter JP. Embolization of type 2 endoleaks after endovascular repair of abdominal aortic aneurysms with use of cyanoacrylate with or without coils. J Vasc Interv Radiol. 2005;16:857-861. https://doi.org/10.1097/01.RVI.0000156495.66062.62
27. Abularrage CJ, Patel VI, Conrad MF, Schneider EB, Cambria RP, Kwolek CJ. Improved results using Onyx glue for the treatment of persistent type 2 endoleak after endovascular aneurysm repair. J Vasc Surg. 2012;56:630-636. https://doi.org/10.1016/j.jvs.2012.02.038
28. Kajiwara K, Yamagami T, Urashima M, Tomiyoshi H, Kakizawa H, Yoshimatsu R, et al. Embolization for type 2 endoleak with sac expansion after endovascular repair of abdominal aortic aneurysm: safety and effectiveness. Springerplus. 2016;5:262. https://doi.org/10.1186/s40064-016-1934-x
29. Massis K, Carson WG 3rd, Rozas A, Patel V, Zwiebel B. Treatment of type II endoleaks with ethylene-vinyl-alcohol copolymer (Onyx). Vasc Endovascular Surg. 2012;46:251-257. https://doi.org/10.1177/1538574412442401
30. Khaja MS, Park AW, Swee W, Evans AJ, Fritz Angle J, Turba UC, et al. Treatment of type II endoleak using Onyx with long-term imaging follow-up. Cardiovasc Intervent Radiol. 2014;37:613-622. https://doi.org/10.1007/s00270-013-0706-z
31. Scallan O, Kribs S, Power AH, DeRose G, Duncan A, Dubois L. Onyx versus coil embolization for the treatment of type II endoleaks. J Vasc Surg. 2021;73:1966-1972. https://doi.org/10.1016/j.jvs.2020.10.069
32. Hamidizadeh R, Nzekwu E, Halliwell O. Factors influencing clinical success following endovascular treatment of type II endoleaks. Can Assoc Radiol J. 2021;72:890-897. https://doi.org/10.1177/0846537120981100
33. Vandenbulcke R, Houthoofd S, Laenen A, Buyck PJ, Mufty H, Fourneau I, et al. Embolization therapy for type 2 endoleaks after endovascular aortic aneurysm repair: imaging-based predictive factors and clinical outcomes on long-term follow-up. Diagn Interv Radiol. 2023;29:331-341. https://doi.org/10.4274/dir.2022.22352
34. Nana P, Panuccio G, Rohlffs F, Torrealba JI, Spanos K, Kolbel T. Early and mid-term outcomes of transcaval embolization for type 2 endoleak after endovascular aortic repair. J Clin Med. 2024;13:3578. https://doi.org/10.3390/jcm13123578
35. Chun JY, Patel S, Ameli-Renani S, Pavlidis V, Morgan R. Embolisation of type 2 endoleaks associated with sac expansion: outcomes from a single-centre cohort. Cardiovasc Intervent Radiol. 2026;49:496-507. https://doi.org/10.1007/s00270-025-04272-8
36. Bredahl KK, Taudorf M, Lonn L, Vogt KC, Sillesen H, Eiberg JP. Contrast enhanced ultrasound can replace computed tomography angiography for surveillance after endovascular aortic aneurysm repair. Eur J Vasc Endovasc Surg. 2016;52:729-734. https://doi.org/10.1016/j.ejvs.2016.07.007
37. DeMartino RR, Breite MD, Neal D, Mendes BC, Colglazier JJ, Stone DH, et al. Incidence, reintervention, and survival associated with type II endoleak at hospital discharge after elective endovascular aneurysm repair in the Vascular Quality Initiative. J Vasc Surg. 2023;78:679-686. https://doi.org/10.1016/j.jvs.2023.05.041
38. Muller-Wille R, Schotz S, Zeman F, Uller W, Guntner O, Pfister K, et al. CT features of early type II endoleaks after endovascular repair of abdominal aortic aneurysms help predict aneurysm sac enlargement. Radiology. 2015;274:906-916. https://doi.org/10.1148/radiol.14140284
39. Ward TJ, Cohen S, Patel RS, Kim E, Fischman AM, Nowakowski FS, et al. Anatomic risk factors for type-2 endoleak following EVAR: a retrospective review of preoperative CT angiography in 326 patients. Cardiovasc Intervent Radiol. 2014;37:324-328. https://doi.org/10.1007/s00270-013-0646-7
40. Jones JE, Atkins MD, Brewster DC, Chung TK, Kwolek CJ, LaMuraglia GM, et al. Persistent type 2 endoleak after endovascular repair of abdominal aortic aneurysm is associated with adverse late outcomes. J Vasc Surg. 2007;46:1-8. https://doi.org/10.1016/j.jvs.2007.02.073
41. Takeuchi Y, Morikage N, Samura M, Sakamoto R, Ike S, Mizoguchi T, et al. Five-year follow-up of randomized clinical trial for pre-emptive inferior mesenteric artery embolization during endovascular aneurysm repair. J Vasc Surg. 2024;80:693-701. https://doi.org/10.1016/j.jvs.2024.04.058
42. Ichihashi S, Takahara M, Fujimura N, Nagatomi S, Iwakoshi S, Bolstad F, et al. Multicentre randomised controlled trial to evaluate the efficacy of pre-emptive inferior mesenteric ar-

tery embolisation during endovascular aortic aneurysm repair on aneurysm sac change: protocol of Clarify IMA study. BMJ Open. 2020;10:e031758. https://doi.org/10.1136/bmjopen-2019-031758
43. Yu HY, Lindstrom D, Wanhainen A, Tegler G, Hassan B, Mani K. Systematic review and meta-analysis of prophylactic aortic side branch embolization to prevent type II endoleaks. J Vasc Surg. 2020;72:1783-1792. https://doi.org/10.1016/j.jvs.2020.05.020
44. Yu HY, Lindstrom D, Wanhainen A, Tegler G, Asciutto G, Mani K. An updated systematic review and meta-analysis of pre-emptive aortic side branch embolization to prevent type II endoleaks after endovascular aneurysm repair. J Vasc Surg. 2023;77:1815-1821. https://doi.org/10.1016/j.jvs.2022.11.042
45. Niklas N, Malec M, Gutowski P, Kazimierczak A, Rynio P. Effectiveness of inferior mesenteric artery embolization on type II endoleak-related complications after endovascular aortic repair (EVAR): systematic review and meta-analysis. J Clin Med. 2022;11:5491. https://doi.org/10.3390/jcm11185491
46. Wu Y, Yin J, Hongpeng Z, Wei G. Systematic review and network meta-analysis of pre-emptive embolization of the aneurysm sac side branches and aneurysm sac coil embolization to improve the outcomes of endovascular aneurysm repair. Front Cardiovasc Med. 2022;9:947809. https://doi.org/10.3389/fcvm.2022.947809
47. Chen Q, Zhang Y, Lei K, Fu L, Zhang D, Sun W, et al. Efficacy and safety of prophylactic intraoperative sac embolization in EVAR for abdominal aortic aneurysm: a meta-analysis. Front Surg. 2022;9:1027231. https://doi.org/10.3389/fsurg.2022.1027231

Original Article

eISSN 2508-2612
https://doi.org/10.64961/kjir.2025.00073
Korean J Interv Radiol 2026;31(2):125-135

KJIR
Korean Journal of
Interventional Radiology

Impact of Tumor Location on Radiofrequency Ablation Outcomes as First-Line Therapy for Hepatocellular Carcinoma

Gwang Hyeon Choi[1], Chang Jin Yoon[2,3,4], Chong-ho Lee[1], Kun Yung Kim[1], Eun Sun Jang[4], Jin-Wook Kim[4], Seung Jae Lee[5,a], Sook-Hyang Jeong[4], Minuk Kim[6], Jae Hwan Lee[2,3,4,*]

[1]Department of Internal Medicine, Seoul National University Bundang Hospital, Seongnam, Republic of Korea
[2]Department of Radiology, Seoul National University Bundang Hospital, Seongnam, Republic of Korea
[3]Department of Radiology, Seoul National University College of Medicine, Seoul, Republic of Korea
[4]Institute of Radiation Medicine, Seoul National University Medical Research Center, Seoul, Republic of Korea
[5]Institute of Health and Environment, Seoul National University, Seoul, Republic of Korea
[6]Department of Radiology, Seoul Metropolitan Government-Seoul National University Boramae Medical Center, Seoul, Republic of Korea

Purpose: Tumor location influences the effectiveness and safety of RFA. This study evaluated RFA outcomes as first-line therapy for HCC < 3 cm, focusing on tumor location impact.

Materials and Methods: In this retrospective cohort study, 281 patients with newly diagnosed HCC < 3 cm in up to three lesions treated with RFA between 2003 and 2019 were analyzed. The tumor location was categorized as superficial (outer third), mid-portion (middle third), or deep (near vena cava), using an imaginary line from the liver surface to the vena cava. Perivascular tumors were defined as those abutting portal or hepatic veins. Recurrence-free survival (RFS) among location groups was compared with risk factors analyzed via Cox regression.

Results: Patients (mean age, 61.1 ± 11.1 years) were predominantly male (73.3%), hepatitis B virus surface antigen–positive (66.2%), and of Child-Pugh class A (97.5%). Deep tumors had shorter RFS than superficial/mid-portion tumors (HR, 1.87; 95% CI, 1.20 to 2.93; p = 0.005), as did perivascular versus non-perivascular tumors (HR, 1.87; 95% CI, 1.16 to 3.00; p = 0.008). Group C (deep + perivascular, n = 10) had shorter RFS than group A (no risk factors: HR, 3.12; 95% CI, 1.50 to 6.45; p = 0.002) and group B (one risk factor: HR, 1.59; 95% CI, 1.05 to 2.40; p = 0.028). Multivariable analysis identified tumor depth, perivascular location, size > 2 cm, creatinine, and prothrombin time as independent predictors of shorter RFS.

Conclusion: Tumor depth and proximity to vasculature independently predict RFS in small HCCs treated with RFA, highlighting the role of tumor location in determining patient prognosis.

Keywords: Hepatocellular carcinoma; Radiofrequency ablation; Prognosis; Local neoplasm recurrence; Neoplasms by site

Received: November 27, 2025; **Revised:** March 23, 2026;
Accepted: March 24, 2026
***Corresponding email:** lzhwanmd@gmail.com

[a]Present address: Department of Applied Statistics, Kyonggi University, Suwon, Republic of Korea

© 2026 Korean Society of Interventional Radiology

This is an Open Access article distributed under the terms of the Creative Commons Attribution Non-Commercial License (http://creativecommons.org/licenses/by-nc/4.0) which permits unrestricted non-commercial use, distribution, and reproduction in any medium, provided the original work is properly cited.

Introduction

RFA is an established first-line treatment for very early (stage 0) and early (stage A) HCC [1,2]. The anatomical tumor location is pivotal in determining not only the RFA feasibility but also its clinical outcomes [3-6]. Tumors located adjacent to extrahepatic organs or major intrahepatic vessels present

unique challenges and are often considered relative contraindications owing to the elevated risk of damaging surrounding tissues [7,8]. RFA efficacy is significantly reduced in perivascular HCCs due to the "heat sink" effect, where blood flow in nearby vessels dissipates heat from the ablation zone, limiting the effectiveness of the procedure and leading to lower overall survival (OS) rates than surgical options [3,4]. Despite these limitations, current international guidelines do not yet integrate anatomical considerations in RFA treatment recommendations, leaving a gap in optimizing treatment for these cases [2,9].

Challenges exist for RFA required at specific tumor locations. RFA is typically performed percutaneously for minimal invasiveness; however, certain tumor locations complicate the procedure [4,8,10]. For superficial or subcapsular tumors, concerns arise regarding the potential for inadequate tumor margin and the risk of tumor seeding and recurrence [11-13]. Deep-seated HCCs, including caudate lobe lesions, further complicate detection and access, making precise targeting during surgery or locoregional treatments challenging [14-16]. These cases are often associated with higher rates of surgical complications and poorer outcomes [14-18].

Previous studies on RFA for challenging tumor locations have focused mainly on technical feasibility in small patient cohorts [19-21] lacking detailed outcome analyses stratified by specific anatomical tumor locations in larger patient samples. Therefore, this study aimed to evaluate RFA outcomes, accounting for anatomical tumor location, which influences treatment efficacy and patient prognosis. By quantifying these effects, this analysis seeks to inform guidelines and aid in developing targeted treatment protocols for HCC based on anatomical considerations.

Materials and Methods

This retrospective cohort study was conducted at a single tertiary academic center, with approval from the Institutional Review Board (14/10/2020) and a waiver of informed consent. A total of 320 treatment-naïve patients with HCC at our institution between May 2003 and December 2019 were initially screened. After applying the eligibility criteria, including exclusion of patients with prior HCC treatment (n = 8), 281 treatment-naïve patients were included in the final analysis. The diagnostic criteria for HCC were based on the international guidelines at the time of diagnosis [22,23]. The inclusion criteria were as follows: (1) newly diagnosed HCC confirmed through international guidelines or biopsy in cases of indeterminate lesions; (2) a maximum of three tumors, each <3 cm in diameter; (3) non-suitability for surgical resection; (4) RFA as the initial therapy; and (5) complete response achieved after a single RFA session, defined as the absence of contrast enhancement in the ablated area during the arterial phase, uniform low attenuation within the ablation zone, and a minimum 0.5–1.0 cm ablative margin of non-enhancing liver tissue surrounding the tumor during the portal venous phase [24]. Exclusion criteria included prior HCC treatment (n = 8), incomplete response post-first ablation (n = 8), presence of extrahepatic malignancies (n = 5), tumors of ≥3 cm (n = 11), concurrent HCC lesions untreated by RFA (n = 5), and lack of follow-up after RFA (n = 2). Following these criteria, 281 patients were included in the final analysis (Fig. 1).

Definition of the Anatomical Location of HCC

Based on previous studies [3,25] tumor depth was categorized as follows (Supplementary Fig. 1): an imaginary line was drawn from the IVC through the tumor center to the nearest liver surface. The tumor depth was classified as superficial,

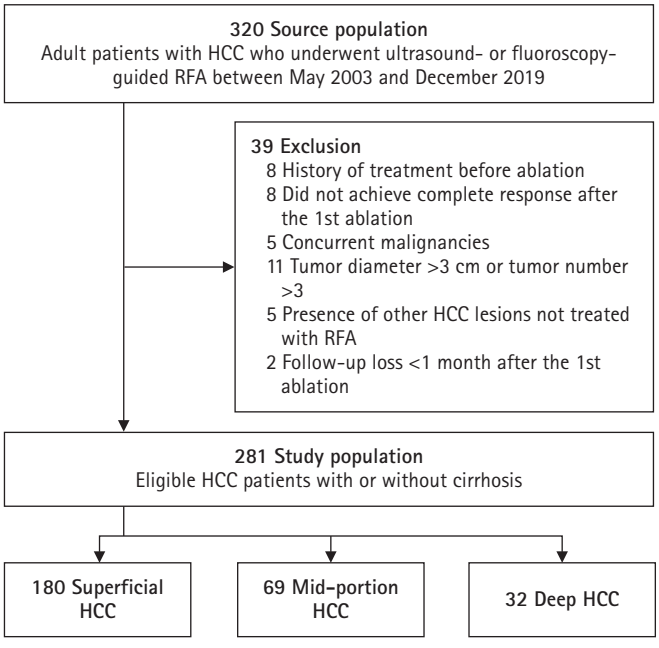


Fig. 1. Patient flow diagram.

middle, or deep according to the position of the tumor center along this line. Tumors with their center in the distal third, closer to the IVC, were classified as deep. A perivascular location was defined as tumors abutting the 1st or 2nd-degree branches of the portal or hepatic vein [4]. Two radiologists, blinded to treatment outcomes, independently reviewed and classified all tumors by consensus based on pre-treatment CT or MRI scans.

RFA Procedures

All RFA procedures were performed on an inpatient basis by one of two radiologists using local anesthesia with conscious sedation. A 17-gauge internally cooled electrode with a manually adjustable active tip (0.5-3 cm; Viva, Starmed, Goyang, Korea) was used for the procedure. Ultrasound guidance facilitated accurate targeting, with intraprocedural monitoring to confirm an adequate peritumoral ablation margin.

For tumors not clearly visible on ultrasound, contrast-enhanced ultrasound, and intraprocedural cone-beam CT scanning were performed in conjunction with RFA under ultrasonography and fluoroscopy guidance, following previously established protocols [26]. In brief, ultrasound contrast agent SonoVue (sulfur hexafluoride microbubbles; Bracco Imaging, Milan, Italy) was initially administered to enhance visualization of the sonographically invisible lesion. Once the lesion was identified, RFA needle placement was performed under ultrasound guidance. Following this, intra-procedural cone-beam CT scanning was conducted to verify the position of the needle, allowing comparison with pre-procedural CT or MRI images to ensure precise placement within the tumor [26,27].

Data Collection, Outcomes, and Follow-up of Patients with HCC

Clinical data for the study group were collected from electronic medical records and included age, sex, HCC etiology, complete blood count, alpha-fetoprotein blood levels, serum aspartate aminotransferase, alanine aminotransferase, albumin, total bilirubin, prothrombin time (PT) as international normalized ratio, creatinine, Child-Pugh score and classification, tumor size, number, location, distribution, and the presence of macrovascular invasion or distant metastasis.

Recurrence was defined as any radiologically confirmed reappearance of HCC after complete response to the index RFA, including local tumor progression, intrahepatic distant recurrence, and extrahepatic recurrence. The primary outcome was recurrence-free survival (RFS), and the secondary outcome was time to progression (TTP) and OS. RFS was defined as the time from the date of RFA procedure to the first recurrence observed on cross-sectional imaging (CT or MRI), death, or the end of follow-up. TTP was defined as the interval from the date of RFA procedure to the date of recurrence confirmed on imaging. OS was defined as the interval from the date of RFA procedure to the date of death. Patients were followed up until December 2022 or for up to 5 years. Mortality data were confirmed through Statistics Korea (governmental census bureau), and the cause of death was verified using medical records.

Statistical Analysis

Baseline patient characteristics were compared using the chi-square test for categorical variables and the t-test for continuous variables. RFS and TTP were estimated using the Kaplan-Meier method and compared with the log-rank test. A Cox proportional hazards model was used in both univariable and multivariable analyses to assess HR and 95% CI for RFS.

To address significant baseline differences, propensity score (PS) matching was applied, reducing the influence of potential confounders and improving the predictive value of tumor location estimates. Nearest-neighbor matching with a caliper of 0.1 was used to match patients in a 1:2 ratio. All p-values were two-sided, with values <0.05 considered statistically significant. Statistical analyses were conducted using SPSS version 21 (IBM Corp., Armonk, NY, USA) and R version 4.0.4 (http://cran.r-project.org/).

Ethics Statement

This study was approved by the Institutional Review Board of Seoul National University Bundang Hospital (approval No. B-1912/580-104). The institutional review board waived the need for informed consent due to the retrospective nature of the study. Consent for publication was obtained for every person's data included in the study.

Results

The baseline characteristics of patients undergoing RFA by

tumor depth are shown in Table 1. Among the 281 patients, the mean age was 61.1 ± 11.1 years, with 73.3% being male, 66.2% hepatitis B virus surface antigen–positive, and 97.5% in Child-Pugh class A. Tumor characteristics, including maximal tumor diameter (17.2 mm, 18.1 mm, and 17.4 mm for superficial, middle, and deep HCC, respectively) and the proportion of patients with a single tumor (93.9%, 91.3%, and 96.6%, respectively), did not differ significantly among groups.

Anatomical distribution showed that superficial and middle HCCs were absent in segment 1, while deep HCCs were not located in segments 3 or 5. Perivascular location was progressively more frequent from superficial to deep HCCs (10.5% for superficial, 18.8% for middle, and 31.3% for deep; p = 0.007). Similarly, Child-Pugh class B status increased with tumor depth (0% for superficial, 2.9% for middle, and 15.6% for deep HCC; p < 0.001).

TTP, RFS, and OS by Tumor Depth before PS Matching

The median follow-up for study patients was 60 months, during which 128 recurrences and 39 deaths were observed. TTP was shortest in deep HCCs, followed by superficial and middle HCCs (median, not reached [NR] vs. 43 months vs. 19 months; p = 0.004) (Fig. 2A). RFS similarly decreased in the order of middle, superficial, and deep HCCs (median, NR vs. 41 months vs. 19 months; p = 0.004 for trend) (Fig. 2B). However, OS was not significantly different among the three groups (Fig. 2C).

Multivariable analysis identified deep HCC as an independent risk factor for shorter RFS (Table 2), with an HR of 2.16 (95% CI, 1.20 to 3.89; p = 0.010) compared to middle HCCs, while superficial HCCs showed no significant association (HR, 1.44; 95% CI, 0.92 to 2.25; p = 0.112). Additional covariates independently linked to shorter RFS included elevated

Table 1. Baseline characteristics of HCC patients who received radiofrequency ablation

	Superficial (n = 180)	Mid (n = 69)	Deep (n = 32)	p-value
Age (years)	61.3 ± 11.2	61.6 ± 10.6	58.6 ± 11.2	0.405
Male sex	131 (72.8)	51 (73.9)	24 (75.0)	0.958
Etiology				0.986
HBV/HCV	120 (66.7)/21 (11.7)	45 (65.2)/9 (13.0)	21 (65.6)/3 (9.4)	
Alcohol/others	36 (20.0)/4 (1.7)	12 (17.4)/3 (4.3)	8 (25.0)/0 (0)	
Maximal tumor diameter (D) (mm)	17.2 ± 5.0	18.1 ± 5.4	17.4 ± 5.4	0.422
D < 20	137 (76.1)	51 (73.9)	23 (71.9)	0.849
20 ≤ D < 30	43 (23.9)	18 (26.1)	9 (28.1)	
Tumor number				
1/2	169 (93.9)/11 (6.1)	63 (91.3)/6 (8.7)	31 (96.9)/1 (3.1)	0.548
Tumor segment				< 0.001
1/2	0 (0)/5 (2.8)	0 (0)/1 (1.4)	5 (15.6)/1 (3.1)	
3/4	19 (10.6)/16 (8.9)	4 (5.8)/5 (7.2)	0 (0)/2 (6.2)	
5/6	23 (12.8)/56 (31.1)	7 (10.1)/19 (27.5)	0 (0)/7 (21.9)	
7/8	7 (3.9)/54 (30.0)	7 (10.1)/26 (37.7)	7 (21.9)/10(31.2)	
Perivascular location				0.007
Portal vein/hepatic vein	15 (8.3)/4 (2.2)	11 (15.9)/2 (2.9)	6 (18.8)/4 (12.5)	
Child-Pugh class B	0 (0)	2 (2.9)	5 (15.6)	< 0.001
Laboratory findings				
WBC (/mm^3)	4.0 (3.9–6.0)	5.2 (4.2–6.4)	4.8 (3.8–6.0)	0.104
PLT (×10^3/mm^3)	119 (83–164)	124 (91–180)	124 (90–159)	0.351
ALT (IU/L)	35 (23–53)	32 (23–44)	37 (28–50)	0.147
ALP (IU/L)	85 (68–105)	88 (69–114)	91 (75–127)	0.215
Albumin (g/dL)	4.0 (3.7–4.3)	4.1 (3.7–4.4)	4.0 (3.4–4.2)	0.159
Total bilirubin (mg/dL)	0.7 (0.5–1.1)	0.9 (0.6–1.1)	1.0 (0.6–1.4)	0.001
Creatinine (mg/dL)	0.8 (0.7–1.0)	0.9 (0.7–1.0)	0.9 (0.7–1.0)	0.030
Prothrombin time (INR)	1.09 (1.04–1.17)	1.09 (1.02–1.15)	1.11 (1.03–1.27)	0.043
AFP (ng/dL)	6.8 (3.4–38.2)	6.2 (3.2–21.6)	7.9 (3.3–34.0)	0.644

Values are presented as mean ± standard deviation or number (%).
HBV, hepatitis B virus; HCV, hepatitis C virus; WBC, white blood cell; PLT, platelet count; ALP, alkaline phosphatase.

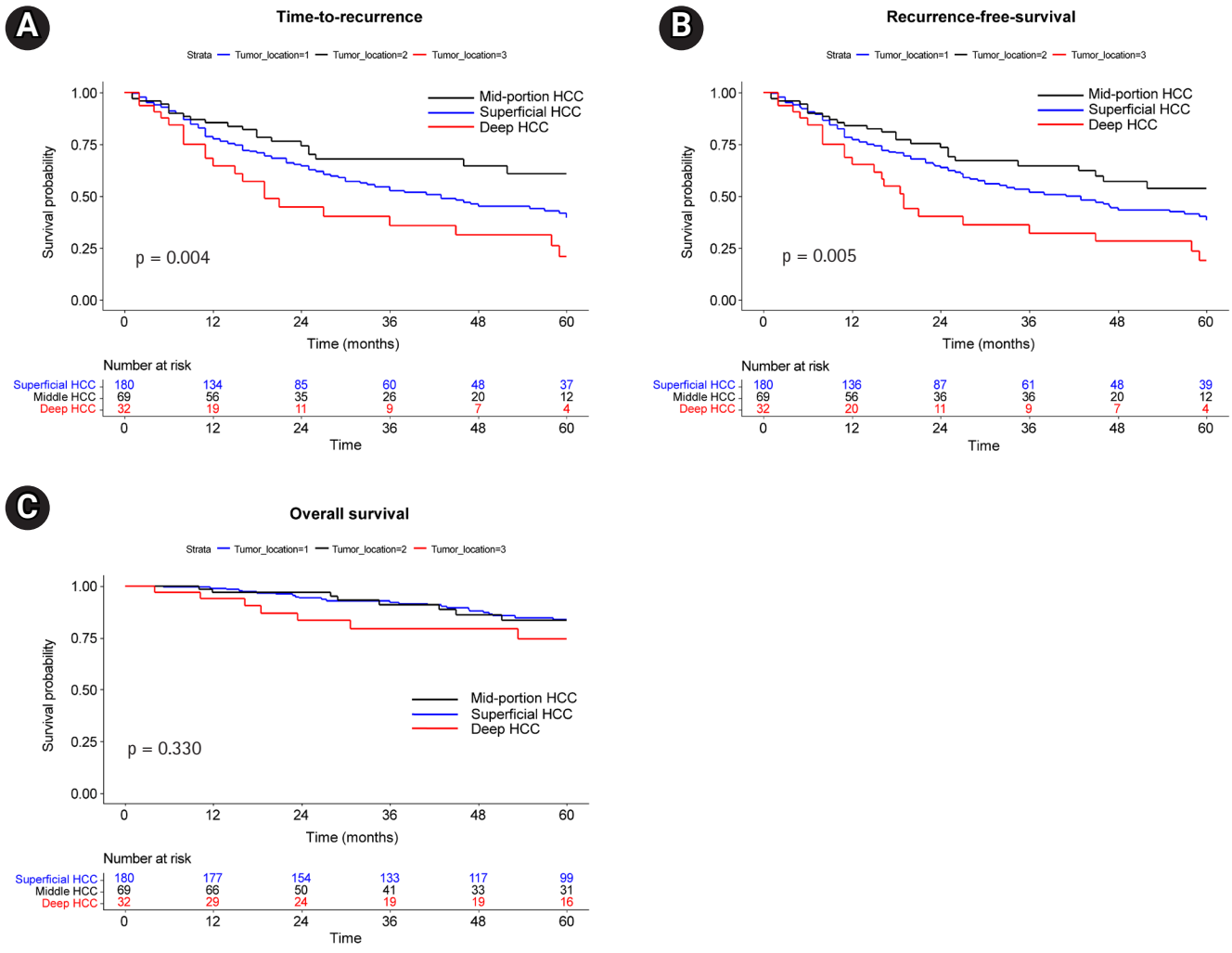


Fig. 2. Kaplan-Meier curve according to tumor depth. (A) Time to recurrence. (B) Recurrence-free survival. (C) Overall survival.

creatinine (HR, 1.14; 95% CI, 1.00 to 1.29; p = 0.042), perivascular location (HR, 1.65; 95% CI, 1.01 to 2.72; p = 0.048), and prolonged PT (HR, 6.84; 95% CI, 1.92 to 24.35; p = 0.003).

TTP and RFS by Perivascular Location

Patients with perivascular tumors had shorter TTP (median, 22 months vs. 52 months; log-rank p = 0.008), RFS (median, 22 months vs. 46 months; p = 0.006), and OS (p = 0.026) compared to those with non-perivascular tumors (Supplementary Fig. 2).

PS-Matched Analyses

Because superficial and middle HCC did not show statistically significant differences in multivariable analysis, they were divided into deep HCC and non-deep HCC groups and PS matching was performed. PS matching yielded 27 pairs (ratio 1:2) of patients from the deep and non-deep HCC groups (Supplementary Table 1), with no significant differences between the matched cohorts. In this matched analysis, the deep HCC group demonstrated a higher risk of shorter TTP (HR, 2.11; 95% CI, 1.08 to 4.09; p = 0.023) and RFS (HR, 2.07; 95% CI, 1.09 to 3.91; p = 0.022) than those in the non-deep HCC group (Fig. 3A, B); however, the OS of patients with deep HCC did not differ significantly from those with non-deep HCC (p = 0.670) (Fig. 3C).

RFS According to the Number of Anatomical Risk Factors

Patients were stratified into three groups based on the presence of two anatomical risk factors (deep HCCs and perivascular location): non-deep, non-perivascular group (n = 217),

Table 2. Multivariable Cox analysis for recurrence-free survival

	Univariable analysis		Multivariable analysis model 1		Multivariable analysis model 2	
	Hazard ratio	p-value	Hazard ratio	p-value	Hazard ratio	p-value
Tumor depth		-		-	-	-
Mid HCC	Reference		Reference			
Superficial 1/3 HCC	1.45 (0.93–2.26)	0.099	1.44 (0.92–2.25)	0.112		
Deep 1/3 HCC	2.48 (1.41–4.37)	0.002	2.16 (1.20–3.89)	0.010		
Perivascular HCC	1.87 (1.16–3.00)	0.010	1.65 (1.01–2.72)	0.048		
Tumor location						
Non-deep, non-perivascular	Reference	-	-	-	Reference	-
Deep or perivascular	1.66 (1.12–2.46)	0.011	-	-	1.60 (1.07–2.40)	0.024
Deep and perivascular	2.99 (1.45–6.18)	0.003	-	-	2.41 (1.08–5.38)	0.031
Maximal tumor diameter ≥ 20 mm	1.51 (1.05–2.18)	0.025	1.56 (1.07–2.26)	0.020	1.62 (1.12–2.34)	0.011
Two HCC	1.28 (0.67–2.43)	0.457	-	-	-	-
Age (years)	1.00 (0.99–1.02)	0.669	-	-	-	-
Male sex	1.23 (0.83–1.81)	0.308	-	-	-	-
PLT (×1,000/mm^3)	0.997 (0.994–1.000)	0.055	0.999 (0.996–1.002)	0.657	0.999 (0.996–1.002)	0.608
ALT (IU/L)	1.000 (0.996–1.003)	0.884	-	-	-	-
Albumin (g/dL)	0.60 (0.42–0.84)	0.003	0.86 (0.57–1.31)	0.483	0.88 (0.58–1.33)	0.536
Total bilirubin (mg/dL)	1.24 (0.95–1.61)	0.113	-	-	-	-
Prothrombin time (INR)	11.05 (3.90–31.28)	<0.001	6.84 (1.92–24.35)	0.003	20.51 (4.20–100.26)	<0.001
Creatinine (mg/dL)	1.13 (1.01–1.28)	0.038	1.14 (1.00–1.29)	0.042	1.14 (1.00–1.29)	0.042
AFP > 20 ng/mL	0.94 (0.64–1.36)	0.725	-	-	-	-

PLT, platelet count.

deep or perivascular group (n = 54), and deep and perivascular group (n = 10).

TTP, RFS, and OS showed a significantly favorable prognosis in the order of the non-deep, non-perivascular; deep or perivascular; and deep and perivascular groups (Fig. 4). Moreover, multivariable Cox analysis (Table 2) demonstrated that the number of anatomical risk factors independently predicted shorter RFS (HR, 1.60; 95% CI, 1.07 to 2.40; p = 0.024 for deep or perivascular HCC; HR, 2.41; 95% CI, 1.08 to 5.38, p = 0.031 for deep and perivascular HCC with reference to non-deep, non-perivascular HCC). Additional factors associated with shorter RFS included maximal tumor size >2 cm (HR, 1.62; 95% CI, 1.12 to 2.34; p = 0.011), elevated creatinine (HR, 1.14; 95% CI, 1.01 to 1.29; p = 0.042), and prolonged PT (HR, 20.51; 95% CI, 4.20 to 100.26; p < 0.001).

Discussion

In this study, patients with deep-seated HCCs and perivascular tumor locations demonstrated significantly shorter RFS and TTP than patients with tumors in less challenging locations. Deep HCCs, specifically, were identified as independent predictors of shorter RFS and TTP. Stratification based on anatomical risk factors showed that patients with both deep and perivascular tumors had the poorest outcomes, underscoring the influence of tumor location on therapeutic efficacy.

Tumor location has a profound impact on the effectiveness of curative therapies for HCC, as it directly affects procedural feasibility and oncologic outcomes [3,4,6-8,10,28]. Anatomically challenging locations, such as perivascular or subcapsular areas, complicate RFA due to technical difficulties in achieving adequate margins and risks of adjacent tissue damage [4,28]. For instance, tumors adjacent to large blood vessels experience the "heat sink" effect, leading to incomplete ablation and higher recurrence rates [3,4]. International guidelines do not yet account for tumor location in treatment planning for HCC [9,29]. However, emerging evidence, including this study, suggests that incorporating location-based considerations could enhance treatment personalization and improve outcomes.

Our findings indicate that deep-seated HCCs were found to be independent predictors of shorter RFS, which underscores the challenges of treating tumors located in these anatomically complex regions. While technical factors, such as achieving adequate ablation margins due to proximity to major blood vessels, contribute to these outcomes, biological and micro-

https://doi.org/10.64961/kjir.2025.00073

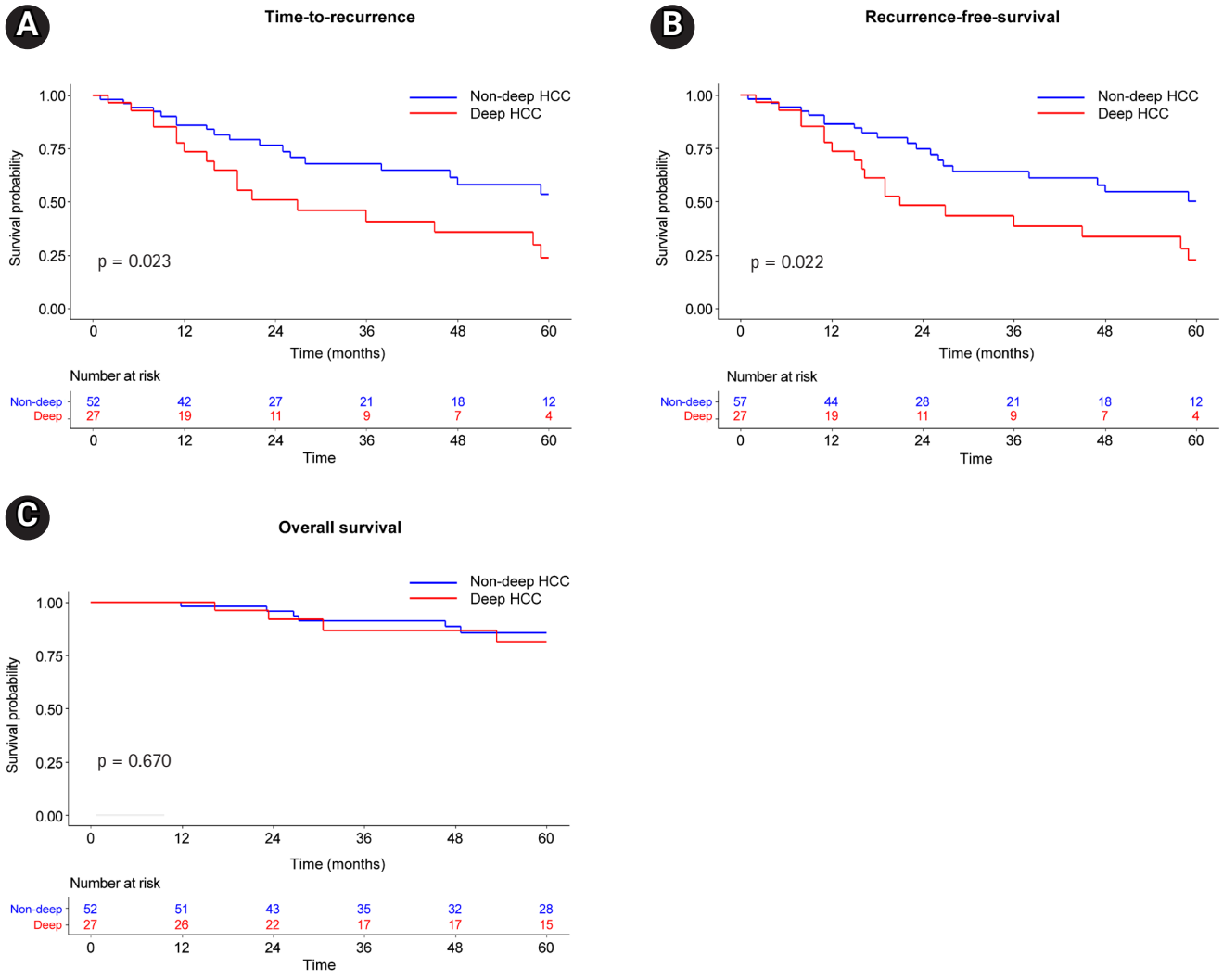


Fig. 3. Kaplan-Meier curve after propensity score matching according to depth. (A) Time to recurrence. (B) Recurrence-free survival. (C) Overall survival.

environmental factors likely play a substantial role. Deep-seated tumors may have reduced immunologic surveillance, potentially enabling tumor cells to evade immune detection and increasing the risk of recurrence [30]. In addition, the unique vascular microenvironment around deep HCCs might support faster tumor regrowth and micrometastasis formation, which standard imaging and local treatment modalities could fail to detect [3,4,31].

These findings highlight the importance of pre-treatment assessment of tumor depth, as deeper tumors are likely to require modified or adjunctive therapeutic approaches, such as the integration of transarterial chemoembolization to complement RFA or microwave ablation [5,31,32]. Clinically, the poorer prognosis for deep-seated HCCs suggests a need for heightened surveillance and consideration of alternative therapies for these patients [21].

Stratifying patients based on anatomical risk factors, such as tumor depth and perivascular proximity, allows for a more nuanced understanding of prognosis post-RFA. In this study, patients grouped by these risk factors showed progressively worse RFS outcomes with increased anatomical complexity. This stratification system could aid clinicians in identifying high-risk patients, guiding treatment selection, and improving patient counseling.

This study has several limitations. As a retrospective, single-center study, it may be subject to inherent biases in patient selection and data collection. Second, the enrollment period spanned more than 15 years, during which RFA devic-

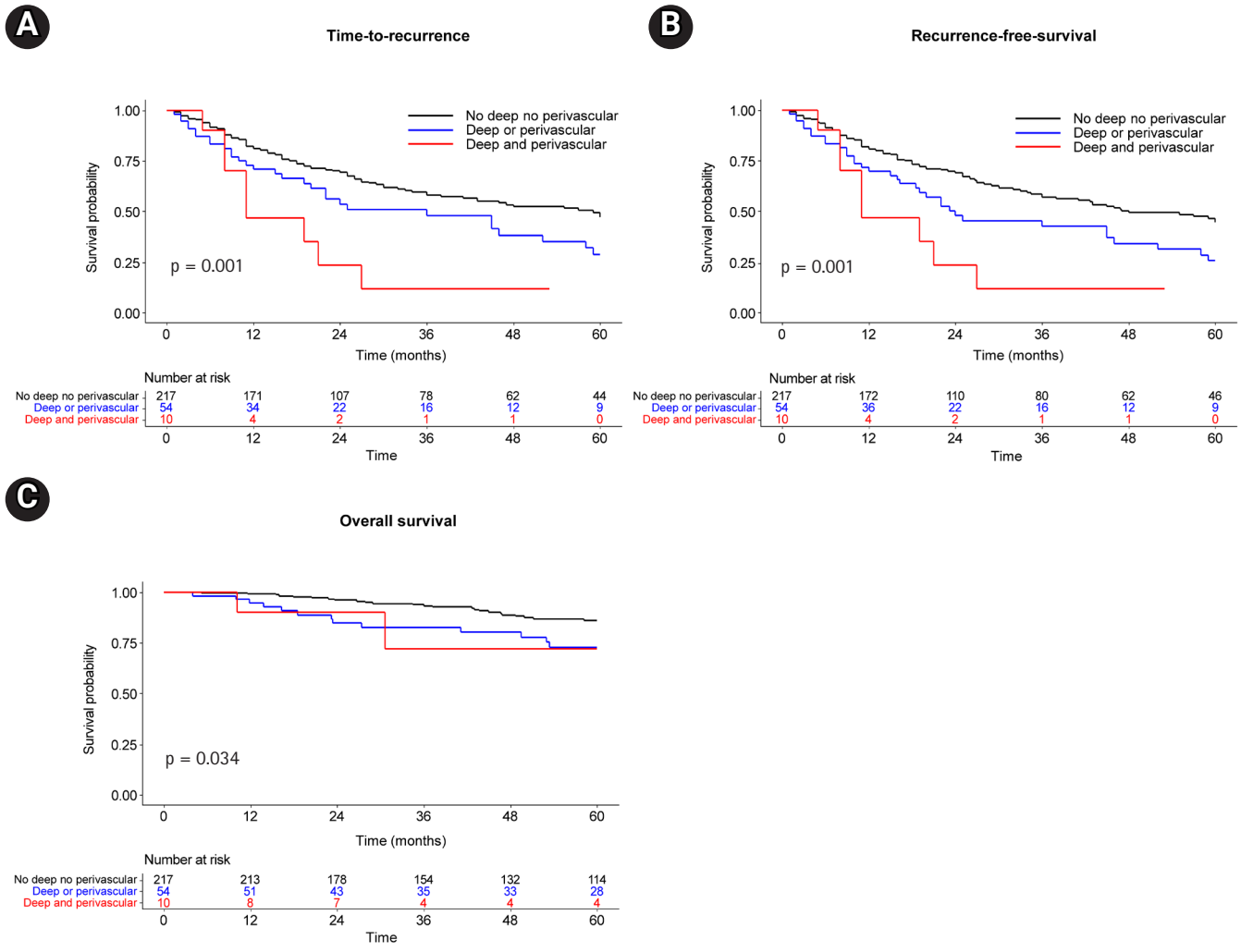


Fig. 4. Kaplan-Meier curve according to deep and/or perivascular location. (A) Time to recurrence. (B) Recurrence-free survival. (C) Overall survival.

es and image-guidance techniques evolved. Such temporal changes may have influenced treatment outcomes, particularly for deep or perivascular tumors that are more dependent on advanced guidance techniques. Therefore, the prognostic effect of anatomical location may not have been constant throughout the study period. Additionally, the modest sample size limits the generalizability of findings to broader populations. Future multi-center, prospective studies are needed to validate these results and further refine anatomical risk stratification in HCC management.

In conclusion, this study emphasizes that tumor location significantly impacts outcomes in HCC patients treated with RFA, particularly in deep and perivascular tumors linked to poorer prognosis. These findings support anatomical risk stratification to guide treatment decisions and suggest updates to clinical guidelines to account for tumor location in HCC management.

Conflict of interest

Kun Yung Kim and Jae Hwan Lee, editors of the *Korean Journal of Interventional Radiology*, were not involved in the editorial evaluation or decision to publish this article. All remaining authors have declared no conflicts of interest.

Funding

This work was supported by the Central Medical Service (CMS) Co., Ltd. Research Fund (Grant number B-2306-835-103).

Acknowledgments

We would like to thank Editage (http://www.editage.com) for editing and reviewing this manuscript for the English language.

Author contributions

Conceptualization: GHC, JHL. Data curation: GHC, KYK, MK. Formal analysis: GHC, SJL, JHL. Investigation: GHC, CHL, CJY. Funding acquisition: JHL. Methodology: GHC, CJY, JHL. Project administration: JHL. Resources: CJY, ESJ, JWK, SHJ. Software: SJL. Supervision: JHL. Validation: GHC, JHL. Visualization: GHC, SJL. Writing - original draft: GHC. Writing - review & editing: all authors.

Data availability statement

The data supporting the findings of this study are available from the corresponding author upon reasonable request.

Supplementary material

The supplementary data are available with this article at https://doi.org/10.64961/kjir.2025.00073.

ORCID

Gwang Hyeon Choi, https://orcid.org/0000-0002-8795-8427
Chang Jin Yoon, https://orcid.org/0000-0002-7660-0489
Chong-ho Lee, https://orcid.org/0000-0003-4021-0240
Kun Yung Kim, https://orcid.org/0000-0002-2018-8130
Eun Sun Jang, https://orcid.org/0000-0003-4274-2582
Jin-Wook Kim, https://orcid.org/0000-0003-0934-3344
Seung Jae Lee, https://orcid.org/0000-0001-5508-8634
Sook-Hyang Jeong, https://orcid.org/0000-0002-4916-7990
Minuk Kim, https://orcid.org/0000-0003-0564-5724
Jae Hwan Lee, https://orcid.org/0000-0001-6513-3224

References

1. Korean Liver Cancer Association (KLCA); National Cancer Center (NCC) Korea. 2022 KLCA-NCC Korea practice guidelines for the management of hepatocellular carcinoma. J Liver Cancer. 2023;23:1-120. https://doi.org/10.17998/jlc.2022.11.07
2. Reig M, Forner A, Rimola J, Ferrer-Fabrega J, Burrel M, Garcia-Criado A, et al. BCLC strategy for prognosis prediction and treatment recommendation: the 2022 update. J Hepatol. 2022;76:681-693. https://doi.org/10.1016/j.jhep.2021.11.018
3. Chen J, Peng K, Hu D, Shen J, Zhou Z, Xu L, et al. Tumor location influences oncologic outcomes of hepatocellular carcinoma patients undergoing radiofrequency ablation. Cancers (Basel). 2018;10:378. https://doi.org/10.3390/cancers10100378
4. Lee S, Kang TW, Cha DI, Song KD, Lee MW, Rhim H, et al. Radiofrequency ablation vs. surgery for perivascular hepatocellular carcinoma: propensity score analyses of long-term outcomes. J Hepatol. 2018;69:70-78. https://doi.org/10.1016/j.jhep.2018.02.026
5. Doyle A, Gorgen A, Muaddi H, Aravinthan AD, Issachar A, Mironov O, et al. Outcomes of radiofrequency ablation as first-line therapy for hepatocellular carcinoma less than 3 cm in potentially transplantable patients. J Hepatol. 2019;70:866-873. https://doi.org/10.1016/j.jhep.2018.12.027
6. Dou JP, Han ZY, Cheng ZG, Liu FY, Yu XL, Yu J, et al. The effect of tumor location on long-term results of microwave ablation for early-stage hepatocellular carcinoma. Abdom Radiol (NY). 2020;45:3923-3933. https://doi.org/10.1007/s00261-020-02472-z
7. Komorizono Y, Oketani M, Sako K, Yamasaki N, Shibatou T, Maeda M, et al. Risk factors for local recurrence of small hepatocellular carcinoma tumors after a single session, single application of percutaneous radiofrequency ablation. Cancer. 2003;97:1253-1262. https://doi.org/10.1002/cncr.11168
8. Teratani T, Yoshida H, Shiina S, Obi S, Sato S, Tateishi R, et al. Radiofrequency ablation for hepatocellular carcinoma in so-called high-risk locations. Hepatology. 2006;43:1101-1108. https://doi.org/10.1002/hep.21164
9. Han S, Sung PS, Park SY, Kim JW, Hong HP, Yoon JH, et al. Local ablation for hepatocellular carcinoma: 2024 expert consensus-based practical recommendation of the Korean Liver Cancer Association. J Liver Cancer. 2024;24:131-144. https://doi.org/10.17998/jlc.2024.08.04
10. Yang W, Yan K, Wu GX, Wu W, Fu Y, Lee JC, et al. Radiofrequency ablation of hepatocellular carcinoma in difficult locations: strategies and long-term outcomes. World J Gastroenterol. 2015;21:1554-1566. https://doi.org/10.3748/wjg.v21.i5.1554
11. Llovet JM, Vilana R, Bru C, Bianchi L, Salmeron JM, Boix L,

et al. Increased risk of tumor seeding after percutaneous radiofrequency ablation for single hepatocellular carcinoma. Hepatology. 2001;33:1124-1129. https://doi.org/10.1053/jhep.2001.24233
12. Espinoza S, Briggs P, Duret JS, Lapeyre M, de Baere T. Radiofrequency ablation of needle tract seeding in hepatocellular carcinoma. J Vasc Interv Radiol. 2005;16:743-746. https://doi.org/10.1097/01.RVI.0000153109.56827.70
13. Jaskolka JD, Asch MR, Kachura JR, Ho CS, Ossip M, Wong F, et al. Needle tract seeding after radiofrequency ablation of hepatic tumors. J Vasc Interv Radiol. 2005;16:485-491. https://doi.org/10.1097/01.RVI.0000151141.09597.5F
14. Tanaka S, Shimada M, Shirabe K, Maehara SI, Tsujita E, Taketomi A, et al. Surgical outcome of patients with hepatocellular carcinoma originating in the caudate lobe. Am J Surg. 2005;190:451-455. https://doi.org/10.1016/j.amjsurg.2004.12.005
15. Sakamoto Y, Nara S, Hata S, Yamamoto Y, Esaki M, Shimada K, et al. Prognosis of patients undergoing hepatectomy for solitary hepatocellular carcinoma originating in the caudate lobe. Surgery. 2011;150:959-967. https://doi.org/10.1016/j.surg.2011.03.005
16. Shimada S, Kamiyama T, Yokoo H, Orimo T, Nagatsu A, Ohata T, et al. Prognoses and clinicopathological characteristics for hepatocellular carcinoma originating from the caudate lobe after surgery. World J Surg. 2019;43:1085-1093. https://doi.org/10.1007/s00268-018-4869-2
17. Yamamoto T, Kubo S, Shuto T, Ichikawa T, Ogawa M, Hai S, et al. Surgical strategy for hepatocellular carcinoma originating in the caudate lobe. Surgery. 2004;135:595-603. https://doi.org/10.1016/j.surg.2003.10.015
18. Liu P, Yang JM, Niu WY, Kan T, Xie F, Li DQ, et al. Prognostic factors in the surgical treatment of caudate lobe hepatocellular carcinoma. World J Gastroenterol. 2010;16:1123-1128. https://doi.org/10.3748/wjg.v16.i9.1123
19. Seror O, Haddar D, N'Kontchou G, Ajavon Y, Trinchet JC, Beaugrand M, et al. Radiofrequency ablation for the treatment of liver tumors in the caudate lobe. J Vasc Interv Radiol. 2005;16:981-990. https://doi.org/10.1097/01.RVI.0000159859.71448.8A
20. Peng ZW, Liang HH, Chen MS, Zhang YJ, Li JQ, Zhang YQ, et al. Percutaneous radiofrequency ablation for the treatment of hepatocellular carcinoma in the caudate lobe. Eur J Surg Oncol. 2008;34:166-172. https://doi.org/10.1016/j.ejso.2007.08.004
21. Nishigaki Y, Tomita E, Hayashi H, Suzuki Y, Iritani S, Kato T, et al. Efficacy and safety of radiofrequency ablation for hepatocellular carcinoma in the caudate lobe of the liver. Hepatol Res. 2013;43:467-474. https://doi.org/10.1111/j.1872-034X.2012.01095.x
22. Bruix J, Sherman M; Practice Guidelines Committee, American Association for the Study of Liver Diseases. Management of hepatocellular carcinoma. Hepatology. 2005;42:1208-1236. https://doi.org/10.1002/hep.20933
23. Marrero JA, Kulik LM, Sirlin CB, Zhu AX, Finn RS, Abecassis MM, et al. Diagnosis, staging, and management of hepatocellular carcinoma: 2018 practice guidance by the American Association for the Study of Liver Diseases. Hepatology. 2018;68:723-750. https://doi.org/10.1002/hep.29913
24. Crocetti L, de Baere T, Lencioni R. Quality improvement guidelines for radiofrequency ablation of liver tumours. Cardiovasc Intervent Radiol. 2010;33:11-17. https://doi.org/10.1007/s00270-009-9736-y
25. Kang TW, Lim HK, Lee MW, Kim YS, Rhim H, Lee WJ, et al. Long-term therapeutic outcomes of radiofrequency ablation for subcapsular versus nonsubcapsular hepatocellular carcinoma: a propensity score matched study. Radiology. 2016;280:300-312. https://doi.org/10.1148/radiol.2016151243
26. Morimoto M, Numata K, Kondo M, Nozaki A, Hamaguchi S, Takebayashi S, et al. C-arm cone beam CT for hepatic tumor ablation under real-time 3D imaging. AJR Am J Roentgenol. 2010;194:W452-W454. https://doi.org/10.2214/AJR.09.3514
27. Lee MW, Kang D, Lim HK, Cho J, Sinn DH, Kang TW, et al. Updated 10-year outcomes of percutaneous radiofrequency ablation as first-line therapy for single hepatocellular carcinoma < 3 cm: emphasis on association of local tumor progression and overall survival. Eur Radiol. 2020;30:2391-2400. https://doi.org/10.1007/s00330-019-06575-0
28. European Association for the Study of the Liver. EASL clinical practice guidelines: management of hepatocellular carcinoma. J Hepatol. 2018;69:182-236. https://doi.org/10.1016/j.jhep.2018.03.019
29. Pietrobon V, Cesano A, Marincola F, Kather JN. Next generation imaging techniques to define immune topographies

in solid tumors. Front Immunol. 2021;11:604967. https://doi.org/10.3389/fimmu.2020.604967
30. Lin CH, Ho CM, Wu CH, Liang PC, Wu YM, Hu RH, et al. Minimally invasive surgery versus radiofrequency ablation for single subcapsular hepatocellular carcinoma ≤ 2026-03-262 cm with compensated liver cirrhosis. Surg Endosc. 2020;34:5566-5573. https://doi.org/10.1007/s00464-019-07357-x
31. Luker GD. Imaging the immune tumor microenvironment to monitor and improve therapy. Radiology. 2021;298:133-134. https://doi.org/10.1148/radiol.2020203799
32. Zheng H, Liu K, Yang Y, Liu B, Zhao X, Chen Y, et al. Microwave ablation versus radiofrequency ablation for subcapsular hepatocellular carcinoma: a propensity score-matched study. Eur Radiol. 2022;32:4657-4666. https://doi.org/10.1007/s00330-022-08537-5

Original Article

eISSN 2508-2612
https://doi.org/10.64961/kjir.2026.00101
Korean J Interv Radiol 2026;31(2):136-144

KJIR
Korean Journal of
Interventional Radiology

Two-Session Catheter-Directed Ethanol Sclerotherapy for Symptomatic Peritoneal Inclusion Cysts: A Preliminary Case Series

Byung Soo Im[1], Ji-Hoon Kim[1], Gun Ha Kim[1], Shakir Ali H. Aljerdah[2], Ji Hoon Shin[1,*]

[1]Department of Radiology and Research Institute of Radiology, Asan Medical Center, University of Ulsan College of Medicine, Seoul, Republic of Korea
[2]Department of Radiology, Najran University, College of Medicine, Najran, Saudi Arabia

Purpose: This study aims to investigate the clinical outcomes and safety of a standardized two-session catheter-directed ethanol sclerotherapy protocol for peritoneal inclusion cysts.

Materials and Methods: Between November 2020 and July 2025, six women (median age, 32.5 years) with symptomatic peritoneal inclusion cysts underwent ethanol sclerotherapy. After complete drainage using an 8.5-Fr or 10.2-Fr pigtail catheter, two sessions of sclerotherapy were performed on consecutive days. In each session, 99.5% ethanol (50% of the aspirated volume, up to 150 mL) was instilled and retained for 20 minutes. Follow-up ultrasound was performed at 1, 3, and 6 months. Technical success was defined as successful completion of both sessions with a 20-minute ethanol retention time, and clinical success was defined as symptom improvement with a >50% decrease in cyst diameter at 3 months.

Results: Technical success was achieved in all cases (6/6, 100%). The median maximum cyst diameter significantly decreased from 14.0 cm (range, 6.0 to 20.0 cm) to 5.25 cm (range, 2.0 to 8.0 cm) at the follow-up within 1 month ($p = 0.03$). Clinical success was achieved in all cases at 3 months (6/6, 100%). No residual cysts were visualized on follow-up ultrasound at 6 months in all patients (6/6, 100%). Anti-Müllerian hormone levels measured in four patients showed heterogeneous changes, precluding definitive conclusions regarding the impact on ovarian reserve. No major complications occurred.

Conclusion: Two-session catheter-directed ethanol sclerotherapy appears to be a safe and effective minimally invasive alternative to surgery for peritoneal inclusion cysts, providing a high rate of complete resolution.

Keywords: Peritoneal inclusion cysts; Ethanol; Sclerotherapy; Drainage; Catheterization

Introduction

Peritoneal inclusion cysts (PICs) are variably sized, mesothelial-lined cysts located within the abdominopelvic cavity. PICs are thought to arise secondary to intra-abdominal inflammation and subsequent cyst formation, with serous fluid originating from the ovarian stroma [1]. Patients typically present with progressive abdominal or pelvic pain and/or a palpable abdominal mass. PICs generally contain clear to yellow serous fluid; however, they may also contain hemorrhagic or gelatinous, discolored fluid [1]. Under normal physiological conditions, peritoneal fluid is produced by the ovaries and resorbed by the peritoneal surface [2]. The absorptive capacity of the peritoneal surface can be impaired, and an inflamma-

Received: April 19, 2026; **Revised:** May 8, 2026; **Accepted:** May 9, 2026
***Corresponding email:** jhshin@amc.seoul.kr

Byung Soo Im and Ji-Hoon Kim contributed equally to this work.

© 2026 Korean Society of Interventional Radiology

This is an Open Access article distributed under the terms of the Creative Commons Attribution Non-Commercial License (http://creativecommons.org/licenses/by-nc/4.0) which permits unrestricted non-commercial use, distribution, and reproduction in any medium, provided the original work is properly cited.

tory exudate may develop due to benign reactions to prior pelvic or abdominal surgery, pelvic inflammatory disease, endometriosis, or inflammatory bowel disease during the third or fourth decade of life, leading to impaired peritoneal resorption [1,3,4]. Inflammatory reactions surrounding surgical interventions may lead to the encapsulation of peritoneal fluid, while increased fluid volumes can stimulate PIC formation.

Pharmacological treatment primarily provides symptomatic relief and lacks a permanent curative effect. This poses challenges for patients wishing to preserve their fertility, as long-term medication use may have adverse implications [1]. While surgical resection remains the conventional approach, it is frequently hampered by dense postoperative adhesions and a high recurrence rate of up to 50%. Furthermore, repeated surgical trauma can exacerbate peritoneal dysfunction [5]. Thus, there is a critical need for a standardized, minimally invasive strategy that ensures long-term success while minimizing surgical morbidity. Simple needle aspiration provides a safe and straightforward method for fluid analysis and symptom management; however, it is almost invariably followed by rapid fluid re-accumulation [1]. Consequently, image-guided sclerotherapy has emerged as a minimally invasive alternative aimed at achieving permanent closure of the cystic space through the induction of mesothelial fibrosis. Nonetheless, the efficacy of sclerotherapy may be hindered by the multiloculated structure of PICs, which can obstruct the sclerosing agent from effectively reaching all sequestered compartments. Traditional sclerotherapy protocols for PICs have been inconsistent, ranging from single-needle aspirations with high recurrence rates to prolonged catheter-based regimens requiring excessive instillations (mean >3 sessions) and varying sclerosing agents [6,7]. To enhance treatment efficacy while minimizing procedural burden and chemical irritation, we hypothesized that a standardized two-session catheter-directed ethanol sclerotherapy protocol could reduce the number of instillations and total hospitalization duration compared to conventional multi-session approaches, while maintaining comparable treatment efficacy. Herein, we report the clinical outcomes and safety of this standardized protocol as a preliminary case series. The term “preliminary” refers to the small patient cohort and relatively short follow-up duration, and specifically reflects our initial clinical experience with this particular standardized two-session protocol and its associated outcome measures, rather than the broader concept of sclerotherapy for PICs, which has been previously reported in the literature.

Materials and Methods

Due to the retrospective nature of this study, the requirement for informed consent was waived by the institutional review board (S2026-0227-0001). This study was conducted in accordance with the Declaration of Helsinki. Between November 2020 and July 2025, six women who were referred by gynecologists underwent a standardized two-session catheter-directed ethanol sclerotherapy protocol for PICs. All patients presented with pelvic pain (n = 5) or a sensation of fullness (n = 1). The median age of the patients was 32.5 years (range, 23 to 48 years). Each patient had a diverse surgical history in the abdominopelvic region (Table 1). The median interval between the previous surgery and sclerotherapy was 14.5 years (range, 1.75 to 28 years). PIC was diagnosed based on clinical history and characteristic findings on ultrasound, CT, or MRI. Imaging features included a multiloculated cystic pelvic mass with thin septations, absence of solid components or internal vascularity on Doppler imaging, and close apposition to the ovary, reflecting entrapped peritoneal fluid within adhesions. Other cystic pelvic lesions, including ovarian cystadenomas, endometriomas, hydrosalpinx, and lymphoceles, were excluded based on their characteristic imaging features (e.g., solid components, high internal echogenicity suggestive of hemorrhagic content, tubular configuration, or typical postoperative location) in conjunction with clinical history. Malignancy was excluded based on imaging findings and tumor markers, including cancer antigen 125, human epididymis protein 4, and the Risk of Ovarian Malignancy Algorithm.

Procedural Details

For the transabdominal percutaneous approach (Figs. 1, 2), the puncture site was first disinfected with povidone-iodine (Betadine, Mundipharma, Basel, Switzerland), and the target lesion was punctured with a 21-gauge, 15-cm Chiba needle (Cook Medical, Bloomington, IN, USA) using a freehand technique. Subsequently, a 0.018-in guidewire (Cook Medical) and a Neff Percutaneous Access Set (Cook Medical) were in-

Table 1. Procedural characteristics and follow-up results of ethanol sclerotherapy

No.	Age (years)	Symptom	Etiology	Access	Catheter	Drainage (mL)	Fluid nature	Ethanol volume (mL), 1st/2nd	Diameter (cm)				AMH (ng/mL)	
									Pre	Within 1 month	3 months	6 months	Pre[a]	Post
1	29	Pelvic pain	Bowel resection for Crohn disease 12 YA	TA	8.5-Fr	1,060	Darkish, thin	100/100	17.5	5.5 (26 days)	1.8	NV	0.92	1.03 (3 months), 0.81 (6 months)
2	48	Pelvic pain	Hysterectomy for myoma 1.8 YA	TA	8.5-Fr	910	Straw, thin	100/100	15	2 (30 days)	NV	NV	NA	NA
3	23	Pelvic pain	Cloacal anomaly correction 22 YA	TA	8.5-Fr	85	Straw, thin	42/42	6	4 (16 days)	NV	NV	NA	3.46 (3 months)
4	43	Pelvic fullness	Cesarean section 14 YA	TV	8.5-Fr	200	Straw, thin	100/100	12.2	7.1 (15 days)	NV	NV	0.09	0.28 (3 months), 0.25 (6 months)
5	29	Pelvic pain	Megacolon operation 28 YA	TA	8.5-Fr	430	Straw, thin	150/150	13	8 (19 days)	NV	NV	2.21	1.47 (3 months), 1.6 (6 months)
6	36	Pelvic pain	Splenectomy and incisional hernia repair 15 YA	TA	10.2-Fr[b]	1,060	Straw, thin	150/150	20[c]	5.0 (19 days)	NV	NV	3.14	2.76 (3 months)

AMH, anti-Müllerian hormone; YA, years ago; TA, transabdominal; NV, non-visualized; NA, not available; TV, transvaginal.
[a]Pre-procedural AMH levels were obtained within 1 week before the procedure.
[b]Catheter upsized from 8.5-Fr to 10.2-Fr due to poor aspiration.
[c]A multiloculated fluid collection.

troduced, and a 0.035-in hydrophilic guidewire (Terumo, Tokyo, Japan) was advanced under fluoroscopic guidance.

In cases requiring a transvaginal approach (Fig. 3), patients were positioned in the lithotomy position. The vaginal area was sterilized with a 0.5% chlorhexidine gluconate solution (Hexitane 0.5%, Firson, Cheonan, Korea). An ultrasound probe with an in-plane endocavitary needle guide (EVN4-9, Aspen Surgical, Caledonia, MI, USA) was inserted. The lesion was punctured using an 18-gauge, 20-cm Chiba biopsy needle (Cook Medical), and a 0.035-in hydrophilic guidewire (Terumo) was advanced into the cyst.

Regardless of the chosen access route, the guidewire was advanced as far as possible to allow adequate coiling within the cyst cavity. Following guidewire placement, an 8.5- or 10.2-Fr pigtail drainage catheter with multiple side holes (Dawson-Mueller Drainage Catheter, Cook Medical) was inserted over the wire.

Following complete aspiration of the cyst contents, the cavity was filled with 10–30 mL of a water-soluble nonionic contrast medium (iobitridol, Xenetix 300 [300 mg I/mL], Guerbet, Villepinte, France) to assess for any leakage into the pelvic cavity (Figs. 1–3). Once the contrast medium was aspirated, the cyst was irrigated with 10–30 mL of lidocaine to alleviate procedural discomfort and then completely aspirated. This was followed by irrigation with 10–30 mL of 99.5% anhydrous ethanol (Taiwan Biotech Co., Ltd., Taoyuan, Taiwan) to ensure the purity of the subsequent sclerotherapy; this pre-wash ethanol was also completely aspirated before therapeutic ethanol was instilled for retention. The cyst was then filled with 99.5% ethanol for retention; the administered volume was equivalent to 50% of the aspirated fluid, with an initial predefined maximum limit of 100 mL. In cyst sclerotherapy, ethanol volume is typically determined as a proportion of the aspirated volume to ensure adequate mucosal contact while minimizing the risk of systemic absorption. Patient pain tolerance was additionally used as a real-time safety parameter, as intraprocedural pain may indicate peritoneal irritation. In the final two patients with larger cysts, the maximum volume was increased to 150 mL based on acceptable pain tolerance and the absence of clinical signs of peritoneal irritation, in order to improve ethanol-cyst wall contact. This represents a within-study protocol modification. To optimize contact between the ethanol and the cyst wall, the catheter was clamped, and

https://doi.org/10.64961/kjir.2026.00101

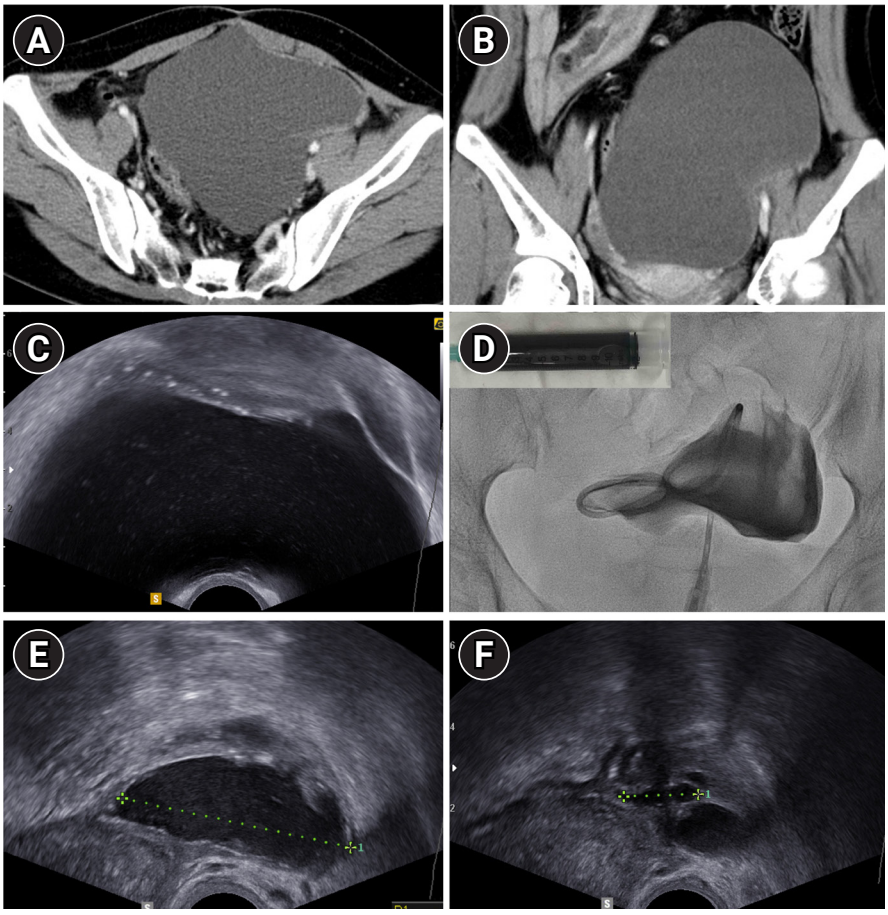


Fig. 1. A 29-year-old female with pelvic pain (case 1). Axial (A) and coronal (B) contrast-enhanced CT scans demonstrated a large cystic lesion (maximum diameter, 17.5 cm) within the pelvis. (C) Transabdominal ultrasound confirmed the presence of the large cystic lesion. (D) Following transabdominal access, an 8.5-Fr pigtail catheter with multiple side holes was inserted. A total of 1,060 mL of darkish, thin fluid was aspirated (inset), and contrast injection confirmed the absence of leakage into the peritoneal cavity. Follow-up transvaginal ultrasound images obtained 26 days (E) and 3 months (F) after two-session ethanol sclerotherapy showed a progressive reduction in cyst size with a flattened appearance; the diameters decreased to 5.5 cm and 1.8 cm, respectively. At the 6-month follow-up, the lesion was no longer visible on ultrasound (not shown).

the patient was instructed to rotate through the supine, bilateral decubitus, and prone positions every 5 minutes. After 20 minutes, the ethanol was aspirated as thoroughly as possible, and the catheter was left in situ overnight for a second session on the following day. The two-session design was based on the rationale that a second ethanol instillation the following day would treat any residual viable mesothelium exposed after initial cyst collapse, thereby maximizing obliteration of the secreting surface while limiting the total procedural burden to a single hospitalization [8,9]. The 20-minute retention time was selected in accordance with previously established protocols for ethanol sclerotherapy of ovarian cysts, which have demonstrated sufficient contact time for mesothelial destruction without increasing the risk of systemic absorption [10,11]. On the following day, after reconfirming the absence of leakage, the second session was performed according to the same standardized protocol, using identical irrigation volumes and a 20-minute ethanol retention time. Upon completion, the catheter was removed, and the patient was monitored for complications prior to discharge on the same day. The procedure was terminated if contrast leakage or intolerable pain occurred. An aliquot of the drained fluid was submitted for cytological examination to exclude malignancy.

For pain management, intracystic lidocaine irrigation (10–30 mL) was used for intraprocedural analgesia, as described above. No routine systemic analgesics or conscious sedation were administered prior to or during the procedure. Additional systemic analgesics (e.g., nonsteroidal anti-inflammatory

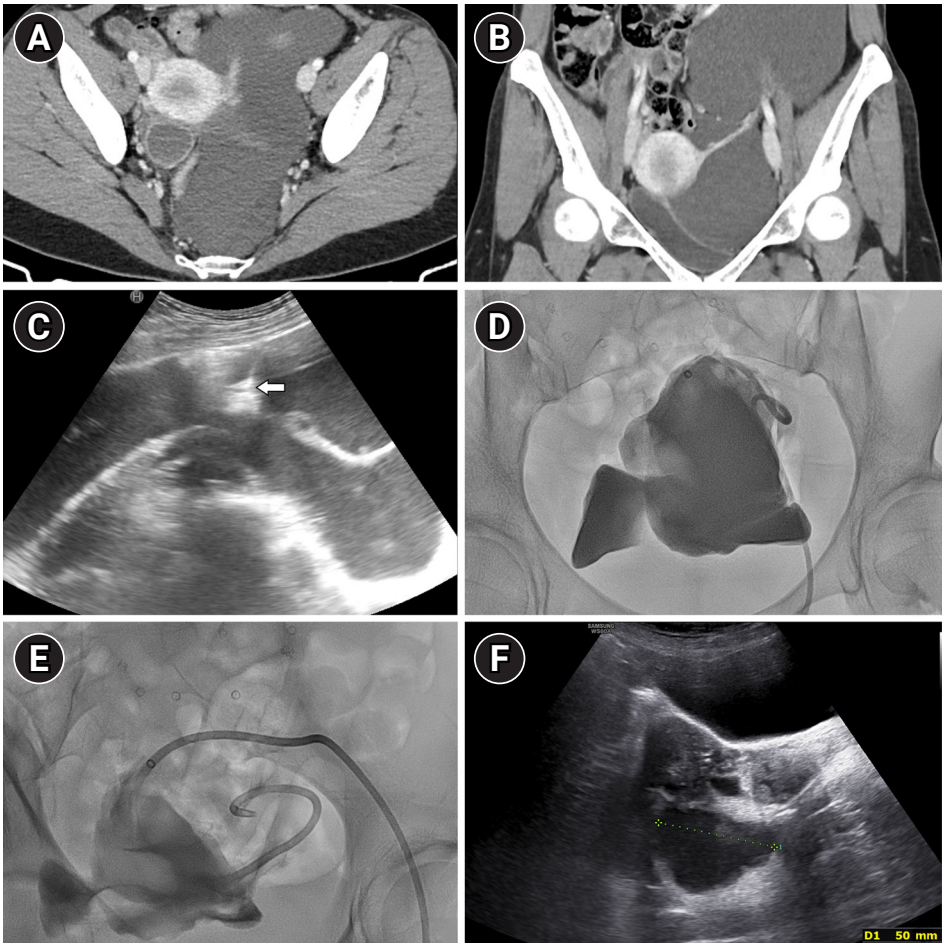


Fig. 2. A 36-year-old female with pelvic pain (case 6). Axial (A) and coronal (B) contrast-enhanced CT scans showed a 20-cm multi-lobulated pelvic cystic lesion. (C) Transabdominal ultrasound showed the initial puncture using a 21-gauge Chiba needle (arrow). (D) Tubogram showed no leakage after 1,060 mL of straw-colored fluid had been drained via an 8.5-Fr pigtail catheter, but further aspiration became difficult. (E) Following an exchange over a guidewire, a 10.2-Fr pigtail catheter was placed, allowing complete aspiration. Tubograms in (D) and (E) show the multi-lobulated nature of the cyst. (F) Follow-up transabdominal ultrasound at 19 days after two-session ethanol sclerotherapy showed a reduction in the lesion size to 5 cm. At the 3-month follow-up, the lesion was no longer visible (not shown).

drugs) were provided on an as-needed basis for postprocedural discomfort during the inpatient stay. Prophylactic antibiotics were not routinely administered.

Definitions and Analysis

Participants were regularly monitored with ultrasound within 1 month (range, 15 to 30 days) and at 3 and 6 months following catheter-directed ethanol sclerotherapy to assess changes in cyst diameter, complications, and recurrence. To evaluate the impact of catheter-directed ethanol sclerotherapy on ovarian reserve, serum anti-Müllerian hormone (AMH) levels were measured within 1 week prior to the procedure and at 3 and 6 months after the procedure, when available.

Technical success was defined as the successful completion of both sessions, with ethanol retained inside the cyst for 20 minutes during each session. Clinical success was characterized by symptomatic improvement and a >50% decrease in cyst diameter at 3 months post-procedure. Symptomatic improvement was assessed using patient-reported outcomes at each follow-up visit, with patients reporting whether their presenting symptoms (pelvic pain or sensation of fullness) had resolved or persisted compared with baseline. Recurrence was defined as the enlargement of the treated PICs on ultrasound during follow-up. Major complications were defined as procedure-related adverse events that caused or prolonged hospitalization, required an invasive procedure for treatment, or resulted in a change in functional status. Minor complications were defined as transient procedure-related

https://doi.org/10.64961/kjir.2026.00101

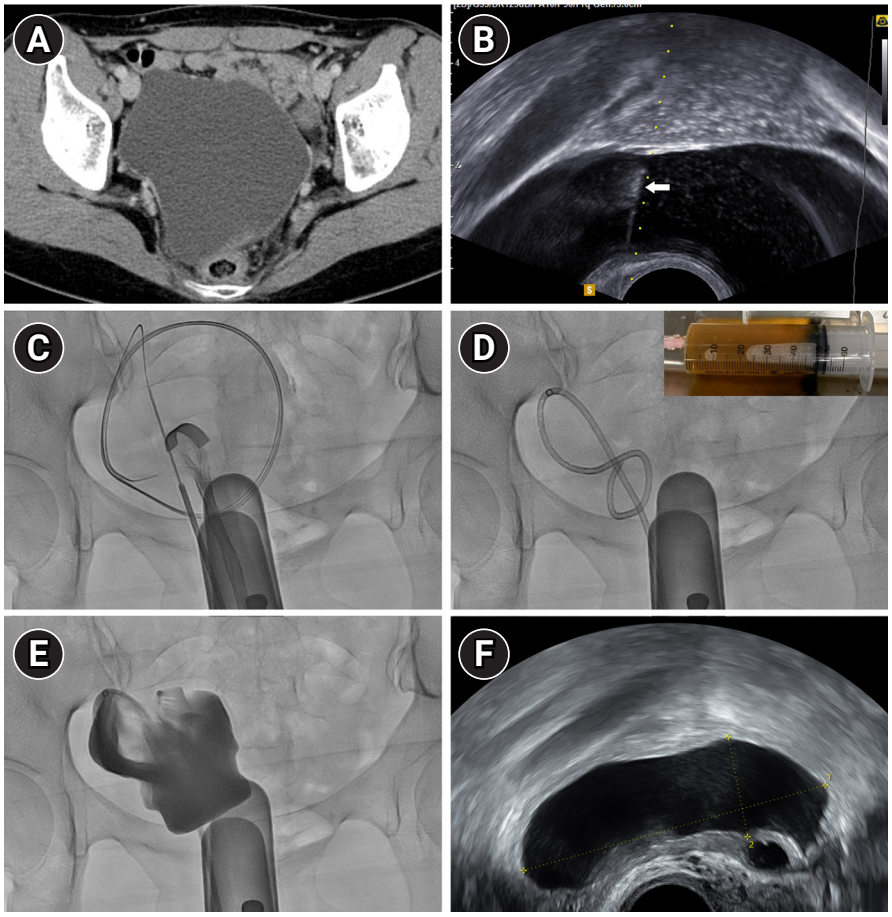


Fig. 3. A 43-year-old female with pelvic fullness (case 4). (A) Axial contrast-enhanced CT showed a 12.2-cm pelvic cystic lesion. Transabdominal access was not feasible owing to overlying bowel loops. (B) Transvaginal ultrasound demonstrated needle tract during puncture with an 18-gauge Chiba needle (arrow). (C, D) Fluoroscopic images showed guidewire insertion, which was followed by the placement of an 8.5-Fr pigtail catheter. Note the evacuated straw-colored fluid (inset in D). (E) Tubogram confirmed no contrast leakage. (F) Follow-up transvaginal ultrasound at 15 days after two-session ethanol sclerotherapy showed that the lesion decreased to 7.1 cm. At the 3-month follow-up, the lesion was no longer visible (not shown).

adverse events requiring nominal or no treatment, with or without overnight hospitalization for observation, and that resolved spontaneously [12].

Continuous variables were expressed as the mean ± standard deviation or median with range, as appropriate, and categorical variables as frequencies and percentages. Changes in maximum cyst diameter between baseline and the first follow-up examination within 1 month after sclerotherapy were assessed using the Wilcoxon signed-rank test. A two-sided $p < 0.05$ was considered statistically significant. All statistical analyses were conducted using SPSS version 26.0 (IBM Corp., Armonk, NY, USA).

Results

A total of six lesions within the pelvic cavity were treated in six patients. The median pre-procedural maximum diameter of the PICs was 14.0 cm (range, 6.0 to 20.0 cm). Access routes were determined based on the cyst location: transvaginal access was employed in one patient (case 4) to avoid the risk of bowel injury, as the transabdominal route was not feasible owing to overlying bowel loops (Fig. 3), while transabdominal access was utilized in the remaining five patients (Figs. 1, 2). For drainage, 8.5-Fr pigtail catheters were used in five patients. However, case 6 required a 10.2-Fr catheter over a guidewire due to inadequate aspiration with the initial catheter (Fig. 2). The median volume of aspirated fluid was 670 mL, which ranged widely (range, 85 to 1,060 mL). The aspirated

fluid was predominantly straw-colored and low-viscosity, except for a darkish, thin fluid in case 1. Cytological analysis of all aspirated fluid specimens was negative for malignant cells.

The volume of ethanol instilled per session ranged from 42 to 150 mL. Technical success was achieved in all cases (100%). Patients were admitted for a scheduled three-day stay, with the first session performed on the day after admission (day 2) and the second session performed on the next morning (day 3), followed by immediate discharge.

Follow-up ultrasound imaging within 1 month demonstrated a marked reduction in cyst size in all patients (Figs. 1–3), with the maximum PIC diameter decreasing from a median of 14.0 cm (range, 6.0 to 20.0 cm) to 5.25 cm (range, 2.0 to 8.0 cm) ($p = 0.03$). At the 3-month follow-up, the cysts were no longer visible in five patients, and in one patient (case 1), the cyst diameter had decreased to 1.8 cm, meeting the criteria for clinical success (Fig. 1). All patients reported resolution of their presenting symptoms at the 3-month follow-up, including pelvic pain in five patients and a sensation of pelvic fullness in one patient. By the 6-month follow-up, no visible cysts remained in any of the patients, confirming sustained resolution and no recurrence in all patients.

No major complications, such as chemical peritonitis, hemorrhage, or bowel injury, were observed; minor complications were limited to transient intraprocedural pain, which resolved with conservative analgesia. AMH levels were available for four patients; levels increased in two patients and decreased in the other two following the procedure.

Discussion

PICs are benign but often symptomatic lesions that predominantly affect premenopausal women with a history of pelvic surgery or inflammation [1]. While surgical resection has traditionally been the primary treatment, high recurrence rates and the risk of adhesion formation have prompted the investigation of less invasive alternatives. This study suggests that ultrasound-guided ethanol sclerotherapy, performed in two sessions, may represent a promising treatment option for PICs in this preliminary series, showing a marked reduction in cyst size within the first month and cyst disappearance in all patients at 6 months. However, given that follow-up was primarily based on ultrasound, small residual or flattened multiloculated fluid collections may have been undetected, and complete radiologic resolution cannot be definitively confirmed.

Our two-session protocol showed favorable preliminary outcomes in terms of efficiency and treatment response compared to the approach reported by Jeong and Kim [6]. Although direct comparison is limited by differences in study era, patient selection, and outcome definitions, their study achieved complete resolution in only 57.1% of cases and required an average of 3.125 sessions (up to 5) with prolonged catheterization until drainage fell below 5 mL [6]. In contrast, our method resulted in no cysts visible on follow-up ultrasound at 6 months in all patients, while requiring only two sessions. This approach eliminates the need for extended catheterization and may simplify the treatment process while suggesting favorable efficacy. Our exclusive use of ethanol also provides a clearer evaluation of its effectiveness compared to previous studies that mixed sclerosing agents [6].

Preservation of ovarian function is an important consideration in the management of PICs, particularly in reproductive-age women [1]. In the present study, AMH levels were available in four patients and showed heterogeneous changes following treatment. Given the small sample size and incomplete data, these findings should be considered exploratory only, and no definitive conclusions can be drawn regarding the impact of the procedure on ovarian reserve. Therefore, these results should be interpreted with caution. Further studies with larger cohorts and systematic hormonal assessment are required to clarify this issue.

The pathogenesis of PICs is linked to the failure of the peritoneal surface to resorb physiological fluid produced by the ovaries, often due to pre-existing adhesions [2,3]. In our cohort, all six patients had clear etiologies involving major abdominal or pelvic surgeries. The clinical challenge is the rapid recurrence of PICs after simple aspiration. By utilizing ethanol as a sclerosing agent, we aimed to denature the mesothelial lining of the cyst wall, thereby preventing further fluid accumulation. This approach is analogous to the principle of ethanol sclerotherapy for endometriomas, which targets the destruction of the active epithelial lining to inhibit recurrence [9]. Our results, showing a 100% technical success rate and absence of visible cysts on ultrasound at 6 months, suggest that ethanol may effectively obliterate these secreting surfaces

in PICs, although larger studies are needed to confirm this mechanism.

Therapeutic efficacy was primarily assessed through changes in the maximum diameter of the cysts. While volumetric reduction may provide a more comprehensive assessment, accurate volume measurement was technically challenging. Due to the inherent nature of PICs, which lack a rigid wall and conform to the shape of adjacent pelvic organs, the cysts often became flattened rather than shrinking proportionally post-sclerotherapy. Consequently, as calculating a precise volume using standard geometric formulas was considered prone to potential error, the maximum diameter was utilized as a more reliable and reproducible metric for follow-up.

Selecting a transabdominal or transvaginal access route is crucial for procedural safety. We primarily used the transabdominal approach, opting for transvaginal access for a deeply located cyst at risk of bowel injury. High-resolution ultrasound guidance facilitated precise needle placement even in complex pelvic environments. Furthermore, using a pigtail catheter for complete drainage before ethanol instillation ensured maximal contact between the sclerosing agent and the cyst wall, which is essential for preventing recurrence [4]. We primarily utilized 8.5-Fr pigtail catheters with multiple side holes (BSL type, Cook Medical) for efficient and thorough drainage. Compared to the standard Dawson-Mueller type, the BSL type features a greater number of side holes distributed over a larger area, which enables more effective evacuation of the cyst fluid from a wider range. However, if initial aspiration with an 8.5-Fr catheter is insufficient—as occurred in one patient in this study—we recommend upsizing to a 10.2-Fr catheter to ensure adequate drainage, which is vital to prevent ethanol dilution and ensure effective contact with the inner surface of the collapsed cyst.

Safety concerns regarding ethanol sclerotherapy include the risks of chemical peritonitis or injury to adjacent adnexal structures. In our series, we limited the maximum ethanol volume to 150 mL per session to minimize potential systemic absorption or leakage. We observed no major complications such as hemorrhage or bowel injury.

Despite its promising results, this study is limited by its small sample size and retrospective design. The small number of patients, although all demonstrated a consistent clinical response, restricted the statistical power of the findings. Additionally, follow-up imaging was primarily performed using ultrasound, which may have limited sensitivity for detecting small residual cysts or flattened multiloculated fluid collections; therefore, true complete radiologic resolution cannot be definitively confirmed. Furthermore, the follow-up duration of 6 months may be insufficient to fully assess long-term durability and recurrence. Although no recurrences were observed during this period, longer-term follow-up data, including the longest follow-up duration for each patient, were not consistently available, and delayed recurrence cannot be excluded. In addition, although the study aimed to apply a standardized protocol, a minor modification was introduced during the study period, with the maximum ethanol volume increased from 100 mL to 150 mL in the final two cases. This within-study adjustment may limit the strict uniformity of the protocol and should be considered when interpreting the results. Future prospective studies with larger cohorts and extended follow-up periods are warranted to validate these findings.

Standardized two-session catheter-directed ethanol sclerotherapy demonstrated promising short-term clinical and radiologic outcomes in this preliminary series of patients with symptomatic PICs. This minimally invasive approach may represent a feasible treatment option and potential alternative to surgery in selected patients, although larger prospective studies with long-term follow-up are required.

Conflict of interest

Gun Ha Kim, a contributing editor of the *Korean Journal of Interventional Radiology*, was not involved in the editorial evaluation or decision to publish this article. All remaining authors have declared no conflicts of interest.

Funding

None.

Acknowledgments

None.

Author contributions

Conceptualization: BSI, JHK, JHS. Data curation: BSI, JHK. Formal analysis: BSI, JHK, GHK, SAHA. Investigation: BSI, JHK. Methodology: BSI, JHK, GHK, SAHA. Project adminis-

tration: BSI, JHK. Resources: BSI, JHK. Software: BSI, JHK. Supervision: JHS. Validation: GHK, SAHA. Visualization: BSI, JHK. Writing - original draft: BSI, JHK. Writing - review & editing: GHK, SAHA, JHS.

Data availability statement

The datasets generated and/or analyzed during the current study are available from the corresponding author on reasonable request.

ORCID

Byung Soo Im, https://orcid.org/0000-0002-0187-9286
Ji-Hoon Kim, https://orcid.org/0000-0002-9280-414X
Gun Ha Kim, https://orcid.org/0000-0001-5042-1637
Shakir Ali H. Aljerdah, https://orcid.org/0009-0006-4289-4809
Ji Hoon Shin, https://orcid.org/0000-0001-6598-9049

References

1. Vallerie AM, Lerner JP, Wright JD, Baxi LV. Peritoneal inclusion cysts: a review. Obstet Gynecol Surv. 2009;64:321-334. https://doi.org/10.1097/OGX.0b013e31819f93d4
2. Koninckx PR, Renaer M, Brosens IA. Origin of peritoneal fluid in women: an ovarian exudation product. Br J Obstet Gynaecol. 1980;87:177-183. https://doi.org/10.1111/j.1471-0528.1980.tb04514.x
3. Hoffer FA, Kozakewich H, Colodny A, Goldstein DP. Peritoneal inclusion cysts: ovarian fluid in peritoneal adhesions. Radiology. 1988;169:189-191. https://doi.org/10.1148/radiology.169.1.3047785
4. Risner V, Gonzales E, McColgan Y, Salazar G. Interventional radiology treatments to address chronic pelvic pain in females. Cardiovasc Intervent Radiol. 2025;48:950-962. https://doi.org/10.1007/s00270-024-03823-9
5. Ross MJ, Welch WR, Scully RE. Multilocular peritoneal inclusion cysts (so-called cystic mesotheliomas). Cancer. 1989;64:1336-1346. https://doi.org/10.1002/1097-0142(19890915)64:6<1336::aid-cncr2820640628>3.0.co;2-x
6. Jeong JY, Kim SH. Sclerotherapy of peritoneal inclusion cysts: preliminary results in seven patients. Korean J Radiol. 2001;2:164-170. https://doi.org/10.3348/kjr.2001.2.3.164
7. Lipitz S, Seidman DS, Schiff E, Achiron R, Menczer J. Treatment of pelvic peritoneal cysts by drainage and ethanol instillation. Obstet Gynecol. 1995;86:297-299. https://doi.org/10.1016/0029-7844(95)00157-m
8. Karakas HM, Yildirim G. Percutaneous treatment of simple renal cysts with 24-h-interval ethanol sclerotherapy. Radiol Bras. 2023;56:8-12. https://doi.org/10.1590/0100-3984.2022.0041
9. Zeng CH, Shin JH. Techniques and clinical outcomes of catheter-directed sclerotherapy using ethanol for ovarian endometriomas. J Korean Soc Radiol. 2026;87:487-495. https://doi.org/10.3348/jksr.2025.0021
10. Han K, Seo SK, Kim MD, Kim GM, Kwon JH, Kim HJ, et al. Catheter-directed sclerotherapy for ovarian endometrioma: short-term outcomes. Radiology. 2018;289:854-859. https://doi.org/10.1148/radiol.2018180606
11. Noma J, Yoshida N. Efficacy of ethanol sclerotherapy for ovarian endometriomas. Int J Gynaecol Obstet. 2001;72:35-39. https://doi.org/10.1016/s0020-7292(00)00307-6
12. Omary RA, Bettmann MA, Cardella JF, Bakal CW, Schwartzberg MS, Sacks D, et al. Quality improvement guidelines for the reporting and archiving of interventional radiology procedures. J Vasc Interv Radiol. 2003;14(9 Pt 2):S293-S295. https://doi.org/10.1097/01.rvi.0000094601.83406.e1

Original Article

eISSN 2508-2612
https://doi.org/10.64961/kjir.2026.00123
Korean J Interv Radiol 2026;31(2):145-155

KJIR
Korean Journal of
Interventional Radiology

Securement of Central Venous Catheters: Suture Fixation vs. Stabilization Devices in a Multicenter Retrospective Study

Jung Ui Hong[1], Yohan Kwon[2], Dong Jae Shim[3,*], Jae Hwan Lee[4,5,6]

[1]Department of Radiology, Inha University College of Medicine, Incheon, Republic of Korea
[2]Department of Radiology, Seoul 88 Clinic, Suwon, Republic of Korea
[3]Department of Radiology, College of Medicine, The Catholic University of Korea, Seoul, Republic of Korea
[4]Department of Radiology, Seoul National University Bundang Hospital, Seongnam, Republic of Korea
[5]Department of Radiology, Seoul National University College of Medicine, Seoul, Republic of Korea
[6]Institute of Radiation Medicine, Seoul National University Medical Research Center, Seoul, Republic of Korea

Purpose: The use of adhesive-pad stabilization devices (SDs) instead of suture fixation (SF) may affect dislocation or infection rates. This study aimed to investigate the impact of SDs compared with SF for securing central venous catheters (CVCs).

Materials and Methods: This multicenter retrospective study was conducted in three tertiary institutions. Two institutions secured CVCs using sutures, whereas one used SDs, between February 2021 and July 2022. Rates of inadvertent dislocation and central line–associated bloodstream infection (CLABSI) were compared using incidence rate ratios (IRRs) from Poisson regression and Kaplan-Meier analysis after propensity-score matching. Factors associated with dislocation and CLABSI were evaluated using Cox proportional hazards analysis.

Results: A total of 2,110 patients (1,045 female; median age, 61 years [IQR, 50 to 72]) underwent CVC placement (SD, 854; SF, 1,256). After propensity-score matching (455 SD, 666 SF), dislocation occurred more frequently in the SD group (5.85 vs. 2.17 per 1,000 catheter-days; IRR, 2.64; 95% CI, 1.36 to 5.34). CLABSI occurred less frequently in the SD group (IRR, 0.19; 95% CI, 0.04 to 0.54). Kaplan-Meier analysis showed similar results. In multivariable analysis, SD was an independent risk factor for dislocation (adjusted HR [aHR], 2.23; 95% CI, 1.11 to 4.48). SD use showed a protective trend against CLABSI but did not reach statistical significance (aHR, 0.49; 95% CI, 0.13 to 1.82). When dislocation was modeled as a competing event, this protective association reached statistical significance (subdistribution HR, 0.19; 95% CI, 0.05 to 0.66).

Conclusion: Securement of CVCs with SDs was associated with a higher rate of catheter dislocation. Although SD use was associated with lower CLABSI rates, this finding requires further validation.

Keywords: Central venous catheters; Equipment failure; Bloodstream infection; Dislodgement; Accidental catheter removal

Received: March 29, 2026; **Revised:** July 4, 2026; **Accepted:** July 4, 2026
***Corresponding email:** interv@catholic.ac.kr

© 2026 Korean Society of Interventional Radiology

This is an Open Access article distributed under the terms of the Creative Commons Attribution Non-Commercial License (http://creativecommons.org/licenses/by-nc/4.0) which permits unrestricted non-commercial use, distribution, and reproduction in any medium, provided the original work is properly cited.

Introduction

A central venous catheter (CVC) plays an essential role in contemporary medicine as a route for fluid therapy and patient monitoring [1]. Maintaining CVC placement for the requested duration is important for patient treatment, particu-

larly in those with limited venous access. Conventionally, catheter hubs or clamps were sutured into the subcutaneous layer to prevent inadvertent dislocation. However, adhesive-pad stabilization devices (SDs) have been recently developed and are increasingly used. These devices secure the hub or clamp with adhesive wings rather than sutures, offering advantages such as reduced pain, shorter application time, and less tissue injury upon removal. A notable limitation of SDs is that they may be more prone to catheter dislocation. Several studies have reported conflicting results regarding suture versus SD fixation [2,3]. The Infusion Nurses Society Infusion Therapy Standards of Practice recommend avoiding sutures, noting that they are associated with needlestick injuries, biofilm formation, and an increased risk of central line–associated bloodstream infection (CLABSI) [4]. This study aimed to compare dislocation and CLABSI rates between SD and suture fixation (SF) in patients with centrally or femorally inserted central catheters (CICC/FICC) using a multicenter, propensity score–matched cohort.

Materials and Methods

Patients

This multicenter retrospective study used data from a previously published study, which was approved by the institutional review board of each participating institution (Incheon Saint Mary's Hospital [No. OC23RIDI0050], Ajou University Hospital [No. AJOUIRB-DB-2024-474], and Seoul National University Bundang Hospital [No. B-2306-836-101]); the data are available to investigators upon reasonable request [5]. The requirement for informed consent was waived due to the study's retrospective nature. The previous study was a before-and-after study evaluating the effect of tissue adhesive on CVC exit-site infection. In this secondary analysis, patients were regrouped by catheter fixation method according to institutional practice, as each institution consistently used either SF or SD throughout the study period. Two institutions secured CVCs by suturing the hub, and one institution fixed the hub or clamp with an SD (StatLock, BD, Franklin Lakes, NJ, USA).

The study retrospectively collected data from patients who underwent CICC or FICC from February 2021 to July 2022, including demographics, comorbidities, purpose of catheterization (medical or surgical), use of tissue adhesive at the exit site, ICU stay, catheterization duration in days, laterality (right or left), number of previous catheterizations, and access site (jugular, subclavian, or femoral). Patients under 19 years of age, outpatients, or those undergoing central line exchange were excluded. The unit of analysis was the catheter episode. In patients who underwent multiple catheterizations, each episode was treated as an independent observation. Electronic case report forms were completed by reviewing daily nursing charts and documenting any inadvertent dislocation, including total dislodgement or partial withdrawal of CVCs. Owing to imbalance between institutional practices, a propensity score–matched dataset was established.

Procedures

All CICC/FICC insertions were performed under ultrasonographic and fluoroscopic guidance in the angiography suite. Jugular or subclavian veins were preferentially accessed; if unavailable, femoral veins were catheterized. Maximal precautions (including sterile drape coverage from head to toe, surgical hand scrubbing, chlorhexidine antisepsis, and wearing surgical gown and gloves) were applied during catheterization. After CVC placement, catheters in the case group were secured with an SD, whereas those in the control group were sutured with nylon thread on both sides of the catheter hub or clamp (Fig. 1). The choice of hub or clamp fixation depended on the length of the external portion of the catheter. Dressing using a transparent film (Tegaderm, 3M, St. Paul, MN, USA) was applied after placement, with clear tape additionally applied at both the proximal and distal ends for reinforcement.

Definitions

Dislocation was defined as any inadvertent catheter movement, including partial withdrawal or complete dislodgement. CLABSI was defined according to the National Healthcare Safety Network as a laboratory-confirmed bloodstream infection not secondary to infection at another body site in a patient with a central line that had been in place for more than two consecutive calendar days [6].

Statistical Analysis

Descriptive statistics summarized demographic and clinical

https://doi.org/10.64961/kjir.2026.00123

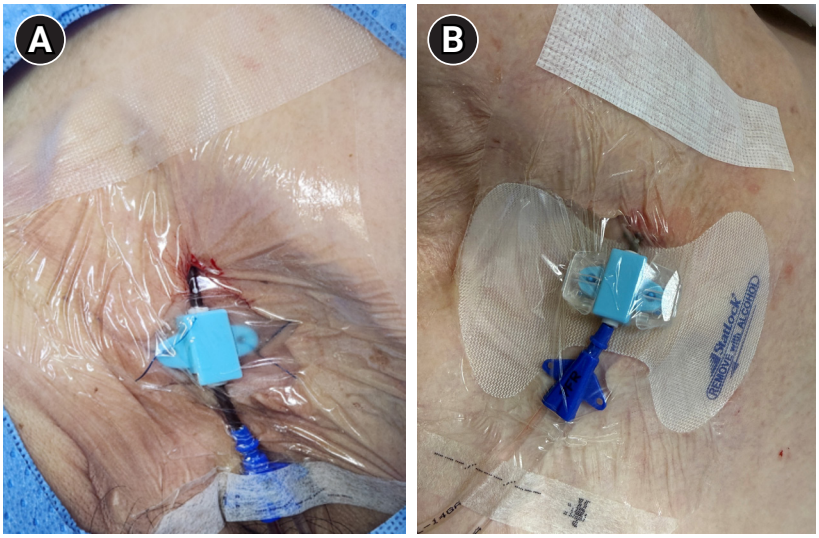


Fig. 1. Representative photographs of catheter securement methods. (A) Suture fixation. (B) Adhesive-pad stabilization device.

features of both groups. Continuous variables are expressed as mean ± standard deviation and were compared using the Mann-Whitney U test or independent t-test, as appropriate, while categorical variables are presented as frequencies with percentages and were compared using the chi-square or Fisher's exact test, as appropriate. Dislocation and CLABSI rates per 1,000 catheter-days were calculated for each group and compared using the incidence rate ratio (IRR) estimated by Poisson regression. Absence of overdispersion was confirmed prior to analysis.

Propensity score matching (PSM) was performed using the MatchIt package (R ver. 4.3.2, The R Foundation, Vienna, Austria) with a nearest-neighbor method at a 1:2 (case:control) ratio. Propensity scores were estimated via logistic regression including the following covariates: age, sex, care setting (ICU vs. general ward), clinical indication (surgical vs. medical), access side (right vs. left), use of tissue adhesive, history of prior catheterization, and comorbidities. A caliper width of 0.15 SDs of the logit of the propensity score was applied, with Mahalanobis distance matching additionally used for age and prior catheterization history. Covariate balance after matching was assessed using standardized mean differences (SMD) and visualized with a Love plot; SMD < 0.1 was considered well-balanced, and SMD < 0.25 acceptable. To account for any residual imbalance after PSM, doubly robust estimation was performed by further adjusting in multivariable Cox regression models.

Kaplan-Meier curves were generated and compared using the log-rank test. Univariable and multivariable Cox proportional hazards regression analyses were performed to identify factors associated with dislocation and CLABSI. For the dislocation analysis, dislocation was defined as the event of interest, while catheter removal, death, and end of the study period were treated as censoring events; an analogous censoring scheme was applied for the CLABSI analysis, with CLABSI defined as the event of interest. In cases where a dislodged catheter was replaced, each catheter insertion was treated as an independent episode with a new follow-up period. The proportional hazards assumption was verified using Schoenfeld residual tests, and stratified Cox models were applied if violations were detected. Multivariable model selection was guided by the Akaike information criterion, and the number of events per variable (EPV) was considered to prevent overfitting.

To evaluate robustness to potential institution-level clustering, sensitivity analyses were performed using a mixed-effects Cox model with matched subclass as a random effect and a Cox model with cluster-robust standard errors. The likelihood ratio test (LRT) was used to assess the significance of the random effect. Cumulative incidence functions were estimated and visualized using the Fine-Gray model, and group differences were assessed using Gray's test. Additionally, to assess the influence of vascular access site, sensitivity analyses were repeated after adjusting jugular versus subclavian access, excluding six patients with femoral access due to sparse data.

All analyses were performed in R version 4.3.2 (The R Foun-

dation), with two-sided p-values < 0.05 considered statistically significant.

Results

Patients and PSM

Among 2,222 eligible patients, 2,110 were included in this study (Fig. 2). CVCs were secured with SDs in 854 patients, whereas 1,256 patients had catheters sutured with nylon. Patient characteristics are presented in Table 1. Due to institutional differences, such as disease severity, catheterization preference, access site, or dwelling time, significant imbalances were observed between groups. A propensity score–matched dataset was generated, including 1,121 patients (SD group: n = 455, age 60.6 ± 16.5 years, female = 281; SF group: n = 666, age 63.8 ± 15.0 years, female = 368). SMD before and after matching, along with the Love plot, demonstrated balanced matching except for ICU stay (SMD = 0.22) after matching (Supplementary Table 1, Supplementary Fig. 1).

Incidence Rate Comparison after PSM

Dislocation occurred more frequently in the SD group (23 patients over 3,933 catheter-days) than in the SF group (15 patients over 6,906 catheter-days). The IRR was 2.64 (95% CI, 1.36 to 5.34) using a Poisson regression model. In contrast, CLABSI occurred more frequently in the SF group (31 patients over 6,906 catheter-days) than in the SD group (three patients over 3,933 catheter-days), with an IRR of 0.19 (95% CI, 0.04 to 0.54). No evidence of overdispersion was detected (dispersion = 0.97, p = 0.999).

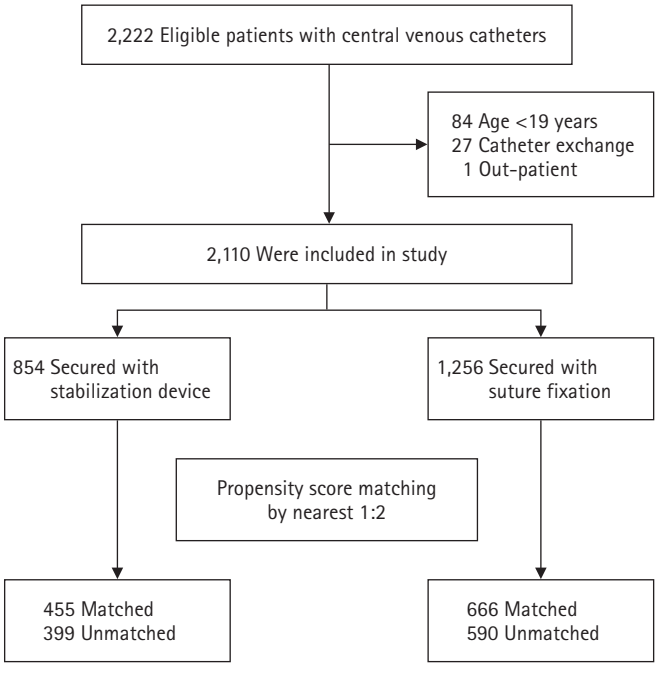


Fig. 2. Patient selection flowchart.

Kaplan-Meier and Log-Rank Analysis

Kaplan-Meier curves demonstrated significant differences in dislocation rates (p = 0.006), with dislocation occurring more frequently in the SD group (Fig. 3). CLABSI rates were significantly higher in the SF group than in the SD group (p = 0.009) (Fig. 4).

Table 1. Patient characteristics

	Overall	Suture	Device	p-value
No.	2,110	1,256	854	
Sex				< 0.001
Female	1,045 (49.5)	674 (53.7)	371 (43.4)	
Male	1,065 (50.5)	582 (46.3)	483 (56.6)	
Age (years)		61 (49–71)	63 (53–73)	< 0.001
Care unit				< 0.001
General wards	1,515 (71.8)	725 (57.7)	790 (92.5)	
ICU	595 (28.2)	531 (42.3)	64 (7.5)	
Clinical indication				< 0.001
Medical	1,229 (58.2)	1,005 (80.0)	224 (26.2)	
Surgical	881 (41.8)	251 (20.0)	630 (73.8)	
Access side				< 0.001
Left	1,956 (92.7)	1,128 (89.8)	828 (97.0)	
Right	154 (7.3)	128 (10.2)	26 (3.0)	
Access site				< 0.001
Jugular	978 (46.4)	213 (17.0)	765 (89.6)	
Subclavian	1,126 (53.4)	1,043 (83.0)	83 (9.7)	
Femoral	6 (0.3)	0 (0)	6 (0.7)	
Use of tissue adhesive				> 0.999
None	1,049 (49.7)	624 (49.7)	425 (49.8)	
Tissue adhesive	1,061 (50.3)	632 (50.3)	429 (50.2)	
Comorbidities				< 0.001
None	465 (22.0)	351 (27.9)	114 (13.3)	
DM	202 (9.6)	153 (12.2)	49 (5.7)	
Cancer	776 (36.8)	333 (26.5)	443 (51.9)	
Immunocompromised	15 (0.7)	13 (1.0)	2 (0.2)	
ESRD	54 (2.6)	24 (1.9)	30 (3.5)	
Multi-comorbidities	598 (28.3)	382 (30.4)	216 (25.3)	
No. of prior catheterizations		1 (1–2)	1 (1–1)	< 0.001
Dwelling time (days)		10 (4–19)	6 (4–8)	< 0.001
Dislocation				0.011
No	2,059 (97.6)	1,235 (98.3)	824 (96.5)	
Yes	51 (2.4)	21 (1.7)	30 (3.5)	

Values are presented as number (%) or median (interquartile range).
ESRD, end-stage renal disease.

https://doi.org/10.64961/kjir.2026.00123

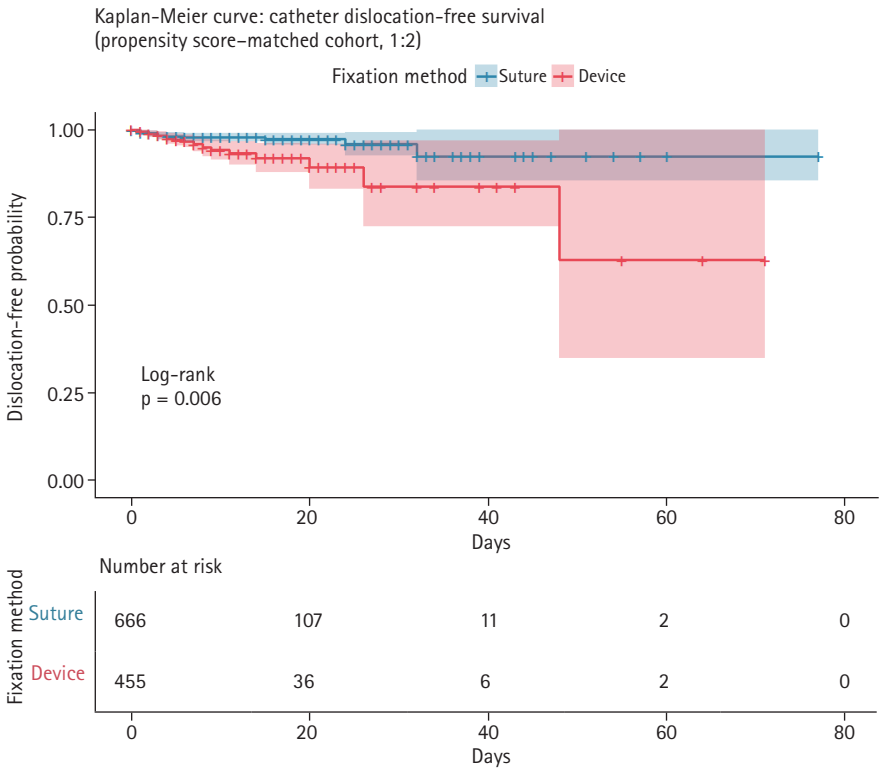


Fig. 3. Kaplan-Meier survival curves for central venous catheter dislocation according to fixation method.

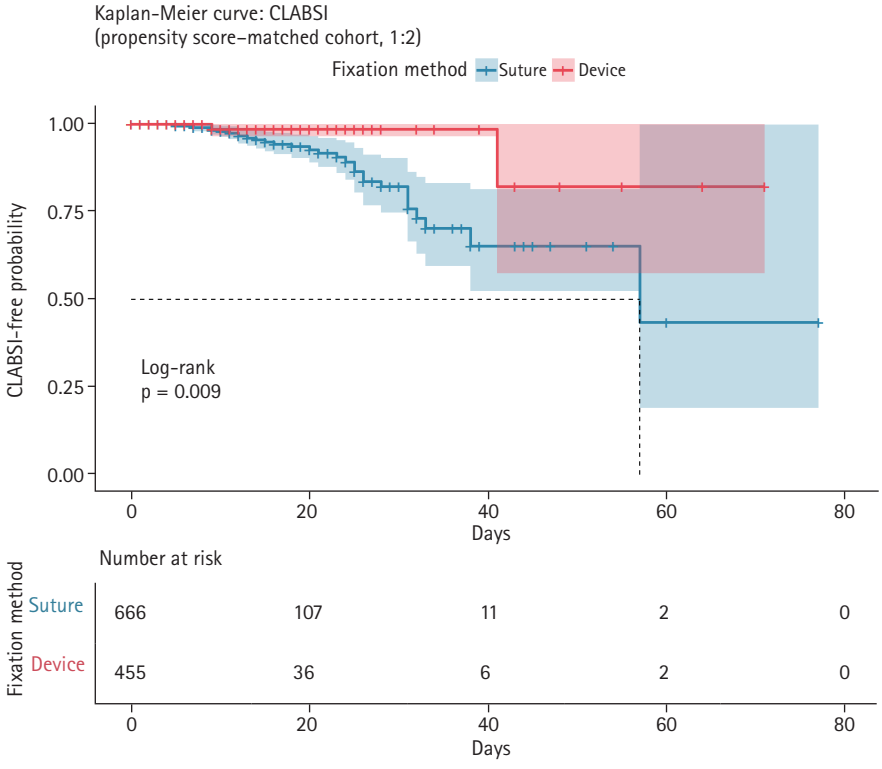


Fig. 4. Kaplan-Meier survival curves for central line–associated bloodstream infection (CLABSI) according to fixation method. Note: Interpretation should consider the low total event count (n = 34), diminishing at-risk numbers in later intervals, and the differential cumulative catheter-days between groups (suture fixation 6,906 vs. stabilization device, 3,933).

Cox-Proportional Hazard Analysis

Univariable analysis indicated that dislocation was more frequent with SD use, older age, and femoral access, and less frequent in patients with surgical indications. In multivariable analysis, stratified by purpose and access site owing to proportional hazards assumption violations, SD use was the only independent predictor of dislocation (adjusted HR, 2.23; 95% CI, 1.11 to 4.48).

Regarding CLABSI, univariable analysis identified protective factors including SD use (HR, 0.24; 95% CI, 0.08 to 0.77), cancer (HR, 0.33; 95% CI, 0.12 to 0.91), and multiple comorbidities (HR, 0.30; 95% CI, 0.13 to 0.70). Significant risk factors included older age (HR, 1.03; 95% CI, 1.01 to 1.06), subclavian access (HR, 2.31; 95% CI, 1.01 to 5.24), and triple-lumen catheter use (HR, 4.00; 95% CI, 1.88 to 8.52). In multivariable analysis, only the use of triple-lumen catheters remained a significant risk factor. Although SD use showed a protective effect in univariable analysis ($p = 0.017$), this effect was not statistically significant in multivariable analysis (HR, 0.49; 95% CI, 0.13 to 1.82; $p = 0.28$), likely owing to limited statistical power (low EPV = 4.3). Detailed results of Cox proportional hazards analyses are shown in Tables 2 and 3. To account for residual imbalance in ICU admission after PSM, doubly robust estimation was performed by additionally adjusting for ICU status in multivariable models; results remained consistent (dislocation: HR, 2.17; 95% CI, 1.10 to 4.29; CLABSI: HR, 0.49; 95% CI, 0.13 to 1.80), supporting the robustness of the primary findings.

Sensitivity Analysis

To further assess robustness to institution-level clustering, sensitivity analyses were performed using a mixed-effects Cox model with matched subclass as a random effect and a Cox model with cluster-robust standard errors. Both approaches yielded results consistent with the primary analysis, with SD use remaining a significant predictor of dislocation across unadjusted and adjusted models (mixed-effects Cox, adjusted: HR, 3.41; 95% CI, 1.73 to 6.73; $p < 0.001$; cluster-robust, adjusted: HR, 3.41; 95% CI, 1.77 to 6.57; $p < 0.001$). The variance of the subclass-level random effect was negligible (variance = 0.0004), and the LRT confirmed no significant clustering within

Table 2. Univariable and multivariable Cox proportional hazards analysis for central venous catheter dislocation

Variable	Univariable		Multivariable	
	HR (95% CI)	p-value	HR (95% CI)	p-value
Treatment				
Suture	Reference	-	Reference	-
Device	2.374 (1.203–4.685)	0.013	2.232 (1.112–4.477)	0.024
Demographics				
Age (per year)	1.028 (1.004–1.053)	0.020	1.009 (0.981–1.037)	0.532
Male sex	1.524 (0.765–3.036)	0.231	-	-
Clinical characteristics				
ICU admission	0.897 (0.408–1.971)	0.787	-	-
Purpose: surgical	0.139 (0.041–0.476)	0.002	Stratified	-
Side: left	1.256 (0.448–3.523)	0.665	-	-
Tissue adhesive fixation	0.840 (0.435–1.622)	0.604	-	-
Prior catheterization (n)	0.679 (0.284–1.621)	0.383	-	-
Access site (ref: jugular)				
Subclavian	0.561 (0.281–1.120)	0.101	Stratified	-
Femoral	6.391 (1.030–39.670)	0.047	Stratified	-
Lumen				
3-Lumen	0.995 (0.432–2.292)	0.991	-	-
Comorbidity (ref: none)				
DM	1.332 (0.410–4.330)	0.633	-	-
Cancer	0.363 (0.117–1.125)	0.079	-	-
ESRD	1.283 (0.249–6.613)	0.766	-	-
Multicomorbidities	1.463 (0.594–3.604)	0.408	-	-

p-values indicate statistical significance ($p < 0.05$). The multivariable model was stratified by surgical purpose and catheter access site to address violations of the proportional hazard assumption (Schoenfeld residual test). Immunocompromised status was merged with "none" due to zero events (n = 5).
DM, diabetes mellitus; ESRD, end-stage renal disease.

Table 3. Univariable and multivariable Cox proportional hazards analysis for CLABSI

Variable	Univariable		Multivariable	
	HR (95% CI)	p-value	HR (95% CI)	p-value
Treatment				
Suture	Reference	-	Reference	-
Device	0.242 (0.075–0.774)	0.017	0.486 (0.130–1.822)	0.285
Demographics				
Age (per year)	1.034 (1.006–1.064)	0.018	-	-
Male sex	0.595 (0.301–1.176)	0.135	-	-
Clinical characteristics				
ICU admission	1.849 (0.951–3.596)	0.070	-	-
Purpose: surgical	0.634 (0.127–3.151)	0.577	-	-
Side: left	1.388 (0.596–3.234)	0.447	-	-
Tissue adhesive (glue)	0.494 (0.232–1.051)	0.067	0.515 (0.240–1.106)	0.089
Prior catheterization	1.125 (0.728–1.739)	0.597	-	-
Access site (ref: jugular/femoral)				
Subclavian	2.305 (1.014–5.240)	0.046	-	-
Lumen				
3-Lumen	4.000 (1.878–8.519)	<0.001	2.928 (1.232–6.961)	0.015
Comorbidity (ref: none)				
DM	0.237 (0.043–1.306)	0.098	-	-
Cancer	0.333 (0.122–0.909)	0.032	-	-
Immunocompromised	0.541 (0.171–1.710)	0.296	-	-
ESRD	0.374 (0.081–1.718)	0.206	-	-
Multicomorbidities	0.297 (0.126–0.701)	0.006	-	-

Bold p-values indicate statistical significance ($p < 0.05$). Femoral access was merged with jugular access due to zero CLABSI events ($n = 6$). The multivariable model was selected based on Akaike information criterion minimization and EPV optimization (EPV = 11.3). Proportional hazards assumption was verified using the Schoenfeld residual test (GLOBAL $p = 0.77$).
CLABSI, central line–associated bloodstream infection; DM, diabetes mellitus; ESRD, end-stage renal disease; EPV, events per variable.

matched subclasses ($p > 0.98$), indicating that PSM adequately addressed group-level confounding.

A competing risk analysis using the Fine-Gray subdistribution hazard model was additionally performed, treating dislocation as a competing event for CLABSI and vice versa. The subdistribution HR for SD use remained consistent in direction with the primary analysis for both outcomes (CLABSI: subdistribution HR [sHR], 0.19; 95% CI, 0.05 to 0.66; $p = 0.009$; dislocation: sHR, 3.51; 95% CI, 1.81 to 6.83; $p < 0.001$), supporting the robustness of the primary findings. Cumulative incidence functions estimated by the Fine-Gray model are presented in Supplementary Fig. 2.

To further evaluate the potential influence of access site on outcomes, access sites including internal jugular, subclavian, and femoral vein were additionally adjusted for in the Cox models after excluding six patients with femoral access due to sparse data precluding stable estimation. After adjustment, SD remained a significant independent predictor of dislocation (HR, 2.77; 95% CI, 1.33 to 5.77; $p = 0.006$). For CLABSI, the protective effect of SD was strengthened and approached statistical significance (HR, 0.21; 95% CI, 0.04 to 1.02; $p = 0.053$), consistent in direction with the primary analysis. The summary of the sensitivity analysis was presented in Table 4.

Discussion

This multicenter retrospective study compared dislocation and CLABSI rates between SD and SF groups in 1,121 propensity score–matched patients who underwent CICC/FICC. The principal findings were twofold: SD use was associated with a significantly higher risk of catheter dislocation (IRR, 2.64; adjusted HR, 2.23), whereas CLABSI occurred less frequently in the SD group based on incidence rate comparison (IRR, 0.19) and Kaplan-Meier analysis. However, the protective effect of SD on CLABSI did not reach statistical significance in multivariable Cox analysis (adjusted HR, 0.49; $p = 0.28$). These results suggest a clinical trade-off between dislocation risk and potential infection benefit when selecting a catheter securement method.

Table 4. Summary of sensitivity analyses for dislocation and CLABSI

Analysis	Dislocation HR (95% CI)	p-value	CLABSI HR (95% CI)	p-value
Primary analysis				
Multivariable Cox (PSM, doubly robust)	2.23 (1.11–4.48)	0.024[a]	0.49 (0.13–1.82)	0.285
Institution-level clustering				
Mixed-effects Cox (random effect: matched subclass), unadjusted	2.46 (1.27–4.75)	0.007	-	-
Mixed-effects Cox (random effect: matched subclass), adjusted	3.41 (1.73–6.73)	< 0.001	-	-
Cox with cluster-robust SE (cluster: matched subclass), unadjusted	2.46 (1.27–4.77)	0.008	-	-
Cox with cluster-robust SE (cluster: matched subclass), adjusted	3.41 (1.77–6.57)	< 0.001	-	-
Competing risk analysis				
Fine-Gray subdistribution hazard model (unadjusted)	3.51 (1.81–6.83)	< 0.001	0.19 (0.05–0.66)	0.009
Access site adjustment				
Cox with access site adjustment (femoral access excluded, n = 6)	2.77 (1.33–5.77)	0.006	0.21 (0.04–1.02)	0.053

All HRs represent stabilization device vs. suture fixation, with suture fixation as the reference group.
CLABSI, central line–associated bloodstream infection; PSM, propensity score matching; SE, standard error.
[a]Stratified by purpose and access site owing to proportional hazards assumption violations.

Regarding catheter dislocation, SD use independently increased the risk approximately 2.2-fold compared with SF. This finding is mechanistically plausible, as sutures anchor the catheter hub directly to subcutaneous tissue, providing firm resistance against outward traction, whereas SDs rely on adhesive bonding to the skin, which is more susceptible to loosening from moisture, perspiration, and patient movement. An in vitro biomechanical study reported that SF using a finger-trap technique withstood dislodgement forces exceeding 76 N [7], consistent with our clinical findings. Karpanen et al. [8] reported a numerically higher rate of unplanned CVC removal in the suture-free group (6%) versus the suture group (2%) in a multicenter randomized feasibility study of 171 patients, although the difference was not statistically significant. Similarly, Mitchell et al.'s CASCADE pilot randomized controlled trial [9] found the highest central venous access device failure rate in the sutureless securement device (StatLock) group (27.3 per 1,000 catheter-days) among four securement methods in 121 ICU patients, though the study was underpowered. Some smaller studies reported no difference or even lower dislodgement rates with sutureless methods; however, these trials used different device types and enrolled substantially smaller cohorts (n = 100–271) [2,3]. Our propensity score–matched analysis of 1,121 patients provides more robust evidence supporting the higher dislocation risk associated with SDs.

The relationship between catheter securement methods and CLABSI is complex. In our study, unadjusted analyses consistently showed a lower CLABSI rate in the SD group: the IRR was 0.19 (95% CI, 0.04 to 0.54), and Kaplan-Meier analysis demonstrated a significant difference (p = 0.009). However, when adjusting for confounders in multivariable Cox regression, the protective effect of SD use was attenuated and no longer statistically significant (HR, 0.49; 95% CI, 0.13 to 1.82; p = 0.28). This attenuation is likely owing to limited statistical power rather than a true absence of effect, as only 34 CLABSI events occurred across both groups, resulting in a low EPV (4.3) in the multivariable model. Cox regression models become unreliable when EPV falls below 10 [10]. Moreover, the low total event count renders the Kaplan-Meier curves for CLABSI (Fig. 4) susceptible to instability in later follow-up intervals, where the number of patients at risk diminishes substantially; this uncertainty is compounded by the differential cumulative exposure between groups (SF: 6,906 vs. SD: 3,933 catheter-days; ratio approximately 1.75:1), which should be considered when interpreting the observed curve separation. This issue of low event rates is not unique to our study; prior securement trials have similarly reported few confirmed CLABSI events despite substantial enrollment [2,9]. The consistency of the direction and magnitude of the protective signal across multiple analytic approaches, including Poisson regression, Kaplan-Meier analysis, and doubly robust sensitivity analysis (HR, 0.49; 95% CI, 0.13 to 1.82), supports this interpretation. Existing systematic reviews, including a Cochrane review and a recent meta-analysis of 46 studies encompassing 10,054 participants, have similarly found no definitive consensus on the optimal securement method for infection prevention, although sutureless devices appear

most promising [11,12]. Taken together, our findings suggest a potential protective effect of SDs against CLABSI, but adequately powered prospective studies are needed to confirm this independently.

Several biological mechanisms may explain the potential association between SF and increased CLABSI risk. Sutures create additional percutaneous puncture sites near the catheter exit, each serving as a potential portal for skin microorganisms [13]; suture material acts as a foreign body promoting biofilm formation and subsequent intravascular migration of colonizing organisms [4,8]; and minor bleeding from suture placement produces a nutrient-rich microenvironment that facilitates bacterial proliferation at the catheter exit site [14]. SDs eliminate these suture-specific risk factors by securing the catheter through adhesive contact alone, without penetrating the skin barrier.

Triple-lumen catheter use was independently associated with CLABSI in our multivariable analysis (HR, 2.93; 95% CI, 1.23 to 6.96), consistent with prior meta-analyses reporting significantly higher infection risks with multilumen catheters (OR, 2.74; 95% CI, 1.84 to 4.07) [15,16], likely owing to increased hub manipulation, which amplifies opportunities for intraluminal contamination [17].

These findings have important clinical implications for catheter securement. In patients at higher infection risk (such as those with prolonged catheterization, immunocompromised status, or triple-lumen catheters), SD use may be preferable despite the higher dislocation risk, given that CLABSI is a serious healthcare-associated infection with an attributable mortality of 12%–25% [18], whereas catheter dislocation is typically manageable with reinsertion. Conversely, in patients for whom catheter dislocation would be particularly consequential, such as those with limited venous access or receiving critical infusions, SF may remain the more appropriate choice. Strategies to mitigate SD-associated dislocation risk, including concurrent use of tissue adhesive at the exit site or integrated securement dressings, warrant further investigation.

This study has several limitations. First, this was a retrospective secondary analysis of data originally collected for a different purpose (tissue adhesive efficacy), and certain variables (such as dressing change frequency and nursing-to-patient ratio) were not systematically recorded. However, PSM with doubly robust estimation and the consistency of results across multiple analytic methods support the validity of our findings. Second, the SD and SF groups were separated by institution rather than randomized within each institution, introducing potential institutional confounding; observed differences may partly reflect institution-level factors rather than securement method. Although PSM balanced most measured covariates and stratified Cox models addressed residual imbalances, unmeasured confounders cannot be fully excluded. A multicenter randomized controlled trial using both securement methods within each institution would be needed to definitively address this limitation. Third, the low CLABSI event rate (34 events across both groups; EPV = 4.3) limited the statistical power of the multivariable analysis. While the protective signal was consistent across all analytic approaches, the study was underpowered to confirm the independent effect of SD use on CLABSI. Notably, however, the Fine-Gray competing risk model—which accounts for dislocation as a competing event—yielded a statistically significant protective effect of SD on CLABSI (sHR, 0.19; 95% CI, 0.05 to 0.66; p = 0.009), and a borderline significant effect was similarly observed after additional adjustment for vascular access site (HR, 0.21; 95% CI, 0.04 to 1.02; p = 0.053). These findings suggest that the protective effect of SD on CLABSI may be real but requires confirmation in larger, adequately powered studies. These findings apply specifically to adhesive-pad SDs, as exemplified by StatLock (BD), and should not be generalized to other CVC securement modalities (including subcutaneous anchor securement systems, tissue adhesives, and integrated securement dressings) without further validation. Lastly, vascular access site (internal jugular, subclavian, and femoral) was not included as a PSM covariate due to strong institution-level preferences, resulting in substantial residual imbalance after matching (SMD, 0.65–0.66). Although a sensitivity analysis adjusting for access site yielded consistent results, the potential influence of this residual imbalance on effect estimates cannot be entirely excluded. Future studies with adequate sample sizes, informed by the effect sizes observed herein, are warranted.

Despite these limitations, the strengths of this study include a large sample size, multicenter design, rigorous statistical methodology with multiple complementary analytic approaches, and clinically relevant dual endpoints encompassing both dislocation and CLABSI.

In conclusion, this multicenter propensity score–matched study demonstrated that catheter SDs were associated with a higher rate of dislocation compared with SF, while multiple analytic approaches consistently suggested a lower CLABSI rate with SD use, which did not reach statistical significance in the primary multivariable analysis but became significant when dislocation was modeled as a competing event.

Conflict of interest

Dong Jae Shim, contributing editor of the *Korean Journal of Interventional Radiology*, was not involved in the editorial evaluation or decision to publish this article. All remaining authors have declared no conflicts of interest.

Funding

None.

Acknowledgments

This manuscript is based on the first author (Jung Ui Hong)'s doctoral dissertation at Inha University.

Author contributions

Conceptualization: DJS. Data curation: YK, JHL, DJS. Formal analysis: DJS. Investigation: DJS. Methodology: YK, JHL, DJS. Project administration: DJS. Resources: DJS. Software: DJS. Supervision: DJS. Validation: DJS. Visualization: DJS. Writing - original draft: JUH, DJS. Writing - review & editing: JUH, DJS.

Data availability statement

The datasets generated or analyzed during the study are available from the corresponding author on reasonable request.

Supplementary material

The supplementary data are available with this article at https://doi.org/10.64961/kjir.2026.00123.

ORCID

Jung Ui Hong, https://orcid.org/0000-0002-9597-5024
Yohan Kwon, https://orcid.org/0000-0001-9502-386X
Dong Jae Shim, https://orcid.org/0000-0001-9596-0765
Jae Hwan Lee, https://orcid.org/0000-0001-6513-3224

References

1. Kehagias E, Galanakis N, Tsetis D. Central venous catheters: which, when and how. Br J Radiol. 2023;96:20220894. https://doi.org/10.1259/bjr.20220894
2. Chen Y, Chen X, Jin X, Zeng X, Cao X, Zhao L. Compare the safety and efficacy of integrated securement device versus suture securement for centrally inserted central venous catheters: a prospective cohort study. Sci Rep. 2025;15:34907. https://doi.org/10.1038/s41598-025-18777-2
3. Molina-Mazon CS, Martin-Cerezo X, Domene-Nieves de la Vega G, Asensio-Flores S, Adamuz-Tomas J. Comparative study on fixation of central venous catheter by suture versus adhesive device. Enferm Intensiva (Engl Ed). 2018;29:103-112. https://doi.org/10.1016/j.enfi.2017.10.004
4. Nickel B, Gorski L, Kleidon T, Kyes A, DeVries M, Keogh S, et al. Infusion therapy standards of practice, 9th edition. J Infus Nurs. 2024;47(1S):S1-S285. https://doi.org/10.1097/NAN.0000000000000532
5. Kwon Y, Shim DJ, Lee JH, Kim D, Baek SH, Kim J, et al. Effect of tissue adhesive application on central line-associated bloodstream infections: a multi-centre retrospective study. J Hosp Infect. 2025;162:153-159. https://doi.org/10.1016/j.jhin.2025.04.030
6. Centers for Disease Control and Prevention. Bloodstream infection event (central line-associated bloodstream infection and non-central line associated bloodstream infection). https://www.cdc.gov/nhsn/pdfs/pscmanual/4psc_clabscurrent.pdf. Published January 2026. Accessed March 2026.
7. Struck MF, Friedrich L, Schleifenbaum S, Kirsten H, Schummer W, Winkler BE. Effectiveness of different central venous catheter fixation suture techniques: an in vitro crossover study. PLoS One. 2019;14:e0222463. https://doi.org/10.1371/journal.pone.0222463
8. Karpanen TJ, Casey AL, Whitehouse T, Timsit JF, Mimoz O, Palomar M, et al. A clinical evaluation of two central venous catheter stabilization systems. Ann Intensive Care. 2019;9:49. https://doi.org/10.1186/s13613-019-0519-6
9. Mitchell ML, Ullman AJ, Takashima M, Davis C, Mihala G, Powell M, et al. Central venous access device securement and dressing effectiveness: the CASCADE pilot randomised controlled trial in the adult intensive care. Aust Crit Care.

2020;33:441-451. https://doi.org/10.1016/j.aucc.2019.10.002
10. Peduzzi P, Concato J, Kemper E, Holford TR, Feinstein AR. A simulation study of the number of events per variable in logistic regression analysis. J Clin Epidemiol. 1996;49:1373-1379. https://doi.org/10.1016/s0895-4356(96)00236-3
11. Ullman AJ, Cooke ML, Mitchell M, Lin F, New K, Long DA, et al. Dressings and securement devices for central venous catheters (CVC). Cochrane Database Syst Rev. 2015;2015:CD010367. https://doi.org/10.1002/14651858.CD010367.pub2
12. Xu H, Hyun A, Mihala G, Rickard CM, Cooke ML, Lin F, et al. The effectiveness of dressings and securement devices to prevent central venous catheter-associated complications: a systematic review and meta-analysis. Int J Nurs Stud. 2024;149:104620. https://doi.org/10.1016/j.ijnurstu.2023.104620
13. Frey AM, Schears GJ. Why are we stuck on tape and suture? A review of catheter securement devices. J Infus Nurs. 2006;29:34-38. https://doi.org/10.1097/00129804-200601000-00007
14. Murga R, Miller JM, Donlan RM. Biofilm formation by gram-negative bacteria on central venous catheter connectors: effect of conditioning films in a laboratory model. J Clin Microbiol. 2001;39:2294-2297. https://doi.org/10.1128/JCM.39.6.2294-2297.2001
15. Lafuente Cabrero E, Terradas Robledo R, Civit Cunado A, Garcia Sardelli D, Hidalgo Lopez C, Giro Formatger D, et al. Risk factors of catheter-associated bloodstream infection: systematic review and meta-analysis. PLoS One. 2023;18:e0282290. https://doi.org/10.1371/journal.pone.0282290
16. Templeton A, Schlegel M, Fleisch F, Rettenmund G, Schobi B, Henz S, et al. Multilumen central venous catheters increase risk for catheter-related bloodstream infection: prospective surveillance study. Infection. 2008;36:322-327. https://doi.org/10.1007/s15010-008-7314-x
17. O'Grady NP, Alexander M, Dellinger EP, Gerberding JL, Heard SO, Maki DG, et al. Guidelines for the prevention of intravascular catheter-related infections. Infect Control Hosp Epidemiol. 2002;23:759-769. https://doi.org/10.1086/502007
18. Centers for Disease Control and Prevention (CDC). Vital signs: central line-associated blood stream infections–United States, 2001, 2008, and 2009. MMWR Morb Mortal Wkly Rep. 2011;60:243-248.

Original Article

eISSN 2508-2612
https://doi.org/10.64961/kjir.2026.00024
Korean J Interv Radiol 2026;31(2):156-163

KJIR
Korean Journal of
Interventional Radiology

Clinical Efficacy and Patency of Stents for Malignant Iliocaval Venous Occlusion

Wonseon Shin[1], Gyoung Min Kim[2,*], Kichang Han[2], Man Deuk Kim[2], Joon Ho Kwon[2], Jong Yun Won[2], Juil Park[2]

[1]Department of Radiology, National Fire Hospital, Eumseong, Republic of Korea
[2]Department of Radiology and Research Institute of Radiological Science, Severance Hospital, Yonsei University College of Medicine, Seoul, Republic of Korea

Purpose: This study aimed to evaluate the clinical efficacy and patency of stents placed for symptomatic iliac vein or IVC obstruction caused by malignant tumors.

Materials and Methods: A total of 34 consecutive patients with malignant iliac vein or IVC obstruction underwent stent placement. We reviewed their electronic medical records, pre- and post-procedural CT scans, and angiograms retrospectively, and evaluated technical success, clinical success, and patient-based and vessel-based reocclusion rates confirmed by follow-up cross-sectional images. The reocclusion rate difference between IVC and iliac stents was also assessed.

Results: All patients complained of leg and/or trunk edema. The stents were placed in the following locations: IVC (n = 9); iliac veins (n = 19); and both IVC and iliac veins (n = 6). Technical success rate was 100% and the clinical success rate was 87.5% during hospitalization. Cross-sectional area of the affected thigh was significantly decreased after stent placement (mean 11.7%, p = 0.003). The median follow-up period was 65 days (Q1–Q3, 28.5–227.3; IQR, 198.8). The patient-based reocclusion rate was 42.8%. The vessel-based reocclusion rates for IVC (12.5%) tended to be lower than those of iliac veins (45.0%), though the difference was not statistically significant (p = 0.194).

Conclusion: Stent insertion for iliac vein or IVC obstruction secondary to malignancy is technically feasible and can help to improve patients' symptoms. IVC stents tend to achieve a higher rate of patency than iliac vein stents.

Keywords: Iliac vein; Vena cava, inferior; Stents; Neoplasm; Venous thrombosis

Introduction

Iliocaval venous obstructions have been successfully treated over the past few decades with minimally invasive interventions such as stent deployment [1,2]. These obstructions are often secondary to cancers. Especially, malignant tumors and their metastases originating from the hepatobiliary system, gastrointestinal tract and genitourinary organs can cause iliocaval venous obstruction. Metastatic lymph nodes or the tumors themselves can cause venous outflow obstruction with or without subsequent venous thrombosis by invasion or extrinsic compression of the iliocaval venous system. Venous thrombosis occurs in more than 1% of cancer patients every year and patients diagnosed with a malignancy have a four-fold higher risk of developing a venous thrombosis [3].

Venous outflow obstruction causes ambulatory venous hypertension, ascites, renal insufficiency, and chronic venous insufficiency [4-7]. Furthermore, venous outflow obstruction caused by venous thromboembolism not only erodes quality

Received: February 5, 2026; **Revised:** July 13, 2026;
Accepted: July 13, 2026
***Corresponding email:** kimgm@yonsei.ac.kr

© 2026 Korean Society of Interventional Radiology

This is an Open Access article distributed under the terms of the Creative Commons Attribution Non-Commercial License (http://creativecommons.org/licenses/by-nc/4.0) which permits unrestricted non-commercial use, distribution, and reproduction in any medium, provided the original work is properly cited.

of life through symptoms that include swelling, pain, and venous stasis ulcer, but also can increase mortality in cancer patients [8].

Traditionally, emergent radiation therapy had been considered the standard treatment for malignant SVC syndrome (SVCS) [9]. In the past decades, endovascular treatment including stent placement, angioplasty, thrombolysis, and thrombectomy has emerged as a superior and faster alternative therapy [10], and is widely accepted as first-line therapy for emergent cases.

Apart from SVCS, malignant iliocaval obstruction, which can be regarded as an analogue of SVCS for the lower extremities, has been investigated far less. In the literature, malignancy-related iliocaval obstruction is treated as a subset of venous obstructions that are due to various causes or that affect various anatomical locations [2,11,12]. There are several clinical studies on the usefulness of stent placement for malignant IVC syndrome [13-18]. And only few studies dealt with iliac vein obstruction [19,20]. Therefore, the purpose of our study was to evaluate the clinical efficacy and patency of the stents placed for symptomatic iliac vein or IVC obstruction caused by tumor invasion or extrinsic compression.

Materials and Methods

This is a single-center, retrospective cohort study. The cases were identified using a searching system of our institution (Severance Clinical Research Analysis Portal). Our institutional review board (Severance Hospital Human Research Protection Center) approved this retrospective study (protocol number: 4-2018-0619), and written informed consent for the procedure was obtained from all patients. Written consent for inclusion in the retrospective study was waived as per our institution's policies.

Patient Population

Thirty-four consecutive patients who underwent iliocaval venous stent placement from May 2003 to October 2014 due to symptomatic malignancy-related iliac vein or IVC occlusion were included in this study. Electronic medical records (EMR) were reviewed to identify basic characteristics, including sex, age, etiology, and the clinical symptoms and signs associated with venous obstruction before and after treatment.

Endovascular Treatment

The malignancy-related iliocaval venous obstructions were diagnosed by CT venography and were confirmed by catheter-based venography in all patients. For the patients with evident venous thrombosis on the pre-procedural CT venography, intravenous heparin infusion (dose, 18 IU/kg/h; target activated partial thromboplastin time range, 40 to 69 seconds) was initiated at least 6 hours before the endovascular procedure. One of two types of retrievable IVC filter (Günther Tulip until August 2014 and Celect from September 2014, Cook Medical, Bloomington, IN, USA) was inserted before the procedure to prevent pulmonary thromboembolism, at the operator's discretion.

For the patient with patent external iliac and femoro-popliteal veins, the femoral fossa was prepared in the usual sterile manner with the patient in the supine position (n = 20). In cases with external iliac vein occlusion and/or thrombosis in the femoro-popliteal vein, we used popliteal access with the patient in the prone position (n = 14). After local anesthesia administration of 2% lidocaine, the common femoral or popliteal vein was punctured under ultrasonographic guidance with a 21-gauge micropuncture introducer set (Cook Medical). A 0.035-inch hydrophilic guide wire (Terumo, Tokyo, Japan) was advanced to the iliac vein, and the introducer sheath with variable size (8–14 Fr) was inserted. After advancing the 0.035-inch guide wire to the iliac vein, a 5-Fr angiography catheter (Omni flush, Angio-Dynamics, Latham, MD, USA, or Contralateral, Boston Scientific, Watertown, MA, USA) was inserted, and pull-back venography was performed.

After confirming the diagnosis and extent of the thrombus, a rotating angiographic catheter was used to inject a small amount of diluted contrast medium to macerate the thrombus, and repetitive aspiration thrombectomy using the 11-Fr percutaneous introducer catheter (Arrow-Flex percutaneous introducer set; Arrow International, Reading, MA, USA) was performed. The manner of aspiration thrombectomy is described elsewhere [21].

For the patients with thrombosis, we injected 3,000 IU of heparin intravenously before aspiration thrombectomy. Heparin was not used during the procedure for the patients without thrombosis.

An endovascular stent was inserted to recanalize the obstructed segment. Four types of self-expandable stents were

placed. These included Hercules (S&G Biotech, Seongnam, Korea), S.M.A.R.T. Control (Cordis, Miami Lakes, FL, USA), E-Luminexx (Bard, Murray Hill, NJ, USA), and Wallstent (Boston Scientific, Galway, Ireland). Stents were chosen individually based on site and size of venous obstruction. Generally, Hercules stents (20–28 mm in diameter) were used for IVC obstructions and the other types of stents (10–14 mm in diameter) were used for iliac venous obstruction. Usually only one stent was deployed for each site of venous obstruction. However, if the length of a stent was shorter than the entire length of malignant venous obstruction, an additional stent was deployed to cover the entire lesion. The additional stent was required in nine cases (IVC, 1; right iliac vein, 3; left iliac vein, 5). Post-stent balloon dilatation was performed in 32 cases of persistent residual stenosis after stent insertion (except for two patients who showed immediate full expansion of the stents). Follow-up CT scans were taken as needed, and at the physician's discretion.

Unless contraindicated (conditions including recent surgery or major hemorrhage, and central nervous system metastases), postprocedural anticoagulation with warfarin and/or enoxaparin was generally administered for 1–3 months.

Follow-up

All patients were followed up by the referring physician till July 2014 or the patient's death. Clinical outcomes were assessed by reviewing the EMR. Radiological follow-up was made at the physician's decision to reevaluate underlying cancer.

Outcomes

The primary outcome of this study was clinical success, which was defined as the reported resolution or improvement of symptoms related to the iliocaval venous obstruction after the interventional procedure. We also reviewed technical success, change of cross-sectional area of mid-thigh, and reocclusion rate. Technical success was defined as successful recanalization of the target lesion and restoration of venous return at the end of the interventional procedure. For more objective response evaluation, pre- and post-procedural cross-sectional areas of ipsilateral mid-thigh (for unilateral iliac vein occlusion) or sum of bilateral mid-thigh (for IVC or both iliac vein occlusion) were measured in cases where both pre- and post-procedural CT scans within 1 month after the procedure covering mid-thigh are available. Occurrence of reocclusion was evaluated by reviewing available follow-up CT scans.

In accordance with the Society of Interventional Radiology Standards of Practice Committee Classification of Complications by Outcome [22], minor and major complications related to the interventional procedure were reviewed retrospectively.

Statistical Analysis

We evaluated patient-based reocclusion rate (number of patients who experienced reocclusion of any stented vessels/number of total patients enrolled) and vessel-based reocclusion rates (number of stented vessels that were reoccluded during follow-up/number of all the stented vessels in the cohort). The difference between IVC and iliac stent reocclusion rates was analyzed by using Fisher's exact test. Pre- and post-procedural mid-thigh areas were compared using a Wilcoxon signed-rank test. Data are presented as the mean ± standard deviation or as the median (range) for continuous variables and proportions (%) for categorical variables. A two-sided significance level of 0.05 was used to evaluate statistical significance. A statistical software package (SPSS Statistics version 20.0.0.2 for Windows, IBM Corp., Armonk, NY, USA) was used for data analysis.

Results

The patients consisted of 18 men and 16 women. Median age was 62.5 years (range, 36 to 89 years). The iliocaval venous obstructions were sequelae of the following cancers: colorectal (n = 9); ureter and bladder transitional cell carcinoma (n = 6); cervical (n = 5); prostate (n = 3); pancreatic cancer (n = 3); and one case each of vaginal, testicular, ovarian, breast, mixed Mullerian tumor, renal cell carcinoma, liposarcoma, and metastasis of unknown origin. Before the interventional treatments, the patients complained of edema occurring in both legs (n = 16), the right leg (n = 8), the left leg (n = 9), or truncal edema (n = 1). One patient with bilateral leg edema also complained of scrotal swelling. Twelve patients (35.3%) had deep vein thrombosis (DVT) associated with the venous obstruction, while 22 patients (64.7%) had symptomatic venous obstruction without thrombosis.

The median time interval between preprocedural CT scan and intervention was 3.5 days (range, 1 to 30 days). Aspiration thrombectomy was performed for all the patients who had DVT (n = 12) and more than 90% of thrombi were removed angiographically in all those patients. The degree of thrombus removal was determined by visual estimation and consensus of two interventional radiologists. Sites of stent deployment were: IVC alone (n = 9); unilateral (n = 14) or bilateral iliac veins (n = 5); and both IVC and iliac vein (n = 6). (Table 1).

During the follow-up period (median, 65 days; range, 1 to 3,650 days), 12 patients (35.3%) died, 21 patients (61.8%) were lost to follow-up, and one patient (2.9%) was alive. The technical success rate was 100% (34/34). Clinical information regarding symptom improvement after intervention was available in only 24 patients (70.6%), and the clinical success rate was 87.5% (21/24). There were no procedure-related complications.

Follow-up CT scans were available in 21 patients (61.8%), and the median time period of imaging follow-up was 65 days (range, 7 to 3,167 days). Both pre- and post-procedural CT scans (within 1 month after the procedure) covering the mid-thigh were available in only 16 patients. Fourteen patients had decreased cross-sectional area of the mid-thigh level and the other two patients did not show a decrease. Mean percent change of the area ([pre-procedural area – post-procedural area]/pre-procedural area) was 11.7% (median, 10.4; Q1–Q3, 5.6 to 17.3; IQR, 11.7; p = 0.003).

Patient-based reocclusion rate was 42.8% (9/21) during the follow-up period. The overall vessel-based reocclusion rate was 35.7% (10/28), where the reocclusion rate of IVC stents was 12.5% (1/8) and that of iliac vein stents was 45% (9/20) (Table 2). The reocclusion rate of IVC stents tended to be lower than that of iliac vein stents, though the result was not statistically significant (p = 0.194) (Figs. 1, 2). Six patients required reintervention (additional stent placement in five patients, sole balloon angioplasty in one patient) and secondary patency was achieved in all cases.

Table 1. Basic characteristics

Characteristic	Value
Age (years)	62.5 (36–89)
Sex	
Male	18 (52.9)
Female	16 (47.1)
Etiology	
Colorectal cancer	9 (26.5)
Transitional cell carcinoma	6 (17.6)
Cervical cancer	5 (14.7)
Prostate cancer	3 (8.8)
Pancreatic cancer	3 (8.8)
Others	8 (23.5)
Cause of obstruction	
Extrinsic compression	12 (35.3)
Invasion	22 (64.7)
Sites of stent	
IVC	9 (26.5)
Iliac veins	19 (55.9)
IVC + iliac veins	6 (17.6)

Values are presented as median (range) or number (%).

Table 2. Reocclusion rates

Site of stents	Reocclusion rate
Patient-based	
Total	42.8 (9/21)
IVC	20.0 (1/5)
Bilateral iliac veins	66.7 (2/3)
Unilateral iliac veins	60.0 (6/10)
IVC + iliac veins	0 (0/3)
Vessel-based	
IVC	12.5 (1/8)
Iliac veins	45.0 (9/20)

Values are presented as % (n/N).

Discussion

Malignancy-related iliocaval venous obstructions have been frequently treated with stenting, yet there is a lack of research regarding the clinical efficacy of stent placement when compared with SVCS. Our study demonstrated a 100% technical success rate and an 87.5% clinical success rate. These results are comparable with previous case studies of stenting for malignant iliocaval obstruction, which reported 94%–100% and 77%–95% technical and clinical success rates, respectively [19,20,23-25].

Clinical success, which was defined as the improvement of symptoms, was not graded nor scored, and was only determined by the physicians' report recorded in EMR. To present more objective results, cross-sectional areas of the mid-thigh were measured on pre- and post-procedural CT scans. Although the cross-sectional areas significantly decreased on post-procedural CT scans compared to those of pre-procedural CT scans, this data was derived from only 47.1% (16/34)

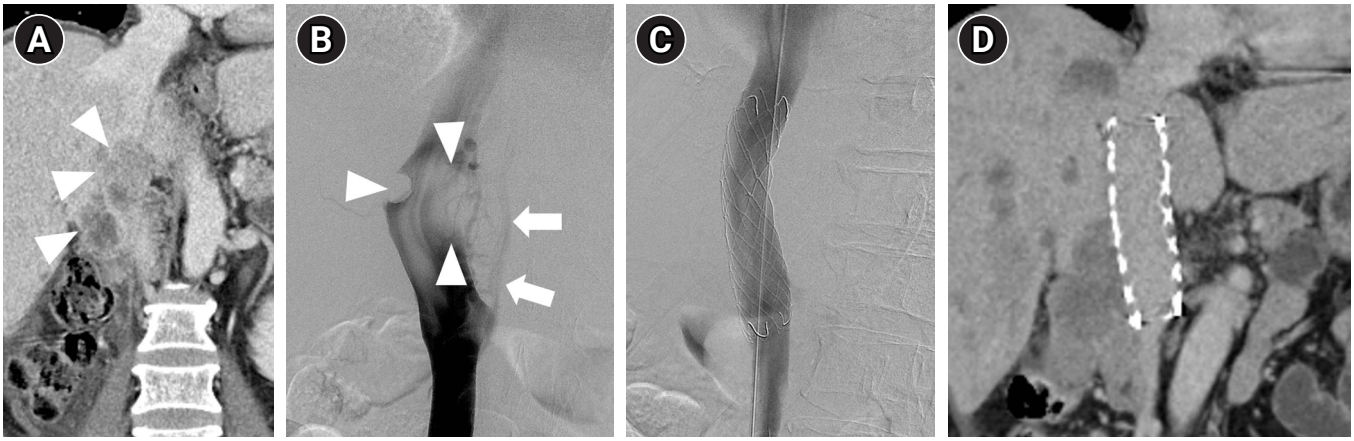


Fig. 1. A 68-year-old man with a history of right nephrectomy due to renal cell carcinoma presented with bilateral leg swelling. (A) CT scan shows a recurrent mass compressing the IVC (arrowheads). (B) Vena cavogram shows filling defects (arrowheads) at the same level. Note the collateral veins (arrows), suggesting IVC stenosis. (C) Vena cavogram shows disappearance of collateral veins, implying decreased pressure gradient, after the deployment of a 24 mm × 10 cm self-expandable stent (Hercules, S&G Biotech). (D) Follow-up CT scan (3 months after intervention) shows a widely patent IVC stent.

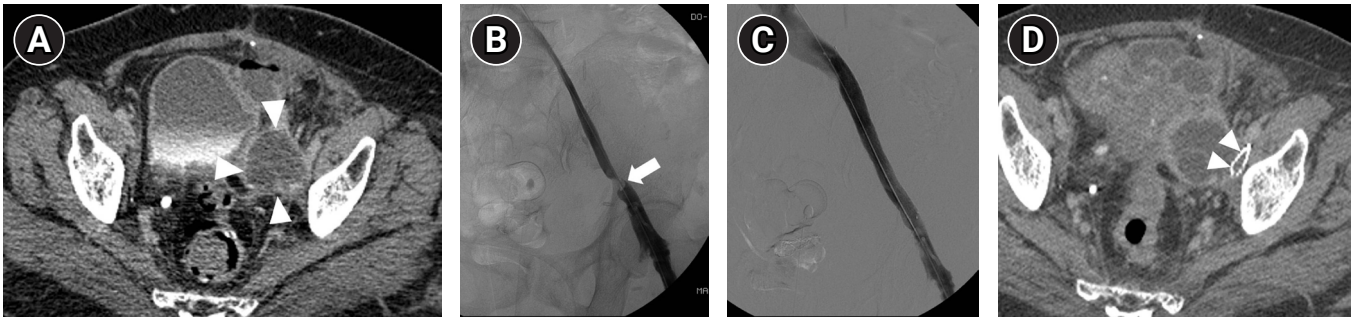


Fig. 2. A 72-year-old woman with a mixed Mullerian tumor complained of left leg swelling. (A) CT scan shows a metastatic lymph node at the left iliac chain (arrowheads). (B) Venography after aspiration thrombectomy shows extrinsic compression (arrow) of the left external iliac vein by the lymph node. (C) After a 14 mm × 10 cm self-expandable stent (E-Luminexx, Bard) was deployed, the venous flow was restored immediately and the edema improved gradually. (D) One month later, the patient complained of recurrent leg swelling. Follow-up CT scan shows a collapsed stent (arrowheads), and recurrent deep vein thrombosis.

of patients. Hence, this result should be considered only as supplementary data.

Reocclusion of the venous stents was not uncommon, and the reocclusion rate was over 40% during the 2-month median follow-up period. At first glance, this reocclusion rate seems to be higher than those of SVC stents, which have reported primary patency from 64% to 92% [23-25]. However, reocclusion of IVC stents occurred in only one patient out of eight in our study, and this rate is comparable with the reported primary patency rates of SVC stents. The previous studies dealing with iliocaval stenting also reported 36.8% of symptom recurrence [19] and 68.8% of primary patency [20], which are similar to the results of our study.

The reocclusion rate of iliac vein stents, though statistically not significant, tended to be higher than that of IVC stents (45% vs. 12.5%, p = 0.194). The low patency rate of iliac vein stents may be explained by the differences in stent diameters. The diameters of IVC stents (range, 20 to 28 mm) were much larger than those of iliac vein stents (range, 10 to 14 mm). Reocclusions are generally amenable to secondary intervention, and the literature reports secondary patency rates ranging from 93%–100% [20,23-25]. Out of nine patients who experienced reocclusion, only 6 patients received reintervention. The remaining three were in poor general condition and did not want to receive further aggressive treatment.

The present study examined both the efficacy and patency of iliocaval stents, but there were many limitations. This was a retrospective study and included a relatively small number of

patients. Because the types of malignancies causing the venous obstructions were so variable, and due to the small number of patients in the study, we could not evaluate the clinical treatment efficacy and stent patency based on cancer type. We experienced a shortage of follow-up data. The majority of enrolled patients were in advanced or terminal stages of cancer and many patients died within a few days of treatment or were transferred to hospice centers or nursing homes and subsequently lost to follow-up. Therefore, we could evaluate clinical improvement of symptoms in only 70.6% (24/34) of the patients, and follow-up CT scans were only available for 61.8% (21/34). Therefore, we cannot insist on the clinical success of our study as a concrete conclusion, because selection bias may have been introduced. Patients who were unavailable for follow-up, including those who died shortly after the procedure or were transferred to hospice care, may have had poorer clinical outcomes. Therefore, the reported clinical success rate may have been overestimated. For the purpose of showing the outcome as objectively as possible, we calculated the change in cross-sectional area of the mid-thigh. But this information was also available in only 16 patients, and the interval between procedure and area measurement varied extremely (29–395 days). The follow-up period, defined as the hospitalization period in this facility, was relatively short and variable because most patients had terminal illnesses and were lost to follow-up after being sent to nursing care facilities. The follow-up CT scans tended to be performed more frequently in patients with persistent or recurrent symptoms, and this may have contributed to an increased reocclusion rate. Another limitation is that the small sample size precluded an adequate statistical analysis to identify factors affecting stent patency.

In conclusion, endovascular stent deployment can be an effective treatment option for malignant iliocaval venous obstruction. This is particularly true in cases of IVC obstruction, where IVC stent placement demonstrates higher patency rates. Although there is a fairly high possibility of reocclusion, especially with iliac vein stent placement, the use of aggressive interventions, including stent deployment, can lead to relief of symptoms for patients suffering from malignant iliocaval venous obstruction. More studies are needed to confirm our results and assess long-term patency.

Conflict of interest

No potential conflict of interest relevant to this article was reported.

Funding

None.

Acknowledgments

None.

Author contributions

Conceptualization: GMK, WS. Data curation: GMK, WS. Formal analysis: WS. Investigation: GMK, KH, MDK, JHK, JYW, JP. Methodology: GMK. Validation: KH, MDK, JHK. Writing - original draft: WS, GMK. Writing - review & editing: KH, JP.

Data availability statement

Data are available upon reasonable request from the corresponding author, subject to ethical and privacy limits.

ORCID

Wonseon Shin, https://orcid.org/0000-0001-5603-737X
Gyoung Min Kim, https://orcid.org/0000-0001-6768-4396
Kichang Han, https://orcid.org/0000-0002-9701-9757
Man Deuk Kim, https://orcid.org/0000-0002-3575-5847
Joon Ho Kwon, https://orcid.org/0000-0002-6178-7252
Jong Yun Won, https://orcid.org/0000-0002-8237-5628
Juil Park, https://orcid.org/0000-0002-5265-8723

References

1. AbuRahma AF, Perkins SE, Wulu JT, Ng HK. Iliofemoral deep vein thrombosis: conventional therapy versus lysis and percutaneous transluminal angioplasty and stenting. Ann Surg. 2001;233:752-760. https://doi.org/10.1097/00000658-200106000-00004
2. Titus JM, Moise MA, Bena J, Lyden SP, Clair DG. Iliofemoral stenting for venous occlusive disease. J Vasc Surg. 2011;53:706-712. https://doi.org/10.1016/j.jvs.2010.09.011
3. Horsted F, West J, Grainge MJ. Risk of venous thromboembolism in patients with cancer: a systematic review and meta-analysis. PLoS Med. 2012;9:e1001275. https://doi.org/10.1371/journal.pmed.1001275

4. Barnes RW, Collicott PE, Sumner DS, Strandness DE Jr. Noninvasive quantitation of venous hemodynamics in the postphlebitic syndrome. Arch Surg. 1973;107:807-814. https://doi.org/10.1001/archsurg.1973.01350230159029
5. Johnson BF, Manzo RA, Bergelin RO, Strandness DE Jr. Relationship between changes in the deep venous system and the development of the postthrombotic syndrome after an acute episode of lower limb deep vein thrombosis: a one- to six-year follow-up. J Vasc Surg. 1995;21:307-312. https://doi.org/10.1016/s0741-5214(95)70271-7
6. Markel A, Manzo RA, Bergelin RO, Strandness DE Jr. Valvular reflux after deep vein thrombosis: incidence and time of occurrence. J Vasc Surg. 1992;15:377-382. https://doi.org/10.1016/0741-5214(92)90259-B
7. Meissner MH, Moneta G, Burnand K, Gloviczki P, Lohr JM, Lurie F, et al. The hemodynamics and diagnosis of venous disease. J Vasc Surg. 2007;46 Suppl S:4S-24S. https://doi.org/10.1016/j.jvs.2007.09.043
8. Sorensen HT, Mellemkjaer L, Olsen JH, Baron JA. Prognosis of cancers associated with venous thromboembolism. N Engl J Med. 2000;343:1846-1850. https://doi.org/10.1056/NEJM200012213432504
9. Straka C, Ying J, Kong FM, Willey CD, Kaminski J, Kim DW. Review of evolving etiologies, implications and treatment strategies for the superior vena cava syndrome. Springerplus. 2016;5:229. https://doi.org/10.1186/s40064-016-1900-7
10. Rachapalli V, Boucher LM. Superior vena cava syndrome: role of the interventionalist. Can Assoc Radiol J. 2014;65:168-176. https://doi.org/10.1016/j.carj.2012.09.003
11. Nazarian GK, Austin WR, Wegryn SA, Bjarnason H, Stackhouse DJ, Castaneda-Zuniga WR, et al. Venous recanalization by metallic stents after failure of balloon angioplasty or surgery: four-year experience. Cardiovasc Intervent Radiol. 1996;19:227-233. https://doi.org/10.1007/BF02577640
12. Xiao L, Tong JJ, Shen J. Endoluminal treatment for venous vascular complications of malignant tumors. Exp Ther Med. 2012;4:323-328. https://doi.org/10.3892/etm.2012.589
13. Kuetting D, Thomas D, Wilhelm K, Pieper CC, Schild HH, Meyer C. Endovascular management of malignant inferior vena cava syndromes. Cardiovasc Intervent Radiol. 2017;40:1873-1881. https://doi.org/10.1007/s00270-017-1740-z
14. Brountzos EN, Binkert CA, Panagiotou IE, Petersen BD, Timmermans H, Lakin PC. Clinical outcome after intrahepatic venous stent placement for malignant inferior vena cava syndrome. Cardiovasc Intervent Radiol. 2004;27:129-136. https://doi.org/10.1007/s00270-003-0009-x
15. Devcic Z, Techasith T, Banerjee A, Rosenberg JK, Sze DY. Technical and anatomic factors influencing the success of inferior vena caval stent placement for malignant obstruction. J Vasc Interv Radiol. 2016;27:1350-1360. https://doi.org/10.1016/j.jvir.2016.02.030
16. Fletcher WS, Lakin PC, Pommier RF, Wilmarth T. Results of treatment of inferior vena cava syndrome with expandable metallic stents. Arch Surg. 1998;133:935-938. https://doi.org/10.1001/archsurg.133.9.935
17. Kishi K, Sonomura T, Fujimoto H, Kimura M, Yamada K, Sato M, et al. Physiologic effect of stent therapy for inferior vena cava obstruction due to malignant liver tumor. Cardiovasc Intervent Radiol. 2006;29:75-83. https://doi.org/10.1007/s00270-004-0324-x
18. Laing AD, Thomson KR, Vrazas JI. Stenting in malignant and benign vena caval obstruction. Australas Radiol. 1998;42:313-317. https://doi.org/10.1111/j.1440-1673.1998.tb00529.x
19. Maleux G, Vertenten B, Laenen A, De Wever L, Heye S, Clement P, et al. Palliative endovascular treatment of cancer-related iliocaval obstructive disease: technical and clinical outcomes. Acta Radiol. 2016;57:451-456. https://doi.org/10.1177/0284185115582059
20. Rabellino M, Moltini P, Di Caro V, Garcia-Monaco R. Symptomatic iliofemoral and iliocaval venous thrombosis in patients with cancer: endovascular treatment. Vasc Endovascular Surg. 2018;52:602-606. https://doi.org/10.1177/1538574418789018
21. Park SI, Lee M, Lee MS, Kim MD, Won JY, Lee DY. Single-session aspiration thrombectomy of lower extremity deep vein thrombosis using large-size catheter without pharmacologic thrombolysis. Cardiovasc Intervent Radiol. 2014;37:412-419. https://doi.org/10.1007/s00270-013-0676-1
22. Omary RA, Bettmann MA, Cardella JF, Bakal CW, Schwartzberg MS, Sacks D, et al. Quality improvement guidelines for the reporting and archiving of interventional radiology procedures. J Vasc Interv Radiol. 2003;14:S293-S295. https://doi.org/10.1097/01.rvi.0000094601.83406.e1

23. Fagedet D, Thony F, Timsit JF, Rodiere M, Monnin-Bares V, Ferretti GR, et al. Endovascular treatment of malignant superior vena cava syndrome: results and predictive factors of clinical efficacy. Cardiovasc Intervent Radiol. 2013;36:140-149. https://doi.org/10.1007/s00270-011-0310-z
24. Nagata T, Makutani S, Uchida H, Kichikawa K, Maeda M, Yoshioka T, et al. Follow-up results of 71 patients undergoing metallic stent placement for the treatment of a malignant obstruction of the superior vena cava. Cardiovasc Intervent Radiol. 2007;30:959-967. https://doi.org/10.1007/s00270-007-9088-4
25. Lanciego C, Pangua C, Chacon JI, Velasco J, Boy RC, Viana A, et al. Endovascular stenting as the first step in the overall management of malignant superior vena cava syndrome. AJR Am J Roentgenol. 2009;193:549-558. https://doi.org/10.2214/AJR.08.1904

Letter-to-Editor

eISSN 2508-2612
https://doi.org/10.64961/kjir.2026.00213
Korean J Interv Radiol 2026;31(2):164-166

KJIR
Korean Journal of
Interventional Radiology

Risk-Adapted Central Venous Catheter Securement: Which Strategy, for Which Catheter, in Which Patient?

Jeong Ho Kim*

Department of Radiology, Gachon University College of Medicine, Incheon, Republic of Korea

We read with great interest the article by Hong et al., "Securement of Central Venous Catheters: Suture Fixation vs. Stabilization Devices in a Multicenter Retrospective Study [1]." The authors should be commended for addressing an important but often overlooked component of central venous catheter (CVC) management. Their study demonstrates an intriguing clinical trade-off: adhesive-pad stabilization devices (SDs) were associated with a higher risk of catheter dislocation than suture fixation (SF), whereas several analyses suggested a potentially lower risk of central line–associated bloodstream infection (CLABSI) with SDs. Beyond the direct comparison of these two techniques, their findings raise a broader and perhaps more clinically relevant question: Should CVC securement be selected according to the individual mechanical and infectious risks of each patient?

CVC securement is sometimes regarded as a minor technical step after successful catheter insertion. However, securement must fulfill two potentially competing objectives: maintaining sufficient mechanical stability to prevent catheter migration or accidental removal while minimizing skin injury and potential routes for microbial colonization. Hong et al. [1] demonstrate this tension particularly well. After propensity-score matching, dislocation occurred more frequently with SDs than with SF, and SD use remained independently associated with dislocation in multivariable analysis (adjusted HR, 2.23; 95% CI, 1.11 to 4.48) [1]. Conversely, CLABSI occurred less frequently in the SD group in incidence-rate and Kaplan-Meier analyses, although the association did not remain statistically significant in the primary multivariable Cox model (adjusted HR, 0.49; 95% CI, 0.13 to 1.82) [1].

These findings suggest that the clinically relevant question may not be whether one securement method is universally superior to another. Rather, the probability and clinical consequences of each complication should be considered for an individual patient. Catheter dislocation may often be managed by reinsertion, but the consequences of catheter loss vary substantially. Accidental removal may be particularly consequential in patients with limited venous access, those receiving continuous vasoactive or other critical infusions, or those in whom repeat catheterization is expected to be technically difficult or hazardous. In such circumstances, maximizing mechanical security may reasonably take priority.

Conversely, the balance may shift in patients expected to require prolonged catheterization or those at particularly high risk for infection. Sutures create additional breaches of the skin barrier adjacent to the catheter exit site and introduce foreign material that may facilitate microbial colonization. Current infusion therapy standards recommend consideration of alternatives to sutures as part of contemporary vascular access management [2]. Although the present study cannot establish a causal protective effect of SDs against CLABSI, the observed signal deserves attention because bloodstream infection can have substantially greater clinical consequences than uncomplicated catheter replacement.

Importantly, however, "sutureless securement" should not

Received: August 19, 2026; **Accepted:** August 25, 2026
***Corresponding email:** ho7ok7@gachon.ac.kr

© 2026 Korean Society of Interventional Radiology

This is an Open Access article distributed under the terms of the Creative Commons Attribution Non-Commercial License (http://creativecommons.org/licenses/by-nc/4.0) which permits unrestricted non-commercial use, distribution, and reproduction in any medium, provided the original work is properly cited.

be considered a single intervention. A recent systematic review and meta-analysis including 46 studies and 10,054 participants demonstrated substantial heterogeneity among catheter types, patient populations, dressings, and securement technologies and emphasized the limited certainty of evidence for several outcomes [3]. A recent prospective cohort study comparing an integrated securement device with sutures for centrally inserted CVCs found no significant difference in complete or partial catheter dislodgement, while the integrated device improved patient comfort and prolonged maintenance intervals [4]. These findings differ somewhat from those of Hong et al. [1] and reinforce the concept that results obtained with one securement technology should not automatically be generalized to all sutureless devices.

Therefore, CVC securement might be better conceptualized as a risk-adapted strategy rather than a binary choice between sutures and SDs. The optimal strategy should consider not only the fixation device but also catheter type, number of lumens, access site, anticipated dwell time, patient mobility or agitation, skin condition, availability of alternative venous access, type of infusion, and the clinical consequences of catheter loss. Nursing factors—including dressing technique, frequency of dressing changes, catheter surveillance, and familiarity with a particular securement system—are also likely to influence outcomes.

The present study itself provides support for such a multidimensional approach. Triple-lumen catheter use was independently associated with CLABSI (adjusted HR, 2.93) [1], consistent with previous evidence linking multilumen catheters with increased bloodstream infection risk [5]. Thus, infection risk cannot be attributed to securement technique alone. Similarly, the mechanical risk of dislocation is likely influenced by patient movement, catheter location, external catheter length, dressing integrity, and local catheter-care practices.

From a practical standpoint, securement could therefore be considered along two principal dimensions: the risk and consequence of catheter dislocation and the risk and consequence of catheter-related infection. A patient with difficult venous access receiving an indispensable continuous infusion may warrant a strategy prioritizing mechanical stability. In contrast, a patient requiring prolonged catheterization who has a high infectious risk and readily available alternative venous access may favor a strategy minimizing skin penetration. Between these extremes, combinations of contemporary technologies—including adhesive-pad devices, integrated securement dressings, tissue adhesives, or subcutaneous anchor systems—may eventually allow securement to be tailored more precisely to individual clinical circumstances.

This interpretation also highlights an important limitation of the study by Hong et al. [1]. SDs were used at one institution, whereas SF was used at the other two institutions [1]. Consequently, securement technique was closely linked to institutional practice. The substantial differences in ICU admission, clinical indication, access site, and catheter dwell time between the original groups suggest important differences in patient populations and catheter-management patterns. Although propensity-score matching and multiple sensitivity analyses strengthen the study, unmeasured differences in nursing care, dressing protocols, patient mobilization, catheter surveillance, and thresholds for catheter replacement cannot be completely separated from the effect of securement technique.

Of particular methodological interest, the analyses described as evaluating institution-level clustering used matched subclass as the random effect or clustering variable rather than institution itself [1]. These analyses appropriately address dependence related to propensity-score matching but do not directly disentangle the effect of institution from that of securement method. Indeed, because securement method was essentially determined by institution, the two effects are intrinsically difficult to separate in the present study design. This limitation does not invalidate the observed association but suggests that the effect estimates should be interpreted as hypothesis-generating rather than strictly causal.

Future studies should therefore move beyond a simple comparison of SF and SD. A prospective multicenter study in which different securement methods are used within each participating institution would reduce institutional confounding. Ideally, randomization should occur at the patient level, with prespecified stratification according to access site, catheter type, number of lumens, and anticipated dwell time. In addition to dislocation and bloodstream infection, patient comfort, skin injury, nursing workload, cost, need for catheter replacement, and consequences of catheter failure should be considered. Such studies could ultimately identify predictors

of mechanical and infectious complications and form the basis of a clinically useful securement algorithm.

Hong et al. [1] have made an important contribution by demonstrating that catheter securement is not merely a procedural detail. Their findings reveal a clinically meaningful tension between mechanical stability and potential infection prevention and provide an opportunity to reconsider how CVC securement is selected. Rather than seeking a universally superior device, the next step should be to identify the optimal strategy for an individual clinical situation.

Thus, rather than asking simply "to tie or not to tie," perhaps the more useful question is: Which securement strategy, for which catheter, in which patient? Answering this question may help transform CVC securement from a matter of institutional preference into an individualized component of vascular access management.

Conflict of interest

No potential conflict of interest relevant to this article was reported.

Funding

None.

Acknowledgments

None.

ORCID

Jeong Ho Kim, https://orcid.org/0000-0002-1404-2821

References

1. Hong JU, Kwon Y, Shim DJ, Lee JH. Securement of central venous catheters: suture fixation vs. stabilization devices in a multicenter retrospective study. Korean J Interv Radiol. 2026;31:145-155. https://doi.org/10.64961/kjir.2026.00123
2. Nickel B, Gorski L, Kleidon T, Kyes A, DeVries M, Keogh S, et al. Infusion therapy standards of practice, 9th edition. J Infus Nurs. 2024;47(1S):S1-S285. https://doi.org/10.1097/NAN.0000000000000532
3. Xu H, Hyun A, Mihala G, Rickard CM, Cooke ML, Lin F, et al. The effectiveness of dressings and securement devices to prevent central venous catheter-associated complications: a systematic review and meta-analysis. Int J Nurs Stud. 2024;149:104620. https://doi.org/10.1016/j.ijnurstu.2023.104620
4. Chen Y, Chen X, Jin X, Zeng X, Cao X, Zhao L. Compare the safety and efficacy of integrated securement device versus suture securement for centrally inserted central venous catheters: a prospective cohort study. Sci Rep. 2025;15:34907. https://doi.org/10.1038/s41598-025-18777-2
5. Templeton A, Schlegel M, Fleisch F, Rettenmund G, Schobi B, Henz S, et al. Multilumen central venous catheters increase risk for catheter-related bloodstream infection: prospective surveillance study. Infection. 2008;36:322-327. https://doi.org/10.1007/s15010-008-7314-x

How I do It

eISSN 2508-2612
https://doi.org/10.64961/kjir.2026.00136
Korean J Interv Radiol 2026;31(2):167-170

KJIR
Korean Journal of
Interventional Radiology

Single-Incision Technique for Placement of Totally Implantable Venous Access Port via the Axillary Vein

Woo Jin Yang[1], **Myung Gyu Song**[2,*], **Tae-Seok Seo**[2]

[1]Department of Radiology, Samsung Medical Center, Sungkyunkwan University School of Medicine, Seoul, Republic of Korea
[2]Department of Radiology, Korea University Guro Hospital, Korea University College of Medicine, Seoul, Republic of Korea

Introduction

Totally implantable venous access ports (TIVAPs) have been widely used to provide long-term central venous access in patients with malignancy [1]. Radiologically guided TIVAP placement has traditionally required two separate incisions: one for percutaneous puncture of the internal jugular vein (IJV), and another for creation of a subcutaneous pocket on the anterior chest wall, with a subcutaneous tunnel connecting the two. Although this conventional approach has been widely accepted, potential drawbacks include pain at the tunneling site, ecchymosis of the skin overlying the tunnel, discomfort with neck movement, and palpation of the catheter over the clavicle [1]. In 2014, the authors introduced a single-incision technique for TIVAP placement via the axillary vein, in which the venipuncture and pocket creation are performed through a single short incision in the infraclavicular area, without a subcutaneous tunnel [1]. Since then, this technique has been used as the default approach at the authors' institution, and TIVAPs have been implanted via the axillary vein in more than 10,000 patients. Whereas the original report described the initial experience in 216 patients [1], this article describes the technique as currently performed, including catheter selection, breast fixation in women, management of technical difficulties, and long-term outcomes.

Received: June 19, 2026; **Revised:** September 15, 2026
Accepted: September 15, 2026
***Corresponding email:** acube808@naver.com

© 2026 Korean Society of Interventional Radiology

This is an Open Access article distributed under the terms of the Creative Commons Attribution Non-Commercial License (http://creativecommons.org/licenses/by-nc/4.0) which permits unrestricted non-commercial use, distribution, and reproduction in any medium, provided the original work is properly cited.

Indications and Pre-procedural Planning

TIVAPs are indicated for long-term venous access, usually for chemotherapy in patients with malignancy, and less often for parenteral nutrition or repeated transfusion. Pre-procedural evaluation includes ultrasound of both axillary veins to assess depth, caliber, and patency at the planned puncture site and to identify anatomic variants or adjacent masses, and review of chest CT, when available, for pre-existing stenosis or thrombosis of the brachiocephalic vein and SVC. In patients with breast cancer, the contralateral side is selected.

Access Strategies

In interventional radiology practice, IJV access is generally preferred for TIVAP placement, and subclavian puncture is largely avoided because of the well-recognized risk of pinch-off syndrome. The IJV approach itself, however, requires a subcutaneous tunnel, and the catheter length is fixed before the tip position is confirmed.

The single-incision technique avoids these requirements by puncturing the axillary vein at the cephalic end of the same incision used for the port pocket [1]. Because the axillary vein is punctured lateral to the first rib, the catheter is already located inside the vessel when it passes between the first rib and the clavicle, eliminating the risk of pinch-off syndrome. The need for a subcutaneous tunnel and a separate neck incision is removed, and the catheter length is fixed only after the tip position is confirmed under fluoroscopy.

The axillary approach is also useful when neck tumor, previous lymph node dissection, or radiation therapy makes IJV access unfavorable.

Technical Procedures (Video 1)

All procedures are performed in an interventional radiology suite under fluoroscopic guidance with bedside ultrasound. The default device is a 6.5-Fr Celsite Discreet port (B. Braun Medical, Boulogne, France), because in an analysis of 209 women with left IJV TIVAPs, an 8-Fr catheter carried a substantially higher cumulative incidence of left innominate vein stenosis than a 6.5-Fr catheter (HR, 20.766; p = 0.005) [2].

The incision line is planned 3 to 4 cm lateral to the junction of the axillary vein and the clavicle, with a length of approximately 2 cm in an oblique vertical orientation. Following sterile preparation and local anesthesia, an oblique vertical skin incision is made. The axillary vein is then punctured under real-time ultrasound guidance at the cephalic end of the incision using a 21-gauge micropuncture needle, with the needle directed medially toward the first rib. A 0.018-inch microwire is advanced through the needle and into the SVC under fluoroscopic guidance, and a microintroducer is then inserted over the microwire [1].

With the microintroducer left in place, the port pocket is created on the medial side of the incision by blunt dissection of the subcutaneous tissue, and gauze packing is applied to the pocket for hemostasis. A 0.035-inch spring guidewire is then advanced into the SVC through the microintroducer, and the microintroducer is exchanged for a peel-away sheath over the guidewire. The catheter is advanced through the peel-away sheath, and the tip is positioned between the upper third of the right atrium and the lower portion of the SVC under fluoroscopic monitoring. The peel-away sheath is removed, the catheter is connected to the port chamber, and the chamber is then placed within the pocket. The incision is closed in layers. Final fluoroscopic and chest radiographic confirmation of catheter tip position is obtained. In female patients, particularly those with pendulous breasts, the catheter tip migrates with positional change between supine and upright postures, which may cause the tip to project against the wall of the SVC. A tip projecting against the SVC wall has been implicated in fibrin sheath and thrombus formation [3], although the effect of breast fixation on these complications has not been evaluated. To reduce this positional migration, the ipsilateral breast is fixed to the abdominal wall with an adhesive nonwoven fabric while the patient is in the sitting position before draping (Fig. 1). In an analysis of 118 women un-

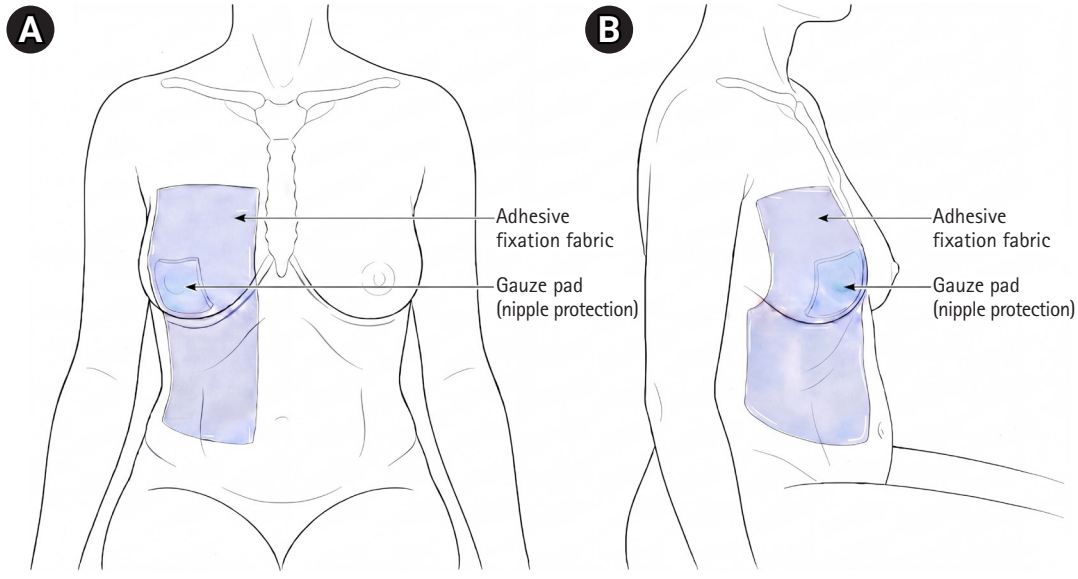


Fig. 1. Ipsilateral breast fixation to reduce catheter tip migration after totally implantable venous access port placement in women with large pendulous breasts. (A) Frontal view showing the adhesive nonwoven fabric sheet applied from the inferior breast onto the upper abdominal wall, spanning the inframammary fold. (B) Lateral view demonstrating the breast held inferiorly against the abdominal wall by the fixation fabric. Fixation is performed in the sitting position to maximize gravitational descent of the breast tissue before adhesion. Gauze padding is placed over the nipple to reduce skin discomfort under the adhesive.

dergoing right axillary TIVAP placement, breast fixation was associated with significantly smaller changes in the distance ratio between the port chamber and the catheter tip on supine and erect chest radiographs [3].

Technical Difficulties and Troubleshooting

Most technical difficulties are resolved with additional manipulation rather than a change of access route. When the axillary vein is small or collapses with respiration, a gentle end-expiratory breath-hold facilitates ultrasound-guided venipuncture. A wire or catheter that enters an unintended vein is redirected under fluoroscopic guidance. Catheter kinking at the cuff-catheter junction is corrected by dissecting the tissue between the puncture tract and the port pocket. Bending of the peel-away sheath, recognized as resistance to catheter passage, is overcome by withdrawing the sheath while advancing the catheter. If the axillary artery is punctured, the needle is removed, manual compression is applied, and the vein is repunctured under ultrasound guidance, or under venographic guidance if a hematoma has collapsed the vein. If access still cannot be obtained, the procedure is converted to either the IJV or the contralateral axillary vein, depending on tumor location and previous surgery or radiation therapy.

Clinical Outcomes

In the authors' initial series of 216 patients, technical success was achieved in all cases. Immediate complications were limited to puncture-site hematoma in two patients (0.9%) [1]. In a long-term analysis of 932 placements over 311,069 catheter days, no catheter fracture from pinch-off syndrome, catheter disconnection, or device inversion was identified [4].

In a cohort of 4,773 patients, symptomatic axillary vein thrombosis developed in 18 patients (0.38%) at a median of 35.5 days after implantation, with pancreatic and lung cancer as independent risk factors [5].

Conclusion

In the authors' practice, single-incision TIVAP placement via the axillary vein has become the default approach. It avoids the drawbacks of subcutaneous tunneling, eliminates the risk of pinch-off syndrome, and has shown high technical success with a low rate of long-term complications, supporting it as a feasible alternative to the conventional two-incision technique.

Conflict of interest

No potential conflict of interest relevant to this article was reported.

Funding

None.

Acknowledgments

None.

Author contributions

Conceptualization: TSS, MGS. Data curation: WJY, MGS. Formal analysis: MGS, TSS. Investigation: MGS, TSS, WJY. Methodology: TSS, MGS, WJY. Project administration: MGS. Resources: MGS, TSS. Supervision: TSS, MGS. Validation: MGS, TSS. Visualization: WJY. Writing - original draft: WJY. Writing - review & editing: WJY, MGS, TSS.

Data availability statement

Data sharing does not apply to this article as no datasets were generated or analyzed during the current study.

Supplementary material

The supplementary data are available with this article at https://doi.org/10.64961/kjir.2026.00136.

ORCID

Woo Jin Yang, https://orcid.org/0000-0003-2392-2174
Myung Gyu Song, https://orcid.org/0000-0002-9861-2886
Tae-Seok Seo, https://orcid.org/0000-0002-4427-0198

References

1. Seo TS, Song MG, Kang EY, Lee CH, Yong HS, Doo K. A single-incision technique for placement of implantable venous access ports via the axillary vein. J Vasc Interv Radiol. 2014;25:1439-1446. https://doi.org/10.1016/j.jvir.2013.12.571
2. Song MG, Seo TS, Kim YH, Cho SB, Chung HH, Lee SH, et

al. Effect of catheter diameter on left innominate vein in breast cancer patients after totally implantable venous access port placement. J Vasc Access. 2018;19:615-619. https://doi.org/10.1177/1129729818765062

3. Song MG, Seo TS, Kim YH, Cho SB, Jung E, Chung HH, et al. Effectiveness of breast fixation to reduce migration of the tip of a totally implantable venous access port in women. J Vasc Access. 2016;17:348-352. https://doi.org/10.5301/jva.5000565
4. Seo TS, Song MG, Kim JS, Choi CW, Seo JH, Oh SC, et al. Long-term clinical outcomes of the single-incision technique for implantation of implantable venous access ports via the axillary vein. J Vasc Access. 2017;18:345-351. https://doi.org/10.5301/jva.5000751
5. Song MG, Seo TS, Yang WJ. Characteristics of symptomatic axillary vein thrombosis after placement of totally implanted venous access port in cancer patients. Iran J Radiol. 2020;17:e102754. https://doi.org/10.5812/iranjradiol.102754

Instructions for authors

KJIR
Korean Journal of
Interventional Radiology

These guidelines outline the requirements for submitting manuscripts to the *Korean Journal of Interventional Radiology* (*KJIR*). Authors should ensure their submissions meet the formatting standards, article type specifications, ethical requirements, and follow the proper submission process.

Table of Contents

Aims and scope
Manuscript Formatting Requirements
Article Types
Author Contributions
Submission Process
References

Aims and scope

Korean Journal of Interventional Radiology, the official English-language journal of the *Korean Society of Interventional Radiology* (*KSIR*), is an international peer-reviewed academic journal dedicated to interventional radiology. *KJIR* will publish cutting-edge and impactful scientific research articles in the field of interventional radiology.

KJIR will feature peer-reviewed original articles, authoritative reviews, systematic reviews and meta-analysis, case reports, and expert opinion on novel techniques and technologies.

Contact Information

KJIR Editorial Office
Room 1401, 42, Seocho-daero 78-gil, Seocho-gu, Seoul, Republic of Korea
Tel: 02-465-9070, Fax: 02-465-9072
E-mail: kjir@ksir.or.kr

Manuscript Formatting Requirements

- **File Format:** Manuscripts must be submitted as a Microsoft Word document (DOC or DOCX).
- **Page Layout:** Use A4 size paper (21.0 cm × 29.7 cm) with **at least 3 cm margins on all sides**.
- **Font and Spacing:** Use a clear, standard font (e.g., Times New Roman) at **11-point size**, and set line spacing to **double-spaced** throughout the document.
- **Page Numbering:** Number all pages consecutively, starting with the title page.
- **Language Policy:** Manuscripts must be written in **English using clear, concise, and professional language**. Authors should ensure proper grammar, spelling, and scientific terminology. The use of acronyms and abbreviations should be minimized. In general, all acronyms and abbreviations must be fully spelled out at their first appearance in the text, followed by the abbreviation in parentheses (e.g., computed tomography (CT)), after which the abbreviation may be used consistently. However, a predefined set of commonly accepted abbreviations may be used without expansion in the title, abstract, main text, tables, and figure legends. Definitions for these terms may be provided only when they appear in reference lists or in direct quotations. While adherence to this convention is not mandatory for peer review or acceptance, it will be applied by the editorial office during the production process of accepted manuscripts. Authors are encouraged to follow these conventions during manuscript preparation to enhance conciseness, particularly with respect to word limits in the abstract and main text. Radiation measurements and laboratory values should conform to the International System of Units (SI) to maintain consistency and standardization. Authors are encouraged to have their manuscripts professionally edited for language clarity before submission, if necessary. The names and locations (city and state/province or country) of the manufacturers of equipment and generic names should be given.

Reporting Standards

- Authors must follow the reporting guidelines relevant to their specific research design, and they are requested to state the guideline used for their study in their manuscript.

The checklists are available in the links provided below;

- Randomized trials – CONSORT Statement (https://www.equator-network.org/reporting-guidelines/consort)
- Observational studies – STROBE Statement (https://www.strobe-statement.org/)
- Systematic reviews and meta-analyses – PRISMA Statement (https://www.equator-network.org/reporting-guidelines/prisma)
- Diagnostic accuracy studies – STARD Statement (https://www.equator-network.org/reporting-guidelines/stard)
- Case reports – CARE Guidelines (https://www.equator-network.org/reporting-guidelines/care)

Article Types

Original Research

- **Scope:** Should present novel techniques, significant new data, or new insights in interventional radiology.
- **Structure:** IMRaD format: **Introduction, Materials and Methods, Results, and Discussion**.
- **Length:** Maximum **3,500 words** (excluding abstract, references, tables, and figure legends).
- **Abstract:** Up to **250 words**, structured (Purpose, Materials and Methods, Results, Conclusion).
- **References:** Up to **40 references**.
- **Tables/Figures:** Maximum **5 tables** and **7 figures**.

Review

- **Scope:** Provide a comprehensive analysis of a topic in interventional radiology.
- **Structure:** Flexible, but typically includes **Introduction, Subsections, and Conclusion**.
- **Length:** Maximum **4,000 words**.
- **Abstract:** Up to **250 words**, systematic review: structured (Background, Methods, Results, Conclusion), narrative review: unstructured typically one or two paragraphs.
- **References:** Up to **100 references**.
- **Tables/Figures:** Maximum **10 figures** and **5 tables**.

Case Report

- **Scope:** Describe unique cases, novel techniques, or rare complications.
- **Structure: Introduction, Case Report, Discussion**.
- **Length:** Maximum **2,500 words**.
- **Abstract:** Up to **125 words**, unstructured.
- **References:** Up to **15 references**.
- **Tables/Figures:** Maximum **3 tables** and **7 figures**.

Technical Note

- **Scope:** Focus on innovative techniques, new devices, or procedural modifications.
- **Structure: Introduction, Materials and Methods, Results, Discussion**.
- **Length:** Maximum **2,500 words**.
- **Abstract:** Up to **250 words**, structured.
- **References:** Up to **15 references**.
- **Tables/Figures:** Maximum **5 tables** and **7 figures**.

Editorial

- **Scope:** Commentary or perspective on interventional radiology topics.
- **Invitation:** Typically invited; unsolicited editorials should be pre-approved by the Editor-in-Chief.
- **Length: 1,000–1,500 words**.
- **References:** Minimal (typically 5–10 references).

Letter-to-Editor

- **Scope:** Commentary or perspective on a published article.
- **Structure:** non-structured. Do not require abstract.
- **Length: 1,000–1,500 words**.
- **Tables and figures:** Three tables or figures are allowed in total.
- **References:** Minimal (typically 5–10 references).

How I do It

- **Scope:** Technical issues on interventional radiology via short comments and video presentation.
- **Structure:** Flexible, both structured or non-structured forms are acceptable. Do not require abstract. It should include video materials including procedural process.
- **Invitation:** Typically invited
- **Length:** Maximum **1,200 words** in text and **6 minutes** in video.
- **References:** up to 5 references.

Author Contributions

All authors must disclose their specific contributions to the work in a designated Author Contributions section using the CRediT Taxonomy of author roles (https://credit.niso.org). For each of the categories below, please enter the initials of the authors who contributed in that category. If listing more than one author in a category, separate each set of initials with a comma. If no one contributed in a category, you may leave that box blank.Submission Process

Online Submission

- All manuscripts must be submitted through KJIR Submission Portal. (https://submit.kjironline.org/)
- First-time users must register; returning authors can log in.

Submission Steps

1. **Manuscript Information** – Enter title, authors, affiliations, and article type.
2. **Cover Letter** – Briefly introduce the submission, highlight significance, and confirm originality.
3. **File Upload** – Upload the manuscript, figures, tables, and supplementary materials as required.
4. **Conflict of Interest and Copyright Forms** – All authors must complete and submit these forms.
5. **Review and Submit** – Ensure compliance with guidelines and finalize submission.

Full Title Page

- Include the following items on the unblinded full title page:
  - Title
  - Abbreviated title
  - Names, affiliations, and addresses of the corresponding author
  - Contact information of the corresponding author
  - Type of manuscript
  - ORCID
  - Acknowledgments
  - Conflict of interest statement
- Each author's full name, not initials, must be provided in the order of first name, middle name, and last name for all participating authors
- The abbreviated title should be no longer than 50 characters (including spaces). When authors from different institutions/addresses are included, the authors should be matched with their organizations by placing the relevant organization number in superscript after each author's name.

Contributor Roles	Definitions
Conceptualization	Ideas; formulation or evolution of overarching research goals and aims.
Data Curation	Management activities to annotate (produce metadata), scrub data and maintain research data (including software code, where it is necessary for interpreting the data itself) for initial use and later reuse.
Formal Analysis	Application of statistical, mathematical, computational, or other formal techniques to analyze or synthesize study data.
Funding Acquisition	Acquisition of the financial support for the project leading to this publication.
Investigation	Conducting a research and investigation process, specifically performing the experiments, or data/evidence collection.
Methodology	Development or design of methodology; creation of models
Project Administration	Management and coordination responsibility for the research activity planning and execution.
Resources	Provision of study materials, reagents, materials, patients, laboratory samples, animals, instrumentation, computing resources, or other analysis tools.
Software	Programming, software development; designing computer programs; implementation of the computer code and supporting algorithms; testing of existing code components.
Supervision	Oversight and leadership responsibility for the research activity planning and execution, including mentorship external to the core team.
Validation	Verification, whether as a part of the activity or separate, of the overall replication/reproducibility of results/ experiments and other research outputs.
Visualization	Preparation, creation and/or presentation of the published work, specifically visualization/data presentation.
Writing – Original Draft Preparation	Creation and/or presentation of the published work, specifically writing the initial draft (including substantive translation).
Writing – Review & Editing	Preparation, creation and/or presentation of the published work by those from the original research group, specifically critical review, commentary or revision – including pre- or post-publication stages.

The corresponding author is responsible for completing this information at submission, and it is expected that all authors would have reviewed, discussed, and agreed to their individual contributions ahead of this time.

The contact information of the corresponding author should include the mailing address, phone number, fax number, and e-mail address.
- ORCID: Authors are encouraged to provide their Open Researcher and Contributor ID (ORCID). To obtain an ORCID, authors can register on the ORCID website at https://orcid.org/.

Any funding, financial, or material support for the work must be disclosed in the conflict-of-interest statement. If none of the authors have conflicts of interest, this should be explicitly stated.

Individuals who contributed to the work but who did not meet the requirements for authorship should be included in the acknowledgments.

Main Document
- The main document is a blinded document for review and should contain the following components in Microsoft Word file, each component starting on a separate page: blinded title page, abstract, main body, references, tables, and figure legends.
- When a blinded main document is submitted, a corresponding non-blinded version must also be uploaded in the Not-for-review section.
- Images should not be embedded in the main document.
- Tables should not be placed within the text. The tables should be placed collectively following the references, each on a separate page.

keywords (index terms) should appear after the abstract.

Figures

All figure parts related to one patient should have the same figure number and use English letters after the numerals to distinguish each figure part, e.g., Fig. 1A, 1B, etc.

Each figure part should be sent as a separate image file.

Labels and arrows should be presented with a professional appearance.

All names and all other identifiers of the patient, authors, and authors' institutions should be removed from the figures.

- After cropping to the area of interest, the images should be at least 300 DPI in resolution and 10-15 cm in width.
- Color figures should be in RGB color mode and line drawings should be black on a white background.
- Figure files should be submitted as TIF/TIFF files.
- Written permission from the prior publisher should be obtained for the use of all previously published illustrations and copies of the permission letter should be submitted.

Video clips

Video clips can be submitted for placement on the journal website. All videos are subject to peer review and can be uploaded as supplementary materials. A video file submitted for consideration for publication should be in complete and final format and at as high a resolution as possible. Any editing of the video will be the responsibility of the author. *KJIR* recommends Quicktime, AVI, MPEG, MP4, or RealMedia file formats not exceeding 30 MB and of less than 5 minutes duration.

Supplementary Data

Nonessential tables and figures may accompany articles as online-only supplementary files. All online only supplementary files should be uploaded separately during the submission process. These files must be referenced in the main text of the manuscript at least once (e.g. Supplementary Table 1).

Peer Review
- Manuscripts undergo peer review by at least two experts in the field.
- *KJIR* uses a double-blind review process for submitted manuscripts. Authors' names, affiliations, or any identifying information should not appear in the main document, figures, appendix, or supplementary materials. If such details are found, the editorial office will either request the corresponding author to resubmit the files with this information removed or will remove it on behalf of the authors before sending the manuscript for external peer review.
- Authors must respond to reviewer comments and submit a revised version if required.

Acceptance and Publication
- Accepted papers will be scheduled for publication in the next available issue.
- Proofs will be sent to the corresponding author for final review.
- There are no **publication charges** (unless specified otherwise by the journal).

- Conflict of Interest and License to Publish forms, available on the *KJIR* website, must be submitted.

References

- The references should start on a separate page and be numbered consecutively as appear in the text.
- All references ought to be cited in the text.
- Reference citations in the text should be identified by numbers in square brackets. e.g., [1].
- Journal names should be abbreviated according to the style of the National Library of Medicine.
- All authors should be listed up to six; when more than six author, the first six author should be given and followed by "et al."
- References should be numbered in the order of citation in the text.
- Use a reference manager (e.g., EndNote, Mendeley) for accurate citation formatting.
- Author(s). Title of the article. Journal name. Year;Volume: page. DOI
- Full page numbers should be used (eg. 112–116).
- *KJIR* encourages use of digital object identifier (DOI) in Reference (e.g. "https://doi.org/article_number").
- Example

Journal articles

Lee S, Shim DJ, Kim D, Cho SB, Baek SH, Lee EW, et al. Angiographic Anatomy of the Prostatic Artery in the Korean Population: A Bicentric Retrospective Study. *Korean J Radiol*. 2024; 25:1011-1021. https://doi.org/10.3348/kjr.2024.0451

Articles in press.

Ko E, Kim J, Gwon DI, Chu HH, Kim GH, Ko GY. Emergency Plug-Assisted Retrograde Transvenous Obliteration (PARTO) for Active Bleeding from Ruptured Gastric Varices. J Vasc Interv Radiol. 2025 Feb 1 [Epub] https://doi.org/10.1016/j.jvir.2025.01.049

Books

Binkert CA, Inferior vena cava filters. In: Mauro MA. Image-guided interventions. 2nd ed. Philadelphia, PA: Elsevier, 2014; e105-e110.

Web contents

Provide the authors, title of the webpage or content; owner of the Web site; URL; publication, update, and access date

Rockville, Estimating the Additional Hospital Inpatient Cost and Mortality Associated With Selected Hospital-Acquired Conditions. Agency for Healthcare Research and Quality. https://www.ahrq.gov/hai/pfp/haccost2017-results.html. Published November 2017. Accessed December 25, 2025

Citations in main text: Number the references in the order in which they appear in the text. Reference numbers appear inline within square brackets.

For further details, contact editor@kjironline.org

By adhering to these guidelines, authors contribute to the quality and impact of the *KJIR*.

Author's checklist

KJIR
Korean Journal of
Interventional Radiology

☐ Cover letter.
☐ All texts files in Microsoft Word format (doc or docx).
☐ Complete Full Title Page as a separate Microsoft Word file
☐ Main Document as a separate Microsoft Word file, including in the order of blinded title page, abstract, keywords, body text, references, tables, and figure legends.
☐ Supplement (if present) as a separate Word document instead of adding it to the end of the main document.
☐ Word limit for abstract
☐ Approximately 5 keywords.
☐ Statement of ethical approval and informed consent at the start of the materials and methods (for manuscripts reporting data from studies involving human participants or animals).
☐ Digital figures must be at least 300 dpi and a minimum of 3 inches to a maximum of 7 inches in width and height.
☐ For previously published materials, send written permission to reprint.

Copyright transfer agreement

KJIR
Korean Journal of
Interventional Radiology

This Copyright Transfer Agreement ("Agreement") sets forth the terms and conditions governing the transfer and use of copyright for manuscripts submitted to the **Korean Journal of Interventional Radiology (KJIR)**.

1. Manuscript Information

- Title of Manuscript:
- Manuscript ID:
- Date of Submission:

2. Grant of License to Publish

In consideration of the review and potential publication of the above-mentioned manuscript, the author(s) hereby grant the **Korean Journal of Interventional Radiology (KJIR)** and its publisher a **worldwide, perpetual, irrevocable, and royalty-free license** to publish, reproduce, distribute, display, archive, translate, and otherwise use the manuscript, in whole or in part, in all forms and media now known or hereafter developed (including print, electronic, online, and offline formats).

The author(s) retain copyright ownership of the manuscript. This license shall take effect upon final acceptance of the manuscript for publication. In the event that the manuscript is rejected or withdrawn prior to acceptance, this Agreement shall be null and void.

3. Rights Retained by the Authors

The author(s) retain copyright in the manuscript and all rights not expressly granted to KJIR. Without limitation, the author(s) retain the right to:

1. Use all or part of the manuscript for non-commercial purposes, including lectures, academic presentations, theses, dissertations, and research reports;
2. Reproduce and distribute the manuscript for educational and research purposes;
3. Post the manuscript on the author's personal website, institutional repository, or other non-commercial platforms;
4. Comply with public access or open access mandates required by funding agencies or governmental bodies.

All such uses must include appropriate citation to the original publication in KJIR.

4. Author Representations and Warranties

The author(s) represent and warrant that:

1. The manuscript is an original work of the author(s) and does not infringe upon any copyright, moral right, patent, or other proprietary right of any third party;
2. The manuscript has not been previously published and is not under consideration for publication elsewhere;
3. Any figures, tables, images, or other materials reproduced from other sources have been used with proper permission, and appropriate acknowledgements are included;
4. All listed authors have substantially contributed to the work and have approved the final version of the manuscript;
5. The corresponding author has been authorized by all co-authors to execute this Agreement on their behalf.

5. Ethics and Conflict of Interest

The author(s) certify that, where applicable, the study was conducted in accordance with relevant ethical standards, including

approval or exemption by an Institutional Review Board (IRB), and that all potential conflicts of interest have been fully disclosed in the manuscript.

6. Open Access Publication

KJIR is an **open access journal.** Upon publication, the final published version of the manuscript (Version of Record) shall be made freely and permanently available to the public without subscription or access fees.

The manuscript shall be published under the **Creative Commons Attribution License (CC BY 4.0),** which permits unrestricted use, distribution, reproduction, and adaptation in any medium, provided that appropriate credit is given to the original author(s) and the source, and any changes made are indicated.

7. Governing Law and Jurisdiction

This Agreement shall be governed by and construed in accordance with the laws of the Republic of Korea. Any dispute arising out of or in connection with this Agreement shall be subject to the exclusive jurisdiction of the courts of the Republic of Korea.

8. Signatures

By signing below, the author(s) acknowledge that they have read, understood, and agreed to the terms of this Agreement.

Corresponding Author

- Name:
- Affiliation:
- Signature:
- Date:

※ The corresponding author confirms that all co-authors have agreed to the terms of this Agreement.